

UC Berkeley

UC Berkeley Electronic Theses and Dissertations

Title

A Unified Approach Toward the Total Synthesis of Lycopodium Alkaloids of the Miscellaneous Class

Permalink

<https://escholarship.org/uc/item/48m5m0q7>

Author

House, Sarah Elizabeth

Publication Date

2010

Peer reviewed|Thesis/dissertation

A Unified Approach Toward the Total Synthesis of *Lycopodium* Alkaloids of the
Miscellaneous Class

By

Sarah Elizabeth House

A dissertation submitted in partial satisfaction of the

requirements for the degree of

Doctor of Philosophy

in

Chemistry

in the

GRADUATE DIVISION

of the

University of California, Berkeley

Committee in charge:

Professor Richmond Sarpong, Chair

Professor K. Peter C. Vollhardt

Professor Leonard F. Bjeldanes

Fall 2010

Abstract

A Unified Approach Toward the Total Synthesis of *Lycopodium* Alkaloids of the Miscellaneous Class

by

Sarah Elizabeth House

Doctor of Philosophy in Chemistry

University of California, Berkeley

Professor Richmond Sarpong, Chair

A unified approach to the total synthesis of *Lycopodium* alkaloids belonging to the miscellaneous class has been developed, wherein a single tetracyclic amine is employed as a common intermediate in synthetic studies toward several alkaloids.

An overview of *Lycopodium* alkaloids is presented, including their structural classification, isolation and biological activity. The biosynthesis of alkaloids in the miscellaneous group is discussed in depth. A summary of previous synthetic work focusing on miscellaneous *Lycopodium* alkaloids is presented, including total syntheses of luciduline, lyconadins A and B and nankakurines A and B. A model study of spirolicidine is discussed.

A biomimetic route to access spirolicidine and nankakurine B has been investigated. In this study, a tetracyclic amine that is a key intermediate in the total synthesis of lyconadin A previously developed in our laboratory is elaborated into a tertiary alcohol that mimics the proposed biosynthetic precursor of nankakurine B. A biomimetic ring-contractive α -hydroxyimine rearrangement to generate nankakurine B has been extensively investigated and found to be disfavored.

The conversion of a tricyclic ketone (first synthesized *en route* to lyconadin A) to the tetracyclic core of serratezomine D has been investigated. The core of this molecule was inaccessible *via* methods employed in the studies toward lyconadin A.

The total synthesis of 1'-*epi*-dihydrolycolucine from the key common tetracyclic amine intermediate has been achieved. Studies toward the synthesis of serratezomine E served as a platform to develop this method and to determine the stereochemical outcome of this reaction.

To my friends, my family and Aidan,
For all of their support and encouragement.

Table of Contents

Acknowledgements	v
------------------	---

Chapter One: The Lycopodium Alkaloid Natural Products

1.1 Introduction	1
1.2 Isolation, Structure and Nomenclature	1
1.3 Biological Activity of the <i>Lycopodium</i> Alkaloids	2
1.4 The Miscellaneous Class of <i>Lycopodium</i> Alkaloids	3
1.5 Biosynthesis of the <i>Lycopodium</i> Alkaloids	4
1.6 Previous Synthetic Work in the Miscellaneous Class	10
1.7 A Unified Approach to Miscellaneous <i>Lycopodium</i> Alkaloids	19
1.8 References	20

Chapter Two: Toward the Total Synthesis of Spirolucidine and Nankakurines A and B

2.1 Retrosynthetic Analysis of Spirolucidine and Nankakurine A	23
2.2 Synthesis of a Tetracyclic Common Intermediate	24
2.3 Imine Route to Spirolucidine and Nankakurine A	29
2.4 Enamide Route to Spirolucidine and Nankakurine A	35
2.5 Oxidation and Rearrangement Studies on Boc-Protected Tetracycle	51
2.6 Synthesis and Exploration of Key Step on Second-Generation Substrates	58
2.7 Conclusion	65

2.8 Experimental Contributions	65
2.9 Experimental Methods	66
2.10 References	77
<i>Appendix One: Spectra Relevant to Chapter Two</i>	79
<i>Chapter Three: Toward the Total Synthesis of Serratezomine D</i>	
<hr/>	
3.1 Introduction	120
3.2 Retrosynthetic Analysis of Serratezomine D	121
3.3 Model Study	122
3.4 Studies Toward the Tetracyclic Core of Serratezomine D	124
3.5 Conclusion	129
3.6 Experimental Contributions	129
3.7 Experimental Methods	130
3.8 References	132
<i>Appendix Two: Spectra Relevant to Chapter Three</i>	133
<i>Chapter Four: Toward the total Synthesis of Serratezomine E and Dihydrolycolucine</i>	
<hr/>	
4.1 Introduction	137
4.2 Retrosynthetic Analysis of Dihydrolycolucine and Serratezomine E	138
4.3 Synthesis of Bicyclic Ketone	139

4.4 Studies Toward Serratezomine E	142
4.5 Studies Toward Dihydrolycolucine	146
4.6 Conclusion	147
4.7 Experimental Contributions	147
4.8 Experimental Methods	148
4.9 References	155
<i>Appendix Three: Spectra Relevant to Chapter Four</i>	156

Acknowledgments

I would like to thank Professor Richmond Sarpong for the opportunity to work in his research group during my time at Berkeley. His constant stream of exciting research ideas and unwavering enthusiasm made working in his group an enjoyable and exciting experience. He cultivated a research environment where students were encouraged to continue to develop intellectually throughout their years in the group, and I have grown immensely as a scientist because of it.

I would also like to thank Professor Gregory B. Dudley at Florida State University, my research advisor during my undergraduate years. He taught me the foundations of research in organic chemistry. In addition, I would like to acknowledge Dr. Hubert Lam for thoroughly training me in proper organic chemical laboratory techniques, even though my first act upon joining the group was to destroy 500 mg of a compound that had taken him six weeks to make.

I am deeply indebted to Dr. Scott West and Dr. Alakesh Bisai, both of whom I worked with very closely with during my time at Berkeley. Much of the work I did was built on a foundation developed by the two of them, and they were both invaluable in helping to familiarize me with the vagaries of working with alkaloids. I am also in debt to Kimberly Larson, Andrew Marcus, Eric Bunnelle and Eric Simmons, the four graduate students that joined the Sarpong group in the class ahead of me. They were instrumental in training me during my first year. To Eric Bunnelle I owe a passion for physical organic chemistry and a cynical streak that will stay with me for life. Andrew was very helpful as a mentor during the short while that we worked on the tetrapetalone project together.

I would be remiss if I did not acknowledge the many people who have worked with me in room 842 Latimer. The undergraduates that worked in the room during my first two years, Amy Lee, Sharon Lee, Allen Hong and Walter Singaram, were enthusiastic and very a constant adventure to spend time with. During my second and third years, Massoud Motamed pushed me to continually grow as a chemist and helped ensure that there was never a dull or silent moment in room 842. Paul Karayan expanded my musical horizons greatly, and Mike Purdham and visiting undergraduate Andrew Hoover made the room a very interesting place to work. During my final year, the combination of Saeed Alzhgari's sunny attitude and Daniel Fischer's impeccable nature photography hanging on the walls practically made me forget that the room has no windows. All of these people helped to make my time at Berkeley the experience that it was, and I will never forget them.

Maryann Robak has been a great friend to me since the moment we met at an on-site visit, long before either of us arrived in Berkeley. I would like to thank her for all of her help and for numerous home-cooked meals. I also want to thank Pete Marsden and Rhia Martin of the Ellman group, both for going to lunch with me regularly and for countless thought-provoking discussions.

Rudi Nunlist and Chris Canlas were both very helpful with NMR studies. I must also thank Pete, Maryann, Daniel and Jess Wood for editing drafts of this thesis. I would like to thank everyone in the Sarpong group for making it a great place to work.

Finally, I would like to thank my friends and family for their support. This would not have been possible without them. I especially want to thank Aidan Scott, whose encouragement helped me see this through to the end.

Chapter One

The Lycopodium Alkaloid Natural Products

1.1 Introduction

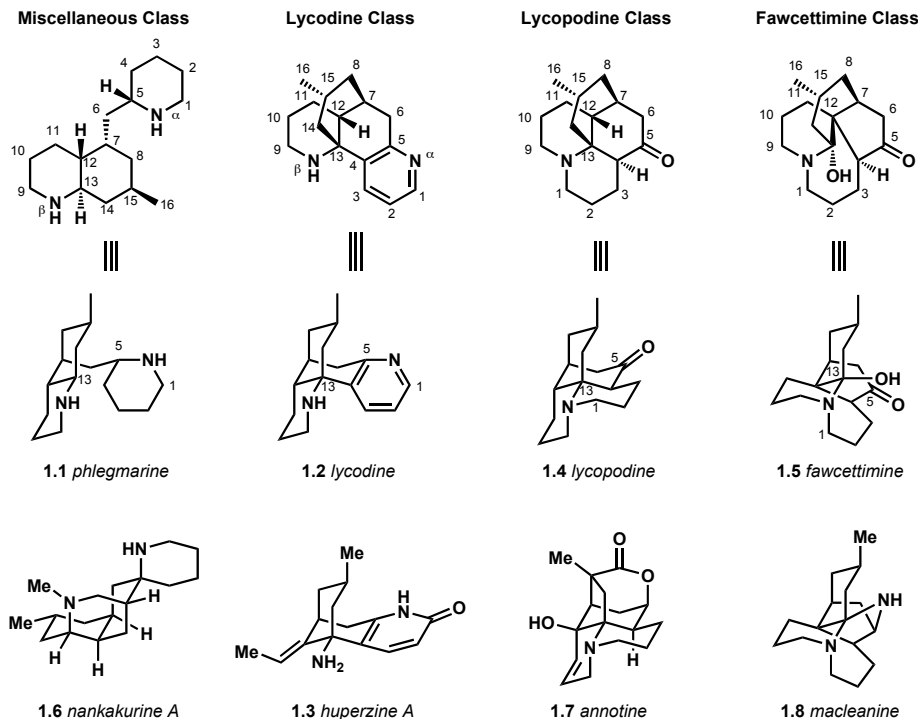
The *Lycopodium* alkaloids are a diverse group of over 250 natural products which possess complex architectures and a range of interesting biological activity, including potent and selective acetylcholinesterase inhibition.¹ The caged, polycyclic structures of these compounds pose significant synthetic challenges. This, combined with the useful bioactivity of these compounds, has led to a host of scientific studies.^{2,3,4} This chapter will begin with an introduction to the structure, nomenclature and biological activity of the *Lycopodium* alkaloids, continue with a discussion of the miscellaneous class of *Lycopodium* alkaloids, then examine the biogenesis and biosynthetic relationships between these compounds, and finally conclude with a summary of previous synthetic efforts toward members of the miscellaneous class of *Lycopodium* alkaloids.

1.2 Isolation, Structure and Nomenclature

There are more than 500 species in the *Lycopodium* family of club mosses.⁴ These low-lying, evergreen mosses are so named because they bear club-shaped strobili that produce the spores they use to reproduce. The first *Lycopodium* alkaloid to be isolated was lycopodine, which was discovered in *Lycopodium complanatum* in 1881 by Bödeker.⁵ Its molecular formula and structure were deduced by Achmatowicz and Uzibelo in 1938.⁶ During the following decade, Marion and Manske isolated thirty-five new *Lycopodium* alkaloids.² Beginning in the 1940's, a systematic study of the structure, synthesis and biogenesis of *Lycopodium* alkaloids was undertaken by several research groups, in particular Ayer, MacLean and Wiesner.⁷ Thus far, the alkaloids of roughly 50 species of *Lycopodium* mosses have been studied, leading to the discovery of more than 250 alkaloids.^{3,4,7}

The *Lycopodium* alkaloids can be divided into four distinct structural classes. These are the lycodine class, the lycopodine class, the fawcettimine class and the miscellaneous class.⁷ Phlegmarine (**1.1**, Figure 1.1) is a member of the miscellaneous class, and is believed to be a key intermediate in the biosynthesis of all four classes of *Lycopodium* alkaloids. Alkaloids that possess a bond between C-4 and C-13 belong to the lycodine class, which is represented here by lycodine (**1.2**) and huperzine A (**1.3**). Scission of the bond between N- α and C-1 and cyclization between C-1 and the remaining nitrogen gives rise to lycopodine (**1.4**). Fawcettimine (**1.5**) is formed from **1.4** by a formal migration of C-4 from C-13 to C-12. All *Lycopodium* alkaloids that do not bear the lycodine, lycopodine or fawcettimine cores belong to the miscellaneous class.

Figure 1.1 The four classes of *Lycopodium* alkaloids.



1.3 Biological Activity of the *Lycopodium* Alkaloids

The most important biological activity that has been discovered in *Lycopodium* alkaloids is selective and reversible acetylcholinesterase inhibition, which is demonstrated by many members of the lycodine class.¹ The inhibition of acetylcholinesterase has been shown to improve symptoms in patients with Alzheimer's disease and to enhance learning and memory. Several of the drugs on the market in the U.S. for the treatment of Alzheimer's disease are acetylcholinesterase inhibitors, including Aricept, Razadyne and Exelon.⁷

Thus far, the *Lycopodium* alkaloid that has demonstrated the most potent acetylcholinesterase inhibition is huperzine A (**1.3**). Huperzine A crosses the blood-brain barrier easily and possesses a prolonged biological half-life. It is an approved treatment for Alzheimer's disease in China and is marketed in the US as a memory supplement.⁷ Many of its structural analogues have been evaluated for bioactivity; however, none have surpassed huperzine A itself.¹

Several *Lycopodium* alkaloids have also demonstrated modest cytotoxicity against certain cancer cell lines. Nankakurine A (**1.6**) exhibited cytotoxicity against human epidermoid carcinoma KB cells ($IC_{50} = 3.1$ ug/mL) and lyconadin A (**1.9**, see Figure 1.2) displayed cytotoxicity against murine lymphoma L1210 cells ($IC_{50} = 0.46$ ug/mL). However, despite the interesting properties displayed by various *Lycopodium* alkaloids, the majority of these compounds have never been screened for biological activity.

1.4 The Miscellaneous Class of *Lycopodium* Alkaloids

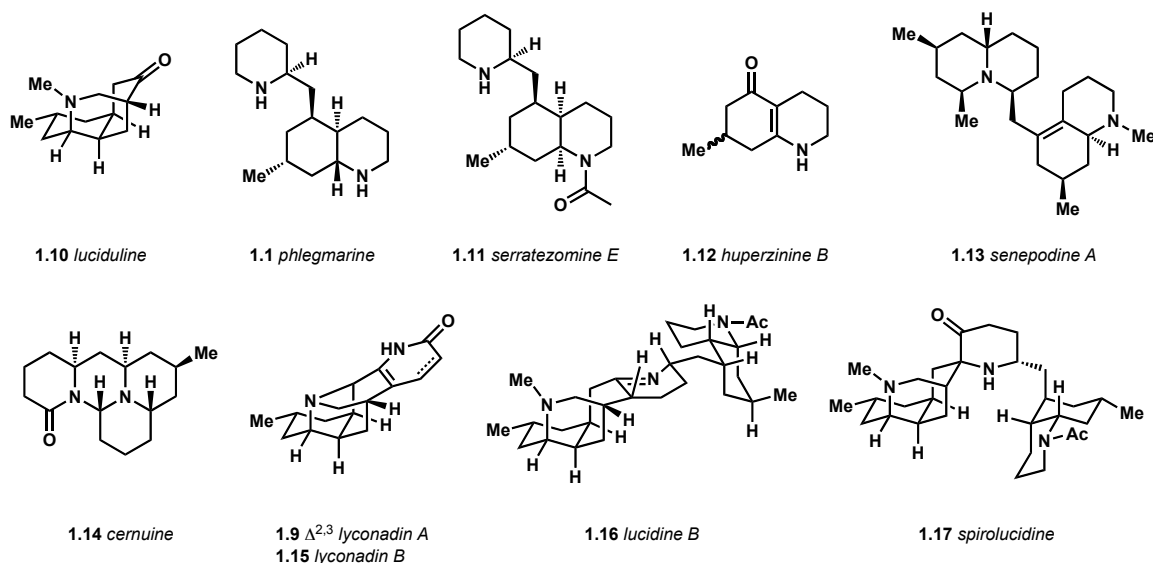
The miscellaneous class of the *Lycopodium* alkaloids contains the most structural diversity of the four classes. To date, more than 60 alkaloids that belong to this class have been isolated. The first of these to be discovered, luciduline (**1.10**, Figure 1.2) was isolated in 1963 from the club moss *Lycopodium lucidulum* by Ayer and co-workers.⁸ Its structure was elucidated in 1979.⁹

Alkaloids in the miscellaneous class do not contain a bond between C-13 and C-4, in contrast to the other three classes. Consequently, many miscellaneous *Lycopodium* alkaloids have only three rings instead of the four commonly present in the other classes. Phlegmarine (**1.1**) and serratezomine E (**1.11**)¹⁰ are typical examples from this class. There are 12 known C₁₆N₂ alkaloids that are close structural analogues of phlegmarine.

To date, five bicyclic miscellaneous *Lycopodium* alkaloids have been isolated,¹¹ the first of which was huperzine B (**1.12**) in 2001.¹² These represent the simplest members of the *Lycopodium* alkaloid family. Luciduline (**1.10**) is an example of a caged tricyclic miscellaneous *Lycopodium* alkaloid that bears a very different skeleton from phlegmarine. Tetracyclic alkaloids such as senepodine A (**1.13**)¹³ and ceruine (**1.14**)¹⁰ also belong to this class.

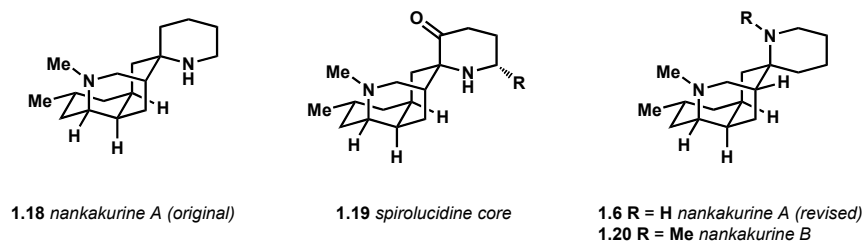
The most structurally complex members of this class are caged structures that contain five to six rings. Lyconadins A (**1.9**)¹⁴ and B (**1.15**)¹⁵, which were isolated from *Lycopodium complanatum* in 2001 and 2006 respectively, have a unique pentacyclic core. There are several alkaloids in this class that possess C₃₀N₃ skeletons, each of which consists of a tetracyclic core with an appended bicycle. Among the first of these to be discovered was lucidine B (**1.16**), whose structure was elucidated in 1979.⁹ Spirolucidine (**1.17**) was isolated from *Lycopodium lucidulum* in 1968,¹⁶ and its structure was determined by X-ray crystallographic analysis of a reduced derivative in 1984.¹⁷

Figure 1.2 Representative miscellaneous *Lycopodium* alkaloids.



The isolation and structural assignment of nankakurine A warrants special examination. Nankakurine A was first isolated by Kobayashi and co-workers in 2004 from the club moss *Lycopodium hamiltonii*.¹⁸ The structure **1.18** (Figure 1.3) was originally proposed for this alkaloid. The stereochemistry at the spiro center was assigned based on both nOe data and its structural similarity to the tetracyclic core of spirolocidine (**1.19**). However, the isolation of nankakurine B (**1.20**) two years later yielded clearer nOe data that led the authors to assign its spiro center the opposite configuration. Because nankakurine A could be converted to nankakurine B through methylation, its structure was revised to **1.6**.¹⁹ This revised structure was confirmed in 2008 after the completion of a total synthesis by Overman, which will be discussed in further detail in section 1.6.4.²⁰

Figure 1.3 Structural assignment of nankakurines A and B.



1.5 Biosynthesis of the *Lycopodium* Alkaloids

1.5.1 Biosynthesis of the lycodine, lycopodine and fawcettimine classes

Studies on the biogenesis of *Lycopodium* alkaloids have been limited in number because of the difficulty in cultivating *Lycopodium* club mosses.¹⁸ Even culturing the tissue of these plants has proven challenging.²¹ Nevertheless, Spenser and others have completed a number of feeding studies that have helped illuminate their biosynthetic pathway.²²

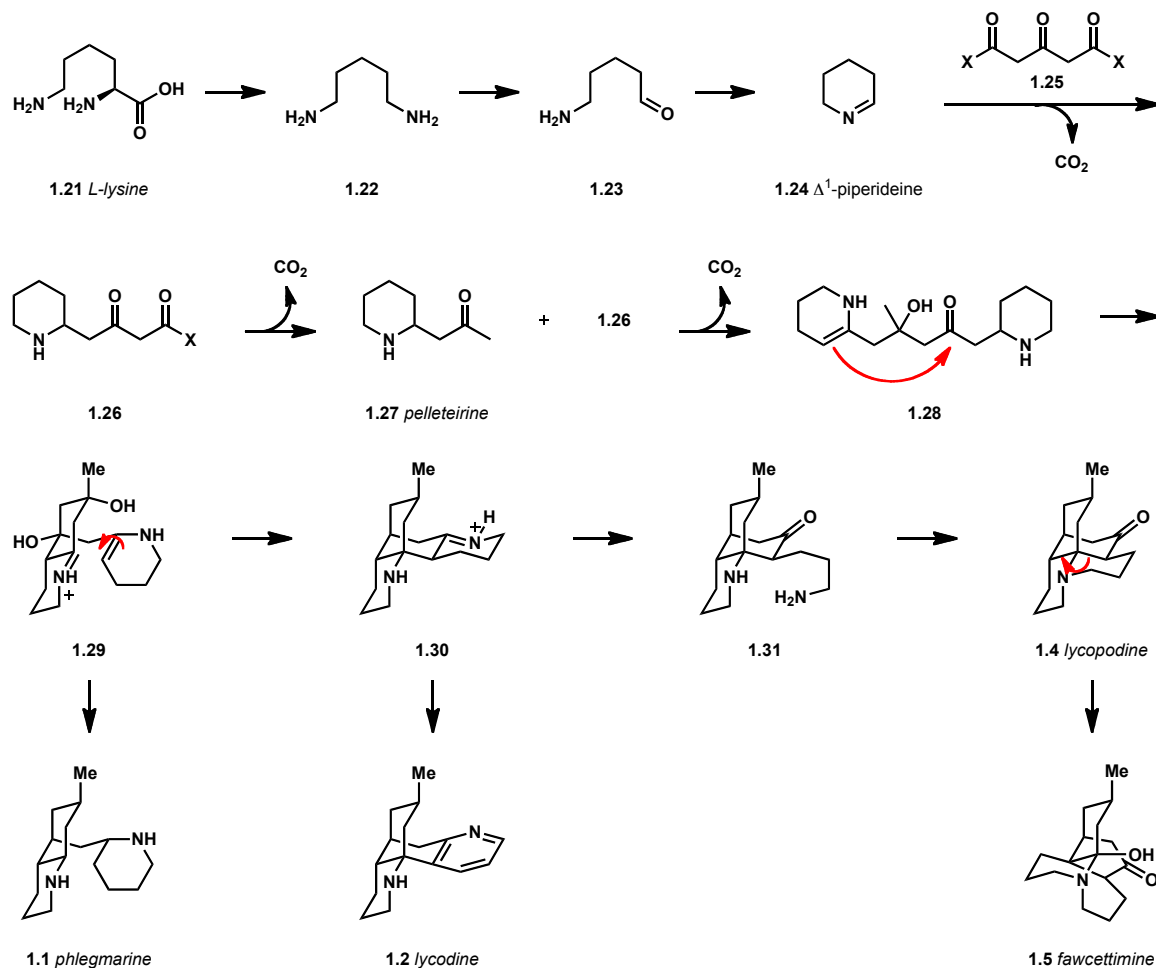
The starting point for the biosynthesis of the *Lycopodium* alkaloids is believed to be L-lysine (**1.21**, Scheme 1.1).^{23,24,25} It is converted through decarboxylation to diamine **1.22**, which is then oxidized to aldehyde **1.23**. Condensation provides Δ^1 -piperideine (**1.24**). The acetone unit is derived from acetone dicarboxylic acid or its bis-CoA ester (**1.25**).²⁶ Decarboxylation followed by addition into **1.24** provides **1.26**, which can undergo a second decarboxylation to afford pelletierine (**1.27**).

Dimerization occurs via an aldol reaction between pelletierine (**1.27**) and **1.26** to afford **1.28**. Cyclization provides tricyclic skeleton **1.29**, which comprises the core of phlegmarine (**1.1**).

The biosyntheses of the lycodine, lycopodine and fawcettimine classes diverge from that of the miscellaneous class. Formation of a bond between C-4 and C-13 of **1.29** gives tetracyclic structure **1.30**, which is oxidized to a pyridine, affording lycodine (**1.2**). Lycodine can then be elaborated into the other members of the lycodine class. For lycopodine, the iminium functionality of **1.29** is

hydrolyzed to form aminoketone **1.31**, which can cyclize to give lycopodine (**1.4**). Migration of the C-4 carbon from C-13 to C-12 furnishes fawcettimine (**1.5**).

Scheme 1.1 Biosynthesis of the lycodine, lycopodine and fawcettimine classes.



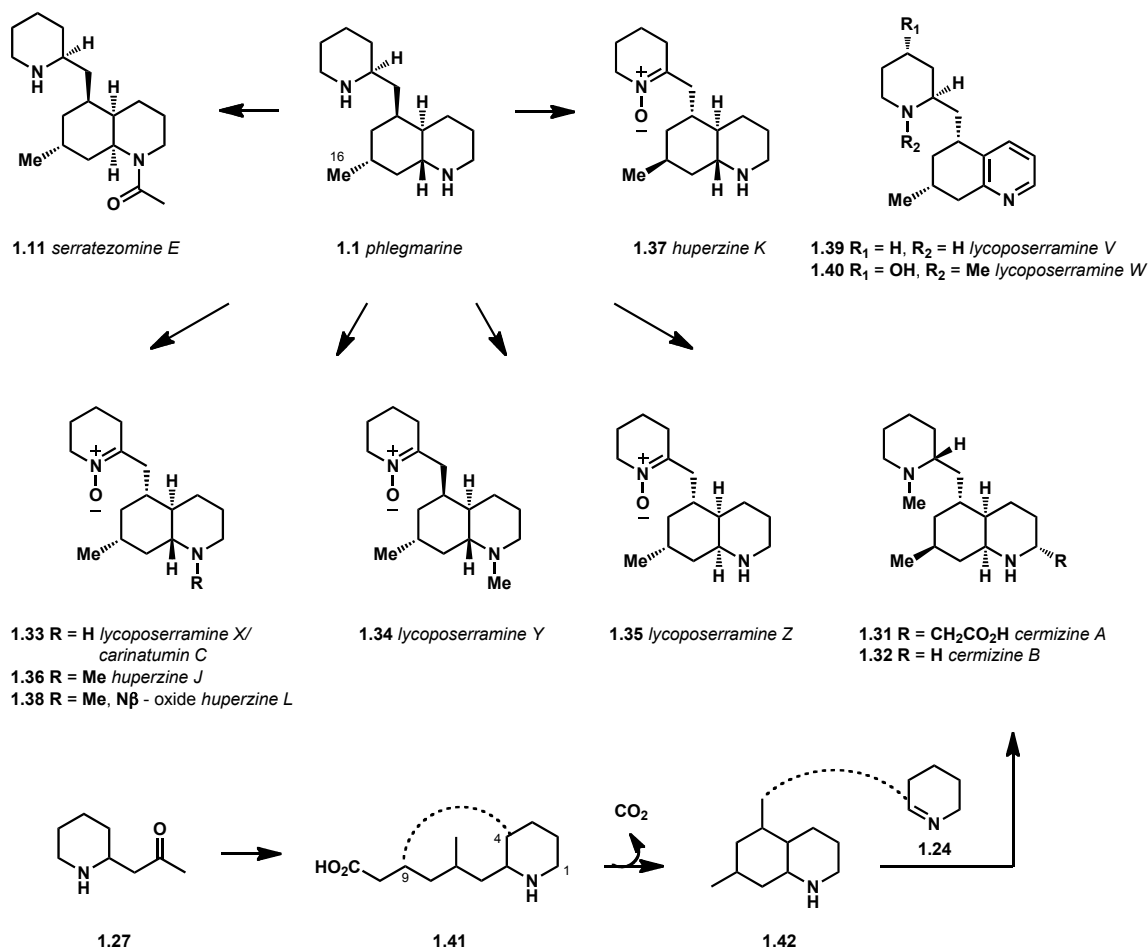
1.5.2 Biosynthesis of the Miscellaneous Class

The majority of the alkaloids in the miscellaneous class are believed to be derived from phlegmarine; however, alternative paths stemming directly from pelletierine have been proposed for certain alkaloids.

A number of alkaloids in the miscellaneous class bear a close structural relationship to phlegmarine. Serratezomine E (**1.11**, Scheme 1.2)¹⁰ and cermizines A (**1.31**) and B¹¹ (**1.32**) differ from phlegmarine only in stereochemistry and substitution pattern. Several derivatives contain a nitron, including lycoposerramines X (**1.33**), Y (**1.34**) and Z (**1.35**)²⁷ and huperzines J – L (**1.36**, **1.37** and **1.38**). Lycoposerramines V (**1.39**) and W (**1.40**)²⁸ contain one ring at the pyridine oxidation level. Phlegmarine may be the biosynthetic precursor for these alkaloids; however, a second biosynthesis has been proposed in which alkaloids such as cermizine A arise from pelletierine (**1.27**) through an intermediate such as

1.41.³ Bond formation between C-4 and C-9 of **1.41** would furnish bicycle **1.42**, and addition of a second Δ^1 -piperidine unit might give the tricyclic alkaloids cermizines A and B.

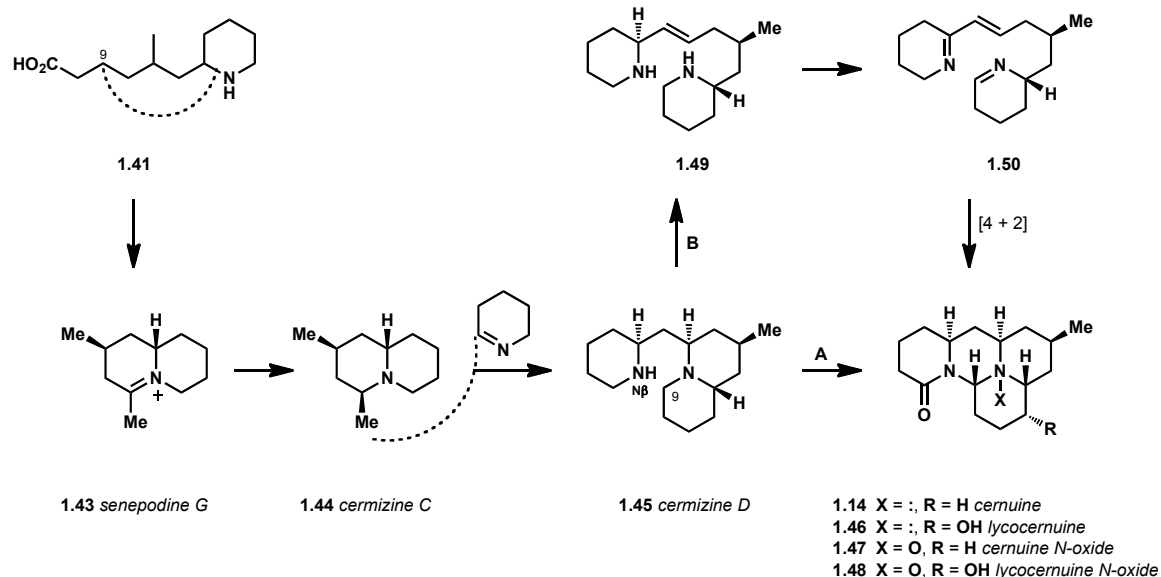
Scheme 1.2 Possible biosynthesis of tricyclic miscellaneous *Lycopodium* alkaloids.



Alternatively, if intermediate **1.41** underwent bond formation between N and C-9 along with decarboxylation, this would furnish bicyclic alkaloids senepodine G (**1.43**, Scheme 1.3) and cermizine C (**1.44**).³ Coupling with an additional Δ^1 -piperidine unit would lead to cermizine D (**1.45**). Bond formation between N- β and C-9 and oxidation, as shown in path A, could lead to cernuine (**1.14**) and lycocernuine (**1.46**) as well as their respective *N*-oxides (**1.47** and **1.48**).

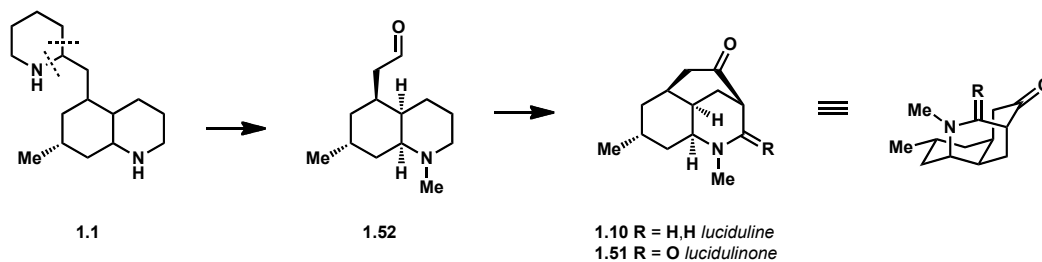
Cernuine (**1.14**) and lycocernuine (**1.46**) have also been postulated to arise from cermizine D (**1.45**) through a rearrangement and cycloaddition sequence (Path B, Scheme 1.3).⁷ Breaking of the C-7 – C-12 bond to give **1.49** followed by oxidation could lead to aza-diene **1.50**, which might undergo a [4+2] cycloaddition to furnish cernuine (**1.14**) and related alkaloids.

Scheme 1.3 Biosynthesis of cermizines A, B and D, cernuine and lycocernuine.



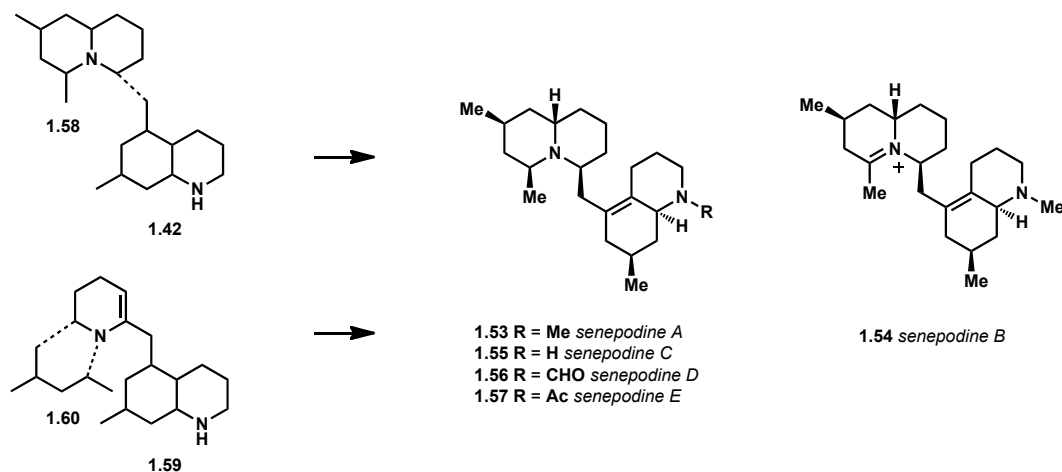
Phlegmarine (**1.1**, see scheme 1.4) is the proposed biogenetic precursor to luciduline (**1.10**) and lucidulinone (**1.51**). This synthesis is presumed to begin with scission of the bond between N- α and C-5 as well as the bond between C-4 and C-5 of **1.1** to produce intermediate aldehyde **1.52**. Cyclization can afford luciduline (**1.10**), and oxidation of that core provides lucidulinone (**1.51**).⁷

Scheme 1.4 Proposed biosynthesis of luciduline and lucidulinone.



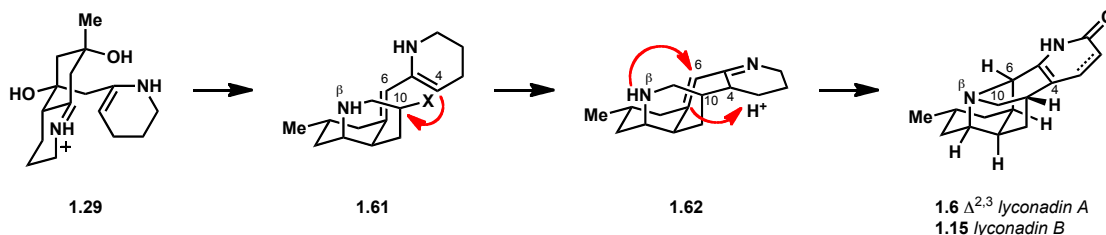
Two biogenetic proposals have been suggested for the synthesis of C₂₂N₂ alkaloids senepodines A – E (**1.53** – **1.57**, Scheme 1.5). The first hypothesizes that a molecule of **1.42** could join with a cermizine C-type C₁₁N unit (**1.58**) to give these structures.³ The other is that the senepodines may arise from phlegmarine-like tricyclic core (**1.59**) through addition to a C₆ unit (**1.60**) derived from two moles of acetyldicarboxylic acid.

Scheme 1.5 Biosynthesis of senepodines A – E.



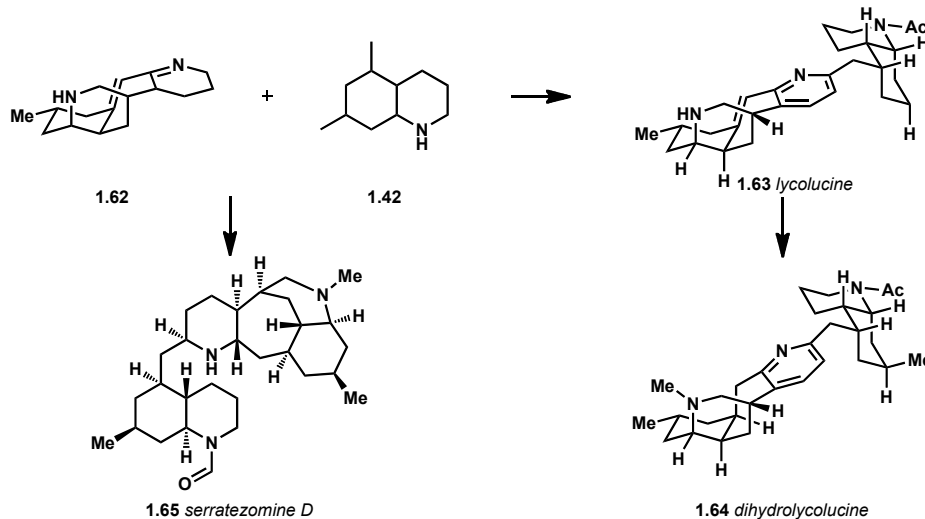
Lyconadin A (**1.9**) is thought to arise from phlegmarine-type structure **1.29** (Scheme 1.6), which is an intermediate in the biogenesis of lycopodine.⁷ Dehydration of **1.29** to give **1.61** could be followed by bond formation between C-4 and C-10 to afford tetracycle **1.62**. Attack of N- β on the alkene functionality of **1.62** would furnish the pentacyclic core of lyconadins A and B.

Scheme 1.6 Biosynthesis of lyconadins A and B.



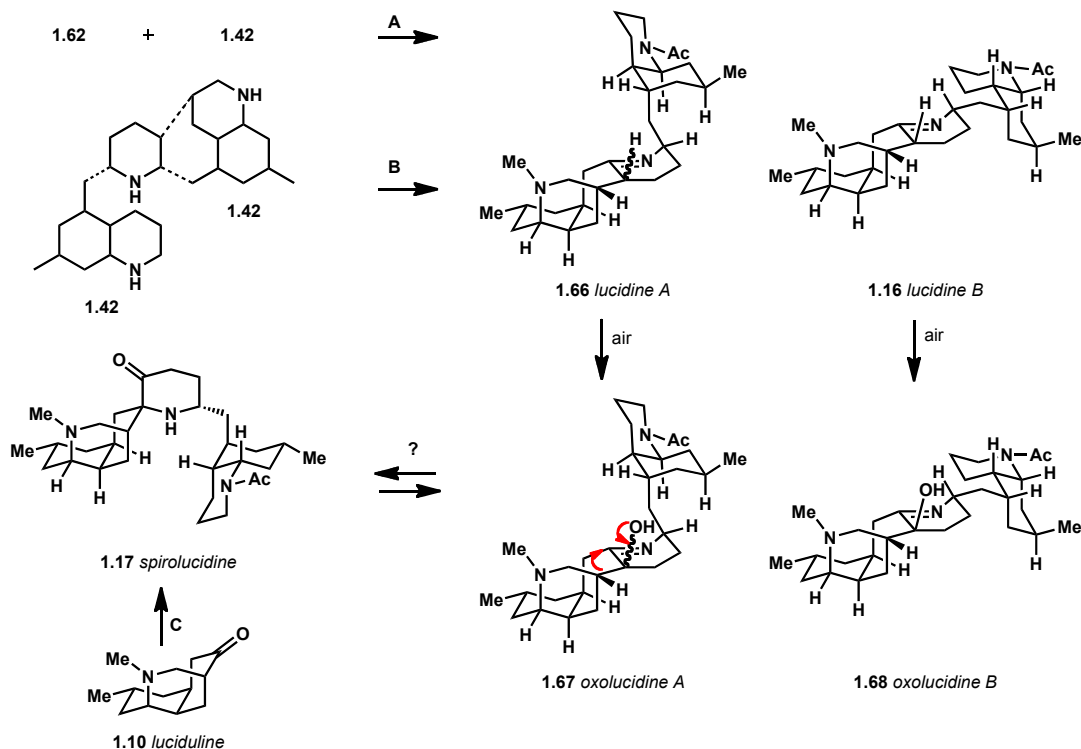
Intermediate **1.62** en route to lyconadin A may also give rise to lycolucine (**1.63**, Scheme 1.7) via coupling with a bicyclic **1.42** unit. Formal addition of hydrogen would yield dihydrolycolucine (**1.64**). Union of **1.62** and **1.42** could also lead to the strained alkaloid serratezomine D (**1.65**).¹⁰

Scheme 1.7 Biosynthesis of lycolucine, dihydrolycolucine and serratezomine D.



A similar coupling of **1.62** and **1.42** could give rise to lucidines A (**1.66**, Scheme 1.8) and B (**1.16**) through path A. The stereochemistry at C-14 of lucidine A remains unsolved, though the rest of the structure has been elucidated by X-ray crystallographic analysis of a derivative.²⁹ Alternatively, lucidine B has been hypothesized by Ayer to arise from the formal coupling of two enantiomeric C₁₁N units (**1.42**) to a single piperidine ring, as shown in path B.⁹

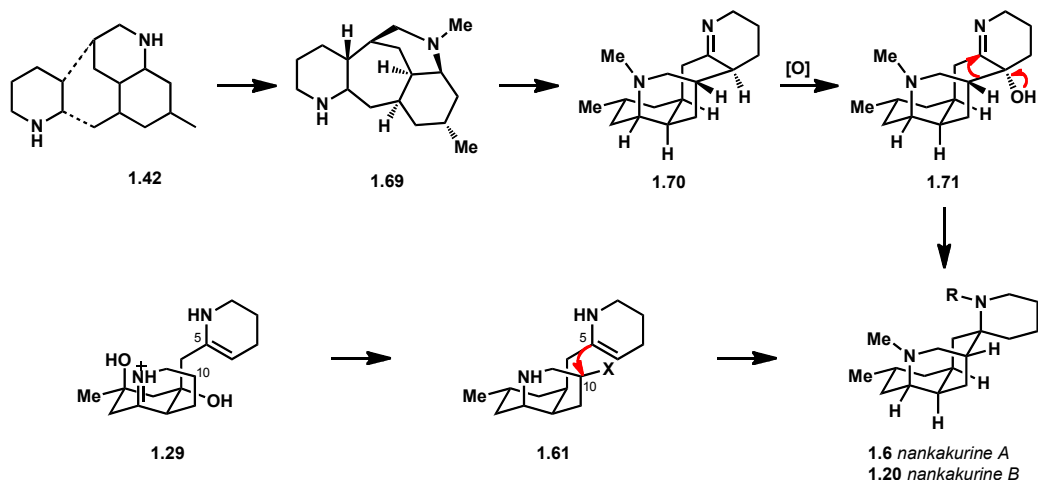
Scheme 1.8 Biosynthesis of lucidines, oxolucidines and spirolucidine.



It has been shown that lucidines A and B oxidize readily in the presence of atmospheric oxygen to form oxolucidines A (**1.67**, Scheme 1.8) and B (**1.68**), respectively. Ayer has proposed that oxolucidine A may be the biosynthetic precursor to spirolocidine (**1.17**) through a ring-contractive skeletal rearrangement; however, the authors were unable to effect this rearrangement by treatment of **1.67** with several acids.²⁹ Ayer has also suggested that spirolocidine may be built from luciduline (**1.10**, Path C), and may actually be the biosynthetic precursor of lucidine A through the reverse rearrangement.¹⁷

Two biosynthetic pathways have been proposed for nankakurines A and B (Scheme 1.9). In the first, intermediate **1.42** is joined with a piperidine unit as shown in Scheme 1.9 to form tetracycle **1.69**. This could undergo an oxidation to imine **1.70** followed by a hydroxylation to afford alcohol **1.71**. Alcohol **1.71** could undergo a ring-contractive skeletal rearrangement analogous to that proposed for spirolocidine to afford nankakurine A after reduction of the carbonyl group. Alternatively, the biosynthesis of nankakurines A and B could proceed through phlegmarine-type intermediate **1.29**. Functionalization of C-10 of **1.29** to form tricycle **1.61** followed by bond formation between C-5 and C-10 would furnish nankakurines A and B.

Scheme 1.9 Biosynthesis of nankakurines A and B.



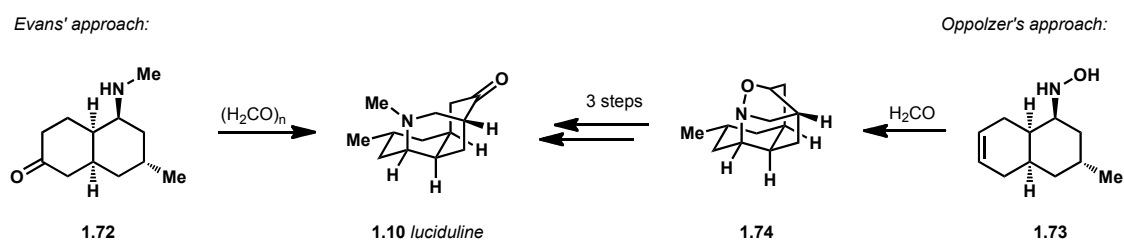
1.6 Previous Synthetic Work in the Miscellaneous Class

Many synthetic efforts have been directed toward constructing members of the miscellaneous class of *Lycopodium* alkaloids. Total syntheses of bicyclic alkaloids senepodine G and cermizine C have been accomplished by Snider³⁰ and Zhang.³¹ Efficient routes have been developed to access a variety of C₁₆N₂ alkaloids, including lycoposerramines V, W,³² X and Z.³³ Cermizine D was built as an intermediate in the total synthesis of cernuine.³⁴

1.6.1 Total synthesis of luciduline

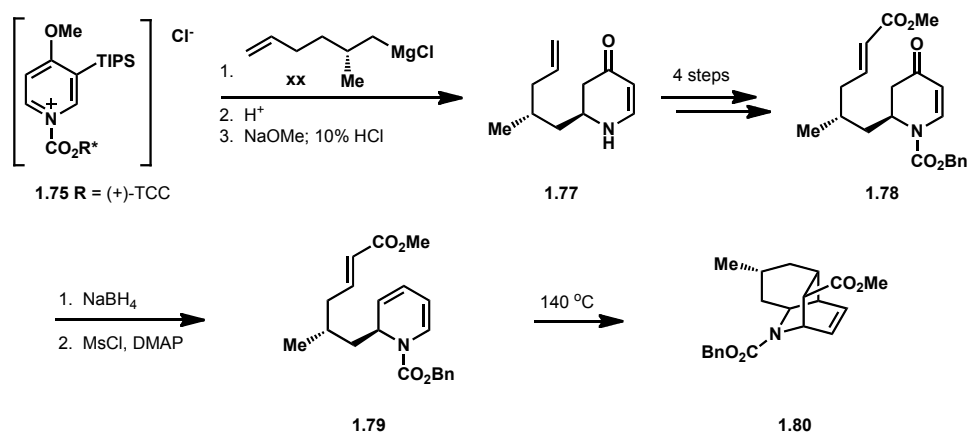
The first total synthesis of a miscellaneous *Lycopodium* alkaloid to be completed was Evans and Scott's racemic synthesis of luciduline in 1972.³⁵ The key step of this synthesis was an intramolecular Mannich reaction utilizing aminoketone **1.72** (Scheme 1.10) and paraformaldehyde to give luciduline. In 1978, Oppolzer and Petrzilka completed the first enantioselective synthesis of (+) – luciduline, beginning from pulegone.³⁶ This synthesis employed a nitron-olefin cycloaddition from bicycle **1.73** as the key step. Tetracycle **1.74** could be converted into luciduline in 3 steps.

Scheme 1.10 Evans' and Oppolzer's approaches to luciduline.



Comins completed an asymmetric synthesis of luciduline beginning with chiral auxiliary-containing salt **1.75** (Scheme 1.11).³⁷ Stereoselective addition of Grignard reagent **1.76** and cleavage of the chiral auxiliary and silyl group afforded **1.77**, which could be converted into dihydropyridine **1.78** in 4 steps. Reduction of the carbonyl and elimination gave diene **1.79**, which underwent intramolecular Diels-Alder cyclization upon heating at 140 °C to yield tetracycle **1.80**.

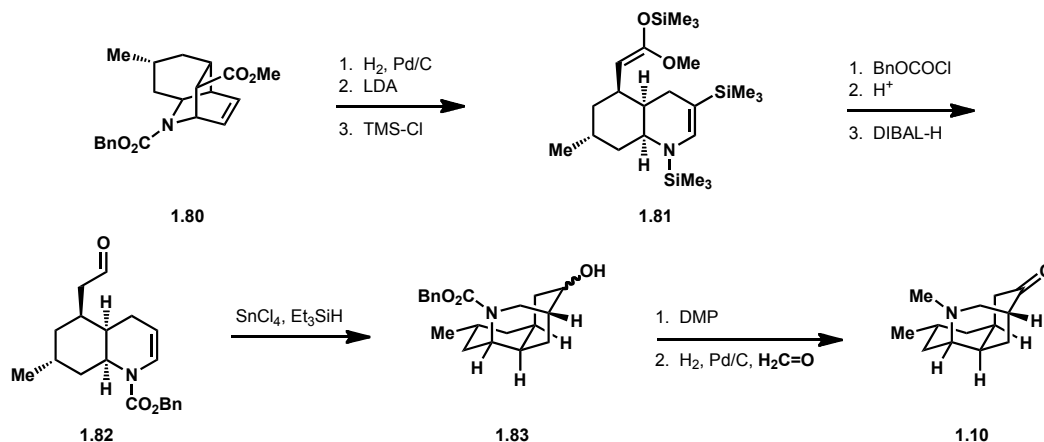
Scheme 1.11 Comins' synthesis of tetracycle **1.80**.



Tetracycle **1.80** was subjected to hydrogenation, retro-Mannich fragmentation and silyl ketene acetal formation to afford bicycle **1.81** (Scheme 1.12). Protection of the nitrogen, removal of the silyl group and DIBAL reduction gave aldehyde **1.82**. Treatment with $SnCl_4$ and Et_3SiH initiated a cationic reductive

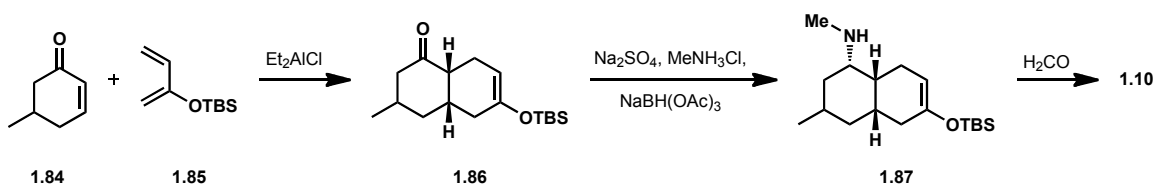
cyclization to afford tricycle **1.83**. Oxidation with DMP followed by one-pot cleavage of the carbamate functionality and reductive methylation yielded luciduline (**1.10**).

Scheme 1.12 Completion of the total synthesis of luciduline.



A fourth total synthesis of luciduline was accomplished by Cheng and Waters in 2010.³⁸ This extremely short synthesis began with a Diels-Alder reaction between enone **1.84** and diene **1.85** (Scheme 1.13). The resultant bicycle (**1.86**) was subjected to reductive amination with methylamine to give bicycle **1.87** followed by treatment with paraformaldehyde to induce a Mukaiyama-Mannich addition that afforded luciduline (**1.10**). They then went on to elaborate luciduline into nankakurines A and B, which will be discussed in section 1.6.5.

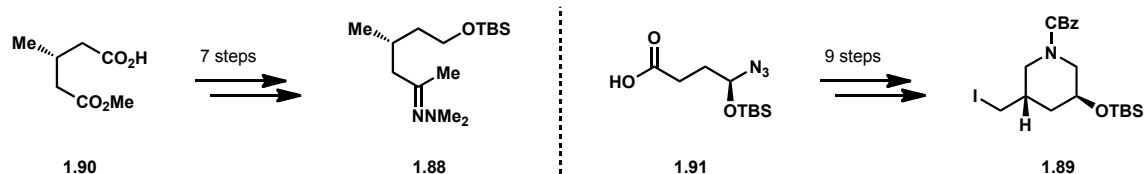
Scheme 1.13 Waters and Cheng's total synthesis of luciduline.



1.6.2 Smith's Total Synthesis of Lyconadins A and B.

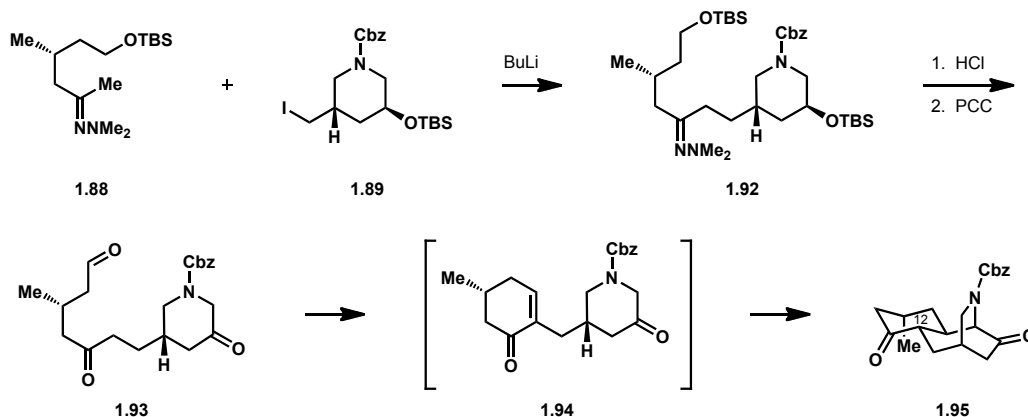
There have been two syntheses of lyconadin A (**1.6**) completed thus far. The first of these was accomplished by Smith and Beshore in 2007.^{39,40} This synthesis utilizes two fragments, hydrazone **1.88** and iodide **1.89** (Scheme 14). Hydrazone **1.88** was constructed in seven steps from (-)-methyl (R)-3-methylglutarate (**1.90**). Azide **1.91** was converted into iodide **1.89** *via* an asymmetric aldol reaction and an S_N2 cyclization in 9 steps.

Scheme 1.14 Smith and Beshore's initial stages of the synthesis of lyconadin A.



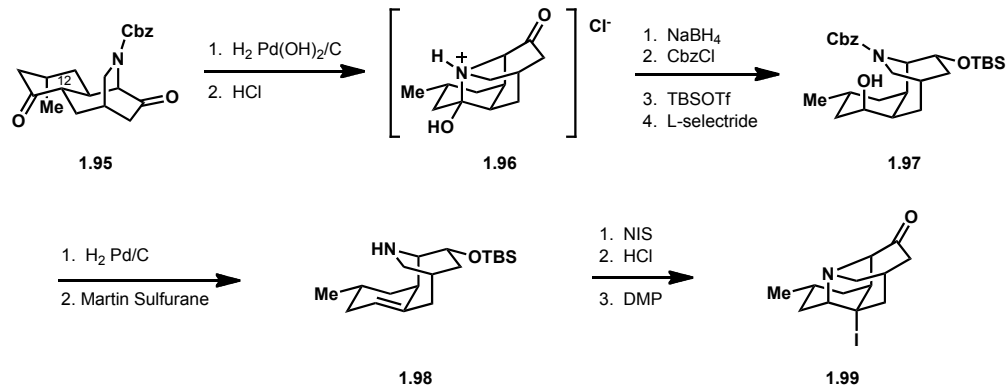
Fragments **1.88** and **1.89** were coupled through nucleophilic displacement of the iodide by the anion of **1.88** to afford hydrazone **1.92** (Scheme 1.15). Acid-mediated hydrolysis of the hydrazone and PCC oxidation afforded aldehyde **1.93**. Treatment of **1.93** with hydrochloric acid led to an aldol condensation, forming intermediate enone **1.94** followed by an *in-situ* conjugate addition to give tricyclic ketone **1.95**.

Scheme 1.15 Synthesis of key tricyclic ketone.



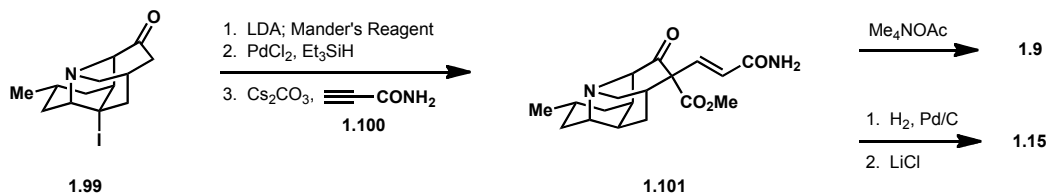
Epimerization of the C-12 stereocenter of **1.95** (see Scheme 1.16) was accomplished by hydrogenolysis to remove the Cbz group and treatment with hydrochloric acid to trap the carbonyl as hemiaminal salt **1.96**. A four-step sequence of protections and reductions furnished alcohol **1.97**. Elimination of water with Martin sulfurane and removal of the Cbz group gave alkene **1.98**. Iodoamination was accomplished by treatment with NIS, and this was followed by removal of the silyl group and oxidation to afford tetracycle **1.99**.

Scheme 1.16 Synthesis of tetracyclic lyconadin core.



Tetracycle **1.99** could be elaborated into both lyconadin A (**1.9**) and lyconadin B (**1.15**, Scheme 1.17). This was accomplished by acylation of **1.99** with Mander's reagent followed by reductive removal of the iodide and Michael addition into propiolamide (**1.100**) to give alkene **1.101**. Alkene **1.101** was then treated with Me_4NOAc to achieve a one-pot decarboxylation, olefin isomerization and condensation that gave lyconadin A (**1.9**). Lyconadin B (**1.15**) was accessed by initial hydrogenation of the alkene functionality of **1.101**, then treatment with LiCl to achieve a similar decarboxylation and cyclization. This synthesis furnished lyconadins A and B in 28 and 29 steps, respectively.

Scheme 1.17 Completion of lyconadins A and B.



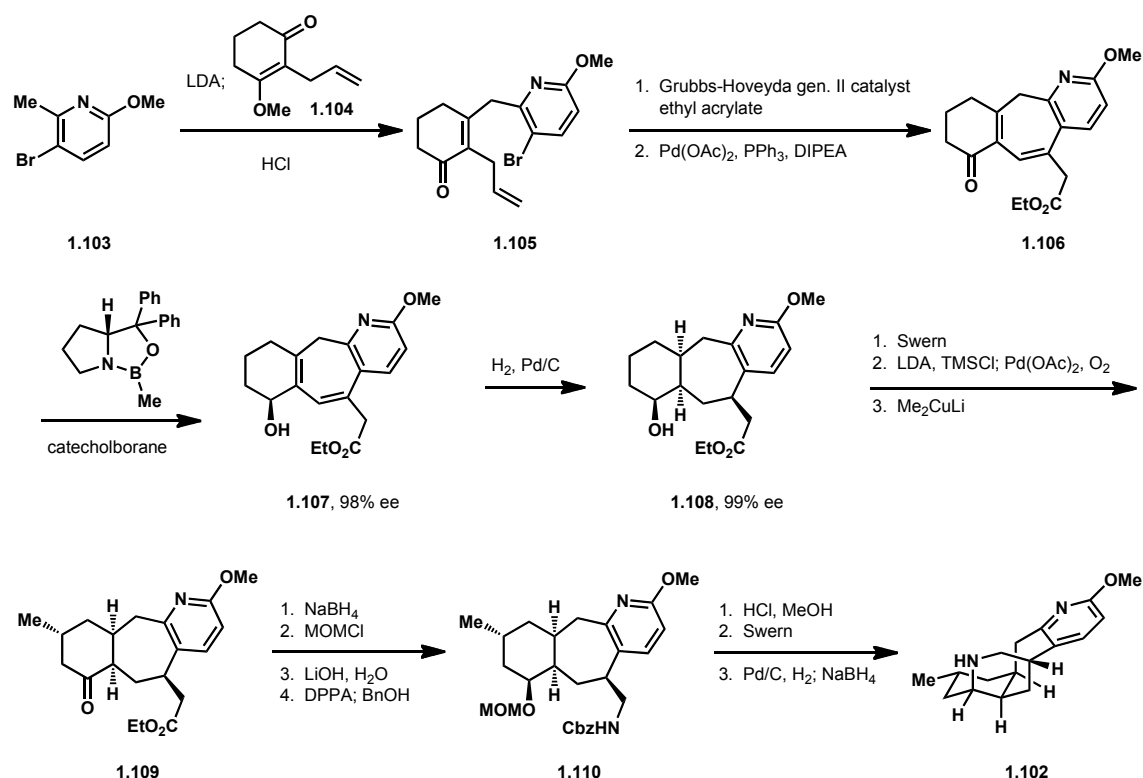
1.6.3 Sarpong's Total Synthesis of Lyconadin A

A second asymmetric synthesis of lyconadin A has been published by the Sarpong research group.^{41,42} This synthesis began with the construction of tetracycle **1.102** as shown in Scheme 1.18. Initial deprotonation of **1.103** with LDA followed by addition to vinylogous ester **1.104** and subsequent hydrolysis with dilute acid produced enone **1.105**. Cross metathesis of the allyl group with ethyl acrylate was accomplished with the Grubbs-Hoveyda second generation catalyst. Subsequent Heck reaction proceeded in excellent yield with concomitant isomerization of the exocyclic olefin into the seven-membered ring to form cycloheptadiene **1.106**.

Enantioselectivity was conferred by a Corey-Bakshi-Shibata (CBS) reduction^{43,44,45} of the carbonyl of **1.106** to afford alcohol **1.107** in high yield and 98% e.e. Hydrogenation with Pd/C gave 8:1 selectivity for alcohol **1.108**, which

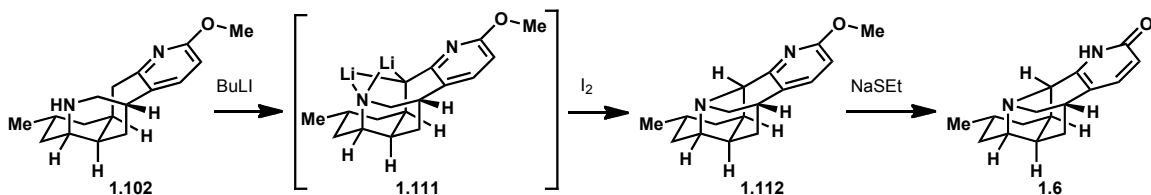
could be recrystallized to afford **1.108** as a single diastereomer in 60% yield and 99% e.e. Swern oxidation was followed by a Saegusa-Ito oxidation sequence and addition of the Gilman reagent to install the critical C-15 methyl group with the correct stereochemistry (**1.109**). The carbonyl of **1.109** was then reduced with NaBH₄ and protected as a MOM ether. Hydrolysis of the ethyl ester and subsequent Curtius rearrangement in the presence of benzyl alcohol provided Cbz-protected amine **1.110**. Removal of the MOM protecting group, Swern oxidation and hydrogenolysis of the Cbz group set the stage for a NaBH₄-mediated reductive amination to close the final bond of tetracycle **1.102**.

Scheme 1.18 Synthesis of tetracycle **1.102**.



The key final C-N bond was closed by treatment of tetracycle **1.102** with two equivalents of BuLi to form dianion **1.111** (Scheme 1.19), which was then oxidized with iodine to afford pentacycle **1.112**. Finally, NaSEt was used to cleave the methyl ether and reveal lyconadin A (**1.6**). This synthesis was accomplished in 17 steps.

Scheme 1.19 Oxidative C-N bond formation and completion of lyconadin A.

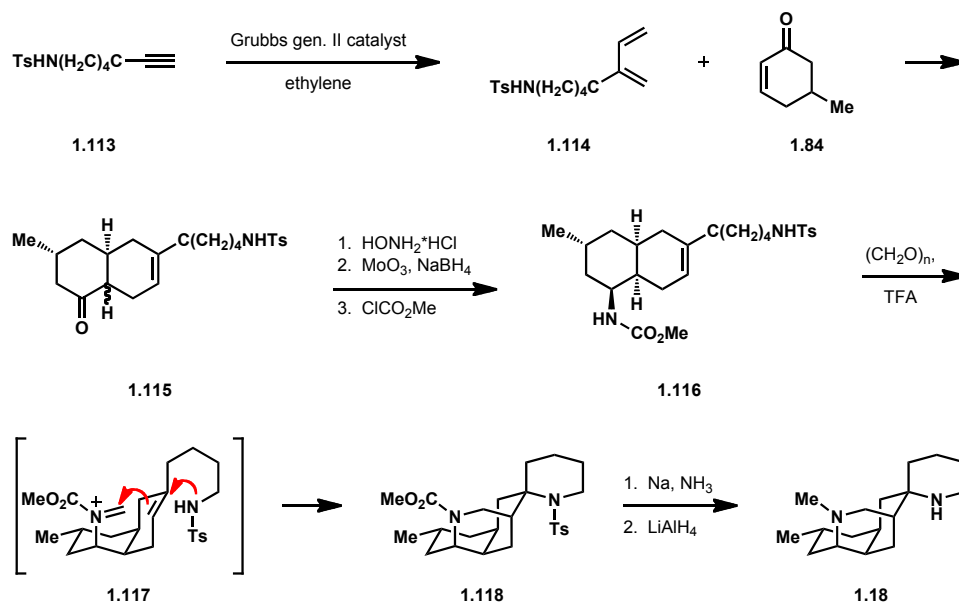


1.6.4 Overman's Total Synthesis of Nankakurines A and B.

The first total synthesis of nankakurines A and B was accomplished by Overman in 2008.²⁰ He constructed both the originally-proposed structure and the revised structure and demonstrated that the revised structure is correct.

The synthesis of the proposed structure of nankakurine A began with enyne metathesis of *N*-tosylalkyne **1.113** (Scheme 1.20) to afford diene **1.114**. Diels-Alder reaction between **1.114** and enone **1.84** afforded bicycle **1.115** as an incidental mixture of diastereomers at the alpha position. Reductive amination was accomplished by treatment with hydroxylamine, then MoO₃ in the presence of NaBH₄. The resultant amine functionality was protected as a methyl carbamate to give **1.116**. Treatment of **1.116** with paraformaldehyde and TFA led to the formation of intermediate iminium ion **1.117**, which underwent the key *N*-terminated aza-Prins cyclization to afford tetracycle **1.118**. Cleavage of the tosyl group and reduction of the carbamate to give the desired *N*-methyl substituent gave rise to the originally-proposed structure of nankakurine A (**1.18**). The ¹H and ¹³C NMR data of this compound were significantly different from that of the natural product; thus, it was surmised that this was not the correct structure of the alkaloid.

Scheme 1.20 Synthesis of the original structure of nankakurine A.

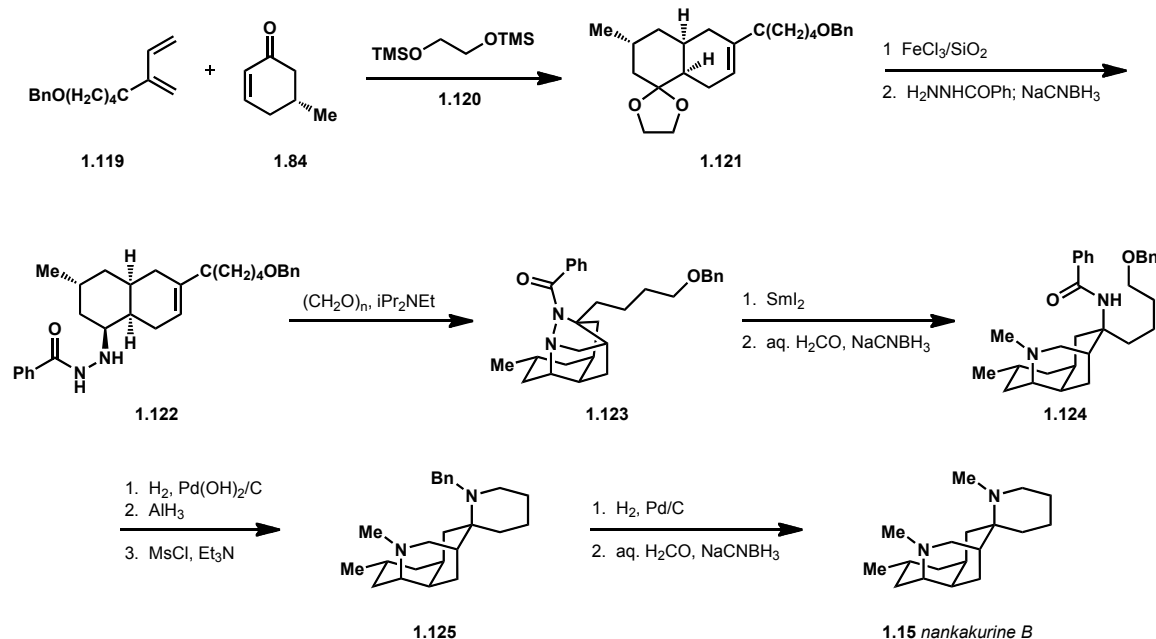


Consequently, the revised structures of nankakurines A and B were synthesized asymmetrically through an analogous route (Scheme 1.21). The *N*-tosyl group was replaced with an OBn group (**1.119**) and enantioenriched enone **1.84** was employed. The Diels-Alder reaction between **1.119** and **1.84** was run in the presence of the bis-TMS ether of ethylene glycol (**1.120**) to trap the product of the reaction as acetal **1.121** in order to avoid epimerization of the stereocenter alpha to the carbonyl. Removal of the ketal was followed by reductive amination with H₂NNHCOPh to afford bicycle **1.122**. Treatment with paraformaldehyde and an

amine base promoted an azomethine imine cycloaddition reaction to give caged structure **1.123**.

Cleavage of the N-N bond of **1.123** was accomplished with SmI_2 and followed by reductive amination with aqueous formaldehyde to give **1.124**. A three-step sequence was employed to convert the benzoyl protecting group into a benzyl group and swap the OBn for an OMs group, which allowed the final ring of nankakurine A to be closed through an $\text{S}_{\text{N}}2$ displacement to afford **1.125**. The benzyl group was removed through hydrogenolysis to afford nankakurine A, which could be converted to nankakurine B (**1.15**) through reductive amination with formaldehyde.

Scheme 1.21 Synthesis of revised structure of nankakurine A and nankakurine B.



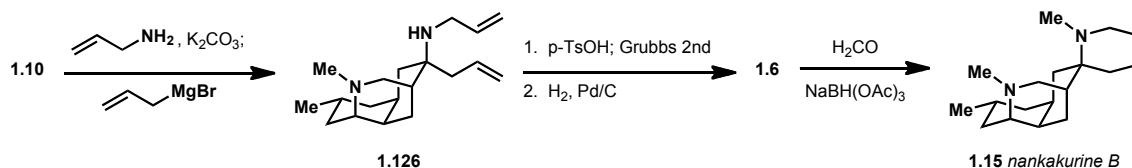
Spectral data for both nankakurines A and B were found to be consistent with that reported for the natural products, confirming these as the correct structures. The syntheses of nankakurines A and B were completed in 13 and 14 steps, in 20% and 16% overall yield, respectively. This synthesis also served to unambiguously confirm the stereochemistry of these two natural products.

1.6.5 Waters and Cheng's Synthesis of Nankakurines A and B.

Waters and Cheng completed a racemic total synthesis of nankakurines A that stemmed from luciduline (**1.10**, see Scheme 1.12).³⁸ Luciduline was synthesized in three steps, as discussed in Section 1.6.1. Stereoselective aminoallylation was accomplished by treating luciduline with allylamine (see Scheme 1.22) then allyl Grignard to afford amine **1.126**. The spirocyclic ring of nankakurine A was formed through ring closing metathesis of **1.126** using Grubbs second generation catalyst. Hydrogenation of the resultant double bond afforded

nankakurine A (**1.6**). Nankakurine A could be converted into nankakurine B (**1.20**) through reductive amination with aqueous formaldehyde and sodium triacetoxyborohydride.

Scheme 1.22 Completion of nankakurines A and B.

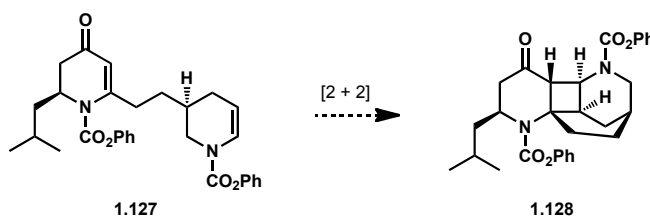


The total synthesis of nankakurines A and B was achieved in 6 and 7 steps respectively in a sequence that employs no protecting groups.

1.6.6 Model Study of Spirolucidine.

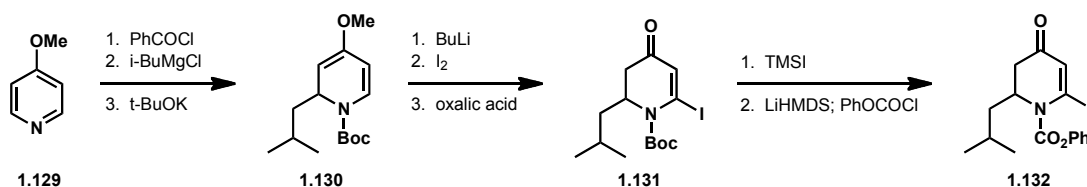
One model study directed toward spirolucidine has been published by Comins and Williams.⁴⁶ In this study, simplified substrate **1.127** (Scheme 1.23) was chosen as a model for a spirolucidine precursor. This approach employed a [2+2] photocycloaddition to form cyclobutane **1.128** as a strategy for setting the spiro center in a stereocontrolled fashion.

Scheme 1.23 Model study of spirolucidine.



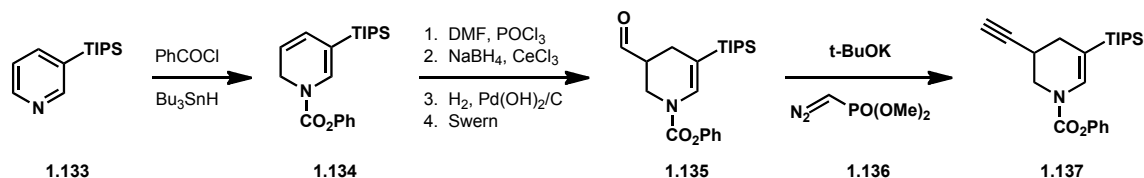
Synthesis of the left half of this substrate commenced with 4-methoxypyridine (**1.129**, Scheme 1.24). Quaternization of the nitrogen followed by addition of isobutyl Grignard and conversion of the *N*-acyl group to a Boc group afforded dihydropyridine **1.130**. Directed lithiation, quenching with iodine and hydrolysis of the methyl enol ether afforded iodide **1.131**. A two-step sequence was employed to exchange the Boc protecting group for a Cbz group, yielding dihydropyridine **1.132**.

Scheme 1.24. Synthesis of spirolucidine model system.



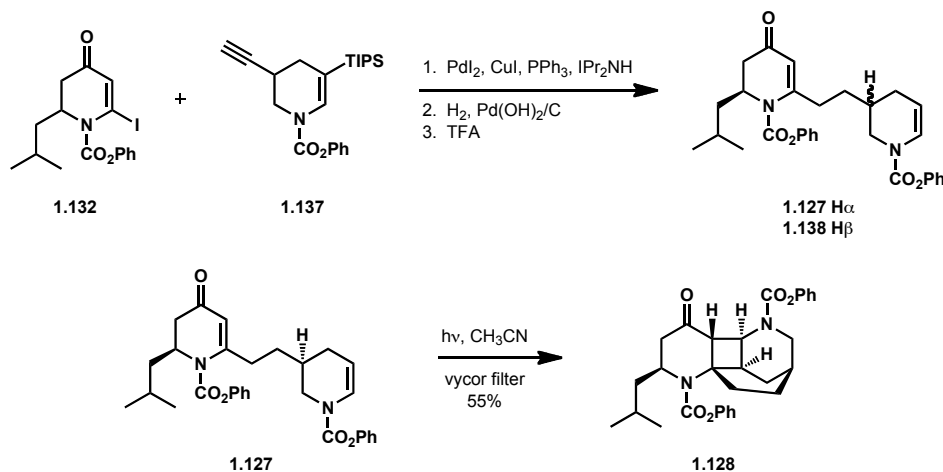
To construct the right-hand fragment, TIPS-substituted pyridine **1.133** (Scheme 1.25) was regioselectively reduced with PhOCOCl and Bu₃SnH to afford dihydropyridine **1.134**. Treatment of **1.134** with the Vilsmeier-Haack reagent was followed by reduction of the aldehyde functionality, selective hydrogenation of one double bond and reoxidation under Swern conditions to give **1.135**. The aldehyde was converted into the corresponding alkyne by treatment with the Gilbert-Seyferth reagent (**1.136**), yielding alkyne **1.137**.

Scheme 1.25 Synthesis of alkyne portion of spiroLucidine model substrate.



Iodide **1.132** (Scheme 1.26) and alkyne **1.137** were joined through a Sonogashira reaction, which was followed by hydrogenation of the alkyne functionality and removal of the TIPS group to give a 1:1 mixture of dihydropyridines **1.127** and **1.138**. Irradiation of **1.127** using a Vycor filter (>210 nm) afforded the desired cyclobutane **1.128** in 55% yield. The opening of the cyclobutane ring was not investigated in this model study, and there has been no follow-up publication to date.

Scheme 1.26. Completion of spiroLucidine model.



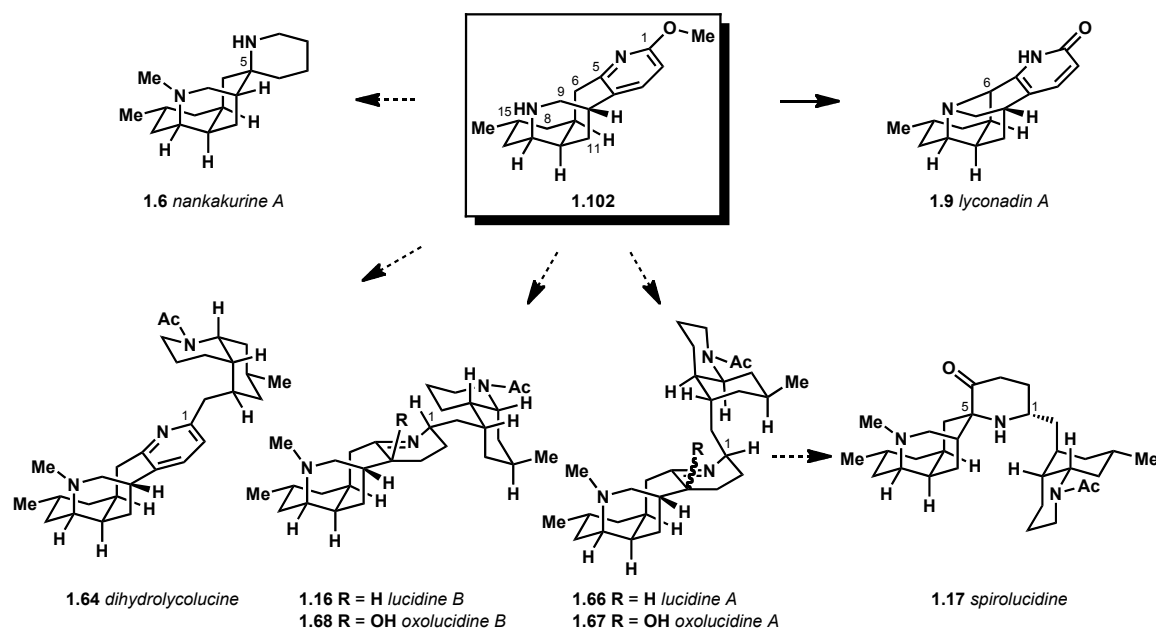
1.7 A Unified Approach to Miscellaneous *Lycopodium* Alkaloids

Our research group has an ongoing synthetic interest in the miscellaneous class of *Lycopodium* alkaloids. We envisioned developing a unified approach to this group of natural products in which various alkaloids could be accessed from a common intermediate. Tetracyclic amine **1.102** (Scheme 1.27) might serve as an

ideal platform for elaboration into multiple natural products. Our lab has already demonstrated that oxidative formation of a C-N bond between the nitrogen and the pseudo-benzylic carbon of **1.102** can give rise to lyconadin A (**1.9**).^{41,42} We imagined that the same tetracycle could be transformed into nankakurine A (**1.6**) through a ring contraction that would install the C-5 spiro center.

We also anticipated that the methyl ether at C-1 of the pyridine of **1.102** could serve as a functional handle to append an additional bicyclic portion to the molecule, which could furnish dihydrolycolucine (**1.64**) and lucidines A (**1.66**) and B (**1.16**). Lucidines A and B are known to undergo facile oxidation to the corresponding oxolucidines (**1.67** and **1.68**) upon exposure to atmospheric oxygen, which would enable us to access those natural products as well. We were intrigued by the possibility of exploring the conversion of oxolucidine A to spirolycolucine (**1.17**), a synthetic transformation that mimics the proposed biogenesis of the molecule.

Scheme 1.27 A unified approach to miscellaneous *Lycopodium* alkaloids.



1.8 References

- Ma, X. Q.; Tan, C. H.; Zhu, D. Y.; Gang, D. R.; Xiao, P. G. *Journal Of Ethnopharmacology* **2007**, *113*, 15.
- Ayer, W. A.; Trifonov, L. S. *Alkaloids (Academic Press)* **1994**, *45*, 233.
- Kobayashi, J.; Morita, H. *Alkaloids (Academic Press)* **2005**, *61*, 1.
- Hirasawa, Y.; Kobayashi, J.; Morita, H. *Heterocycles* **2009**, *77*, 679.
- Bödeker, K. *Justus Liebigs Ann. Chem.*, **1881**, *208*, 363.
- Achmatowicz, O.; Uzieblo, W. *Rocz. Chem.*, **1938**, *18*, 89 (94 in English).
- Ma, X.; Gang, R. *Nat. Prod. Rep.* **2004**, *21*, 752.

-
- ⁸ Ayer, W. A.; Berezows, J.; Law, D. A. *Can. J. Chem.* **1963**, *41*, 649.
- ⁹ Ayer, W. A.; Browne, L. M.; Nakahara, Y.; Tori, M.; Delbaere, L. T. J. *Can. J. Chem.* **1979**, *57*, 1105.
- ¹⁰ Kubota, T.; Yahata, H.; Yamamoto, S.; Hayashi, S.; Shibata, T.; Kobayashi, J. *Bioorg. Med. Chem. Lett.* **2009**, *19*, 3577.
- ¹¹ Morita, H.; Hirasawa, Y.; Shinzato, T.; Kobayashi, J. *Tetrahedron* **2004**, *60*, 7015.
- ¹² Yuan, S.; Zhao, Y.; Feng, R. *Junshi Yixue Kexueyuan Yuankan* **2001**, *25*, 57.
- ¹³ Morita, H.; Hirasawa, Y.; Yoshida, N.; Kobayashi, J. *Tetrahedron Lett.* **2001**, *42*, 4199.
- ¹⁴ Kobayashi, J.; Hirasawa, Y.; Yoshida, N.; Morita, H. *J. Org. Chem.* **2001**, *66*, 5901.
- ¹⁵ Ishiuchi, K. I.; Kubota, T.; Hoshino, T.; Obara, Y.; Nakahata, N.; Kobayashi, J. *Bioorg. Med. Chem.* **2006**, *14*, 5995.
- ¹⁶ Ayer, W. A.; Masaki, N.; Nkunika, D. S. *Can. J. Chem.* **1968**, *46*, 363.
- ¹⁷ Ayer, W. A.; Ball, L. F.; Browne, L. M.; Tori, M.; Delbaere, L. T. J.; Silverberg, A. *Can. J. Chem.* **1984**, *62*, 298.
- ¹⁸ Hirasawa, Y.; Morita, H.; Kobayashi, J. *Org. Lett.* **2004**, *6*, 3389.
- ¹⁹ Hirasawa, Y.; Kobayashi, J.; Obara, Y.; Nakahata, N.; Kawahara, N.; Goda, Y.; Morita, H. *Heterocycles* **2006**, *68*, 2357.
- ²⁰ Nilsson, B. L.; Overman, L. E.; Alaniz, J. R.; Rohde, J. M. *J. Am. Chem. Soc.* **2008**, *130*, 11297.
- ²¹ Ma, X. Q.; Gang, D. R. *Phytochemistry* **2008**, *69*, 2022.
- ²² Hemscheidt, T.; Spenser, I. D. *J. Am. Chem. Soc.* **1996**, *118*, 1799.
- ²³ Gupta, R. N.; Castillo, M.; Maclean, D. B.; Spenser, I. D.; Wrobel, J. T. *J. Am. Chem. Soc.* **1968**, *90*, 1360.
- ²⁴ Castillo, M.; Gupta, R. N.; Ho, Y. K.; MacLean, D. B.; Spenser, I. D. *Can. J. Chem.* **1970**, *48*, 2911.
- ²⁵ Castillo, M.; Gupta, R. N.; MacLean, D. B.; Spenser, I. D. *Can. J. Chem.* **1970**, *48*, 1893.
- ²⁶ Hemscheidt, T. *Top. Curr. Chem.* **2000**, *209*, 175.
- ²⁷ Katakawa, K.; Kitajima, M.; Yamaguchi, K.; Takayama, H. *Heterocycles*, **2006**, *69*, 223.
- ²⁸ Shigeyama, T.; Katakawa, K.; Kogure, N.; Kitajima, M.; Takayama, H. *Org. Lett.* **2007**, *9*, 4069.
- ²⁹ Tori, M.; Shimoji, T.; Shimura, E.; Takaoka, S.; Nakashima, K.; Sono, M.; Ayer, W. *Phytochemistry* **2000**, *53*, 503.
- ³⁰ Snider, B. B.; Grabowski, J. F. *J. Org. Chem.* **2007**, *72*, 1039.
- ³¹ Cui, L.; Peng, Y.; Zhang, L. *J. Am. Chem. Soc.* **2009**, *131*, 8394.
- ³² Shigeyama, T.; Katakawa, K.; Kogure, N.; Kitajima, M.; Takayama, H. *Org. Lett.* **2007**, *20*, 4069.
- ³³ Tanaka T.; Kogure, N.; Kitajima, M.; Takayama, H. *J. Org. Chem.* **2009**, *74*, 8675.
- ³⁴ Nishikawa, Y.; Kitajima, M.; Takayama, H. *Org. Lett.* **2008**, *10*, 1987.
- ³⁵ Scott, W. L.; Evans, D. A. *J. Am. Chem. Soc.* **1972**, *94*, 4779.
- ³⁶ Oppolzer, W.; Petrzilka, M. *Helv. Chim. Acta* **1978**, *61*, 2755.
- ³⁷ Comins, D. L.; Brooks, C. A.; Al-awar, R. S.; Goehring, R. R. *Org. Lett.* **1999**, *1*, 229.
- ³⁸ Cheng, X.; Waters, S. P. *Org. Lett.* **2010**, *12*, 205.
- ³⁹ Beshore, D. C.; Smith, A. B., III *J. Am. Chem. Soc.* **2007**, *129*, 4148.

-
- ⁴⁰ Beshore, D. C.; Smith, A. B., III *J. Am. Chem. Soc.* **2008**, *130*, 13778.
- ⁴¹ Bisai, A.; West, S. P.; Sarpong, R. *J. Am. Chem. Soc.* **2008**, *130*, 7222.
- ⁴² West, S. P.; Bisai, A.; Lim, A. D.; Narayan, R. R.; Sarpong R. *J. Am. Chem. Soc.* **2009**, *131*, 11187.
- ⁴³ Corey, E. J.; Bakshi, R. K. *Tetrahedron Lett.* **1990**, *31*, 611–614.
- ⁴⁴ Corey, E. J.; Bakshi, R. K.; Shibata, S. *J. Am. Chem. Soc.* **1987**, *109*, 5551–5553.
- ⁴⁵ Corey, E. J.; Bakshi, R. K.; Shibata, S.; Chen, C. P.; Singh, V. K. *J. Am. Chem. Soc.* **1987**, *109*, 7925–7926.
- ⁴⁶ Comins, D. L.; Williams, A. L. *Org. Lett.* **2001**, *3*, 3217.

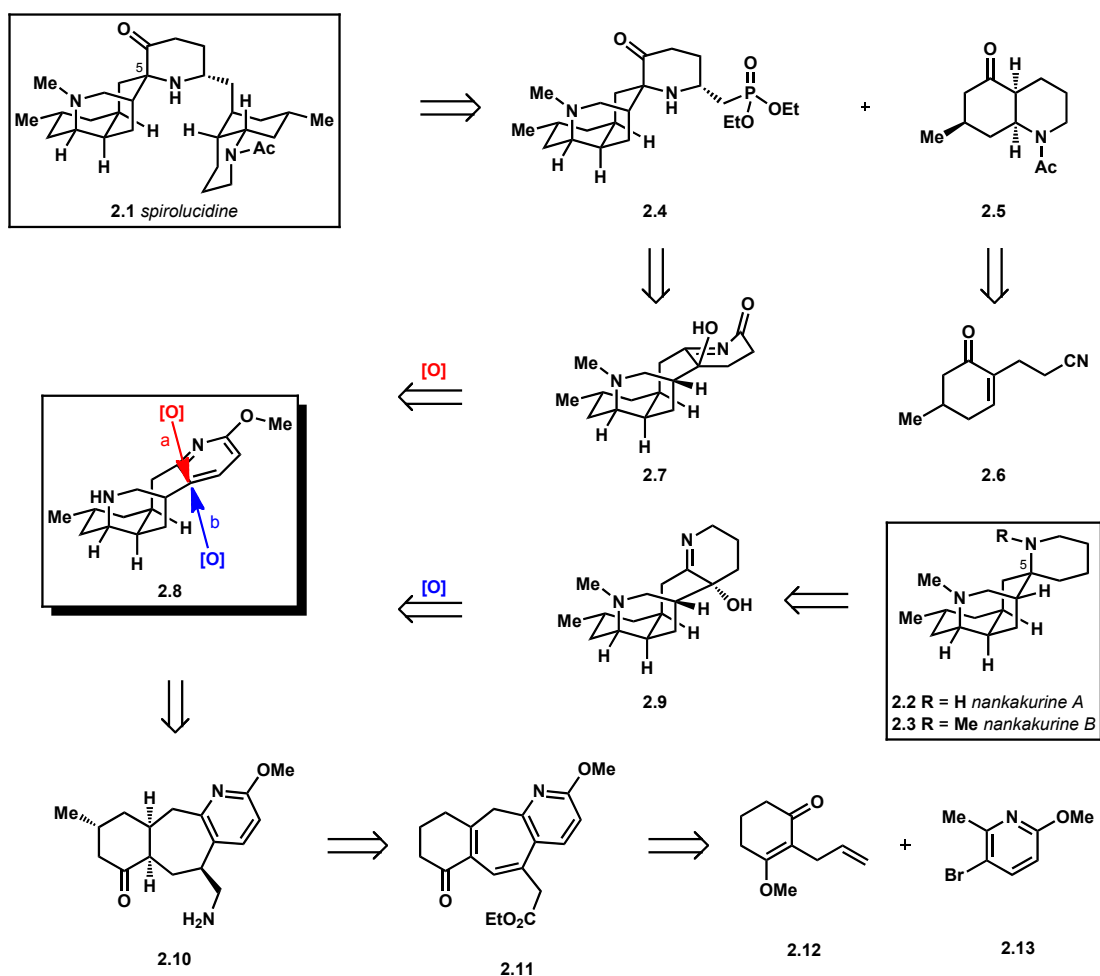
Chapter Two

Toward the Total Synthesis of Spirolucidine and Nankakurines A and B

2.1 Retrosynthetic Analysis of Spirolucidine and Nankakurine A

Spirolucidine (**2.1**, Scheme 2.1) and nankakurines A and B (**2.2** and **2.3**) were chosen as initial targets to demonstrate the generality of our unified approach to miscellaneous *Lycopodium* alkaloids. Spirolucidine was envisioned to arise from a late-stage Horner-Wadsworth-Emmons reaction between tetracyclic phosphonate **2.4** and bicyclic ketone **2.5**. Bicycle **2.5** could be generated from nitrile **2.6**, a known compound.¹ Spirocycle **2.4** would be derived from tetracycle **2.7** through a ring-contractive α -hydroxyimine rearrangement. Tetracycle **2.7** could arise from tetracyclic amine **2.8** through an oxidation event occurring from the β -face of the pyridine (Path a).

Scheme 2.1 Retrosynthesis of nankakurine A and spirolucidine.



Nankakurine A (**2.2**) could arise from an analogous α -hydroxyimine rearrangement of tetracyclic alcohol **2.9**. Alcohol **2.9** would be derived from the common tetracyclic intermediate (**2.8**) through an oxidation event on the α -face of the pyridine ring (Path b).

Tetracycle **2.8** was previously synthesized by our group *en route* to lyconadin A.^{2,3} It arises from an intramolecular reductive amination of tricyclic aminoketone **2.10**, which in turn is derived from ester **2.11**. The ultimate starting materials for this synthesis are vinylogous ester **2.12** and bromomethoxypicoline **2.13**.

The α -hydroxyimine rearrangement is known to be stereospecific;⁴ therefore, controlling the stereochemistry of the oxidation of tetracycle **2.8** should allow us to control the configuration of the C-5 spiro center. This would enable us to selectively synthesize nankakurine A or spirolicidine. This system presented an opportunity to explore the inherent facial selectivity of tetracycle **2.8** towards oxidation, as well as an opportunity to investigate reagent-controlled methods of accessing the disfavored stereoisomer in order to ultimately synthesize both natural products.

2.2 Synthesis of a Tetracyclic Common Intermediate

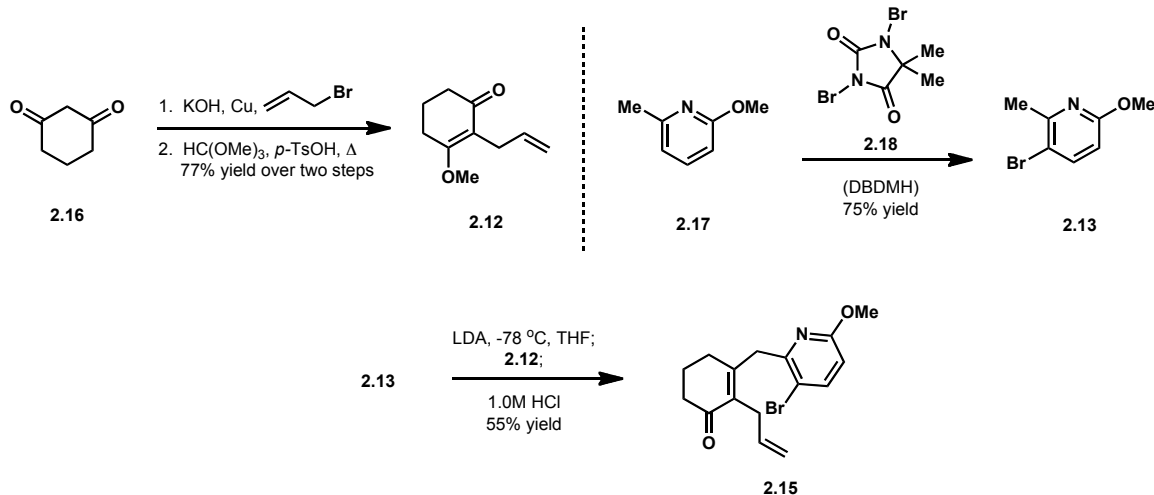
For our initial investigations into the oxidation reactivity of tetracycle **2.8**, we chose to use amine **2.14** (Figure 2.1), which does not bear the C-15 methyl group, as a model system. Installation of the methyl group adds three steps to the synthetic sequence, and we anticipated that its absence would not significantly affect the reactivity of the system. The synthesis of tetracycle **2.14** was carried out largely according to a route developed by Scott West and Alakesh Bisai in our research group during the course of their studies on lyconadin A.^{2,3}

Figure 2.1 Model substrate for tetracycle **2.8**.



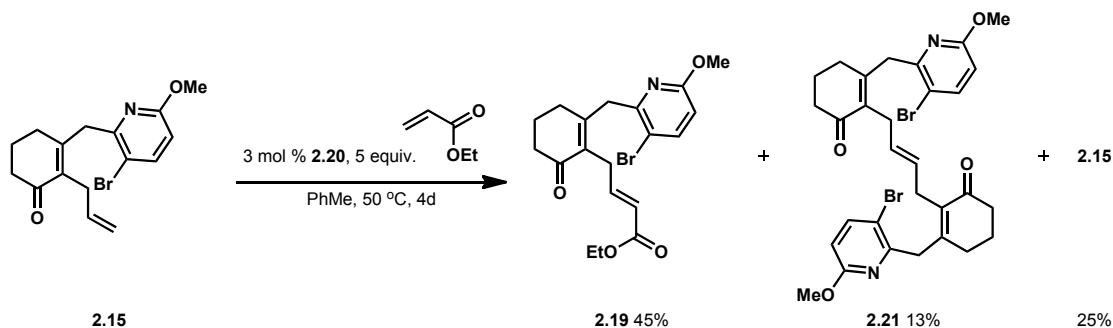
The synthesis commenced with the generation of enone **2.15** (Scheme 2.2). Allylation of 1,3-cyclohexanedione (**2.16**) was followed by treatment with trimethylorthoformate to afford vinylogous ester **2.12** in 77% yield over 2 steps. Bromomethoxypicoline **2.13** was generated from methoxypicoline **2.17** via treatment with the mild brominating agent 1,3-dibromo-5,5-dimethylhydantoin (DBDMH, **2.18**) for 48 h. Deprotonation of **2.13** was accomplished by treatment with LDA. The resultant anion was treated with vinylogous ester **2.12**, then dilute HCl to afford enone **2.15**.

Scheme 2.2 Synthesis of enone 2.15.



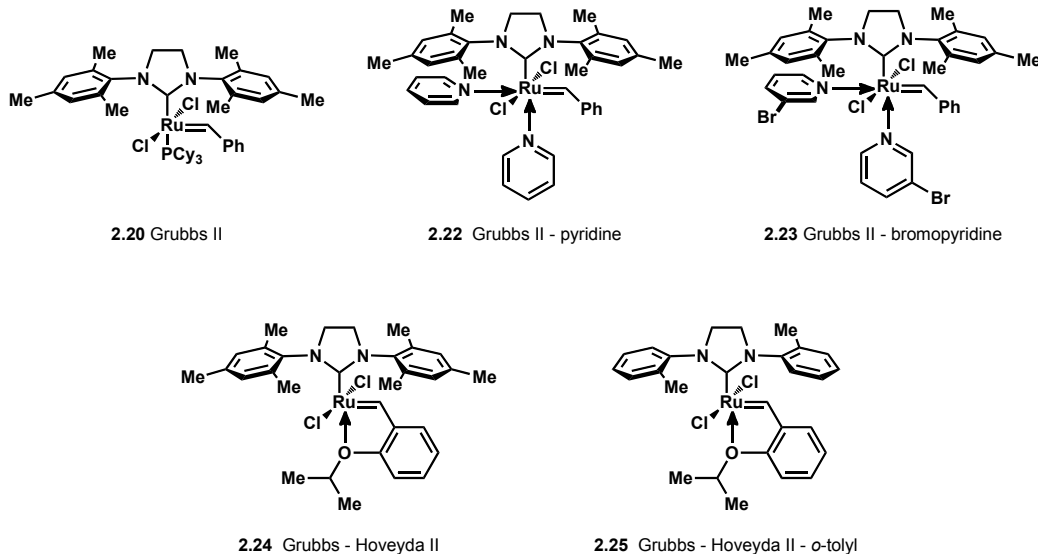
The next step in the synthetic sequence was conversion of enone **2.15** to ester **2.19** via cross metathesis (Scheme 2.3). This reaction was initially run with Grubbs second generation cross metathesis catalyst (**2.20**, Figure 2.2), but suffered from low conversion to product and formation of a significant amount of homodimerized product **2.21**. The desired product (**2.19**) was obtained in a modest 45% yield. Homodimer **2.21** was found to be a competent reaction partner and can be converted to ester **2.19**. However, this reaction proceeded much more slowly than the reaction of **2.19**. Therefore, we wished to minimize the formation of **2.21** while maximizing the conversion of starting material to **2.19**.

Scheme 2.3 Cross metathesis of enone 2.15.



Several cross metathesis catalysts, solvents and temperatures were screened to find conditions that would accomplish this goal with minimal catalyst loading (Table 2.1). Reactions were run at 0.1M to avoid excessive homodimerization. The yield improved to 53% when the reaction was run at room temperature (entry 2). This was presumed to occur because the lower temperature slowed the rate of catalyst decomposition. No improvement in yield was observed by changing the catalyst to Grubbs II-pyridine (**2.22**, entry 3) or Grubbs II bromopyridine (**2.23**, entry 4).

Figure 2.2 Cross Metathesis Catalysts



The Grubbs-Hoveyda second generation catalyst **2.24** offered a marked improvement in yield, affording 88% of the desired product (entry 5). Neither increasing the temperature to 60 °C nor switching the solvent to DCM and running the reaction at 40 °C offered any improvement in yield (entries 6 and 7). Employing the *o*-tolyl Grubbs-Hoveyda II catalyst (**2.25**) also offered a similar yield (entry 8). It was found that when 10 equivalents of ethyl acrylate were used, the catalyst loading of **2.25** could be decreased to 2 mol% without a decrease in yield (entry 9).

Table 2.1 Optimization of cross-metathesis conditions.

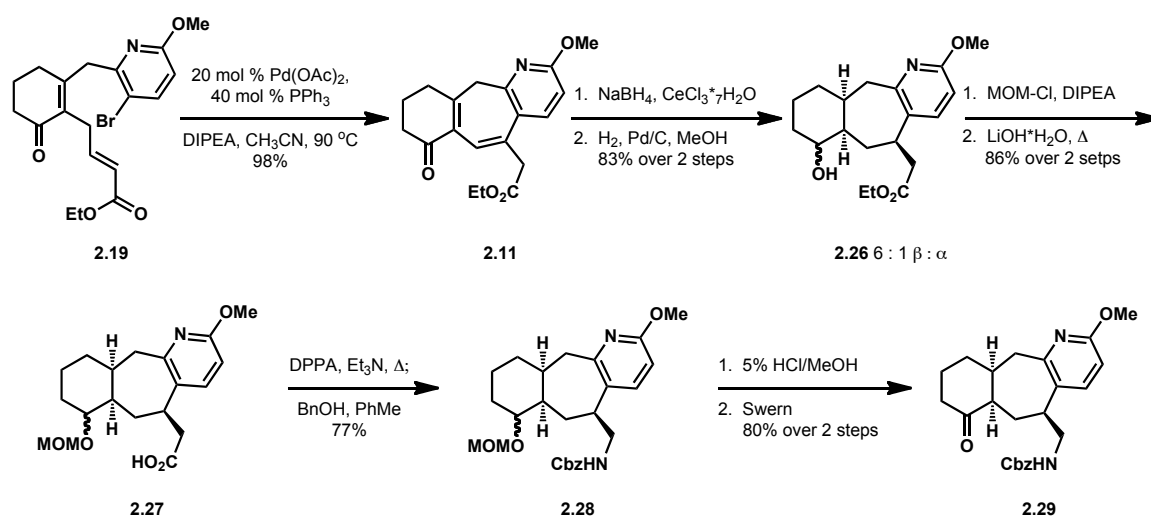


Entry	Catalyst	Cat. loading (mol %)	Equiv. ethyl acrylate	Solvent	Temp. (°C)	Yield (%)	Recovered s.m. (%)	Homodimer (%)
1	2.20	3	5	PhH	50	45	25	13
2	2.20	3	5	PhH	r.t.	53	28	11
3	2.22	3	5	PhH	r.t.	45	26	10
4	2.23	3	5	PhH	r.t.	44	31	19
5	2.24	3	5	PhH	r.t.	88	—	trace
6	2.24	3	10	DCM	40	83	—	trace
7	2.24	3	10	PhH	60	87	—	trace
8	2.25	3	10	PhH	60	85	—	trace
9	2.25	2	10	PhH	r.t.	86	—	trace

With optimal conditions for the cross metathesis reaction identified, we proceeded with the synthesis of **2.14** according to the previously developed route (Scheme 2.4). Ester **2.19** was subjected to an intramolecular Heck reaction that proceeded with concomitant migration of the exocyclic olefin into conjugation to afford **2.11** in 98% yield. Luche reduction followed by hydrogenation gave alcohol **2.26** as a 6:1 mixture of diastereomers at the carbon bearing the hydroxyl, with the β -OH stereoisomer predominating. This diastereomeric mixture was of no consequence in the overall synthesis, since this stereocenter was destroyed several steps later.

Alcohol **2.26** was protected as a MOM acetal, and the ester functionality was saponified by heating in the presence of lithium hydroxide to afford acid **2.27**. A Curtius rearrangement was achieved by heating the acid in the presence of DPPA, then benzyl alcohol to afford Cbz-protected amine **2.28**. The MOM acetal was removed by treatment with dilute HCl in methanol, and Swern oxidation yielded tricyclic ketone **2.29**.

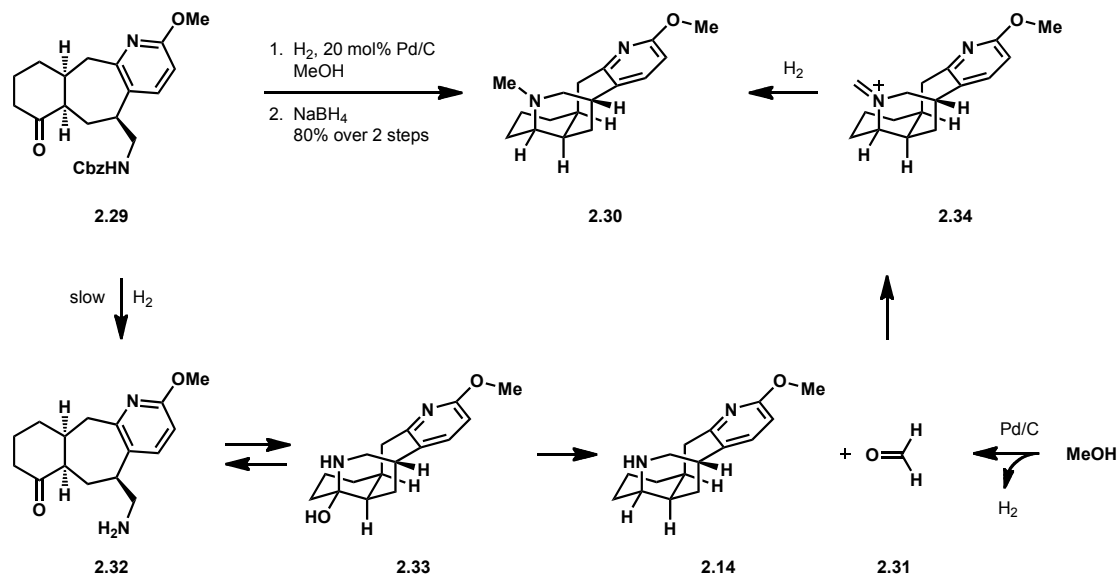
Scheme 2.4 Synthesis of ketone **2.29**.



Ketone **2.29** was subjected to hydrogenolysis over palladium on carbon in methanol to cleave the Cbz protecting group (Scheme 2.5). The crude material was treated with NaBH₄ to complete an intramolecular reductive amination. To our surprise, the product we obtained from this reaction was *N*-methylated tetracycle **2.30**. This was presumed to occur via a transfer hydrogenation process in which some of the methanol was converted into formaldehyde (**2.31**). Cleavage of the Cbz group of **2.29** gives rise to an equilibrium mixture of aminoketone **2.32** and hemiaminal **2.33**. Hemiaminal **2.33** could undergo the desired intramolecular reductive amination to afford tetracycle **2.14**. Tetracycle **2.14** then presumably underwent a condensation with formaldehyde to give rise to iminium ion **2.34**, which was reduced *in situ* to afford *N*-methylated tetracycle **2.30**. This methylation process was found to be competitive with the hydrogenolysis of the Cbz group,

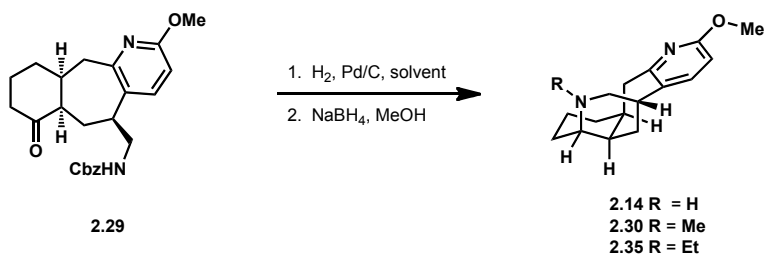
generating significant amounts of tetracycle **2.30** before the starting material was fully consumed.

Scheme 2.5 Formation of *N*-methylated tetracycle **2.30**.



Although the natural products nankakurine A, nankakurine B and spirolucidine all bear an *N*-methyl group, we were concerned about installing it at this stage. We anticipated that it would be necessary to protect the nitrogen with an electron-withdrawing group to avoid undesired reactivity of the amine during oxidative chemistry we planned to employ during the late stages of the synthesis. Therefore we sought conditions in which this adventitious methylation would be minimized or suppressed entirely.

We found that increasing the catalyst loading to 50 weight % and decreasing the reaction time to two hours favored the formation of the desired product, affording **2.14** and **2.30** in a 5:1 ratio after reductive amination (Table 2.2, entry 2). Increasing the catalyst loading further to 100 mol% and decreasing the reaction time to 1h did not offer further improvement, and instead gave a mixture of desired product **2.14**, *N*-methylated product **2.30** and starting material (entry 3). Changing the solvent to ethanol brought the ratio of **2.14** to ethylated product **2.35** up to 9:1. The reaction yielded only starting material if run in THF (entry 5), but utilizing EtOAc as the solvent gave complete conversion to tetracycle **2.14** without any formation of side products (entry 6). These optimized conditions of 50 mol% catalyst in ethyl acetate allowed us to obtain multigram quantities of tetracycle **2.14**.

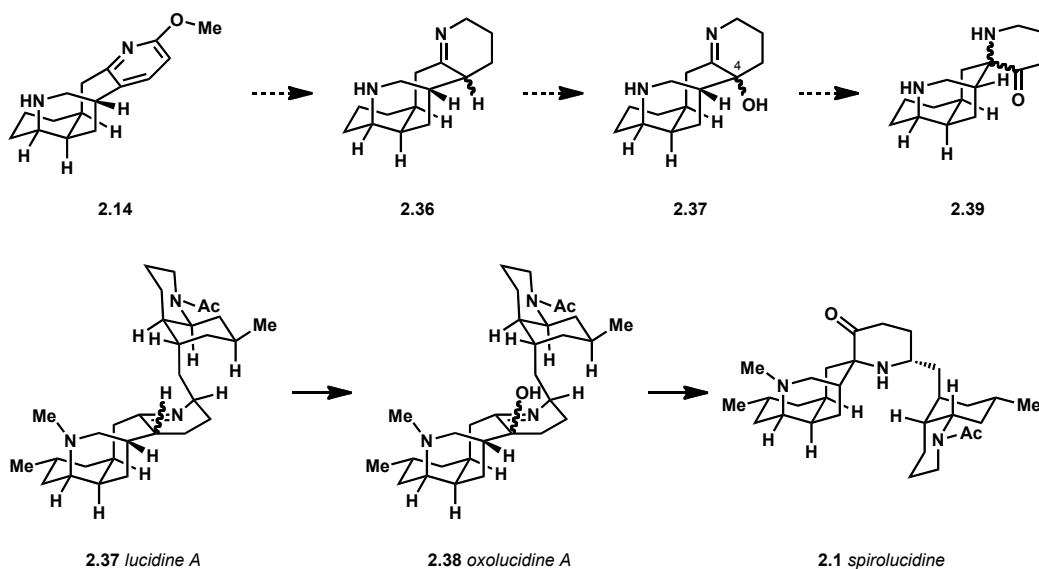
Table 2.2 Hydrogenolysis and reductive amination of **2.14**.

Entry	Cat. Loading	Solvent	Time (h)	Result
1	20 weight %	MeOH	12	complete conversion to 2.30
2	50 weight %	MeOH	2	5:1 2.14 to 2.30
3	100 weight %	MeOH	1	3:3:1 2.14 to 2.30 to s.m.
4	50 weight %	EtOH	2	9:1 2.14 to 2.35
5	50 weight %	THF	6	s.m.
6	50 weight %	EtOAc	3	exclusively 2.14 , 92% yield

2.3 Imine Route to Spirolucidine and Nankakurine A

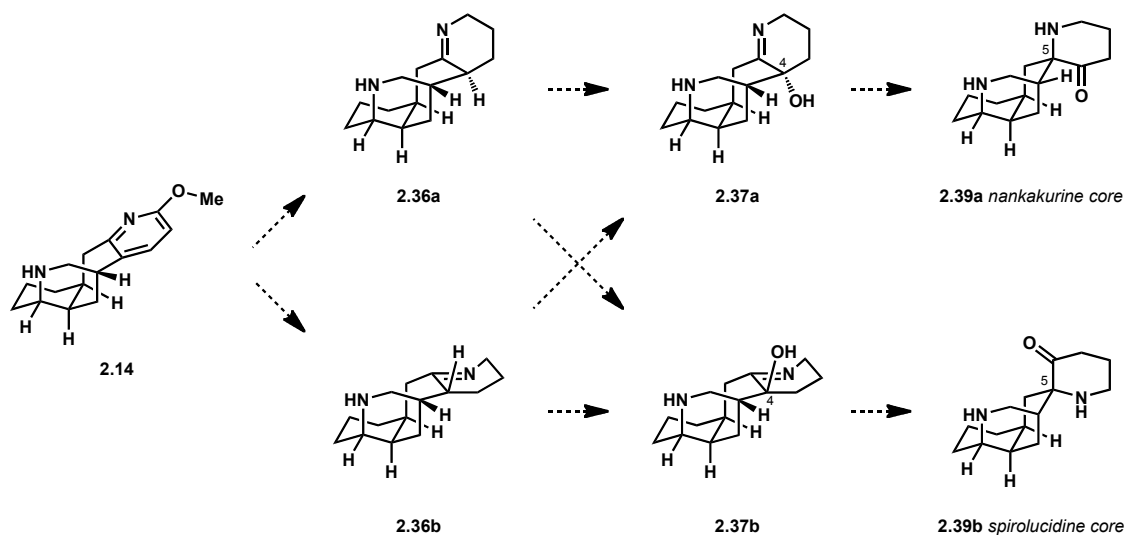
With the desired tetracycle (**2.14**) in hand, we sought to explore its transformation into the spirolucidine and nankakurine cores. We initially chose to explore a biomimetic route (Scheme 2.6) in which tetracycle **2.14** would be elaborated into imine **2.36**. We intended to test whether imine **2.36** would undergo a facile oxidation to α -hydroxyimine **2.37**, a transformation analogous to the oxidation of lucidine A (**2.37**) to oxolucidine A (**2.38**). We would then effect an α -hydroxyimine rearrangement on tetracycle **2.37** to generate the spirocyclic core of nankakurine A and spirolucidine (**2.1**). This, too, is analogous to the proposed biogenesis of these molecules (see section 1.5).

Scheme 2.6 Biomimetic route to the nankakurine and spirolicudine cores.



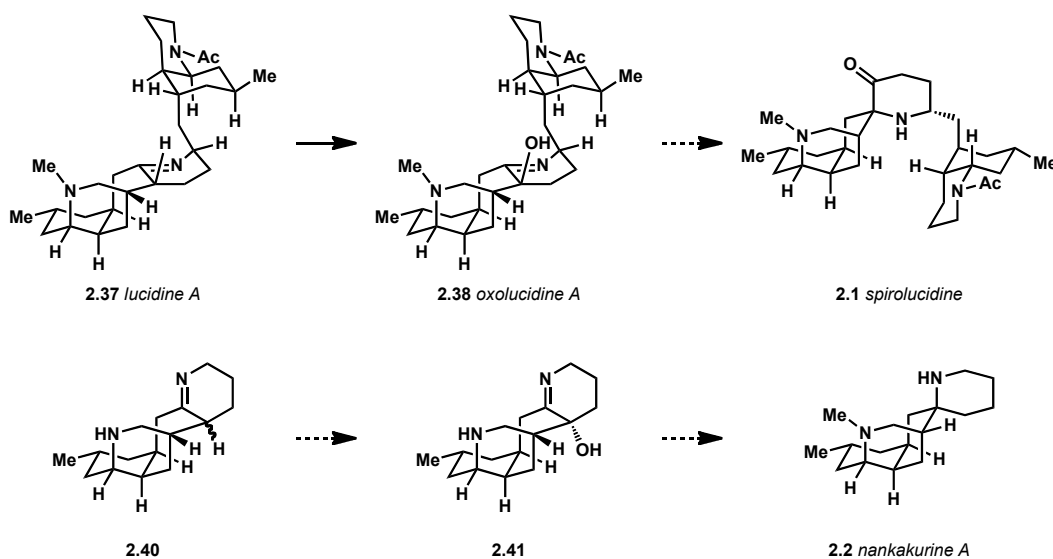
Because of the stereospecific nature of the α -hydroxyimine rearrangement,⁴ the configuration of the C-4 stereocenter of **2.37** was expected to control the stereochemistry of the spiro center of **2.39**. Hydroxyimine **2.37a** (Scheme 2.7) would give rise to the nankakurine core (**2.39a**), whereas hydroxyimine **2.37b** would generate the core of spirolicudine (**2.39b**). Therefore, the stereochemistry with which the oxidation of **2.36** to **2.37** took place would determine which natural product target we would access. It is possible that the stereochemical outcome of this oxidation is controlled by the configuration at C-4 of imine precursor **2.36**. In this case, the ultimate configuration of **2.39** would be determined by the reductive process that created the C-4 stereocenter of **2.36**. By selectively accessing imine **2.36a** or **2.36b**, we could generate the core of nankakurine A or spirolicudine. On the other hand, if the oxidation of **2.36** to **2.37** were to proceed through a planar intermediate, then the stereochemistry of the oxidation would depend on the overall conformation and steric bias of the tetracycle. We might see exclusive formation of either **2.37a** or **2.37b**, regardless of whether we began with imine **2.36a** or **2.36b**.

Scheme 2.7 Stereochemical possibilities for the biomimetic route.



The α -hydroxyl group is thought to be β in oxolucidine A (**2.38**), which differs from our substrate in that it bears an appended bicyclic portion at C-1 (Scheme 2.8). It is possible that this C-1 bicycle plays an important role in biasing the conformation of the system towards hydroxylation from the β -face. Tetracycle **2.40**, which does not bear a C-1 bicycle, might show a preference for oxidation from the α -face to afford hydroxyimine **2.41**. If this were the case, it would account for the opposite configurations in the spiro centers of nankakurine A and spiroLucidine.

Scheme 2.8 Pathways to spiroLucidine and nankakurine A.

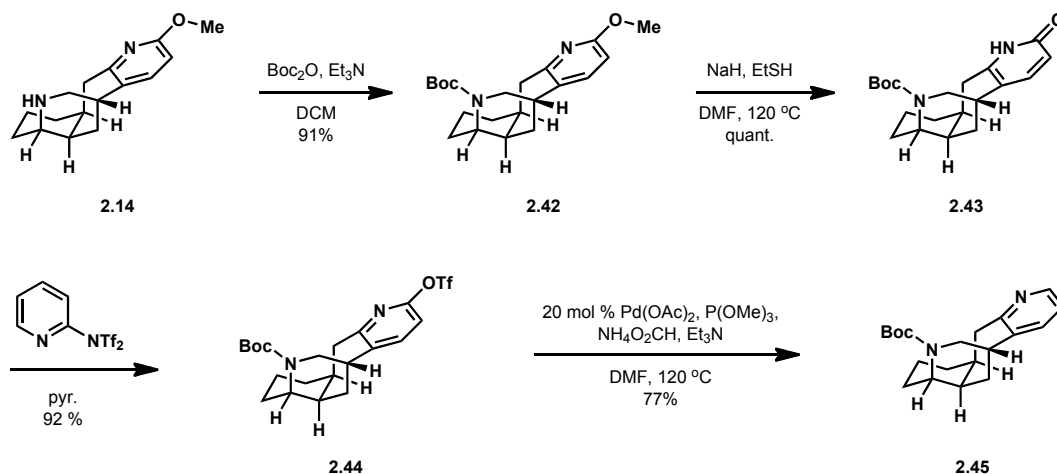


We were interested in testing the feasibility of the oxidation of **2.36** to **2.37**. We also wished to explore the innate stereoselectivity of this reaction and determine whether we could perturb it through reagent control to allow us to

access **2.37a** or **2.37b**. Accomplishing these goals would give us access to the cores of nankakurine A and spirolucidine.

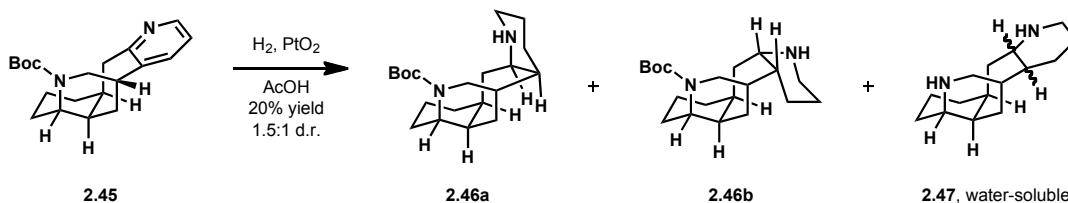
With these goals in mind, we continued the synthesis by protecting tetracyclic amine **2.14** as a Boc carbamate (**2.42**, Scheme 2.9). The methyl ether of **2.42** could be cleaved by heating in the presence of NaSEt to reveal pyridone **2.43**. The pyridone was converted into the corresponding pyridine triflate (**2.44**) by treatment with Comins Reagent and was subsequently transformed to pyridine **2.45** by catalytic reduction with Pd(OAc)₂ and ammonium formate.⁵

Scheme 2.9 Synthesis of pyridine **2.45**.



The reduction of pyridine **2.45** proved difficult. Stirring under hydrogen with Adams' catalyst for 2 d gave a mixture of two piperidine products, presumed to be **2.46a** and **2.46b**, in a 1.5:1 ratio and a combined 20% yield (Scheme 2.10). The stereochemistry of the major product was not determined at this stage. The low recovery appeared to be the result of partial cleavage of the Boc group under the acidic reaction conditions. This produced a diamine product (**2.47**) that had significant water solubility.

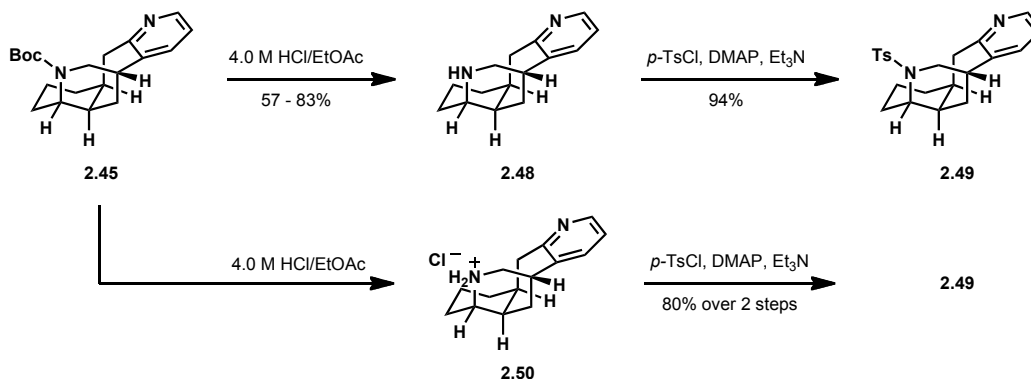
Scheme 2.10 Hydrogenation of pyridine **2.45**.



Consequently, we elected to switch from the Boc protecting group to the more robust tosyl group (Scheme 2.11). This could be accomplished by removal of the Boc group from tetracyclic pyridine **2.45** with 3.0 M hydrochloric acid in ethyl acetate to afford secondary amine **2.48** in 57 - 83% yield. The variability in yield is believed to stem from the water-solubility of amine **2.48**, which made extraction

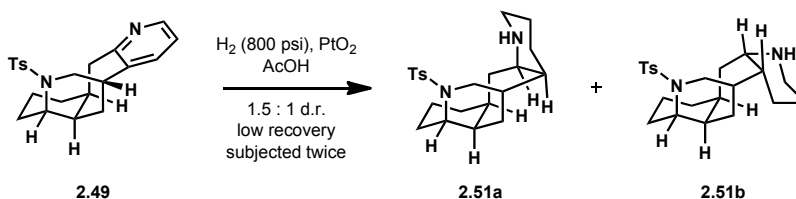
from aqueous media difficult even at pH = 14. Pyridine **2.48** could be protected by treatment with *p*-TsCl, DMAP and triethylamine to afford tosyl amide **2.49** in 94% yield. An alternate approach was also developed wherein pyridine **2.45** was treated with anhydrous hydrochloric acid, and salt **2.50** was isolated by removal of volatiles, bypassing the need for an aqueous extraction. Salt **2.50** was converted into tosyl-protected tetracycle **2.49** by treatment with *p*-TsCl in 80% yield over two steps.

Scheme 2.11 Protecting group swap.



Hydrogenation of tosyl-protected pyridine **2.49** was accomplished at elevated hydrogen pressure with Adams' catalyst to afford a 1.5:1 mixture of piperidines **2.51a** and **2.51b** (Scheme 2.12). This reaction was sluggish and required two subjectings to reaction conditions to go to completion. It was also discovered that the piperidine products were partially water-soluble, even with the tosyl protecting group intact. This led to loss of material with each resubjection. Therefore, we screened several hydrogenation catalysts for efficacy.

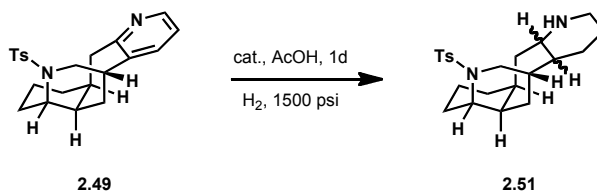
Scheme 2.12 Hydrogenation of pyridine **2.49**.



Because of the reluctance of the pyridine group to undergo this hydrogenation, a stoichiometric amount of catalyst was employed in the screening. The substrate was heated in acetic acid in the presence of the catalyst for 24 h under 1700 psi hydrogen pressure (Table 2.3). Rhodium on carbon as the catalyst led to only trace recovery of material (entry 1). Adams' catalyst gave complete conversion to product in a 3:1 d.r. in a modest 29% yield (entry 2). Palladium hydroxide led to exclusive formation of a single piperidine product (entry 3). Although the prospect of accessing a single diastereomer was exciting, this reaction gave low recovery and

only 50% conversion to product. The best yield was obtained with rhodium on alumina (entry 4), which showed a reversal of stereochemical preference to afford the two piperidine products in a 1:2.3 ratio.

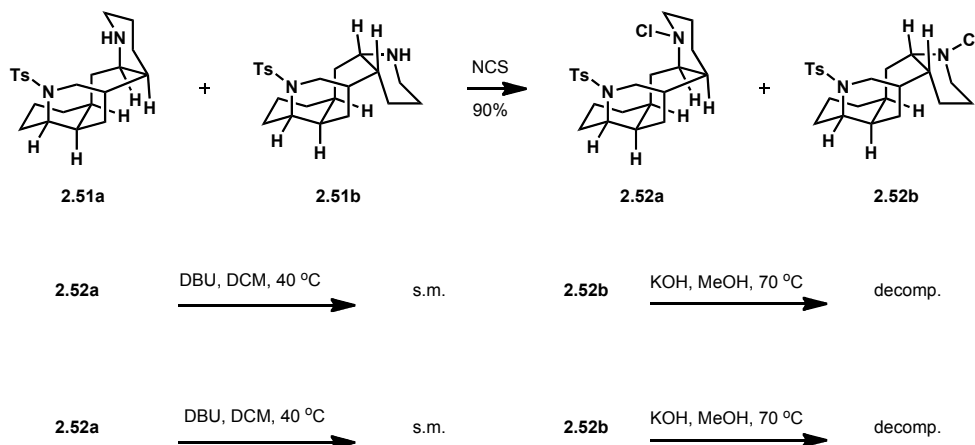
Table 2.3 Catalyst screen for hydrogenation of pyridine **2.49**.



Entry	Catalyst	Conversion	Recovery	d.r.
1	5% Rh/C	—	trace	—
2	PtO ₂	complete	29%	3:1
3	Pd(OH) ₂ /C	50%	4%	0:1
4	Rh/Al ₂ O ₃	complete	70%	1:2.3

The mixture of piperidines **2.51a** and **2.51b** obtained by hydrogenation over Adams' catalyst was treated with NCS to generate the corresponding *N*-chloro compounds **2.52a** and **2.52b** (Scheme 2.13). The two stereoisomeric compounds could be separated by column chromatography at this stage. Regioselective elimination of hydrochloric acid to afford the more highly-substituted imine was plausible according to conditions that had literature precedent.⁶ Heating *N*-chloro compounds **2.52a** and **2.52b** resulted in starting material for both isomers, whereas treating the compounds with KOH in MeOH at 70 °C led to decomposition. Attempts to convert piperidines **2.51a** and **2.51b** to the corresponding *N*-iodo compounds using I-Cl and NIS were met with failure, giving only decomposition products.

Scheme 2.13 Attempted imine synthesis.

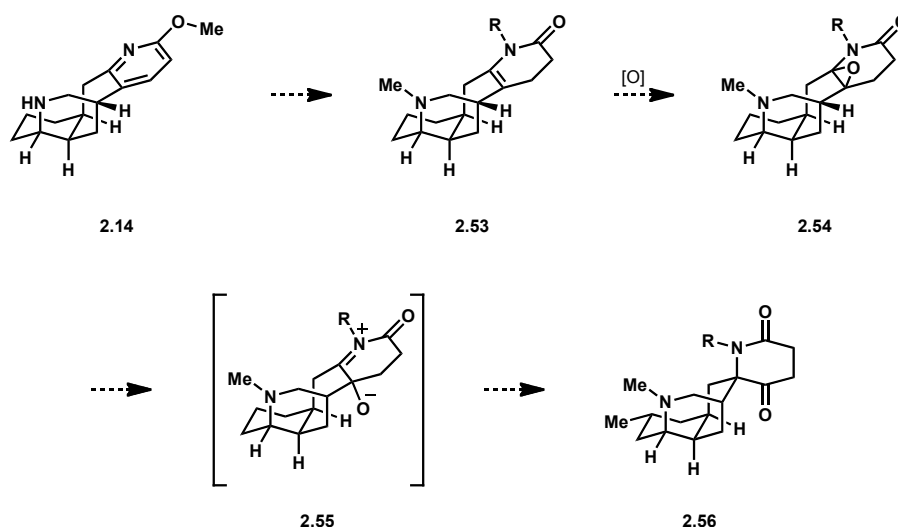


Because the imine formation chemistry was proving difficult and the hydrogenation of pyridine **2.49** represented a significant bottleneck in the generation of sufficient quantities of **2.51** with which to explore this chemistry, we decided to revise our synthetic route.

2.4 Enamide Route to Spirolucidine and Nankakurine A

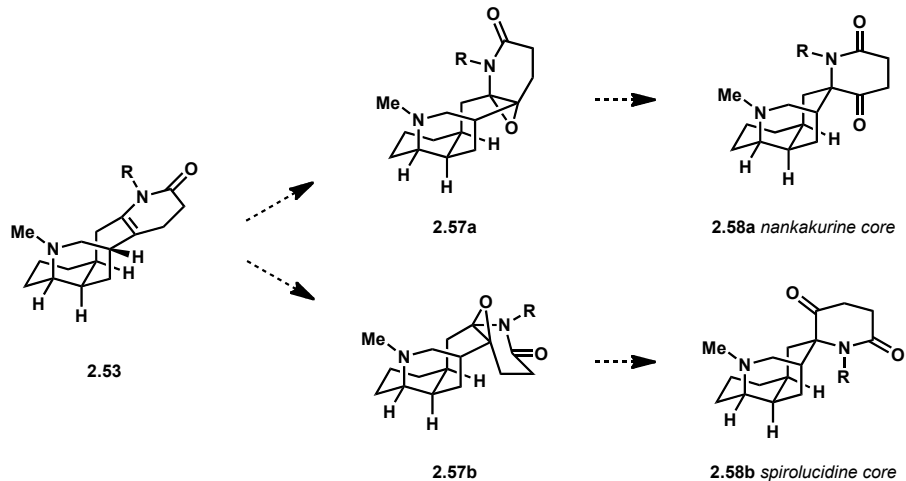
In our revised route to nankakurine A and spiroLucidine, we sought to elaborate tetracycle **2.14** into enamide **2.53** (Scheme 2.14). The C-4 spiro center could then be installed through the epoxidation and subsequent ring-contractive α -hydroxyimine rearrangement of **2.53**. Aminoepoxide **2.54** could undergo fragmentation to form zwitterionic intermediate **2.55**, which is activated to undergo the desired ring contraction and afford spirocycle **2.56**. Similar transformations have been shown in the literature to occur spontaneously,⁷ or to be initiated by Lewis acidic reagents such as TiCl_4 .⁴

Scheme 2.14 Enamide route to the core of nankakurine A.



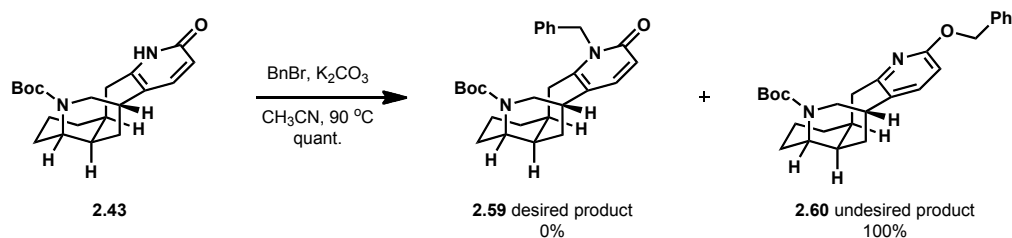
Once again, the stereochemistry of the oxidation would determine the ultimate configuration of the spiro center, and therefore the most readily accessible natural product (Scheme 2.15). Epoxidation of enamide **2.53** from the top face would ultimately give rise to nankakurines A and B *via* aminoepoxide **2.57a** and spirocycle **2.58a**, whereas epoxidation from the bottom face would lead to spiroLucidine through analogous intermediates **2.57b** and **2.58b**. We were interested in exploring the innate facial selectivity of tetracycle **2.53**, as well as investigating methods of reversing the inherent selectivity through reagent control to generate either core.

Scheme 2.15 Stereochemistry of the epoxidation and rearrangement of **2.53**.



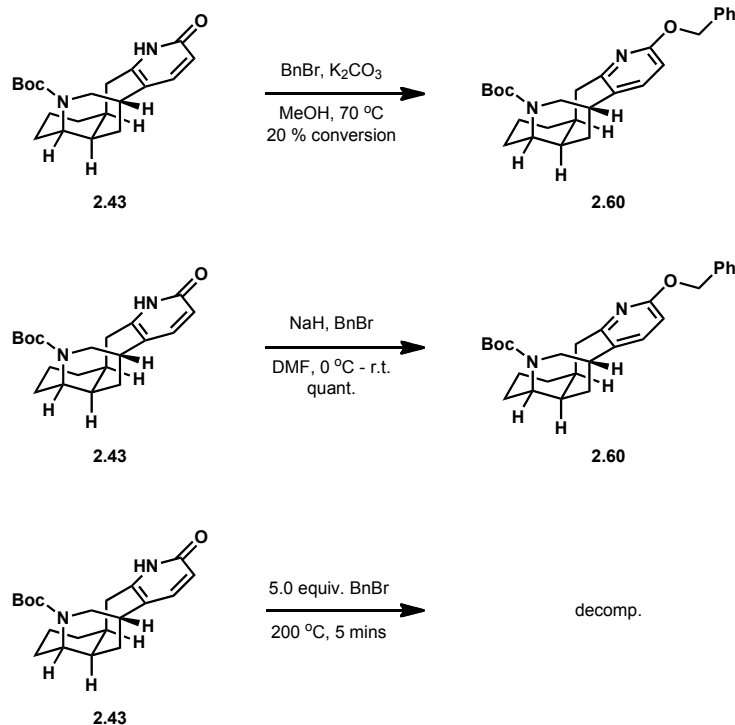
This synthetic effort commenced with pyridone **2.43** (Scheme 2.16). The first step was a seemingly trivial benzyl protection of the pyridone nitrogen. Treatment of **2.43** under literature-precedented pyridone *N*-benzylation conditions consisting of heating in the presence of potassium carbonate and benzyl bromide in acetonitrile led to a single product which was thought to be **2.59**. However, when repeated attempts to reduce this material all met with failure, the identity of **2.59** was called into question. Further investigation revealed that the product of this reaction was in fact *O*-benzylated tetracycle **2.60**.

Scheme 2.16 Attempted benzylation of pyridone **2.43**.



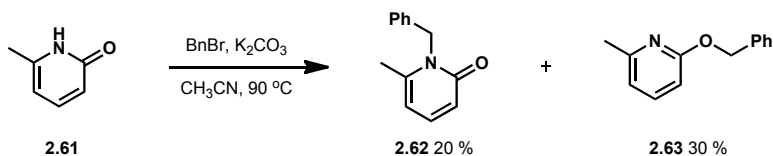
Other benzylation conditions were then investigated (Scheme 2.17). Changing the solvent from acetonitrile to methanol⁸ resulted in a 20% conversion to *O*-benzylated product **2.60**. Employing sodium hydride in DMF⁹ also gave exclusively *O*-benzylated tetracycle **2.60**. Stirring pyridones in neat benzyl bromide at high temperatures has been shown to favor selective *N*-benzylation;¹⁰ however, tetracyclic pyridone **2.43** underwent complete decomposition within five minutes at 200 °C in benzyl bromide. No trace of *N*-benzylated pyridone **2.59** was observed under any of the reaction conditions tested.

Scheme 2.17 Further benzylation attempts with pyridone **2.43**.



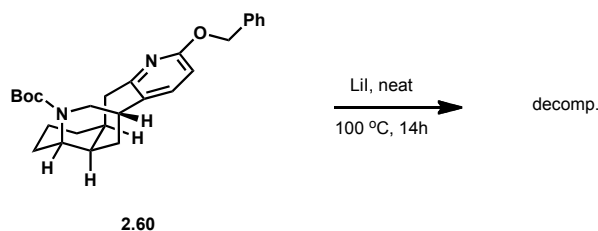
We hypothesized that the steric bulk of the C-5/C-6 substituents on pyridone **2.43** could be biasing it toward *O*-benzylation rather than *N*-benzylation. To gain insight into this possibility, the regioselectivity of the benzylation of model pyridone **2.61** was studied (Scheme 2.18). Treatment of **2.61** with benzyl bromide and potassium carbonate at 90 °C led to formation of *N*-benzylated pyridone **2.62** and *O*-benzylated pyridone **2.63** in a 1:1.5 ratio and 50% combined yield. Because this model substrate is less sterically congested at the nitrogen than tetracyclic pyridone **2.43**, this result suggested that it would be very difficult to achieve selective *N*-benzylation of **2.43**.

Scheme 2.18 Benzylation of model substrate **2.61**.



Isomerization of *O*-benzylated pyridine substrates to the tautomeric *N*-benzylated pyridones has been demonstrated by Anderson and coworkers *via* heating in the presence of lithium iodide.¹¹ Because *O*-benzylated pyridine **2.60** could be formed in quantitative yield, this isomerization was investigated (Scheme 2.19). Unfortunately, heating tetracycle **2.60** at 100 °C with LiI for 14 h resulted in complete decomposition.

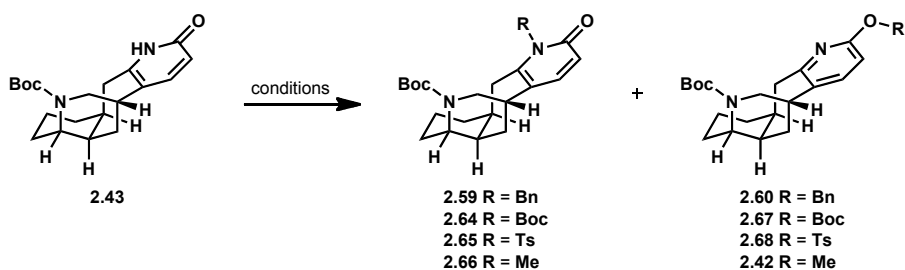
Scheme 2.19 Attempted isomerization of *O*-benzylpyridine **2.60**.



Having met with little success at forming *N*-benzylpyridone **2.59**, functionalization with groups other than benzyl was pursued (Table 2.4). Boc protection has been demonstrated on sterically hindered tetrasubstituted pyridones;¹² however, attempted Boc protection of **2.43** led to the recovery of starting material (entry 1). Treatment of **2.43** with BuLi and *p*-TsCl gave a 2:3 mixture in favor of undesired *O*-functionalized pyridine **2.68** (entry 2). This was the first time that *N*-functionalization of pyridone **2.43** had been observed.

Because no reaction conditions had yet shown a preference for *N*-alkylation of **2.43**, the sterically smaller alkylating agent methyl iodide was investigated next.¹³ Stirring pyridone **2.43** in neat methyl iodide for an extended period of time (5 d) resulted in starting material (entry 3). Heating **2.43** in acetonitrile with potassium carbonate and methyl iodide gave a 1:1 mixture of *N*- and *O*-benzylated products **2.66** and **2.69** (entry 4). Changing the base to sodium hydride and the solvent to DMF afforded a 1.4:1 ratio of compounds in favor of the desired *N*-methylated product **2.66** (entry 5).

Table 2.4 Functionalization of pyridone **2.43**.



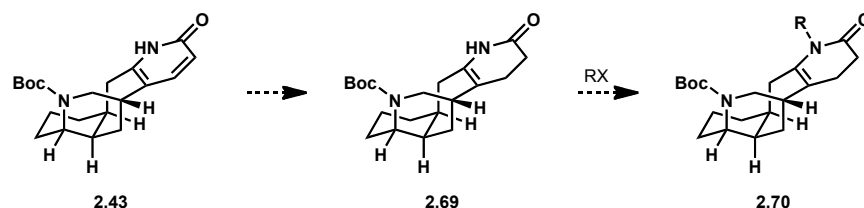
Entry	Electrophile	Conditions	T (°C)	Time	Desired Product	Conversion	Product Ratio
1	Boc ₂ O	Et ₃ N, DCM	0 - r.t.	12h	2.64	0%	—
2	<i>p</i> -TsCl	BuLi, THF	-78 - r.t.	12h	2.65	complete	2:3 2.68 : 2.65
3	MeI	neat	r.t.	5 d	2.66	0 %	—
4	MeI	K ₂ CO ₃ , CH ₃ CN	90	12h	2.66	66%	1:1 2.66 : 2.69
5	MeI	NaH, DMF	0 - r.t.	12h	2.66	complete	1.4:1 2.66 : 2.42

This 1.4:1 ratio of **2.66** to **2.42** was the highest ratio in favor of *N*-methylation over *O*-methylation that could be achieved. Although *O*-methylated

pyridone **2.42** could be resubjected to cleavage of the ether and methylation of the pyridone without significant loss of substrate, recycling over 40% of the material each time this reaction was run was deemed inefficient.

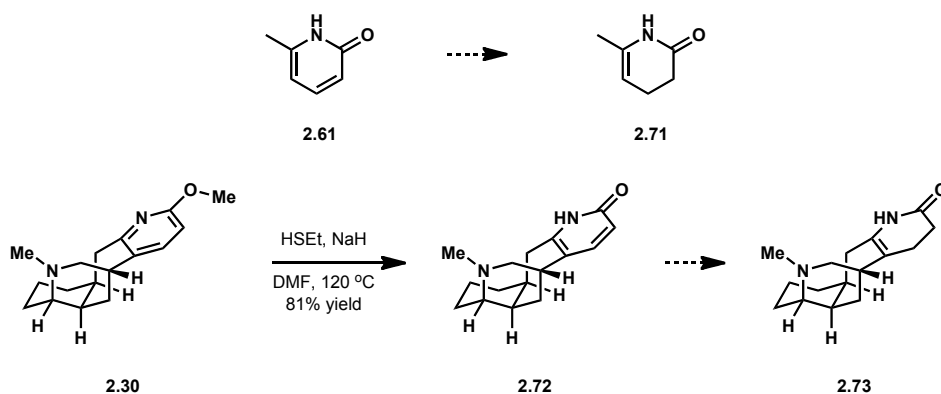
We elected to bypass this pyridone *N*-functionalization reaction entirely by attempting to effect a direct 1,4-reduction on pyridone **2.43** (Scheme 2.20) to afford enamide **2.69**, which could then be protected to give **2.70**. *N*-alkylation was expected to be significantly more favored for enamide **2.69** than for pyridone **2.43** because *O*-alkylation of enamide **2.69** would not generate an aromatic system.

Scheme 2.20 Planned reduction and protection of pyridone **2.43**.



In addition to pyridone **2.43**, two other pyridone substrates were screened (Scheme 2.21). Simple pyridone **2.61** was selected as a suitable model system for testing reduction conditions. *N*-methylated pyridone **2.72** was also employed in this study. It was generated from methoxypyridine **2.30** *via* heating in the presence of NaSEt.

Scheme 2.21 Pyridone substrates screened for 1,4-reduction.

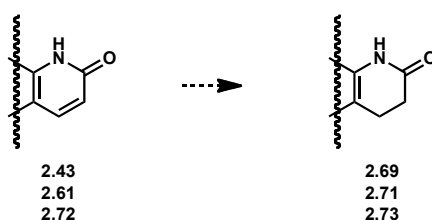


The screen of reduction conditions commenced with the common 1,4-reducing agent L-selectride (Table 2.5, entry 1), which has been shown to effect 1,4-reductions on *N*-alkylated pyridones.^{14,15} However, in the case of pyridone **2.61**, treatment with L-selectride resulted in recovery of starting material. K-selectride provided similar results, even at elevated temperature (entry 2). Stryker's reagent did not accomplish the desired reduction of pyridone **2.61** and returned the starting material unchanged (entry 3). Employing TMS-Cl as an additive with Stryker's reagent has been shown to enhance the reactivity of substrates towards reduction.¹⁶ These reaction conditions resulted in *O*-silylation of pyridone **2.61** (entry 4).

Attempted borane¹⁴ and diimide¹⁷ reductions of the pyridone substrates led to recovered starting materials (entries 5 – 7). The reducing agent derived from addition of NaBH₄ to RuCl₃ has been shown to selectively reduce mono- and disubstituted olefins;¹⁸ however, treatment of pyridone **2.43** with this reagent resulted in polymerization (entry 8).

Several sets of dissolving metal conditions were also screened. SmI₂ is a mild electron source that can reduce α,β -unsaturated amides when used in concert with additives such as dimethylacetamide¹⁹ and HMPA.²⁰ Treating pyridone **2.61** with SmI₂ using either acetamide or HMPA as an additive resulted in recovery of starting material (entries 9 and 10). Magnesium has been employed as an electron source for the 1,4-reduction of pyridones.²¹ Pyridone **2.43**, however, showed no conversion to product under these reaction conditions (entry 11).

Table 2.5 1,4-Reduction screen of pyridone substrates **2.43**, **2.61** and **2.72**.

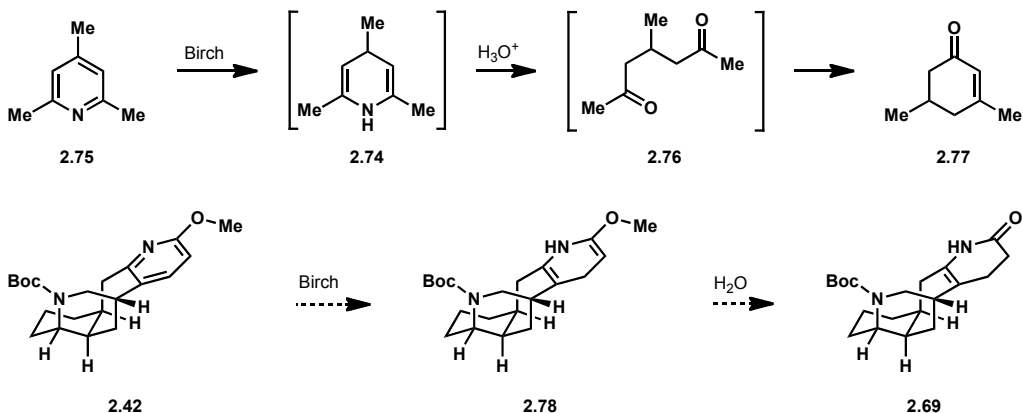


Entry	Substrate	Reagents	Intended Product	Result
1	2.61	L-selectride, THF, -35 °C	2.71	s.m.
2	2.43	K-selectride, 60 °C	2.69	s.m.
3	2.61	[(Ph ₃ P)CuH] ₆	2.71	s.m.
4	2.61	[(Ph ₃ P)CuH] ₆	2.71	
5	2.61	BH ₃ ·THF, 60 °C	2.71	s.m.
6	2.72	<i>p</i> -TsNHNH ₂ , Et ₃ N, MeOH	2.73	s.m.
7	2.43	<i>p</i> -TsNHNH ₂ , Et ₃ N, MeOH	2.69	s.m.
8	2.43	RuCl ₃ ·H ₂ O, NaBH ₄	2.69	polymerization
9	2.61	SmI ₂ , CH ₃ C(O)NMe ₂ , <i>t</i> -BuOH, THF	2.71	s.m.
10	2.61	SmI ₂ , HMPA, <i>t</i> -BuOH, THF	2.71	s.m.
11	2.43	Mg, MeOH	2.69	s.m.

Another potential strategy to access enamide **2.69** involved a Birch reduction of methoxypyridine **2.42**. Examples of employing Birch reduction conditions to access dihydropyridines such as **2.74** (Scheme 2.22) from pyridines such as **2.75** are rare in the literature. Typically, the dihydropyridine products are immediately hydrolyzed to generate dicarbonyl products such as **2.76**, which can go on to intramolecular aldol condensations to form enones such as **2.77**.^{22,23} Although no literature precedent for the Birch reduction of 2-alkyloxy pyridines could be found,

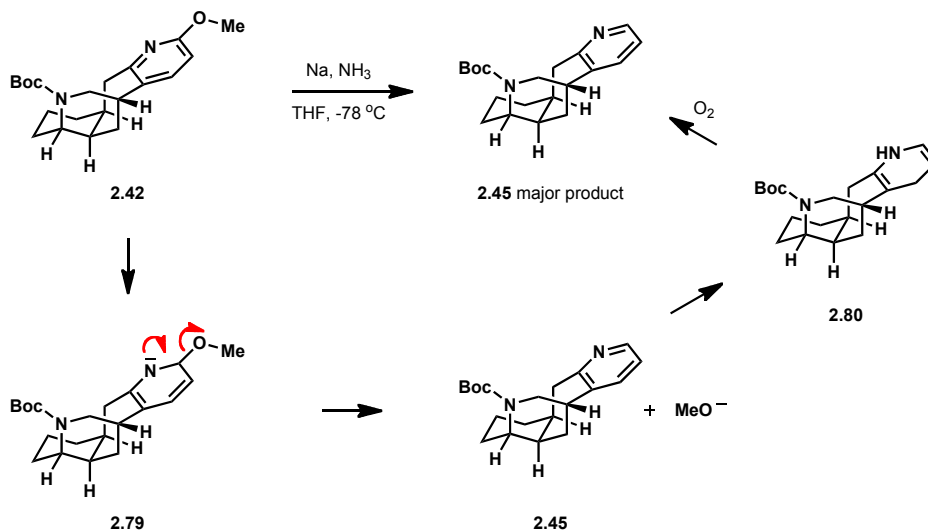
this could potentially be adapted to this synthesis through reduction of methoxypyridine **2.42** to methyl enol ether **2.78**, followed by hydrolysis to afford enamide **2.69**.

Scheme 2.22 Birch reduction pathways.



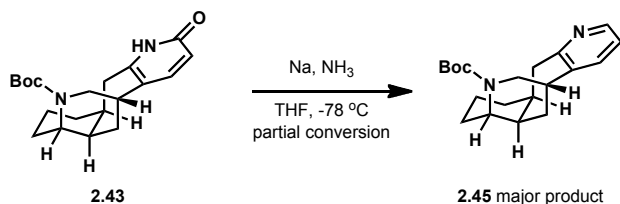
The major product isolated from the Birch reduction of methoxypyridine **2.42** proved to be pyridine **2.45** (Scheme 2.23). This presumably arose from initial reduction of methoxypyridine **2.42** to produce anion **2.79**, which could eject methoxide to generate pyridine **2.45**. Pyridine **2.45** could possibly undergo a second reduction to afford dihydropyridine **2.80** under the reaction conditions. However, **2.80** may be rapidly reoxidized to **2.45** upon exposure to atmospheric oxygen during the work-up.

Scheme 2.23 Birch reduction of methoxypyridine **2.24**.



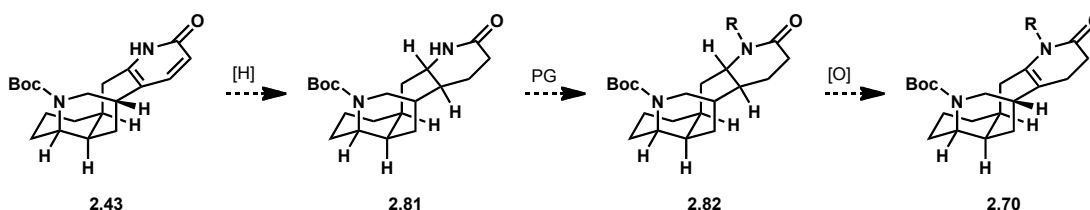
Pyridone **2.43** was also treated with Birch reduction conditions (Scheme 2.24). This reaction did not go to completion, but the major product was once again pyridine **2.45**.

Scheme 2.24 Birch reduction of pyridone **2.43**.



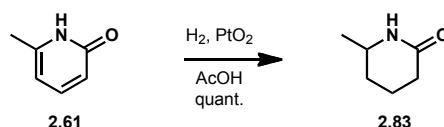
A route in which pyridone **2.43** was initially subjected to a double reduction to afford lactam **2.81** was also considered (Scheme 2.25). The nitrogen of lactam **2.81** could be protected to afford tetracycle **2.82**, bypassing the selectivity issues encountered with the pyridone, and the substrate could subsequently be oxidized to enamide **2.70**.

Scheme 2.25 Planned synthesis of enamide **2.70**.



The hydrogenation was initially tested on model pyridone **2.61** (Scheme 2.26). Upon exposure to a hydrogen atmosphere in the presence of Adams' catalyst and acetic acid,²⁴ pyridone **2.61** underwent smooth conversion to lactam **2.83** in quantitative yield.

Scheme 2.26 Reduction of model pyridone **2.61**.

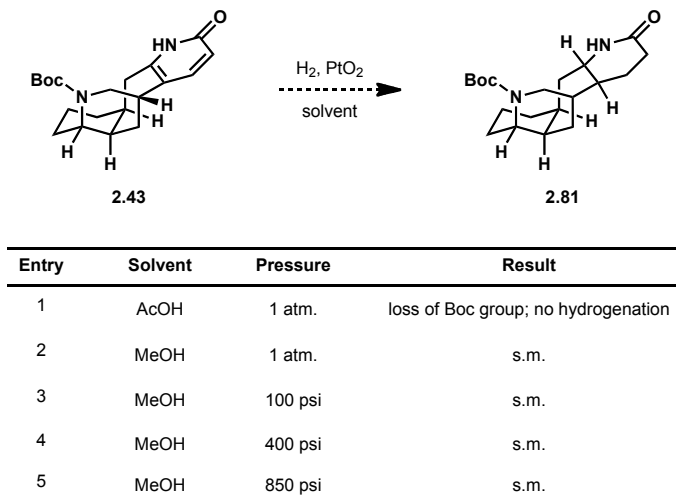


When tetracyclic pyridone **2.43** was subjected to the same reaction conditions, hydrogenation was not observed (Table 2.6, entry 1). The only reaction that took place was partial cleavage of the Boc protecting group. This prompted the conclusion that pyridone **2.61** was not an effective model for pyridone **2.43**.

Hydrogenation of pyridone **2.43** was also attempted using methanol as solvent.²⁵ Reduction was not observed at one atmosphere of H₂ pressure (entry 2), so elevated pressures were investigated. Unfortunately, starting material was also

recovered from the reaction when it was run with 100, 400 or 800 psi of H₂ (entries 3 – 5).

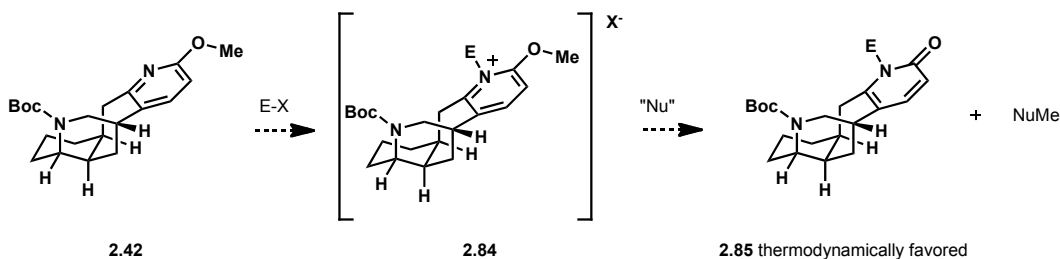
Table 2.6 Hydrogenation of pyridone **2.43**.



This string of unsuccessful reduction attempts led us to conclude that the reduction of unprotected pyridone **2.43** would be difficult to achieve.

An alternative route to synthesize *N*-functionalized pyridone **2.43** was needed. Because direct *N*-functionalization of pyridone **2.43** had proven problematic, and reduction of pyridone **2.43** without a protecting group on the nitrogen was not feasible, a strategy involving quaternization of the nitrogen of methoxypicoline **2.42** was pursued (Scheme 2.27). This would require alkylation of methoxypyridine **2.42** to form a salt such as **2.84**. Subsequent cleavage of the methyl ether through a Krapcho process would afford pyridone **2.85**. Treatment of **2.84** with a nucleophile was expected to result in conversion to pyridone **2.85** rather than reversion to methoxypyridine **2.42** because pyridones are typically more thermodynamically stable as compared to their corresponding hydroxypyridine tautomers.¹¹

Scheme 2.27 Salt formation route to pyridone **2.85**.



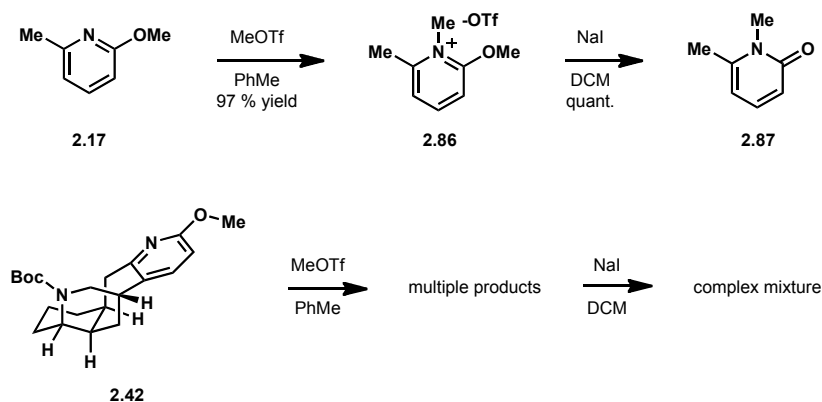
A survey of the literature revealed few conditions known to effect quaternization of 2-oxygenated pyridines.²⁶ These reactions typically require

methyl triflate as an alkylating agent; less reactive electrophiles are usually not sufficient.²⁷ This is likely the result of the unusually low nucleophilicity of the 2-alkoxyppyridine nitrogen. The strongly electron-withdrawing inductive effect of the O-alkyl substituent dominates its competing electron-donating resonance effect. This confers atypical reactivity on the 2-alkoxyppyridine relative to other pyridines; for example, protonation of the pyridine nitrogen in substrates containing the 2-methoxyppyridine moiety has never been observed in any of our studies. Substrates such as **2.42** can be extracted from acidic solutions of pH < 0 without any detectable loss of material into the aqueous layer.

This study began with model methoxyppyridine **2.17** (Scheme 2.28). Treatment of **2.17** with MeOTf in toluene afforded desired quaternary pyridinium salt **2.86** in 97% yield. Salt **2.86** could be smoothly converted to *N*-methyl pyridone **2.87** by stirring with sodium iodide in dichloromethane.

Encouraged by this result, we subjected tetracyclic methoxyppyridine **2.42** to the same reaction conditions. This led to loss of the Boc group and formation of multiple products. Treatment of this mixture with sodium iodide did not yield any trace of desired pyridone product **2.66**.

Scheme 2.28 Quaternization of methoxyppyridine substrates with MeOTf.

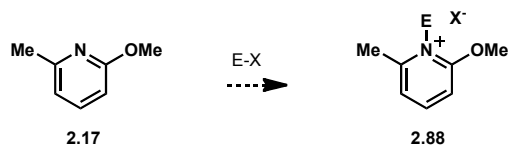


Electrophiles less reactive than methyl triflate were also tested for competence in the quaternization of methoxyppyridine **2.42** (Table 2.7). Treatment of **2.17** with methyl chloroformate followed by sodium hydride and hydrochloric acid was expected to effect a quaternization with subsequent reduction and hydrolysis to afford enamine **2.89** (see Figure 2.3);²⁸ however, this reaction resulted in decomposition (entry 1). Exposing methoxypicoline **2.17** to methyl chloroformate alone resulted in starting material; stirring in the presence of benzyl bromide also gave no reaction (entries 2 and 3).

Stirring **2.17** in neat methyl iodide resulted in 20% conversion to a new product (entry 4). Upon examination, this product proved not to be salt **2.92**, but rather *N*-methylpyridone **2.87** (Figure 2.3). This is presumed to have occurred through the initial formation of salt **2.92**, followed by *in situ* conversion to pyridone **2.87** by attack of the iodide counterion.

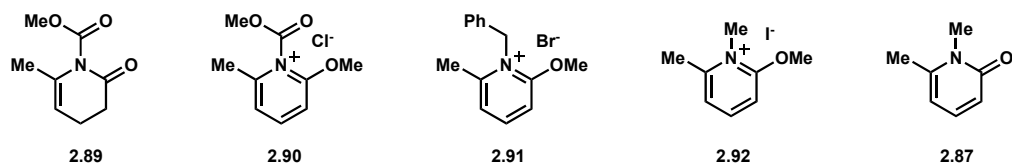
In an attempt to drive the reaction to completion, it was heated at 40 °C; however, this resulted in multiple products believed to arise from methylation of the pyridine ring (entry 5). Addition of lithium chloride shut down the reaction and afforded only starting material (entry 6).

Table 2.7 Attempted quaternization of methoxypyridine substrates.



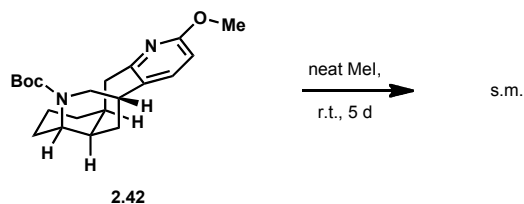
Entry	Electrophile	Conditions	Time	Intended Product	Result
1	ClCO ₂ Me	CH ₃ CN; NaBH ₄ ; HCl	4 h	2.89	decomp.
2	ClCO ₂ Me	CH ₃ CN	4 h	2.90	s.m.
3	BnBr	DCM	1 d	2.91	s.m.
4	Mel	neat, r.t.	3 d	2.92	20% conversion to 2.87
5	Mel	neat, 40 °C	1 d	2.87	multiple products
6	Mel	LiCl	1 d	2.87	s.m.

Figure 2.3 Intended products of methoxypyridine quaternization reactions.



Stirring methoxypyridine **2.17** in neat methyl iodide at room temperature had yielded the best results for quaternization, so tetracycle **2.42** was treated with these conditions (Scheme 2.29). Unfortunately, this reaction gave only starting material even after stirring for five days at 23 °C.

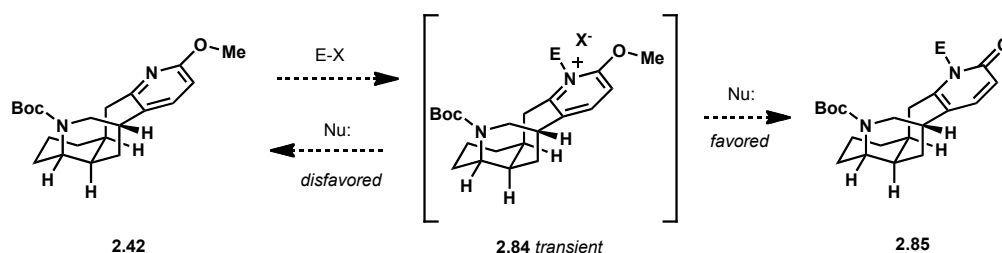
Scheme 2.29 Attempted isomerization of methoxypyridine **2.42** with MeI.



Although isolation of quaternized salt **2.84** had not been achieved, we were encouraged by the observation that *N*-methylpyridone **2.87** could be generated (Table 2.7, entry 4). This result suggested that quaternized salt **2.92** had formed transiently under the reaction conditions. We reasoned that perhaps tetracycle

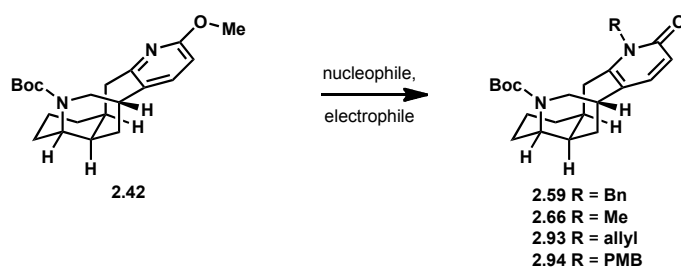
2.42 could be converted to pyridone **2.85** in one pot through the intermediacy of an analogous salt (**2.84**, Scheme 2.30). This would involve treating **2.42** with an electrophile and a nucleophile in the same reaction vessel. Once again, we predicted that this potentially reversible reaction would yield *N*-alkylpyridone **2.85** rather than the corresponding *O*-alkylpyridine because of the greater thermodynamic stability of the pyridone.

Scheme 2.30 One-pot route from pyridine **2.42** to pyridone **2.85**.



On the basis of the success of *in situ* generation of iodide ions for converting salt **2.92** to pyridone **2.87** (see Table 2.7, entry 4), metal iodides were selected as suitable nucleophiles to be tested for a one-pot methoxypyridine to *N*-alkylpyridone isomerization reaction (Table 2.8). Benzyl bromide was initially employed as the electrophile. Heating methoxypyridine **2.42** in acetonitrile in the presence of benzyl bromide and sodium iodide led to decomposition over the course of two days (entry 1). Changing the solvent to DMF and heating at 120 °C yielded the same result (entry 2). Heating **2.42** with neat lithium iodide also led to decomposition (entry 3).

Table 2.8 Direct one-pot isomerization of tetracycle **2.42** to pyridone products.

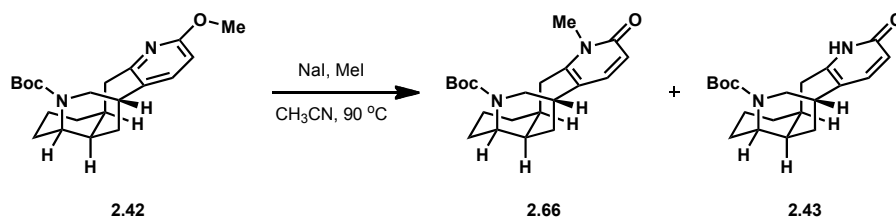


Entry	Electrophile	Nucleophile	Solvent	T (°C)	Time	Intended Product	Result
1	BnBr	Nal	CH ₃ CN	90	2 d	2.59	decomp.
2	BnBr	Nal	DMF	120	1 d	2.59	decomp.
3	BnBr	Lil	—	100	2 d	2.59	decomp.
4	allyl-Br	Nal	CH ₃ CN	100	14 h	2.93	decomp.
5	allyl-I	Nal	CH ₃ CN	90	14 h	2.93	decomp.
6	PMB-Cl	Nal	CH ₃ CN	90	1 d	2.94	decomp.
7	MeI	Nal	DMF	120	15 h	2.66	decomp.
8	MeI	Nal	CH ₃ CN	90	1 d	2.66	50% conversion

Our focus then shifted to electrophiles other than benzyl bromide. Utilizing allyl bromide, allyl iodide or PMB-Cl afforded only decomposition products (entries 4 – 6). Treating **2.42** with methyl iodide in DMF at 120 °C resulted in decomposition. However, heating methoxypyridine **2.42** with methyl iodide and sodium iodide in acetonitrile at 90 °C for one day resulted in 50% conversion to desired *N*-methylpyridone **2.66** (entry 8).

Optimized conditions for the conversion of methoxypyridine **2.42** to *N*-methylpyridone **2.66** were then sought (Table 2.9). Reaction time and concentration were varied, as was the number of equivalents of both methyl iodide and sodium iodide. Complete conversion to **2.66** could be achieved by treating methoxypyridine **2.42** (0.020 M in acetonitrile) with 5 equivalents of sodium iodide and 10 equivalents of methyl iodide for two days (entry 1). It was found that increasing the reaction concentration threefold to 0.060 M decreased the reaction time to 32 h (entry 2). Increasing the concentration further to 0.12 M and heating for 20 hours led to conversion of 10% of the desired product (**2.66**) into des-*N*-methylpyridone **2.43**. At concentrations of 0.20 M, this undesired reactivity could be almost completely suppressed by careful monitoring of the reaction progress (entry 4); however, at a concentration of 1.0 M, the formation of pyridone **2.43** became competitive with the formation of the desired product. This led to isolation of a mixture of desired pyridone **2.66** and des-methylated pyridone **2.43** in a 3:1 ratio along with remaining starting material **2.42** (entry 5). Thus, optimized conditions for the conversion of **2.42** to **2.66** consisted of heating a 0.20 M solution of **2.42** in acetonitrile with 10 equivalents of sodium iodide and 20 equivalents of methyl iodide at 90 °C for approximately 8 h. This afforded desired pyridone product **2.66** in 88% isolated yield (entry 4).

Table 2.9 Optimization of direct isomerization of **2.42** to **2.66**.

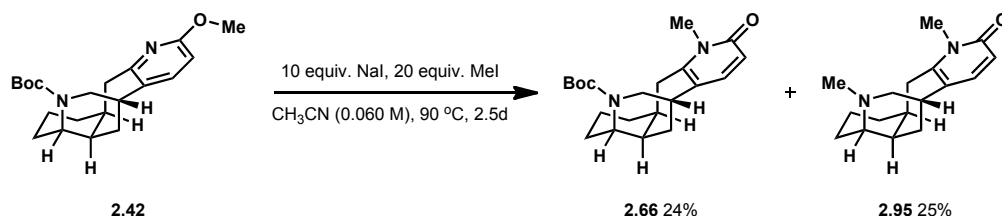


Entry	NaI (equiv)	MeI (equiv)	CH ₃ CN (M)	T (h)	Result
1	5	10	0.020	48	complete conversion to 2.66
2	5	10	0.060	32	complete conversion to 2.66
3	10	20	0.12	20	10:1 ratio of 2.66 to 2.43
4	10	20	0.20	7.5	88% yield, trace 2.43 , trace s.m.
5	10	20	1.0	9	3:1 ratio of 2.66 to 2.43 , trace s.m.

It was discovered that even at the low reaction concentration of 0.060 M, heating this reaction mixture for an extended period of time (>48 h) resulted in partial cleavage of the Boc protecting group (Scheme 2.31). Desired product **2.66**

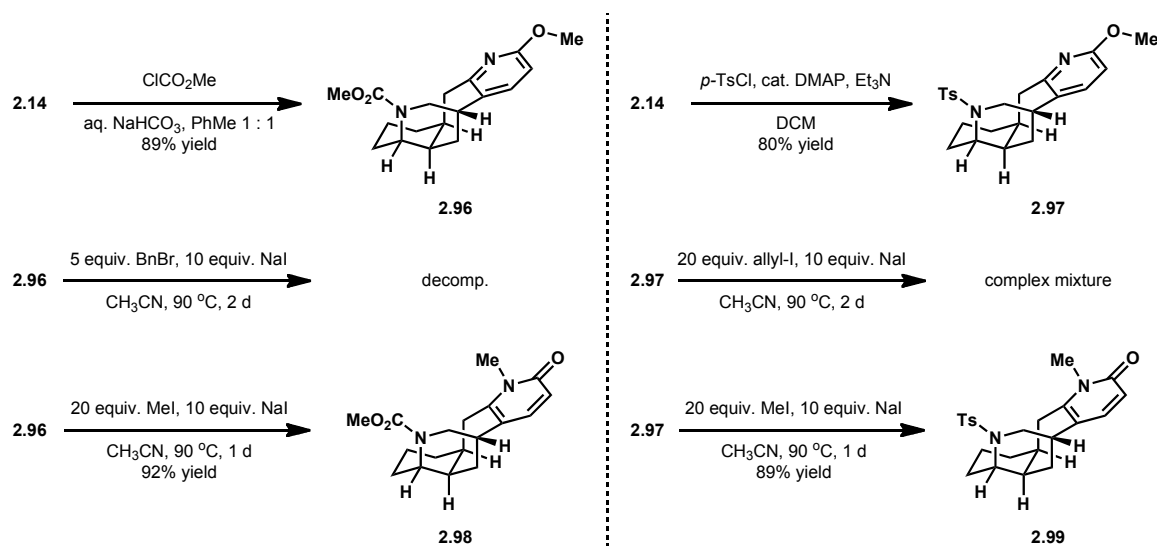
was isolated in 24% yield, while *N*-methylated pyridone **2.95** was isolated in 25% yield. The remainder of the material was presumed to have undergone a second *N*-methylation to afford a water-soluble quaternary ammonium salt that was lost during aqueous work-up.

Scheme 2.31 Byproduct of direct isomerization at extended reaction times.



This observation led us to speculate that the sensitivity of the Boc group toward the reaction conditions could be the factor that led to repeated decomposition during the screen of electrophiles other than methyl iodide. In order to explore this possibility, substrates bearing two different protecting groups were synthesized. Tetracyclic amine **2.14** could be protected as either a methyl carbamate (**2.96**, see Scheme 2.32) or a tosylate (**2.97**) in high yields under standard conditions. Unfortunately, attempts to effect the direct isomerization of methyl carbamate-protected tetracycle **2.96** to the corresponding *N*-benzylated pyridone resulted in decomposition. Similarly, attempts to convert tosyl-protected pyridone **2.97** to the corresponding *N*-methylpyridones were met with failure. Both substrates, however, smoothly underwent the one-pot direct isomerization reaction to the corresponding *N*-methylpyridones under the conditions initially optimized for substrate **2.42**. Pyridone **2.98** was produced in a 92% yield, whereas tosyl-protected pyridone **2.99** was isolated in 89% yield.

Scheme 2.32 Protecting group screen for direct isomerization.

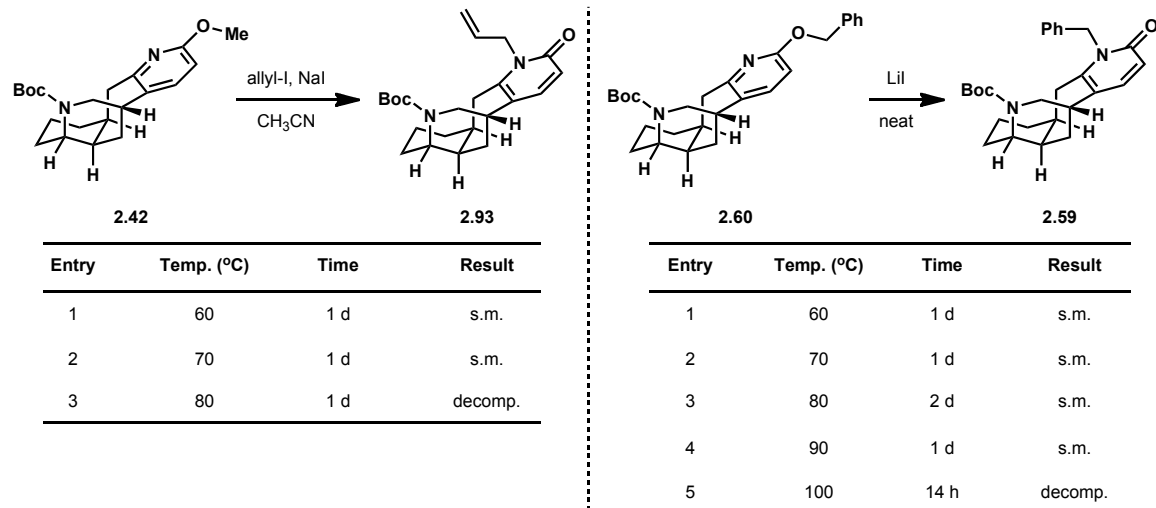


The development of a method to secure tetracyclic *N*-methylpyridones such as **2.66**, **2.98** and **2.99** represented a significant breakthrough in the progress toward spirolicidine and nankakurine B. Both of these natural products bear a methyl group on that nitrogen; installation of the methyl group at this point is therefore advantageous in that it would render a late-stage deprotection and reductive amination sequence unnecessary.

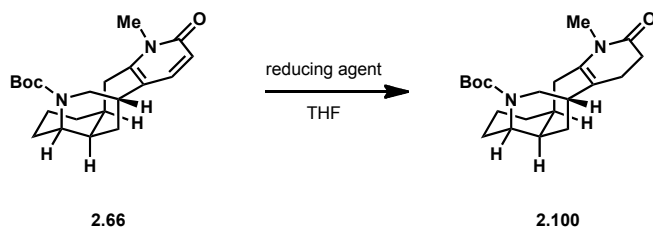
Nevertheless, we had two concerns about installing an *N*-methyl group at this stage of the synthesis. First, we were concerned about potential unwanted reactivity of a tertiary amine in anticipated subsequent oxidation chemistry. Second, accessing nankakurine B through a reductive amination of nankakurine A was expected to be an easier process than accessing nankakurine A *via* the demethylation of nankakurine B. Therefore, the installation of an easily-removable protecting group on the pyridone nitrogen of **2.43** was still desirable.

Because changing the protecting group on tetracycle **2.14** had not allowed us to access *N*-alkylpyridones other than *N*-methylpyridones, we focused on a different aspect of this reaction. During direct isomerization reactions with methyl iodide, we regularly observed starting material in the reaction flask even after 48 h. However, when electrophiles other than methyl iodide were employed, complete decomposition was observed in as little as 14 h. We hypothesized that this discrepancy could arise as the result of differences in stability between various *N*-alkylpyridones. We speculated that perhaps the desired *N*-allylated and *N*-benzylated products were being formed, but underwent rapid decomposition under the reaction conditions.

A systematic temperature study was then undertaken to identify a window of temperatures in which the desired isomerization reaction would take place but the product would not decompose (Table 2.10). Two reactions were chosen for study: the isomerization of methoxypyridine **2.42** to *N*-allylated pyridone **2.93**, and the isomerization of *O*-benzylpyridine **2.60** to *N*-benzylpyridone **2.59**. It was found that the allylation reaction showed only unchanged starting material when heated for a day at 60 or 70 °C (entries 1 and 2), but underwent decomposition at 80 °C (entry 3). *O*-benzylpyridine **2.60** was stable to reaction conditions at temperatures as high as 90 °C (entries 1 – 4), but showed no conversion to product. When heated to 100 °C, **2.60** rapidly decomposed (entry 5).

Table 2.10 Temperature study of direct isomerization to pyridones.

We elected to move forward in the synthesis with *N*-methylpyridone substrate **2.66**. Our focus now shifted to the 1,4-reduction of the pyridone moiety. *N*-benzylated¹⁵ and *N*-methylated¹⁴ pyridones have been shown to undergo conjugate reductions at the unsubstituted position with L-selectride at -35 °C. Accordingly, pyridone **2.66** was treated with these reaction conditions (Table 2.11, entry 1). This resulted in the recovery of starting material.

Table 2.11 Reduction of *N*-methylpyridone **2.66**.

Entry	Reducing Agent	Equivalents	Temp. (°C)	Time	Result
1	L-selectride	2	-35	45 min.	s.m.
2	L-selectride	5	-35	1 h	s.m.
3	L-selectride	10	-35	3 h	s.m.
4	L-selectride	10	0	3 h	s.m.
5	L-selectride	2	r.t.	3 h	partial conversion; 50% recovery by weight
6	L-selectride	10	r.t.	3 h	decomp.
7	K-selectride	10	-35	45 min.	s.m.
8	K-selectride	10	0	3 h	s.m.
9	K-selectride	10	r.t.	6 h	s.m.
10	K-selectride	10	65	3 h	60 % yield

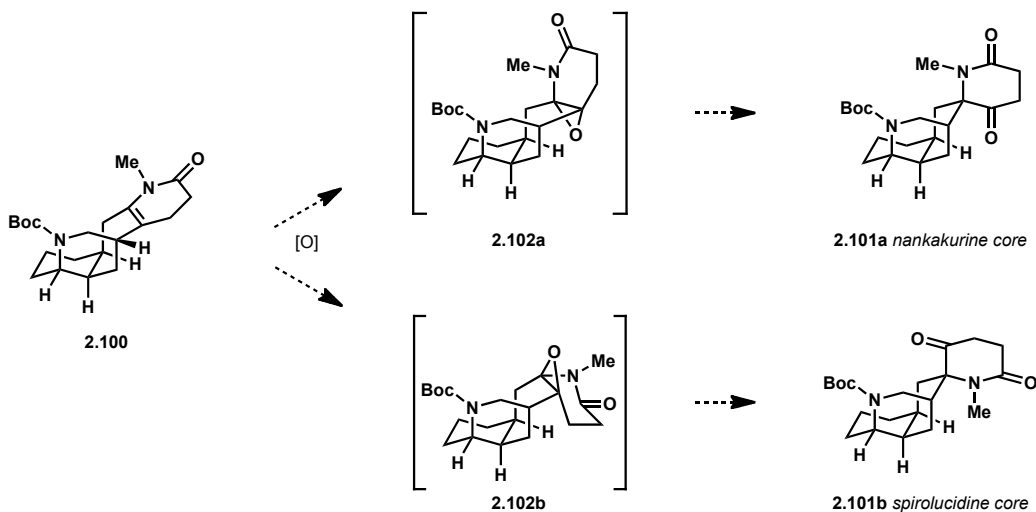
The reactivity of pyridone **2.66** was tested at several temperatures. It was found that temperatures of 0 °C and lower gave no conversion to product, even when as many as 10 equivalents of reducing agent were used (entries 2 - 4). At room temperature, the material underwent partial conversion to product as well as partial decomposition (entry 5). Heating this reaction at 65 °C resulted in complete decomposition (entry 6).

K-selectride was also tested as a reducing agent. It was found that at -35 °C, 0 °C and room temperature, starting material was recovered (entries 7 - 9). Happily, heating at 65 °C for 3 h gave the complete conversion of **2.66** to enamide **2.100**, which was isolated in 60% yield (entry 10).

2.5 Oxidation and Rearrangement Studies on Boc-Protected Tetracycle

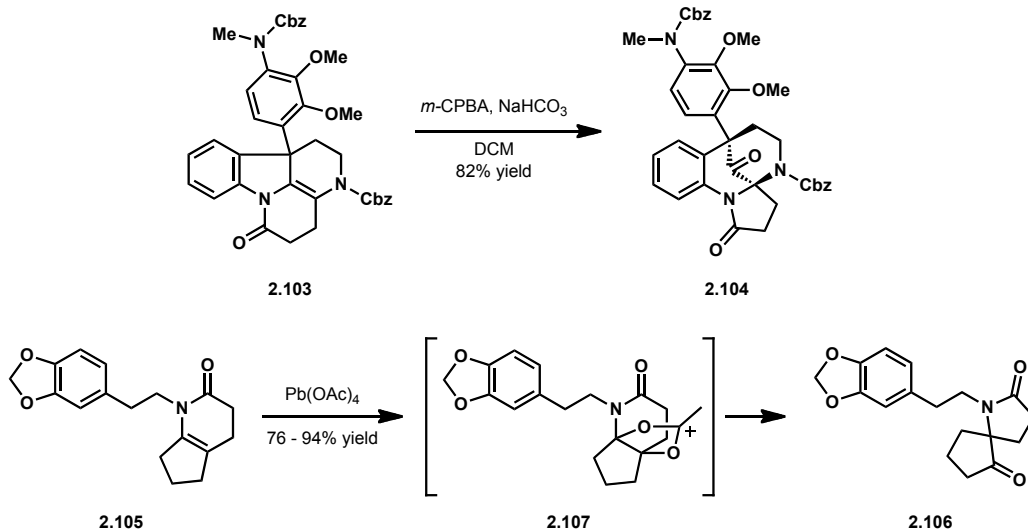
We then screened conditions to effect the oxidation and ring-contractive rearrangement of **2.100** to the nankakurine and spiroLucidine cores (**2.101a** and **2.101b** respectively, see Scheme 2.33) through the intermediacy of aminoepoxides **2.102a** and **2.102b**.

Scheme 2.33 Proposed oxidation and rearrangement of enamide **2.100**.



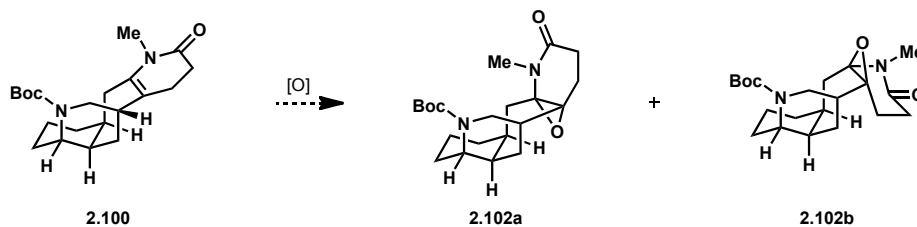
Similar oxidation and rearrangement sequences of enamides have been demonstrated in the literature to take place upon treatment with *m*-CPBA. Fukuyama used this method to convert enamide **2.103** (Scheme 2.34) to spirocycle **2.104** in a key step of the total synthesis of haplophytine.⁷ $\text{Pb}(\text{OAc})_4$ has also been employed to effect similar ring-contractive rearrangements in a complex natural product setting by Spitzer.²⁹ Enamide **2.105** was converted to spirocycle **2.106**, a key intermediate in the total synthesis of cephalotaxine. This rearrangement is believed to proceed via bridged acetate species **2.107**.

Scheme 2.34 Precedented oxidation/rearrangement sequences.



Accordingly, *m*-CPBA was initially tested for efficacy in the oxidation and rearrangement of enamide **2.100** (Table 2.12). This resulted in the formation of a complex mixture of products that included partial incorporation of *m*-chlorobenzoic acid (*m*-CBA, entry 1). Running the reaction in the presence of sodium bicarbonate⁷ failed to suppress this undesired side reaction, affording a similar product mixture (entry 2). Treatment of enamide **2.100** with Pb(OAc)₄ resulted in the recovery of starting material (entry 3). Employing NBS and water³⁰ as an oxidizing agent afforded nonspecific decomposition (entry 4).

Table 2.12 Screening of oxidative conditions upon enamide **2.100**.

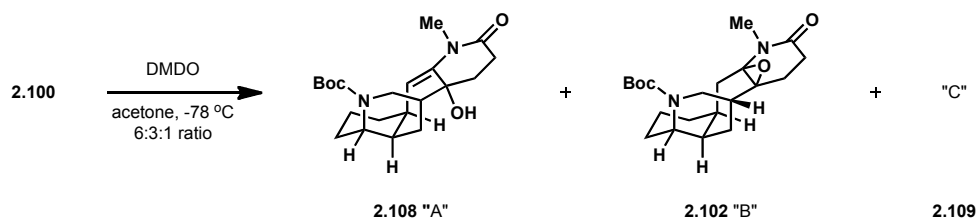


Entry	Oxidant	Other Conditions	T (°C)	Result
1	<i>m</i> -CPBA	DCM	0 - r.t.	complex mixture; partial <i>m</i> -CBA incorporation
2	<i>m</i> -CPBA	NaHCO ₃ , DCM	0 - r.t.	complex mixture; partial <i>m</i> -CBA incorporation
3	Pb(OAc) ₄	PhH	85	s.m.
3	NBS	H ₂ O, DCM	0 - r.t.	decomp.

A two-step oxidation and rearrangement sequence was then pursued. Isolation of sensitive aminoepoxides derived from the oxidation of enamide double bonds has been demonstrated in the literature by employing DMDO as an

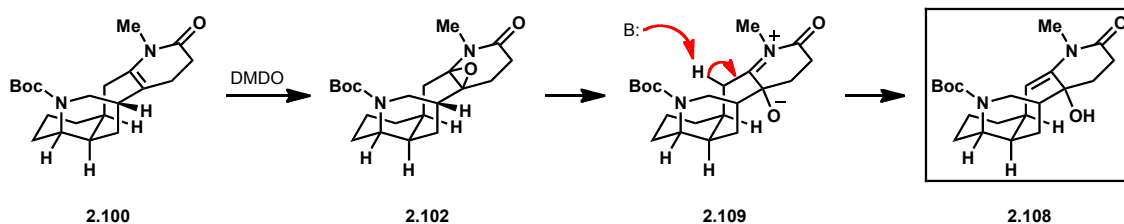
oxidant.^{4,31,32} Treatment of enamide **2.100** with freshly-generated DMDO in acetone at -78 °C resulted in the formation of three distinct products in a 6:3:1 ratio (Scheme 2.35).

Scheme 2.35 DMDO oxidation of enamide **2.100**.



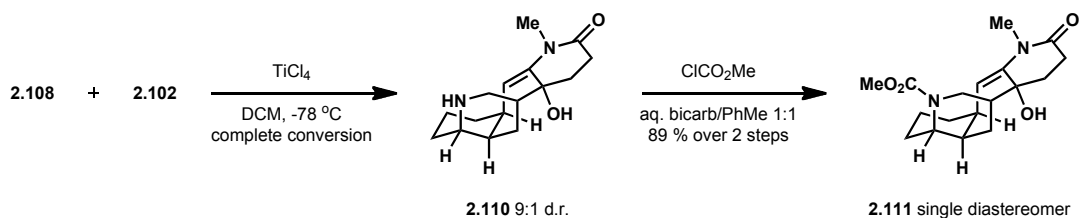
The three products formed from the oxidation of **2.100** with DMDO were dubbed A, B and C respectively. Compounds A and B were very difficult to separate ($R_f = 0.21$ for both compounds), but extensive column chromatography allowed isolation of a sample of A that was analytically pure. To our surprise, the major product (A) proved to be a single diastereomer of enamide **2.108**. This was thought to arise from initial epoxidation of enamide **2.100** to form aminoepoxide **2.102** (Scheme 2.36), which could fragment to form zwitterionic intermediate **2.109**. A final proton transfer would afford enamide **2.108**.

Scheme 2.36 Proposed formation of major enamide product **2.108**.



Spectral data for product B were consistent with a single diastereomer of epoxide **2.102**. No information had yet been gleaned about the stereochemistry of **2.108** or **2.102**. To test whether **2.108** and **2.102** had both been oxygenated from the same face or from opposite faces, the crude reaction mixture obtained from the DMDO epoxidation of **2.100** was treated with TiCl_4 (Scheme 2.37). This resulted in cleavage of the Boc group and the isolation of tetracycle **2.110** as a 9:1 mixture of diastereomers. Amine **2.110** could be protected as a methyl carbamate to afford **2.111** in 89% yield over two steps as a single diastereomer. This suggested that **2.108** and **2.102** both result from oxidation of enamide **2.100** from the same face.

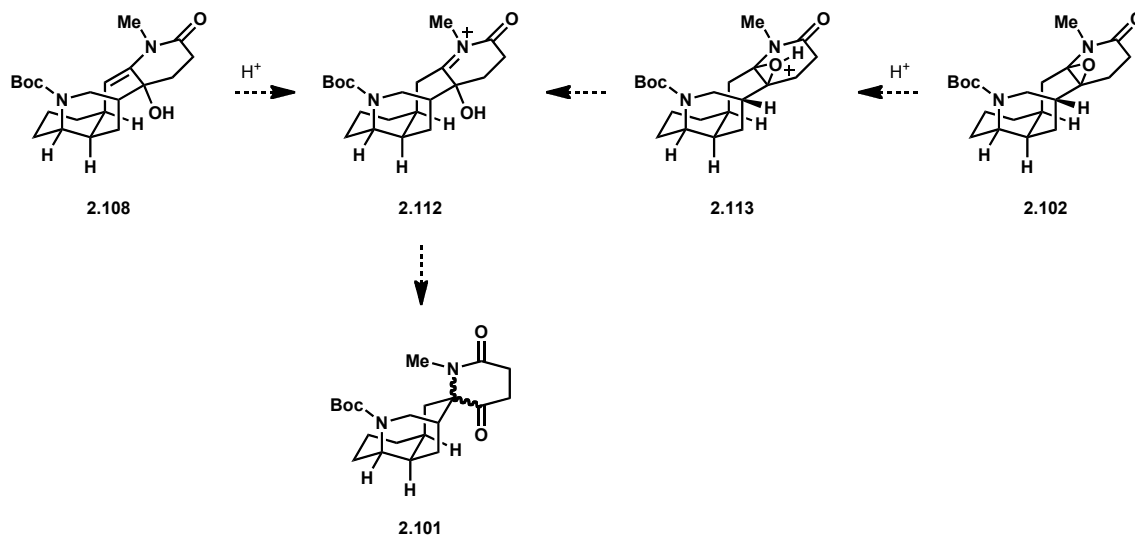
Scheme 2.37 Exploring the stereochemistry of enamide **2.108** and epoxide **2.102**.



This result had several exciting implications. Because **2.108** and **2.102** together accounted for more than 90% of the material, this demonstrated that tetracyclic enamide **2.100** has an inherent preference of at least 9:1 for oxidation from a single face. This reactivity would allow us to access the core of a single natural product without needing to rely on reagent control to confer selectivity.

Furthermore, this meant that the mixture of **2.108** and **2.102** could be employed in the key step as-is, bypassing the need for a difficult separation. Both enamide **2.108** and epoxide **2.102** should give the same activated intermediate (**2.112**, Scheme 2.38) upon treatment with acid. While aminoepoxide **2.102** could become protonated on the epoxide oxygen (**2.113**) and then fragment to give iminium ion **2.112**, enamide **2.108** would merely need to become protonated on the enamide in order to afford the same zwitterion. Therefore we expected enamide **2.108** to be equally competent to aminoepoxide **2.102** in the key ring-contractive rearrangement to generate **2.101**.

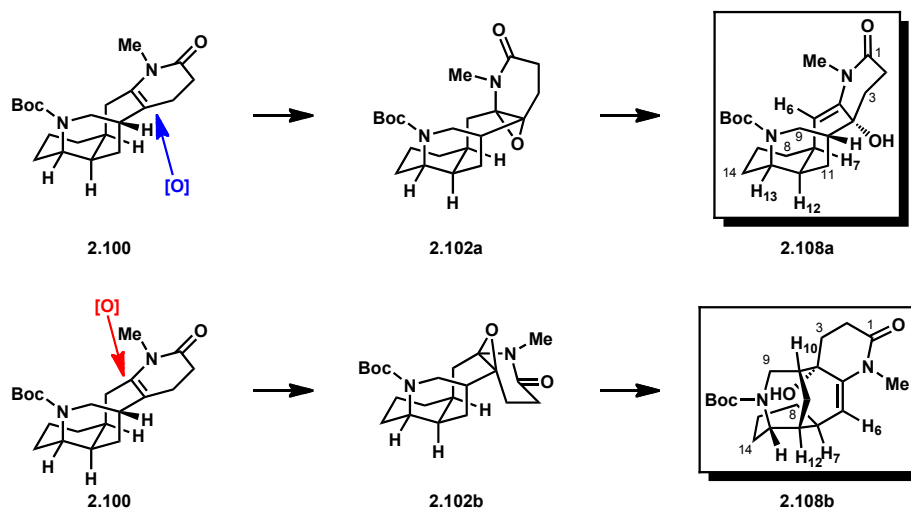
Scheme 2.38 Expected equivalence of aminoepoxide **2.102** and enamide **2.108**.



Compound **C** (**2.109**) was difficult to study because it was only isolated in trace quantities and was relatively unstable. This material was assumed to be the minor product resulting from epoxidation from the disfavored face of enamide **2.100**. Because it comprised less than 10% of the material obtained from the DMDO oxidation, its identity was not pursued at this juncture.

Our next task was to determine the stereochemistry of **2.102** and **2.108**. Epoxidation of enamide **2.100** from the bottom face would give rise to alcohol **2.108a** (see Scheme 2.39), whereas epoxidation of **2.100** from the top face would ultimately give rise to alcohol **2.108b**. Simple modeling suggested that these two diastereomeric alcohols would adopt very different conformations. Alcohol **2.108a** was expected to reside in a conformation similar to other tetracyclic compounds that had been studied. Alcohol **2.108b**, on the other hand, would need to undergo a significant conformation change of the seven-membered ring in order to place the enamide atoms in a *syn*-coplanar arrangement. This would result in the lactam functionality of **2.108b** being oriented almost opposite that of **2.108a**. In alcohol **2.108a**, both the C-9 – C-13 piperidine ring and the C-7 – C-8 – C-13 – C-15 cyclohexane ring sit in chair conformations, whereas in **2.108b** they must adopt twist boat conformations. This, in combination with the significant steric interaction expected between the hydroxyl group and H-8_{ax}, suggested that enamide **2.108b** would be significantly more strained than enamide **2.108a**. On the basis of this analysis, we hypothesized that the major product would be enamide **2.108a**, resulting from epoxidation from the bottom face.

Scheme 2.39 The two stereoisomers of enamide **2.108**.



The significant conformational differences between enamides **2.108a** and **2.108b** suggested that NOESY spectroscopy would be an effective tool for differentiating the two. Very different NOESY cross peaks were expected for each diastereomer. The most informative signals were expected to be those of H-6. In structure **2.108b**, H-6 is oriented toward the outer face of the seven-membered ring, whereas in structure **2.108a** this proton is oriented toward the top of the C-8 – C-14 cyclohexane ring. Thus, we expected the NOESY correlations of H-6 to be diagnostic.

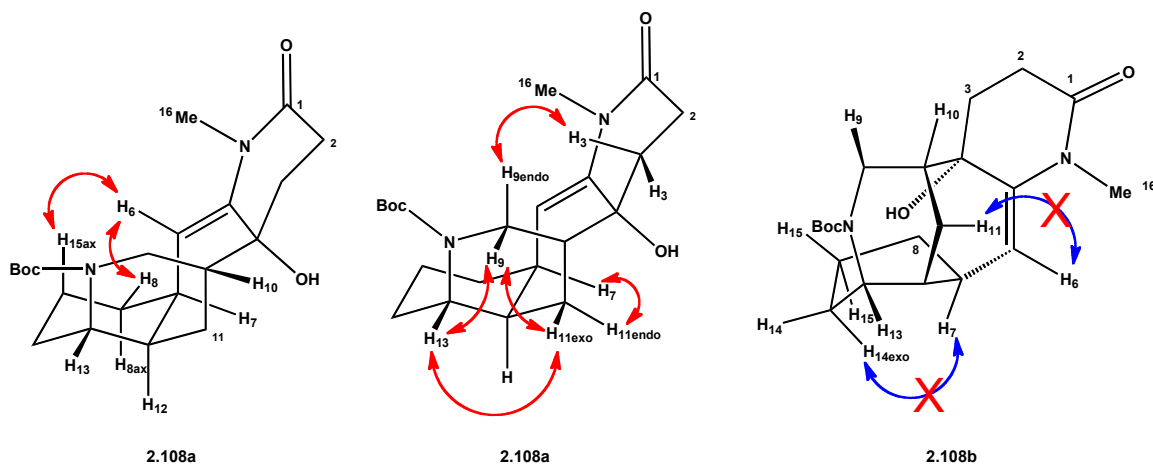
The NOESY spectrum of enamide **2.108** showed two telling cross-peaks for H-6 (**2.108a**, Figure 2.4). One was a correlation with H-15_{ax}, and the other was with H-8_{eq}. This was consistent with structure **2.108a**, wherein the caged structure of

the molecule brings H-6 and H-15_{ax} into very close proximity. H-6 is also oriented toward C-8, and was expected to interact with H8_{eq}. In structure **2.108b**, however, the conformation of the seven-membered ring results in H-6 pointing away from both C-8 and C-15. Several atoms are in between H-6 and H-15 in this structure, and a NOESY correlation between these protons appears extremely unlikely.

Evidence against structure **2.108b** can be found in the lack of certain diagnostic NOESY cross peaks that would be expected of that molecule. Most notably, a NOESY correlation was not observed between H-11_{endo} and H-6 (see Figure 2.4). Excluding vicinal and geminal protons, H-11_{endo} would be the closest proton to H-6 in structure **2.108b**. The absence of a correlation between these two protons is strong evidence against this structure.

Further support for structure **2.108a** can be found in the correlations of the C-9 – C-13 piperidine ring. NOESY cross-peaks of H-9_{exo}/H-11_{exo}, H-11_{exo}/H-13, and H-13/H-9_{exo} indicate that the C-9 – C-13 piperidine ring adopts a chair conformation, and these three protons reside in the three axial positions. The boat-like conformation of the C-9 – C-13 piperidine ring in **2.108b** places H-9_{exo} and H-13 in quasi-equatorial positions, where a NOESY correlation between them is unlikely to be present.

Figure 2.4 Selected NOESY correlations for the two stereoisomers of **2.108**.



The presence of a cross-peak between H-11_{endo} and H-7 is consistent with structure **2.108a**, where H-11_{endo} and H-7 are in quasi-1,3-diaxial positions on the seven-membered ring. In structure **2.108b**, these two protons are much further apart and a NOESY correlation was not expected. Furthermore, H-11_{endo} is closer to H-6 than to H-7 in structure **2.108b**; observing a H-11_{endo}/H-7 cross peak without observing a H-11_{endo}/H-6 cross peak would be very surprising in the case of structure **2.108b**.

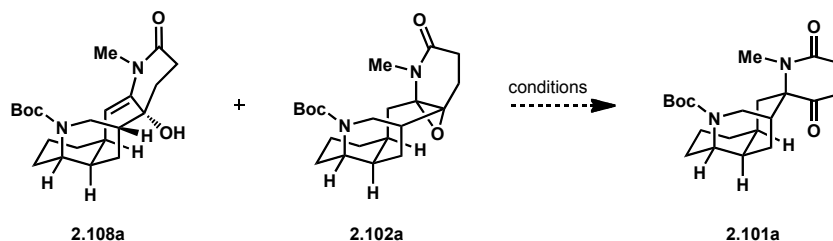
Finally, there isn't an observable NOESY cross-peak between H-14_{exo} and H-7. This correlation is expected in structure **2.108a**, where the cyclohexane ring containing C-14 and C-7 sits in a twist boat conformation and those two protons occupy the flagpole positions.

In conclusion, the NOESY data for compound **2.108** was consistent with structure **2.108a**. The product of the DMDO oxidation of enamide **2.100** was therefore concluded to be **2.108a**, in which oxidation took place from the bottom face. Enamide **2.108a** would ultimately give rise to the core of the natural product nankakurine B (**2.2**, see Figure 2.1) after the key rearrangement.

With key intermediate **2.108a** in hand, we turned our attention to identifying suitable conditions to effect the key hydroxyimine rearrangement. The mixture of enamide **2.108a** and aminoepoxide **2.102a** was used as the substrate for these reactions.

Both protic and Lewis acids were screened (Table 2.13). Employing *p*-toluenesulfonic acid in DCM at 60 °C led to decomposition (entry 1). Neither repeating this reaction without an aqueous work-up nor reducing the temperature to r.t. gave better results (entries 2 and 3). Running the reaction at 0 °C afforded a mixture of starting material and decomposition with no sign of the desired product (entry 4). Changing the acid to CSA⁴ or TFA also resulted in decomposition (entries 5 and 6).

Table 2.13 Attempts to effect the key ring contraction.



Entry	Conditions	Solvent	T (°C)	Result
1	<i>p</i> -TsOH	PhH	60	decomp.
2	<i>p</i> -TsOH, no aq. workup	PhH	60	decomp.
3	<i>p</i> -TsOH	PhH	r.t.	decomp.
4	<i>p</i> -TsOH	PhH	0	s.m. + partial decomp.
5	CSA	DCM	r.t.	decomp.
6	TFA	DCM	r.t.	decomp.
7	TiCl ₄	DCM	-78	loss of Boc
8	TiCl ₄	DCM	-78 - r.t.	decomp.
9	TiCl ₄	DCM	0 °C	decomp.
10	BF ₃ ·OEt ₂	DCM	r.t.	decomp.
11	AgClO ₄	DCM	r.t.	decomp.

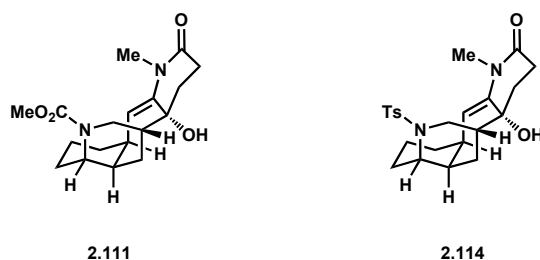
The Lewis acid screen commenced with TiCl₄, which had been shown to remove the Boc group from **2.108a** and **2.102a** at -78 °C (entry 7). Allowing the reaction to warm to room temperature or running it at 0 °C led to decomposition (entries 8 and 9). Employing BF₃·OEt₂ or silver perchlorate also led to decomposition (entries 10 and 11).

One common theme of many of the decomposition reactions was the loss of the Boc group. Removal of the Boc group would reveal a secondary amine, which could open up many decomposition pathways. It was therefore decided that it was necessary to construct a substrate that bore a less acid-labile protecting group on the tetracycle nitrogen.

2.6 Synthesis and Exploration of Key Step on Second-Generation Substrates

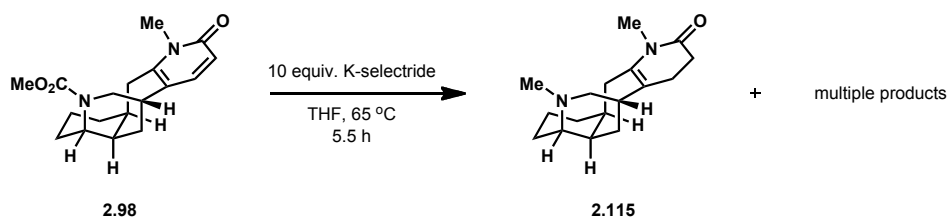
Two second-generation targets were chosen for testing the key ring-contractive rearrangement (Figure 2.5). These were methyl carbamate-protected enamide **2.111** and tosyl-protected enamide **2.114**.

Figure 2.5 Second-generation targets.



Tetracyclic pyridones **2.98** and **2.99** had already been synthesized (see Scheme 2.32). We intended to transform these into the corresponding enamides through the same synthetic sequence that had been employed for Boc-protected pyridone **2.42**. However, difficulties were encountered immediately. Treating tetracycle **2.98** with K-selectride at 65 °C led to multiple products, including the reduction of the methyl carbamate protecting group to the corresponding *N*-methyl compound (**2.115**, Scheme 2.40).

Scheme 2.40 K-selectride reduction of **2.98**.

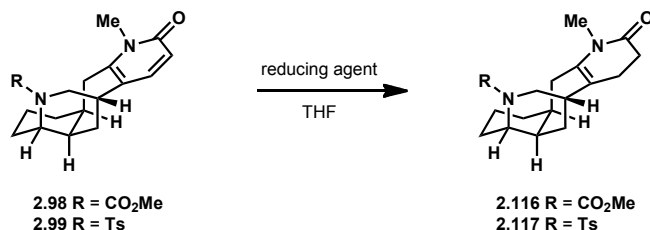


Consequently, a screen of reduction conditions was revisited (Table 2.14). Heating either pyridone **2.98** or **2.99** with K-selectride at 65 °C led to overreduction (entries 1 and 2); lowering the amount of reducing agent from 10 equiv to 5 equiv gave the same result (entry 3). Lowering the temperature to 40 °C resulted in starting material, even after a prolonged heating time of 48 h (entry 4).

The stronger reducing agent L-selectride was also tested. Although stirring pyridone **2.98** or pyridone **2.99** with 10 equiv. of L-selectride at -45 °C led to 50%

conversion to the respective products (entries 5 and 6), increasing the reaction temperature to 0 °C gave complete conversion for substrate **2.98**, affording enamide **2.116** in 77% isolated yield (entry 7). Tosyl-protected substrate **2.99** underwent 85% conversion to product under these conditions and gave 47% isolated yield of **2.117** (entry 8). Further increasing the reaction temperature to r.t. led once again to overreduction (entry 9).

Table 2.14 Screen of reduction conditions for pyridones **2.98** and **2.99**.



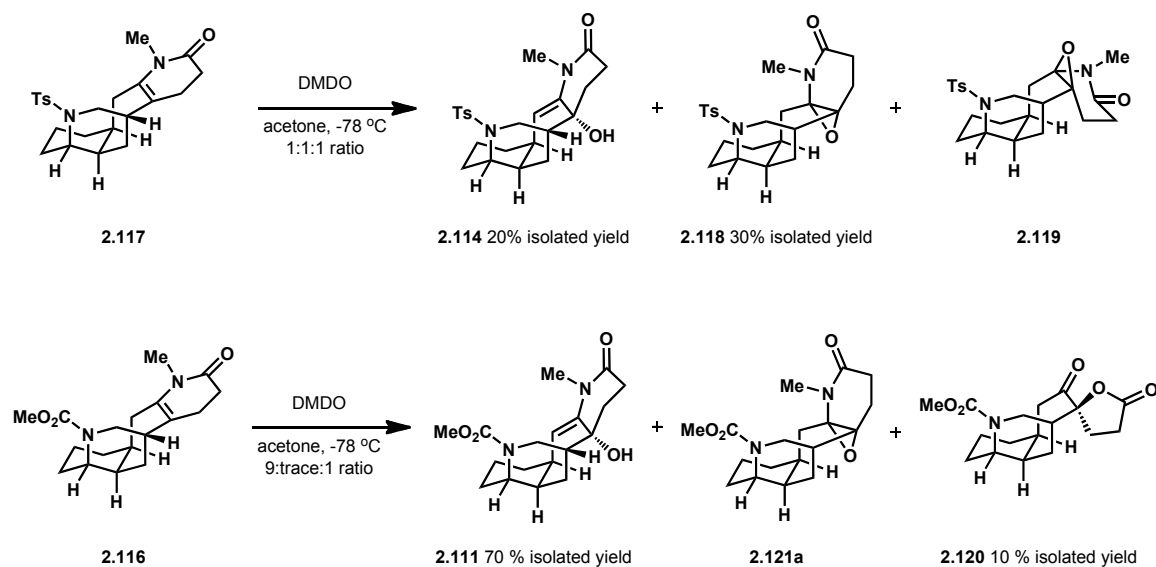
Entry	Substrate	Reducing Agent	Equivalents	Temp. (°C)	Time (h)	Product	Result
1	2.98	K-selectride	10	65	5.5	2.116	overreduction
2	2.99	K-selectride	10	65	3	2.117	overreduction
3	2.98	K-selectride	5	65	5.5	2.116	overreduction
4	2.98	K-selectride	10	40	48	2.116	s.m.
5	2.98	L-selectride	10	-45	5	2.116	50% conversion
6	2.99	L-selectride	10	-45	5	2.117	50% conversion
7	2.98	L-selectride	10	0	5	2.116	complete conversion, 77% isolated yield
8	2.99	L-selectride	10	0	2.5	2.117	85% conversion, 47% isolated yield
9	2.98	L-selectride	10	r.t.	4.5	2.116	overreduction

Optimized conditions, consisted of treating pyridones **2.98** and **2.99** with 10 equiv. of L-selectride at 0 °C. Although the 47% yield obtained in the case of tosyl-protected pyridone **2.99** was not synthetically tenable, it allowed us to access enough material to test the subsequent steps.

Each enamide was then oxidized with DMDO (Scheme 2.41). Tosyl-protected substrate **2.117** yielded a 1:1:1 mixture of enamide **2.114**, aminoepoxide **2.118** and a non-isolable product presumed to stem from epoxide **2.119**. Enamide substrate **2.117** showed a decrease in facial selectivity from the 9:1 demonstrated by Boc-protected substrate **2.100** to 2:1 in favor of oxidation from the bottom face.

Gratifyingly, treatment of methyl carbamate-protected substrate **2.116** with DMDO produced enamide **2.111** and the minor diastereomer (**2.120**) in a 6:1 ratio. Epoxide **2.121a** was not present in detectable amounts; it appeared to have undergone complete conversion to enamide tautomer **2.111** under the reaction conditions. Enamide **2.111** was isolated in 70% yield as a single diastereomer.

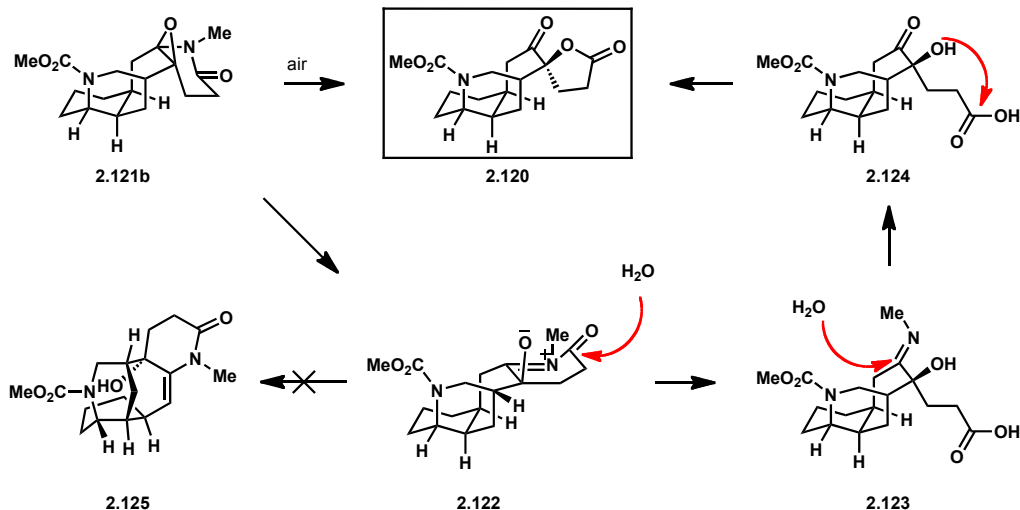
Scheme 2.41 Oxidation and rearrangement of enamides **2.116** and **2.117**.



This reaction also afforded an unexpected opportunity to isolate and characterize the minor product formed by the DMDO epoxidation of **2.116**. It was found that within one hour of exposure to atmospheric air and moisture, the minor product had undergone complete conversion to a lactone, spectral data for which were consistent with spirocycle **2.120**. This product is thought to arise from initial epoxidation of enamide **2.116** from the top face to afford epoxide **2.121b** (Scheme 2.42), followed by fragmentation to afford zwitterionic intermediate **2.122**. This activated intermediate could undergo hydrolysis of the amide bond to afford tricycle **2.123**, then a second hydrolysis of the imine to generate ketone **2.124**. Intramolecular lactonization of hydroxyacid **2.124** would afford lactone **2.120**.

Generation of a similar lactone product from enamide **2.111** was never observed, even after prolonged benchtop storage. Enamide **2.111** appeared to be indefinitely stable. By the same token, the enamide product **2.125** was never observed to arise from the minor product of a DMDO epoxidation of **2.116**. This difference in reactivity can be attributed to the high strain inherent in forming enamide **2.125** (see Scheme 2.42). Rather than undergoing a charge-quenching proton transfer, intermediate **2.122** could remain in activated zwitterionic form long enough for hydrolysis to occur.

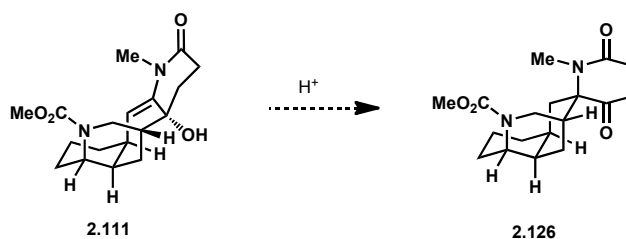
Scheme 2.42 Suspected reaction pathway of minor product.



A route was now in place to generate key enamide **2.111** as a single, clean product, which allowed us to study the ring-contractive rearrangement of **2.111** to form the core of nankakurine B.

The efficacy of protic acids to effect the rearrangement of **2.111** to **2.126** was tested first (Table 2.15). Treating **2.111** with *p*-toluenesulfonic acid at room temperature resulted in decomposition (entry 1). Utilizing hydrochloric acid in dioxane as solvent at 80 °C or TFA at 0 °C also resulted in decomposition (entries 2 and 3). $\text{HBF}_4 \cdot \text{OEt}_2$ was tested in the hopes that an acid with a non-coordinating conjugate base would mitigate some of the decomposition pathways; however, the result of this reaction was nonspecific decomposition (entry 4). Stirring **2.111** over silica gel as a mild proton source returned the starting material unchanged (entry 5).

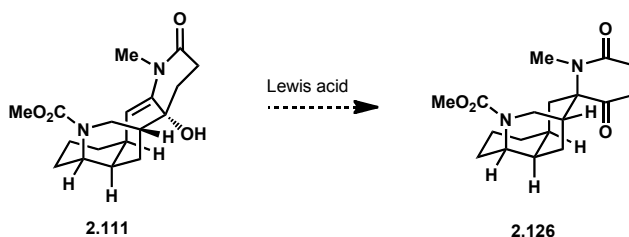
Table 2.15 Acidic conditions to effect the key step.



Entry	Acid	Solvent	Temp. (°C)	Result
1	<i>p</i> -TsOH	PhH	r.t.	decomp.
2	4.0 M HCl	dioxane	80	decomp.
3	TFA	DCM	0 - r.t.	decomp.
4	$\text{HBF}_4 \cdot \text{OEt}_2$	DCM	0	decomp.
5	SiO_2	DCM	r.t.	s.m.

Lewis acids were then tested (Table 2.16). Stirring enamide **2.111** with $\text{BF}_3 \cdot \text{OEt}_2$ returned starting material at -78 and at 0 °C (entries 1 and 2). At room temperature, this reagent caused decomposition of the substrate (entry 3). If the reaction was initiated at 0 °C and allowed to warm slowly to room temperature over the course of 3 hours, the methyl carbamate protecting group was cleaved, but none of the desired semipinacol reactivity was observed (entry 4). Employing $\text{Cu}(\text{OTf})_2$ led to the formation of multiple products, including partial oxidation of **2.111** to an aromatic product (entry 5). Heating enamide **2.111** in the presence of PtCl_2 or PdCl_2 at 80 °C resulted in recovery of starting material (entries 6 and 7). Increasing the temperature to 100 °C resulted in decomposition with PtCl_2 case, but still gave starting material with PdCl_2 (entries 8 and 9). Activation of the electron-rich enamide alkene with PtCl_2 and hydrochloric acid at 60 °C³³ resulted in decomposition (entry 10).

Table 2.16 Lewis acid screen to effect the key step.



Entry	Lewis Acid	Solvent	Temp. (°C)	Result
1	$\text{BF}_3 \cdot \text{OEt}_2$	DCM	-78	s.m.
2	$\text{BF}_3 \cdot \text{OEt}_2$	DCM	0	s.m.
3	$\text{BF}_3 \cdot \text{OEt}_2$	DCM	r.t.	decomp.
4	$\text{BF}_3 \cdot \text{OEt}_2$	DCM	0 - r.t.	removal of carbamate
5	$\text{Cu}(\text{OTf})_2$	DCM	-78	mult. prods including oxidation to aromaticity
6	PtCl_2	PhMe	80	s.m.
7	PdCl_2	PhMe	80	s.m.
8	PtCl_2	PhMe	100	decomp.
9	PdCl_2	PhMe	100	s.m.
10	$\text{PtCl}_2, \text{HCl}$	dioxane	60	decomp.

Several conditions that were neither acidic nor Lewis acidic were screened for suitability in initiating the key step (Table 2.17). Tertiary alcohols can be cleaved to generate radicals by stirring with hypervalent iodine reagents while irradiating with visible light.³⁴ We theorized that generating a radical at C-4 might induce the desired ring contraction. However, treating enamide **2.111** under these reaction conditions led to decomposition (entry 1).

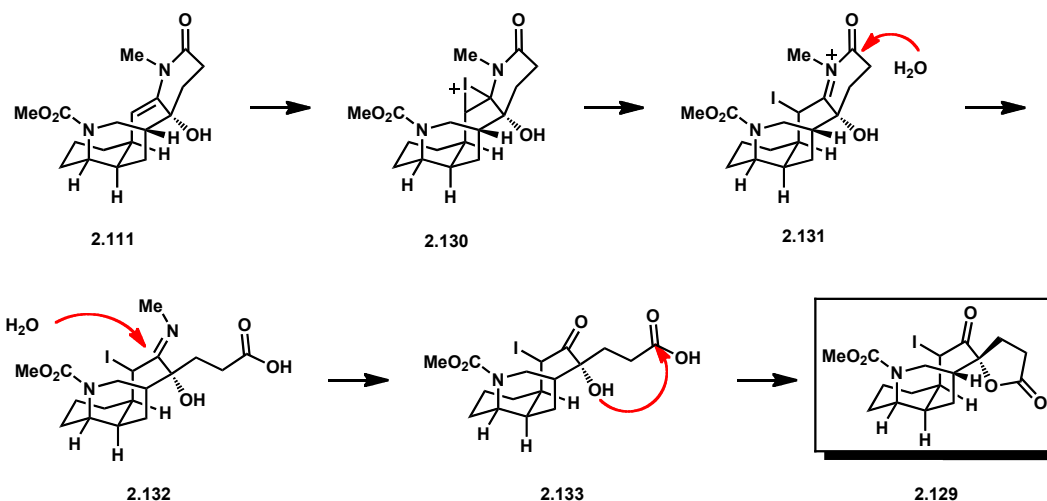
Electrophilic halogen sources were tested for their ability to activate the enamide double bond of **2.111** (Table 2.17). These reagents would generate halogenated products such as **2.127** after activation of the olefin and ring contraction; the halogen atom would be reductively cleaved at a later stage. Stirring **2.111** with NBS led to the formation of multiple products (entry 2). Utilizing molecular iodine with DBU led to decomposition (entry 3). Employing NIS in the presence of magnesium sulfate, however, led to the unexpected formation of product **2.129** (see Scheme 2.43).

Table 2.17 Miscellaneous conditions to effect the key step.

Entry	Reagent	Solvent	Temp. (°C)	Intended Product	Result
1	PhI(OAc) ₂ , visible light	DCM	r.t.	2.126	decomp.
2	NBS	DCM	-10	2.127	mult. prods
3	I ₂ , DBU	DCM	40	2.128	decomp.
4	NIS, MgSO ₄	DCM	-50	2.128	2.129

Iodide **2.43** is thought to arise from initial activation of the enamide double bond of **2.111** to give iodonium ion **2.130** (Scheme 2.43), which could be in equilibrium with iminium ion **2.131**. This activated intermediate could remain in the reaction flask until work-up, at which point water could hydrolyze first the amide bond to give imine **2.132**, which would subsequently be converted to ketoacid **2.133**. Lactonization of **2.133** would afford spirocyclic iodide **2.129**.

Scheme 2.43 Formation of iodide **2.129**.

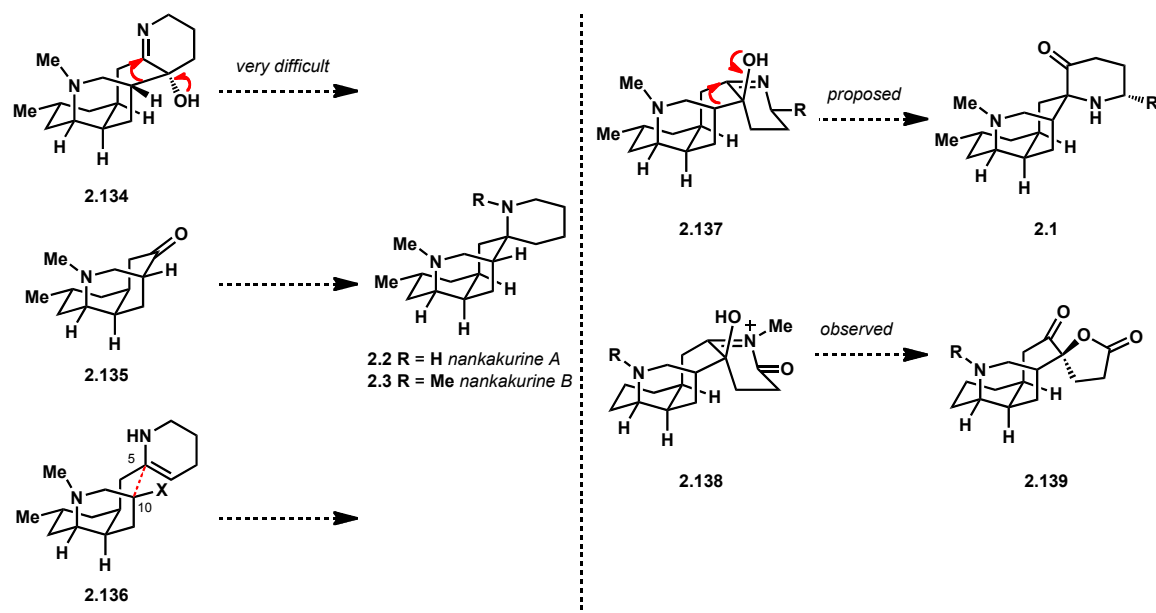


This result was very discouraging. Although it appeared that activation of the enamide double bond of **2.111** had been accomplished, the desired ring contraction had failed to take place. This suggested that the desired reaction pathway was significantly disfavored.

Having explored a variety of methods to effect the rearrangement of [6,6,7,6]-tetracyclic system **2.111** to [6,6,6,6]-spirocyclic system **2.126** without success, we concluded that this transformation is quite disfavored and would most likely proceed through a high-energy transition state. This has several implications for the proposed biogenesis of nankakurines A and B through the rearrangement of **2.134** (Scheme 2.44).³⁵ It may be more likely that nankakurine A arises from the elaboration of luciduline³⁶ (**2.135**) or *via* direct C-5 to C-10 bond formation of intermediate **2.136**, rather than through the ring-contractive rearrangement of an analogue of oxolucidine such as **2.134**. This could explain why such an analogue has never been isolated from nature.

This work also gives several insights into the proposed biosynthesis of spirolicidine (**2.1**). Spirolicidine has been proposed to arise from the ring-contractive rearrangement of **2.137**. However, every tetracyclic structure bearing oxygenation from the top face that was synthesized during this study was observed to undergo rapid hydrolysis of the enamide functionality rather than a ring-contractive rearrangement. This could indicate that this is not the synthetic path followed in nature, or that this reaction is mediated by an enzyme which suppresses hydrolysis and accelerates the ring contraction.

Scheme 2.44 Biosynthetic implications for nankakurines A and B and spirolicudine.



2.7 Conclusion

Key enamide intermediate **2.111** was synthesized and methods to effect its biomimetic conversion to the tetracyclic core of nankakurine A were extensively investigated. This transformation was found to be extremely difficult to achieve. A one-pot reaction for direct isomerization of 2-methoxypyridines to *N*-methylpyridones has been developed. The inherent facial selectivity of tetracycle **2.111** was studied and found to be up to 9:1 in favor of oxidation from the bottom face. Through this study, valuable insights have been gained into the potential biogenesis of the natural products spirolicudine and nankakurines A and B.

2.8 Experimental Contributions

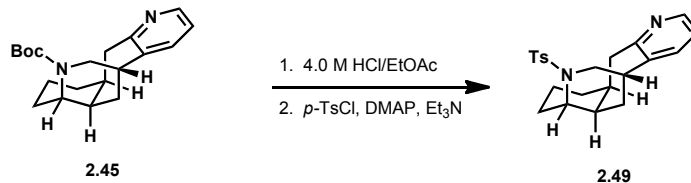
Significant contributions to this research were made by both Dr. Alakesh Bisai, a post-doctoral researcher in our group, and Scott West, a graduate student in our group. Drs. West and Bisai initially developed and executed the synthesis of common tetracyclic intermediate **2.14** (Schemes 2.2 and 2.4). All synthetic steps in this sequence were run according to methods developed by these investigators except for the cross metathesis of **2.15** (Table 2.1) and the hydrogenolysis studies and subsequent reductive amination of **2.29** (Table 2.2).

2.9 Experimental Methods

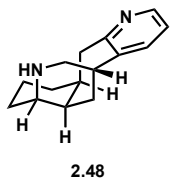
Materials and Methods

Unless otherwise stated, reactions were performed in oven-dried glassware fitted with rubber septa under a nitrogen atmosphere and were stirred with Teflon-coated magnetic stirring bars. Liquid reagents and solvents were transferred via syringe using standard Schlenk techniques. Tetrahydrofuran (THF) and diethyl ether (Et₂O) were distilled over sodium/benzophenone ketyl. Dichloromethane (CH₂Cl₂), toluene, and benzene were distilled over calcium hydride. Acetonitrile was distilled over potassium carbonate. *N,N*-Diisopropylethylamine (DIPEA) was distilled over calcium hydride prior to use. All other solvents and reagents were used as received unless otherwise noted. Reaction temperatures above 23 °C refer to oil bath temperature, which was controlled by an OptiCHEM temperature modulator. Thin layer chromatography was performed using SiliCycle silica gel 60 F-254 precoated plates (0.25 mm) and visualized by UV irradiation and anisaldehyde or potassium permanganate stain. SiliCycle Silia-P silica gel (particle size 40-63 μm) was used for flash chromatography. Melting points were recorded on a Laboratory Devices Mel-Temp 3.0 and are uncorrected. ¹H and ¹³C NMR spectra were recorded on Bruker AVB-400, DRX-500, AV-500 and AV-600 MHz spectrometers with ¹³C operating frequencies of 100, 125, 125 and 150 MHz, respectively. Chemical shifts (δ) are reported in ppm relative to the residual solvent signal (δ = 7.26 for ¹H NMR and δ = 77.0 for ¹³C NMR). Data for ¹H NMR spectra are reported as follows: chemical shift (multiplicity, coupling constants, number of hydrogens). Abbreviations are as follows: s (singlet), d (doublet), t (triplet), q (quartet), m (multiplet), br (broad). IR spectra were recorded on a Nicolet MAGNA-IR 850 spectrometer and are reported in frequency of absorption (cm⁻¹). Only selected IR absorbencies are reported. High resolution mass spectral data were obtained from the Mass Spectral Facility at the University of California, Berkeley.

Experimental Procedures

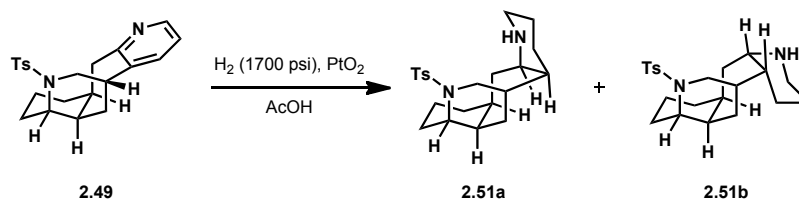


Pyridine 2.49: To a stirred solution of HCl (4.0 M in EtOAc, 300 μ L) was added pyridine **2.45** (14.7 mg, 0.0448 mmol). The solution was stirred for 3 h, at which point 3.0 M NaOH was added until the solution reached pH = 14 (1 mL). The mixture was extracted with DCM (3 x 10 mL). The combined organic extracts were dried over MgSO₄ filtered and concentrated under vacuum to afford 10.2 mg (83% yield) of tetracycle **2.48**. The crude material was used without purification in the next step.

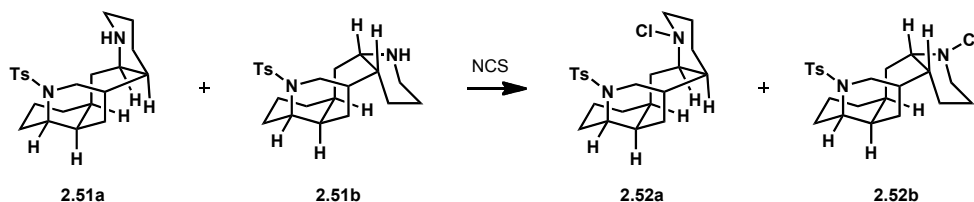


¹H NMR (500 MHz, CDCl₃) δ 7.31 (d, J = 4.8 Hz, 1H), 6.32 (d, J = 7.5 Hz, 1H), 6.04 – 5.96 (m, 1H), 3.82 (t, J = 13.9 Hz, 1H), 2.32 (d, J = 11.8 Hz, 1H), 2.25 (dd, J = 11.5, 4.4 Hz, 1H), 2.06 (s, 1H), 1.86 (dd, J = 15.2, 4.1 Hz, 1H), 1.73 (s, 1H), 1.13 (d, J = 12.8 Hz, 1H), 1.07 – 0.97 (m, 1H), 0.85 (d, J = 13.8 Hz, 3H), 0.70 (m, 4H), 0.46 – 0.35 (m, 2H).

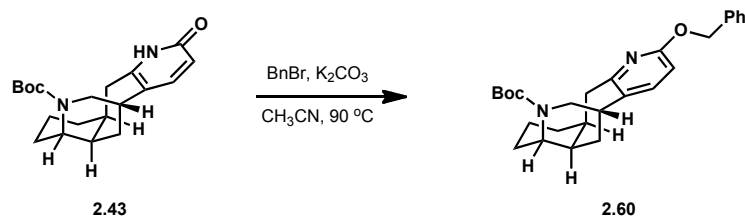
To a solution of tetracycle **2.48** (8.5 mg, 0.0372 mmol), DMAP (2.5 mg, 0.0205 mmol), and *p*-TsCl (22.0 mg, 0.115 mmol) in DCM (0.4 mL) was added triethylamine (30 μ L 0.216 mmol). The reaction was stirred at rt for 21h, then poured into 1.0 M NaOH (2 mL). The mixture was extracted with DCM (3 x 10 mL). The combined organic extracts were dried over MgSO₄ filtered and concentrated under vacuum. The crude material was purified by flash chromatography (49:1 DCM/MeOH to 19:1 DCM/MeOH) to afford 13.3 mg (94% yield) of pyridine **2.49** as a white solid. **¹H NMR** (500 MHz, CDCl₃) δ 8.47 – 8.23 (m, 1H), 7.64 (d, J = 8.2 Hz, 2H), 7.32 (d, J = 7.9 Hz, 3H), 7.02 (dd, J = 7.4, 4.9 Hz, 1H), 4.69 – 4.51 (m, 1H), 4.24 (d, J = 11.7 Hz, 1H), 3.48 (s, 1H), 2.93 (d, J = 18.1 Hz, 2H), 2.87 (dd, J = 15.7, 3.6 Hz, 1H), 2.78 (dd, J = 11.8, 4.4 Hz, 2H), 2.43 (s, 3H), 2.09 (m, 2H), 1.99 (br, s, 1H), 1.89 (m, 1H), 1.81 (d, J = 13.4 Hz, 2H), 1.69 (m, 1H), 1.55 – 1.44 (m, 2H).



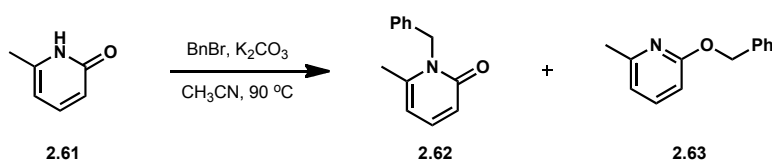
Piperidine 2.51: Pyridine **2.49** (6.8 mg, 0.0158 mmol) and PtO₂ (1.9 mg, 0.00837 mmol) were suspended in AcOH (400 μ L) and placed in a high pressure bomb. The bomb was evacuated and backfilled with hydrogen 3 times. The reaction mixture was placed under a hydrogen atmosphere (1700 psi) and stirred at rt for 1 d, then poured onto sat. KOH (0.3 mL). The mixture was extracted with DCM (3 x 10 mL) and EtOAc (3 x 10 mL). The combined organic extracts were dried over MgSO₄ filtered and concentrated under vacuum to afford 1.8 mg (30% yield) of piperidine **2.51** as a 3:1 mixture of diastereomers. The crude material was used in the next step without purification. Major diastereomer: ¹H NMR (500 MHz, CDCl₃) δ 7.65 (d, J = 8.2 Hz, 2H), 7.32 (d, J = 7.4 Hz, 2H), 4.18 (d, J = 11.8 Hz, 1H), 3.22 (dd, J = 10.4, 5.0 Hz, 1H), 3.16 – 2.97 (m, 1H), 2.89 – 2.65 (m, 3H), 2.42 (s, 3H), 2.21 (m, 1H), 2.08 (m, 2H), 1.98 (m, 3H), 1.86 – 1.30 (m, 9H), 0.91 – 0.80 (m, 2H). Minor diastereomer: ¹H NMR (diagnostic peaks) (500 MHz, CDCl₃) δ 3.87 (d, J = 11.1 Hz, 1H), 3.64 (dd, J = 16.1, 8.5 Hz, 1H), 3.00 (s, 1H), 2.40 (d, J = 2.8 Hz, 3H), 2.32 (dd, J = 11.0, 2.4 Hz, 1H).



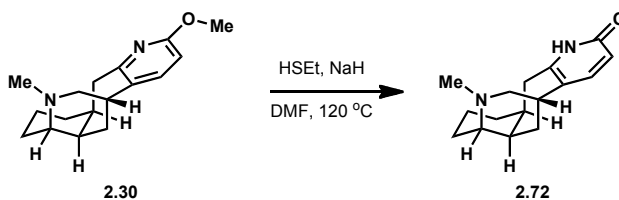
N-chloro tetracycle 2.52: A round-bottom flask was charged with piperidine **2.52** (1.8 mg, 0.00463 mmol), NCS (1.3 mg, 0.00974 mmol) and DCM (0.5 mL). The reaction was stirred for 6 h at rt. Volatiles were removed under vacuum and the residue was purified by flash chromatography (3:1 hexanes/EtOAc to 2:1 hexanes/EtOAc) to afford 1.4 mg (70% yield) of the major diastereomer of **2.52** and 0.4 mg (20% yield) of the minor diastereomer of **2.52**. Major product: ¹H NMR (500 MHz, CDCl₃) δ 7.70 (d, J = 8.1 Hz, 2H), 7.37 (d, J = 8.0 Hz, 2H), 3.91 (d, J = 11.1 Hz, 1H), 3.73 – 3.67 (m, 2H), 3.01 (t, J = 10.4 Hz, 2H), 2.86 (d, J = 15.4 Hz, 1H), 2.71 – 2.59 (m, 2H), 2.53 (d, J = 13.8 Hz, 1H), 2.48 (s, 3H), 2.36 (d, J = 8.7 Hz, 2H), 2.29 – 2.01 (m, 5H), 1.85 – 1.74 (m, 1H), 1.46 (m, 5H), 0.99 – 0.83 (m, 3H). Minor product: ¹H NMR (500 MHz, CDCl₃) δ 7.64 (d, J = 8.2 Hz, 2H), 7.33 (d, J = 8.1 Hz, 2H), 4.17 (d, J = 12.2 Hz, 1H), 3.37 (dd, J = 9.8, 4.4 Hz, 1H), 3.00 (m, 2H), 2.87 (d, J = 14.3 Hz, 1H), 2.76 (dd, J = 23.3, 13.1 Hz, 1H), 2.54 (br, s, 1H), 2.43 (s, 3H), 2.41 (d, J = 2.9 Hz, 1H), 2.17 (s, 1H), 2.12 (dd, J = 12.1, 3.6 Hz, 1H), 2.08 – 1.89 (m, 3H), 1.88 – 1.69 (m, 5H), 1.67 – 1.58 (m, 2H), 1.44 (d, J = 16.8 Hz, 1H), 1.36 – 1.29 (m, 2H), 0.85 (m, 1H).



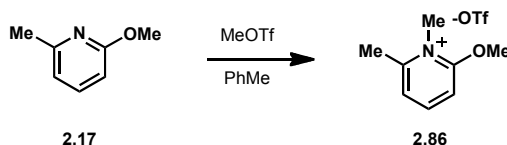
O-benzylated pyridine 2.60: To a stirred suspension of pyridone **2.43** (5.1 mg, 0.0145 mmol), K_2CO_3 (10.0 mg, 0.0724 mmol) and acetonitrile (2 mL) was added benzyl bromide (10 μL , 0.0841 mmol). The vial was sealed and heated at 90 $^\circ\text{C}$ for 4 h. The reaction was allowed to cool to rt and poured onto water (2 mL). The aqueous layer was extracted with EtOAc (3 x 10 mL), and the combined organic layers were dried over MgSO_4 filtered and concentrated under vacuum. The crude product was purified by flash chromatography (19:1 hexanes/EtOAc) to give 6.4 mg (quant. yield) of pyridine **2.60**. R_f 0.50 (9:1 hexanes/EtOAc); $^1\text{H NMR}$ (400 MHz, CDCl_3) δ 7.50 (d, $J = 7.6$ Hz, 2H), 7.40 (t, $J = 7.3$ Hz, 2H), 7.37 – 7.27 (m, 2H), 6.56 (d, $J = 8.1$ Hz, 1H), 5.38 (dd, $J = 12.3, 12.3$ Hz, 2H), 4.20 (d, $J = 13.6$ Hz, 1H), 3.82 (t, $J = 14.9$ Hz, 1H), 3.64 (br, s, 1H), 3.36 (dd, $J = 13.7, 5.2$ Hz, 1H), 2.95 – 2.76 (m, 3H), 2.20 – 1.98 (m, 4H), 1.85 (d, $J = 13.3$ Hz, 1H), 1.78 (m, 1H), 1.59 (m, 3H), 1.36 (s, 9H).



N-benzylpyridone 2.62 and O-benzylpyridine 2.63: A round-bottom flask equipped with a reflux condenser was charged with pyridone **2.61** (321.6 mg, 2.95 mmol), K_2CO_3 (636.5 mg, 4.61 mmol) and acetonitrile (30 mL). Benzyl bromide (540 μL , 4.61 mmol) was added, and the reaction mixture was heated at reflux for 6 h. The reaction was allowed to cool to rt and poured onto water (10 mL). The aqueous layer was extracted with EtOAc (3 x 25 mL), and the combined organic layers were dried over MgSO_4 , filtered and concentrated under vacuum. The crude product was purified by flash chromatography (19:1 hexanes/EtOAc to 1:1 hexanes/EtOAc) to afford 175 mg (30% yield) of pyridine **2.63** and 113 mg (20% yield) of pyridone **2.62**. Pyridine **2.63**: R_f 0.25 (33:1 DCM/MeOH); $^1\text{H NMR}$ (500 MHz, CDCl_3) δ 7.51 – 7.42 (m, 3H), 7.38 (dd, $J = 10.1, 4.6$ Hz, 2H), 7.31 (dd, $J = 13.9, 6.6$ Hz, 1H), 6.73 (d, $J = 7.2$ Hz, 1H), 6.60 (d, $J = 8.2$ Hz, 1H), 5.37 (s, 2H), 4.13 (q, $J = 7.1$ Hz, 1H), 2.47 (s, 3H). Pyridone **2.62**: R_f 0.84 (33:1 DCM/MeOH); $^1\text{H NMR}$ (500 MHz, CDCl_3) δ 7.31 (t, $J = 7.4$ Hz, 2H), 7.28 – 7.20 (m, 3H), 7.15 (d, $J = 7.4$ Hz, 2H), 6.55 (d, $J = 9.1$ Hz, 1H), 6.03 (d, $J = 6.8$ Hz, 1H), 5.36 (s, 2H), 2.27 (s, 3H).



Pyridone 2.72: A Schlenk flask was charged with NaH (25.7 mg, 60% dispersion in mineral oil, 0.643 mmol) and DMF (1 mL) and cooled to 0 °C. EtSH (90 μ L, 1.22 mmol) was added dropwise *via* syringe at 0 °C. Tetracycle **2.30** was dissolved in DMF (0.7 mL) and added dropwise to the reaction mixture. The reaction was stirred at 0 °C for 20 min, then allowed to warm to rt. The Schlenk tube was then sealed and heated at 120 °C for 12 hours. The reaction was allowed to cool to rt and quenched with H₂O (2 mL). The mixture was extracted with DCM (3 x 10 mL). The combined organic extracts were dried over MgSO₄, filtered and concentrated under vacuum to afford 12.0 mg (81% yield) of pyridone **2.72** as a white solid. The material was used in the next step without purification. *R_f* 0.31 (19:1 DCM/MeOH); ¹H NMR (400 MHz, CDCl₃) δ 11.65 – 11.60 (br s, 1H), 7.17 (d, *J* = 8.8 Hz, 1H), 6.30 (d, *J* = 9.1 Hz, 1H), 4.76 – 4.52 (t, *J* = 13.9 Hz, 1H), 2.90 (d, *J* = 11.3 Hz, 1H), 2.62 (br, s, 1H), 2.33 (dd, *J* = 11.4, 4.2 Hz, 1H), 2.27 (dd, *J* = 15.5, 3.5 Hz, 1H), 2.16 (d, *J* = 13.1 Hz, 2H), 2.10 (br, s, 1H), 2.06 (s, 3H), 1.96 – 1.83 (m, 2H), 1.81 – 1.55 (m, 5H), 1.37 (dd, *J* = 19.7, 8.2 Hz, 1H).

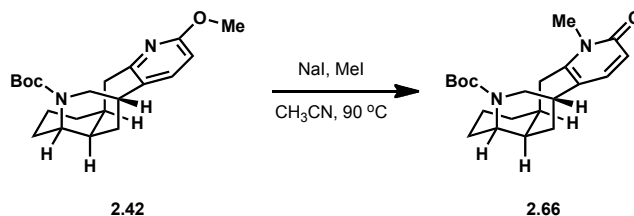


Triflate salt 2.86: A round-bottom flask was charged with methoxypyridine **2.17** (56.4 mg, 0.458 mmol) and toluene (2 mL). The solution was cooled to 0 °C and MeOTf (80 μ L, 0.707 mmol) was added dropwise. Solids began forming after 5 min. The ice bath was removed and the reaction was allowed to warm to rt. After 1 h, volatiles were removed to afford 127.5 mg (97% yield) of triflate salt **2.86** as a white solid. The material was used in the next step without purification. ¹H NMR (500 MHz, CDCl₃) δ 8.26 – 8.18 (m, 1H), 7.39 (d, *J* = 8.8 Hz, 1H), 7.32 (d, *J* = 7.7 Hz, 1H), 4.29 (s, 3H), 3.99 (s, 3H), 2.77 (s, 3H).

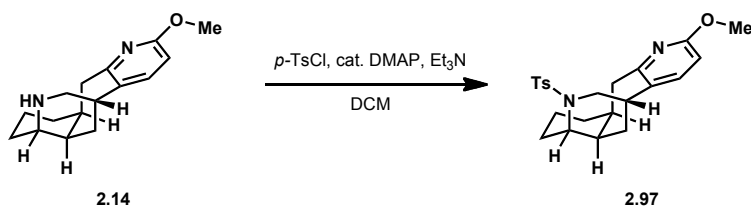


N-methylpyridone 2.87: Triflate salt **2.86** (8.4 mg, 0.0292 mmol) was suspended in DCM (0.5 mL) in a round-bottom flask open to atmosphere. NaI (7.2 mg, 0.0480 mmol) was added and the reaction was stirred for 24 h. The solution was poured onto water (2 mL) and extracted with EtOAc (3 x 10 mL). The combined organic

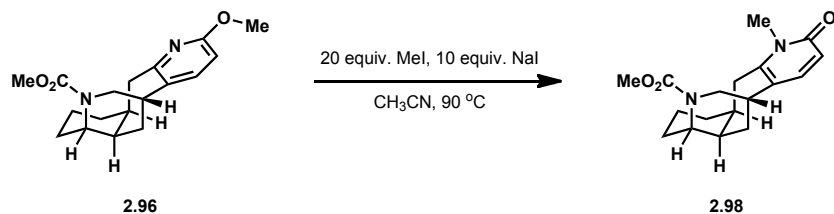
extracts were dried over MgSO_4 , filtered and concentrated under vacuum to afford 3.5 mg (quant. yield) of pyridone **2.87**. $^1\text{H NMR}$ (500 MHz, CDCl_3) δ 7.21 (dd, $J = 9.0, 6.9$ Hz, 1H), 6.47 (d, $J = 9.1$ Hz, 1H), 6.04 (d, $J = 6.8$ Hz, 1H), 3.53 (s, 3H), 2.35 (s, 3H).



3.79 (dd, $J = 26.1, 10.4$ Hz, 1H), 3.63 (d, $J = 3.5$ Hz, 1H), 3.57 (s, 3H), 3.39 (dd, $J = 13.7, 5.6$ Hz, 1H), 2.90 – 2.80 (m, 2H), 2.76 (dd, $J = 16.1, 4.1$ Hz, 1H), 2.16 – 1.99 (m, 3H), 1.94 (dd, $J = 19.7, 13.1$ Hz, 1H), 1.80 (d, $J = 11.5$ Hz, 1H), 1.77 – 1.69 (m, 2H), 1.64 – 1.47 (m, 2H); $^{13}\text{C NMR}$ (151 MHz, CDCl_3) δ 161.56, 157.67, 155.96, 141.12, 132.36, 106.82, 57.04, 53.19, 52.10, 50.59, 43.81, 38.67, 38.30, 34.74, 34.41, 33.30, 30.43, 17.71; **IR** (film) ν_{max} 2923, 1709, 1596, 1477, 1303, 1258, 1224, 1190, 1088, 1034 cm^{-1} ; **HRMS** (ESI) m/z 317.1863 [(M+H) $^+$]; calculated for $[\text{C}_{18}\text{H}_{25}\text{N}_2\text{O}_3]^+$: 317.1860]; **MP** 111 – 114 $^\circ\text{C}$.

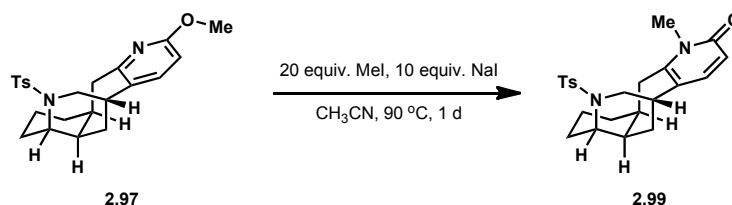


Tosyl-protected tetracycle 2.97: To a stirred solution of tetracycle **2.14** (21.1 mg, 0.0817 mmol), *p*-TsCl (30.1 mg, 0.158 mmol) and DMAP (2.8 mg, 0.0229 mmol) in DCM (1 mL) was added triethylamine (30 μL , 0.214 mmol). The reaction was stirred for 14 h, then poured into a 1:1 mixture of 3.0 M NaOH and brine (3 mL) and extracted with DCM (3 x 10 mL). The combined organic extracts were dried over MgSO_4 , filtered and concentrated under vacuum. The crude material was purified by flash chromatography (19:1 DCM/MeOH) to afford 26.5 mg (80% yield) of tetracycle **2.97**. R_f 0.19 (19:1 DCM/MeOH); $^1\text{H NMR}$ (600 MHz, CDCl_3) δ 7.63 (d, $J = 8.3$ Hz, 2H), 7.31 (t, $J = 10.0$ Hz, 2H), 7.21 (t, $J = 8.7$ Hz, 1H), 6.47 – 6.42 (m, 1H), 4.50 (dd, $J = 15.4, 13.9$ Hz, 1H), 4.17 (dt, $J = 11.5, 1.8$ Hz, 1H), 3.91 (s, 3H), 2.93 (d, $J = 12.7$ Hz, 1H), 2.88 – 2.84 (m, 1H), 2.78 – 2.67 (m, 3H), 2.42 (d, $J = 7.3$ Hz, 3H), 2.19 – 2.07 (m, 2H), 1.98 (d, $J = 2.6$ Hz, 1H), 1.89 – 1.77 (m, 3H), 1.68 (tt, $J = 13.5, 4.1$ Hz, 1H), 1.53 – 1.43 (m, 2H); $^{13}\text{C NMR}$ (151 MHz, CDCl_3) δ 161.70, 158.54, 143.33, 141.30, 133.28, 131.39, 129.52, 127.83, 106.75, 59.10, 55.64, 53.22, 43.89, 39.90, 39.37, 35.29, 34.77, 34.20, 31.94, 21.49, 16.59; **IR** (film) ν_{max} 2925, 1599, 1574, 1479, 1424, 1324, 1302, 1266, 1155, 1089, 1053 cm^{-1} ; **HRMS** (ESI) m/z 413.1887 [(M+H) $^+$]; calculated for $[\text{C}_{23}\text{H}_{29}\text{N}_2\text{O}_3\text{S}]^+$: 413.1893]. **MP** decomp. 258- 259 $^\circ\text{C}$.

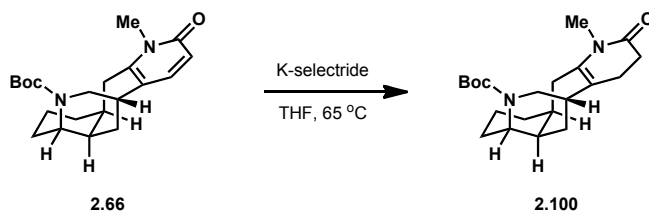


Tetracyclic pyridone 2.98: To a suspension of tetracycle **2.96** (466.9 mg, 1.49 mmol) and NaI (1.144 g, 7.64 mmol) in CH_3CN (10.5 mL) was added MeI (1.9 mL, 30.5 mmol). The vial was sealed and heated at 90 $^\circ\text{C}$ for 9 h until TLC showed complete consumption of starting material. The orange suspension was poured into a 1:1 mixture of sat. NaHCO_3 and sat. NaHSO_3 (20 mL) and extracted with DCM (3 x

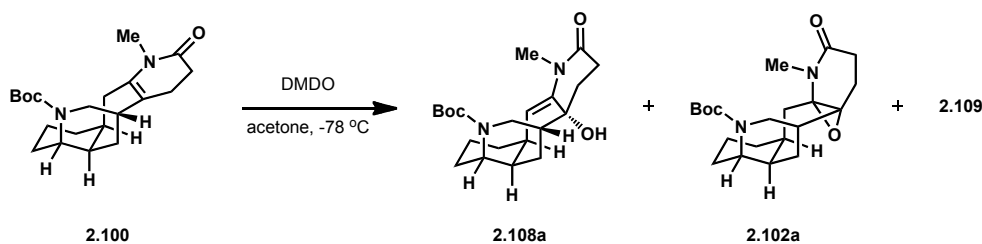
50 mL). The combined organic extracts were dried over MgSO_4 , filtered and concentrated under vacuum. The crude material was purified by flash chromatography (49:1 DCM/MeOH) to afford 430 mg (92% yield) of pyridone **2.98** as a white solid. R_f 0.21 (19:1 DCM/MeOH); $^1\text{H NMR}$ (500 MHz,) δ 7.04 (d, J = 9.2 Hz, 1H), 6.38 (d, J = 9.2 Hz, 1H), 4.24 – 4.15 (m, 1H), 3.61 (s, 3H), 3.59 (s, 3H), 3.56 (d, J = 6.9 Hz, 1H), 3.26 (dd, J = 13.7, 5.1 Hz, 1H), 2.95 (d, J = 11.6 Hz, 1H), 2.82 (dd, J = 16.8, 3.8 Hz, 1H), 2.74 (br, s, 1H), 2.07 – 1.94 (m, 3H), 1.94 – 1.67 (m, 5H), 1.56 (m, 2H); $^{13}\text{C NMR}$ (126 MHz,) δ 163.33, 155.90, 148.10, 142.91, 122.81, 116.75, 57.24, 52.23, 51.29, 39.13, 38.28, 35.47, 34.62, 34.38, 34.09, 32.31, 30.52, 17.60; **IR** (film) ν_{max} 2921, 1705, 1657, 1587, 1533, 1440, 1417, 1300, 1192, 1085 cm^{-1} ; **HRMS** (ESI) m/z 317.1861 [(M+H) $^+$]; calculated for $[\text{C}_{18}\text{H}_{25}\text{N}_2\text{O}_3]^+$: 317.1860]; **MP** 182 – 184 $^\circ\text{C}$.



Tetracyclic pyridone 2.99: To a suspension of tetracycle **2.97** (17.0 mg, 0.0412 mmol) and NaI (100 mg, 0.667 mmol) in CH_3CN (2.6 mL) was added MeI (200 μL , 3.21 mmol). The vial was sealed and heated at 90 $^\circ\text{C}$ for 20 h until TLC showed complete consumption of starting material. The orange suspension was poured into a 1:1 mixture of sat. NaHCO_3 and sat. NaHSO_3 (2 mL) and extracted with DCM (3 x 10 mL). The combined organic extracts were dried over MgSO_4 , filtered and concentrated under vacuum to afford 15.1 mg (89% yield) of tetracycle **2.99** as a white solid. The material was used in the next step without purification. R_f 0.23 (19:1 DCM/MeOH); $^1\text{H NMR}$ (600 MHz, CDCl_3) δ 7.62 (d, J = 8.1 Hz, 2H), 7.32 (d, J = 8.1 Hz, 2H), 7.01 (d, J = 9.2 Hz, 1H), 6.37 (d, J = 9.1 Hz, 1H), 4.34 (dd, J = 16.4, 13.0 Hz, 1H), 4.16 (d, J = 11.6 Hz, 1H), 3.64 (s, 3H), 2.94 (d, J = 12.7 Hz, 1H), 2.83 (dd, J = 16.5, 3.5 Hz, 1H), 2.75 (s, 1H), 2.67 (d, J = 1.9 Hz, 1H), 2.64 (dd, J = 11.7, 4.2 Hz, 1H), 2.42 (s, 3H), 2.11 (m, 1H), 2.03 (d, J = 12.8 Hz, 1H), 1.96 (s, 1H), 1.85 – 1.68 (m, 4H), 1.59 – 1.52 (m, 1H), 1.48 (m, 1H); $^{13}\text{C NMR}$ (151 MHz, CDCl_3) δ 163.33, 149.22, 143.65, 142.88, 129.62, 127.81, 121.93, 116.55, 99.95, 58.86, 55.39, 39.64, 39.45, 36.02, 34.92, 34.82, 34.68, 32.44, 31.81, 21.49, 16.57; **IR** (film) ν_{max} 2915, 1659, 1593, 1535, 1452, 1415, 1330, 1160, 1084, 1043 cm^{-1} ; **HRMS** (ESI) m/z 413.1889 [(M+H) $^+$]; calculated for $[\text{C}_{23}\text{H}_{29}\text{N}_2\text{O}_3\text{S}]^+$: 413.1893]; **MP** decomp. 222 – 223 $^\circ\text{C}$.

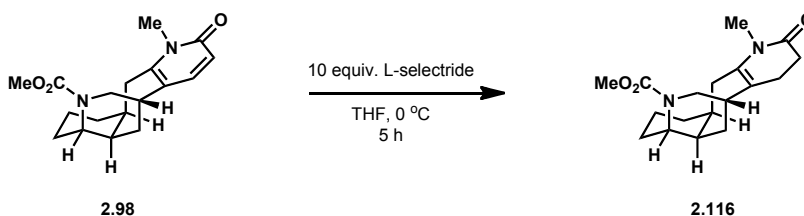


Enamide 2.100: To a solution of pyridone **2.66** (14.3 mg, 0.0399 mmol) in THF (0.5 mL) was added K-selectride (210 μL , 1.0M solution in THF, 0.210 mmol) and the vial was sealed and heated at 60 $^\circ\text{C}$ for 19 h. The reaction was cooled to 0 $^\circ\text{C}$ and quenched by dropwise addition of brine (0.21 mL), 30% aq. H_2O_2 (0.53 mL) and 3.0 M NaOH (0.21 mL). The mixture was allowed to warm to rt, then extracted with DCM (3 x 15 mL). The combined aqueous extracts were dried over MgSO_4 , filtered and concentrated under vacuum to afford 13.8 mg (96% yield) of enamide **2.100** as a foam. The material was used in the next step without purification. R_f 0.25 (19:1 DCM/MeOH); $^1\text{H NMR}$ (400 MHz, CDCl_3) δ 4.32 (d, $J = 13.3$ Hz, 1H), 3.41 (br, s, 1H), 3.04 (s, 3H), 3.01 – 2.78 (m, 3H), 2.46 – 2.38 (m, 2H), 2.22 (m, 4H), 2.07 – 1.94 (m, 1H), 1.90 (m, 2H), 1.80 (m, 2H), 1.70 – 1.58 (m, 2H), 1.52 (m, 2H), 1.41 (s, 9H); $^{13}\text{C NMR}$ (126 MHz, CDCl_3) δ 171.64, 154.00, 135.68, 124.15, 79.27, 57.59, 51.81, 39.58, 39.16, 36.02, 34.28, 33.44, 33.16, 32.28, 30.52, 30.34, 29.00, 28.53, 18.12; **IR** (film) ν_{max} 3359, 2972, 2926, 1699, 1423, 1365, 1314, 1251, 1162, 1076 cm^{-1} ; **HRMS** (ESI) m/z 361.2491 [(M+H) $^+$; calculated for $[\text{C}_{21}\text{H}_{33}\text{N}_2\text{O}_3]^+$: 361.2486].

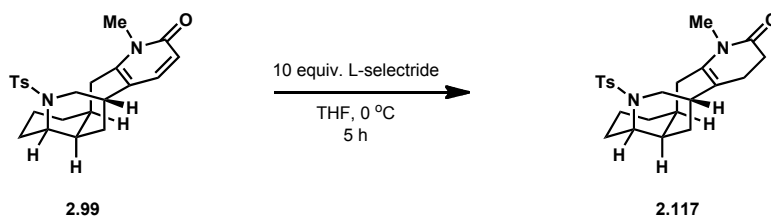


Enamide 2.102a: A vial was charged with enamide **2.100** (50.8 mg, 0.141 mmol) and acetone (1.7 mL). The reaction was cooled to -78 $^\circ\text{C}$ and DMDO (5.3 mL, 0.0525 M in acetone, 0.278 mmol) was added dropwise over 10 min. The reaction was stirred at -78 $^\circ\text{C}$ for 1 h, then allowed to warm to rt. Volatiles were removed under vacuum to afford 54 mg (quant. yield) of enamide **2.108a**, epoxide **2.102a** and minor product **2.109** in a 6:3:1 ratio. A sample of enamide **2.108a** was purified by flash chromatography (99:1 DCM/MeOH) for analysis. Enamide **2.108a**: R_f 0.21 (19:1 DCM/MeOH); $^1\text{H NMR}$ (500 MHz, CDCl_3) δ 4.98 (s, 1H), 4.13 (d, $J = 14.3$ Hz, 1H), 3.50 – 3.41 (m, 1H), 3.17 – 3.07 (m, 4H), 2.88 (d, $J = 13.5$ Hz, 1H), 2.82 (s, 1H), 2.79 – 2.69 (m, 1H), 2.60 (d, $J = 12.7$ Hz, 1H), 2.50 – 2.43 (m, 1H), 2.19 (m, 1H), 1.96 – 1.80 (m, 3H), 1.76 (s, 2H), 1.71 – 1.41 (m, 4H), 1.39 (s, 9H); $^{13}\text{C NMR}$ (126 MHz,) δ 170.37, 154.44, 142.00, 118.50, 79.39, 73.31, 57.04, 46.67, 40.38, 37.35, 36.46, 35.17, 32.95, 32.04, 30.90, 30.41, 28.52, 28.36, 18.63; **IR** (film) ν_{max} 3398, 2931, 1669, 1627, 1420, 1365, 1162, 1080 cm^{-1} ; **HRMS** (ESI) m/z 399.2264 [(M+Na) $^+$; calculated for $[\text{C}_{21}\text{H}_{32}\text{N}_2\text{O}_4\text{Na}]^+$: 399.2254]. COSY, HMQC, HMBC and NOESY data for

2.108a is included with ^1H and ^{13}C . Epoxide **2.102a**: R_f 0.21 (19:1 DCM/MeOH); ^1H NMR (diagnostic peaks) (400 MHz, CDCl_3) δ 4.21 (dd, $J = 14.6, 4.6$ Hz, 1H), 3.61 – 3.54 (m, 1H), 3.41 (dd, $J = 14.6, 6.7$ Hz, 1H), 3.21 (s, 3H), 2.40 – 2.32 (m, 2H), 1.46 (s, 9H).

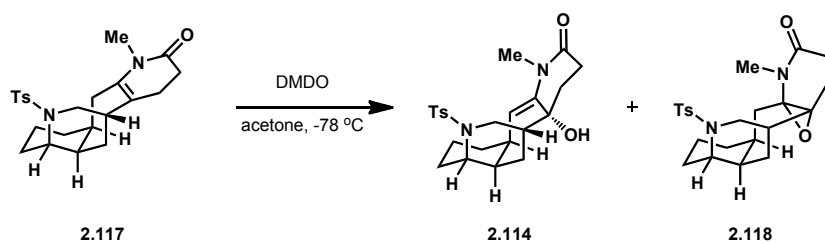


Enamide 2.116: A round-bottom flask was charged with pyridone **2.98** (15.7 mg, 0.496 mmol) and THF (0.30 mL). The reaction was cooled to 0 °C and L-selectride (250 μL , 1.0M solution in THF, 0.250 mmol) was added dropwise over 5 min. The reaction was stirred at 0 °C for 4 h. A second portion of L-selectride (250 μL , 1.0M solution in THF, 0.250 mmol) was added dropwise over 5 min. The reaction was stirred at 0 °C for a further 4 h, then quenched by dropwise addition of brine (0.50 mL), 30% aq. H_2O_2 (1.25 mL) and 3.0 M NaOH (0.50 mL). The mixture was allowed to warm to rt, then extracted with DCM (3 x 15 mL). The combined organic extracts were dried over MgSO_4 , filtered and concentrated under vacuum. The crude material was purified by flash chromatography (DCM to 49:1 DCM/MeOH) to afford 12.1 mg (77% yield) of enamide **2.116** as a foam. R_f 0.17 (19:1 DCM/MeOH); ^1H NMR (600 MHz, CDCl_3) δ 4.30 (d, $J = 13.3$ Hz, 1H), 3.61 (s, 3H), 3.45 (s, 1H), 3.04 (s, 3H), 2.97 (dd, $J = 13.3, 3.5$ Hz, 1H), 2.88 (m, 2H), 2.43 – 2.20 (m, 5H), 2.16 – 2.08 (m, 1H), 2.04 – 1.93 (m, 1H), 1.91 (m, 2H), 1.83 (m, 2H), 1.69 – 1.59 (m, 2H), 1.56 – 1.44 (m, 2H); ^{13}C NMR (151 MHz, CDCl_3) δ 171.69, 155.07, 135.89, 124.36, 57.90, 52.02, 51.73, 39.33, 38.97, 35.75, 34.11, 33.32, 33.02, 32.28, 30.64, 30.13, 28.73, 17.81; IR (film) ν_{max} 3481, 2914, 1705, 1668, 1440, 1377, 1327, 1225, 1194, 1087, 1033 cm^{-1} ; HRMS (ESI) m/z 319.2022 [(M+H) $^+$; calculated for $[\text{C}_{18}\text{H}_{27}\text{N}_2\text{O}_3]^+$: 319.2016].

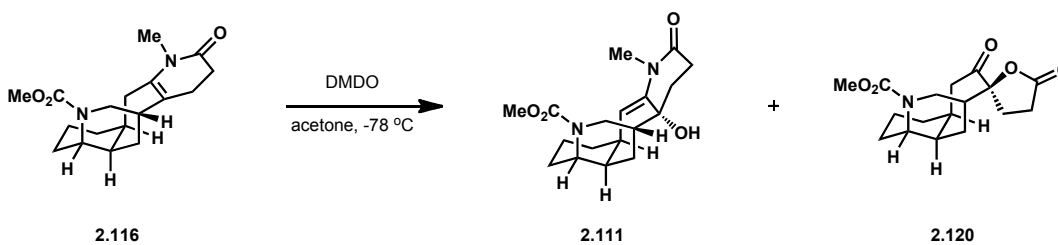


Enamide 2.117: A round-bottom flask was charged with pyridone **2.99** (5.1 mg, 0.0124 mmol) and THF (0.30 mL). The reaction was cooled to 0 °C and L-selectride (1.0M solution in THF, 120 μL , 0.120 mmol) was added dropwise over 5 mins. The reaction was stirred at 0 °C for 2.5 h, then quenched by dropwise addition of brine (0.12 mL), 30% aq. H_2O_2 (0.30 mL) and 3.0 M NaOH (0.12 mL). The mixture was allowed to warm to r.t., then extracted with DCM (3 x 10 mL). The combined organic extracts were dried over MgSO_4 , filtered and concentrated under vacuum.

The crude material was purified by flash chromatography (DCM to 49:1 DCM/MeOH) to afford 2.5 mg (49% yield) of enamide **2.117** as a foam. R_f 0.17 (19:1 DCM/MeOH); $^1\text{H NMR}$ (500 MHz, CDCl_3) δ 7.67 (d, $J = 8.4$ Hz, 2H), 7.33 (d, $J = 7.7$ Hz, 2H), 4.15 (dd, $J = 25.5, 12.0$ Hz, 1H), 3.67 (dd, $J = 18.3, 10.5$ Hz, 1H), 3.08 (s, 3H), 2.86 (d, $J = 14.9$ Hz, 1H), 2.75 – 2.64 (s, 1H), 2.54 (dd, $J = 11.4, 3.6$ Hz, 1H), 2.49 – 2.38 (m, 4H), 2.23 (m, 4H), 2.13 – 1.99 (m, 1H), 1.91 (s, 2H), 1.79 (d, $J = 12.1$ Hz, 1H), 1.68 (m, 3H), 1.50 – 1.41 (m, 2H).

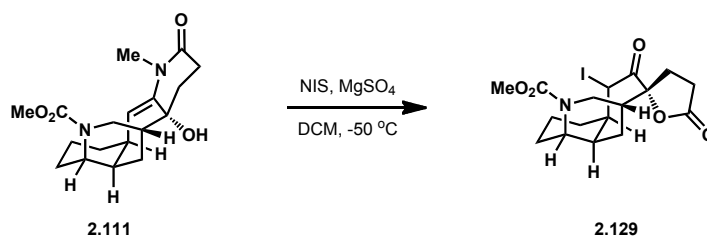


Enamide 2.114: A vial was charged with enamide **2.117** (2.5 mg, 0.00603 mmol) and acetone (350 μL). The reaction was cooled to $-78\text{ }^\circ\text{C}$ and DMDO (150 μL , 0.0645 M in acetone, 0.00967 mmol) was added dropwise. The reaction was stirred at $-78\text{ }^\circ\text{C}$ for 1 h, then allowed to warm to rt. Volatiles were removed under vacuum and the material was purified by flash chromatography (99:1 DCM/MeOH to 49:1 DCM/MeOH) to afford 0.3 mg (20% yield) of enamide **2.114** and 0.8 mg (30% yield) of aminoepoxide **2.118**. Enamide **2.114:** R_f 0.17 (19:1 DCM/MeOH); $^1\text{H NMR}$ (500 MHz, CDCl_3) δ 7.58 (d, $J = 8.2$ Hz, 2H), 7.31 (d, $J = 7.9$ Hz, 2H), 5.11 (d, $J = 2.9$ Hz, 1H), 4.05 (d, $J = 13.2$ Hz, 1H), 3.28 (s, 3H), 2.86 (s, 2H), 2.73 – 2.64 (m, 2H), 2.62 (br, s, 1H), 2.58 – 2.44 (m, 3H), 2.43 (s, 3H), 2.18 (dd, $J = 15.0, 12.2$ Hz, 2H), 1.86 (br, s, 2H), 1.80 (s, 1H), 1.74 (s, 1H), 1.63 (m, 3H), 1.42 (m, 2H). Aminoepoxide **2.118:** R_f 0.27 (19:1 DCM/MeOH); $^1\text{H NMR}$ (600 MHz, CDCl_3) δ 7.66 (d, $J = 8.3$ Hz, 2H), 7.37 (d, $J = 8.1$ Hz, 2H), 4.42 (d, $J = 12.7$ Hz, 1H), 3.57 – 3.49 (m, 1H), 3.24 – 3.19 (s, 3H), 2.96 – 2.87 (m, 1H), 2.62 (d, $J = 5.5$ Hz, 1H), 2.48 – 2.31 (m, 9H), 2.20 (d, $J = 25.0$ Hz, 1H), 1.75 (m, 2H), 1.52 – 1.34 (m, 1H), 0.88 (t, $J = 7.0$ Hz, 1H).



Enamide 2.111: A vial was charged with enamide **2.116** (38.6 mg, 0.121 mmol) and acetone (2.0 mL). The reaction was cooled to $-78\text{ }^\circ\text{C}$ and DMDO (3.8 mL, 0.0645 M in acetone, 0.245 mmol) was added dropwise over 10 min. The reaction was stirred at $-78\text{ }^\circ\text{C}$ for 1 h, then allowed to warm to rt. Volatiles were removed under vacuum and the material was purified by flash chromatography (99:1 DCM/MeOH to 49:1 DCM/MeOH) to afford 28.4 mg (70% yield) of enamide **2.111** and 4.0 mg (10% yield) of lactam **2.120**. Enamide **2.111:** R_f 0.20 (19:1 DCM/MeOH); $^1\text{H NMR}$

(500 MHz, CDCl₃) δ 4.97 (d, J = 2.6 Hz, 1H), 4.21 (dd, J = 14.5, 2.4 Hz, 1H), 3.54 (s, 3H), 3.48 (d, J = 3.5 Hz, 1H), 3.11 (dd, J = 14.5, 4.3 Hz, 1H), 3.08 (s, 3H), 2.93 (dd, J = 14.0, 2.5 Hz, 1H), 2.84 (s, 1H), 2.78 – 2.64 (m, 2H), 2.47 (dt, J = 16.5, 3.4 Hz, 1H), 2.17 (tt, J = 13.6, 6.8 Hz, 1H), 2.06 – 1.92 (m, 1H), 1.91 – 1.82 (m, 1H), 1.82 – 1.70 (m, 2H), 1.70 – 1.54 (m, 4H), 1.53 – 1.44 (m, 1H); ¹³C NMR (126 MHz,) δ 170.61, 142.46, 118.51, 73.36, 57.70, 51.94, 46.72, 39.94, 37.38, 36.15, 34.98, 33.04, 31.99, 31.32, 30.13, 29.70, 28.48, 18.70; IR (film) ν_{max} 3369, 2924, 2855, 1669, 1627, 1456, 1417, 1261, 1178, 1125, 1084 cm⁻¹; HRMS (ESI) m/z 335.1967 [(M+H)⁺; calculated for [C₁₈H₂₇N₂O₄]⁺: 335.1965]. Lactam **2.120**: ¹H NMR (500 MHz, CDCl₃) δ 4.32 (dd, J = 14.6, 2.5 Hz, 1H), 3.70 (s, 3H), 3.58 – 3.51 (m, 1H), 3.36 – 3.26 (m, 2H), 2.81 (dd, J = 13.5, 2.5 Hz, 1H), 2.51 – 2.43 (m, 2H), 2.42 – 2.34 (m, 2H), 2.31 – 2.18 (m, 2H), 2.17 – 2.07 (m, 1H), 2.05 – 1.86 (m, 3H), 1.77 – 1.62 (m, 3H), 1.56 – 1.42 (m, 2H); ¹³C NMR (151 MHz, CDCl₃) δ 206.18, 175.53, 155.82, 92.64, 56.68, 52.53, 45.65, 43.73, 37.73, 36.52, 36.01, 32.63, 31.26, 30.56, 29.06, 27.91, 17.31.



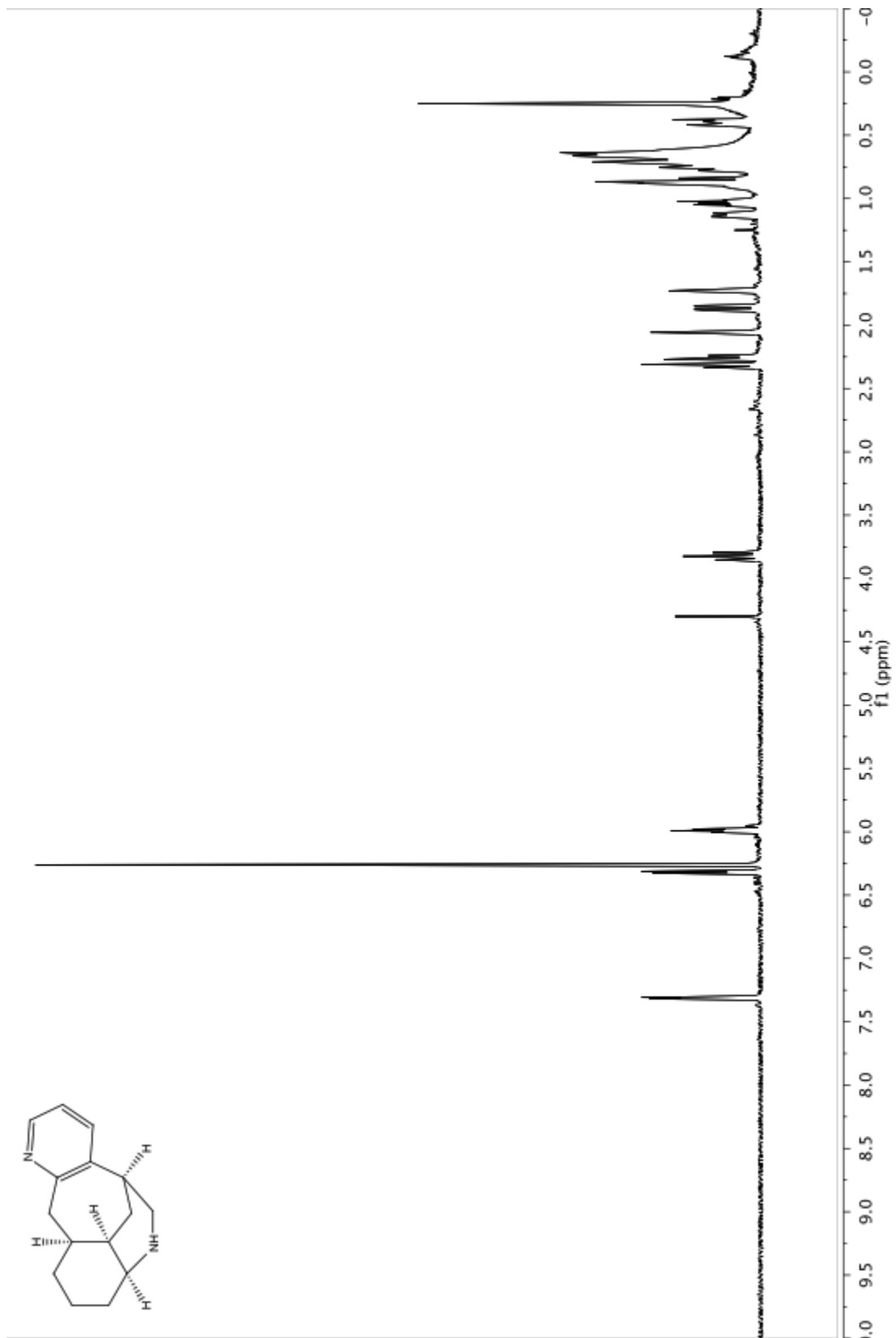
Iodide 2.129: A vial was charged with NIS (2.9 mg, 0.0129 mmol), MgSO₄ (21.7 mg, 0.180 mmol) and DCM (0.5 mL). The reaction mixture was cooled to -50 °C and a solution of enamide **2.111** (1.8 mg, 0.00538 mmol) in DCM (0.2 mL) was added dropwise. The reaction was allowed to warm to rt and stirred for 12h. The reaction mixture was poured into brine (2 mL) and extracted with DCM (3 x 10 mL). The combined organic extracts were dried over MgSO₄, filtered and concentrated under vacuum to afford 2 mg (83% yield) of iodide **2.129**. R_f 0.20 (19:1 DCM/MeOH); ¹H NMR (600 MHz,) δ 4.53 (s, 1H), 3.44 (s, 3H), 3.21 (d, J = 2.2 Hz, 2H), 3.17 (s, 1H), 3.02 (ddd, J = 12.4, 10.2, 6.4 Hz, 1H), 2.94 – 2.87 (m, 1H), 2.59 – 2.49 (m, 2H), 2.37 (m, 2H), 2.00 (d, J = 5.5 Hz, 1H), 1.90 (d, J = 2.9 Hz, 1H), 1.86 – 1.75 (m, 3H), 1.71 – 1.61 (m, 2H), 1.51 (m, 2H); ¹³C NMR (151 MHz, CDCl₃) δ 176.81, 176.45, 167.88, 99.98, 85.17, 73.08, 62.44, 57.92, 46.16, 44.62, 39.57, 38.99, 33.23, 31.38, 29.82, 28.77, 17.52.

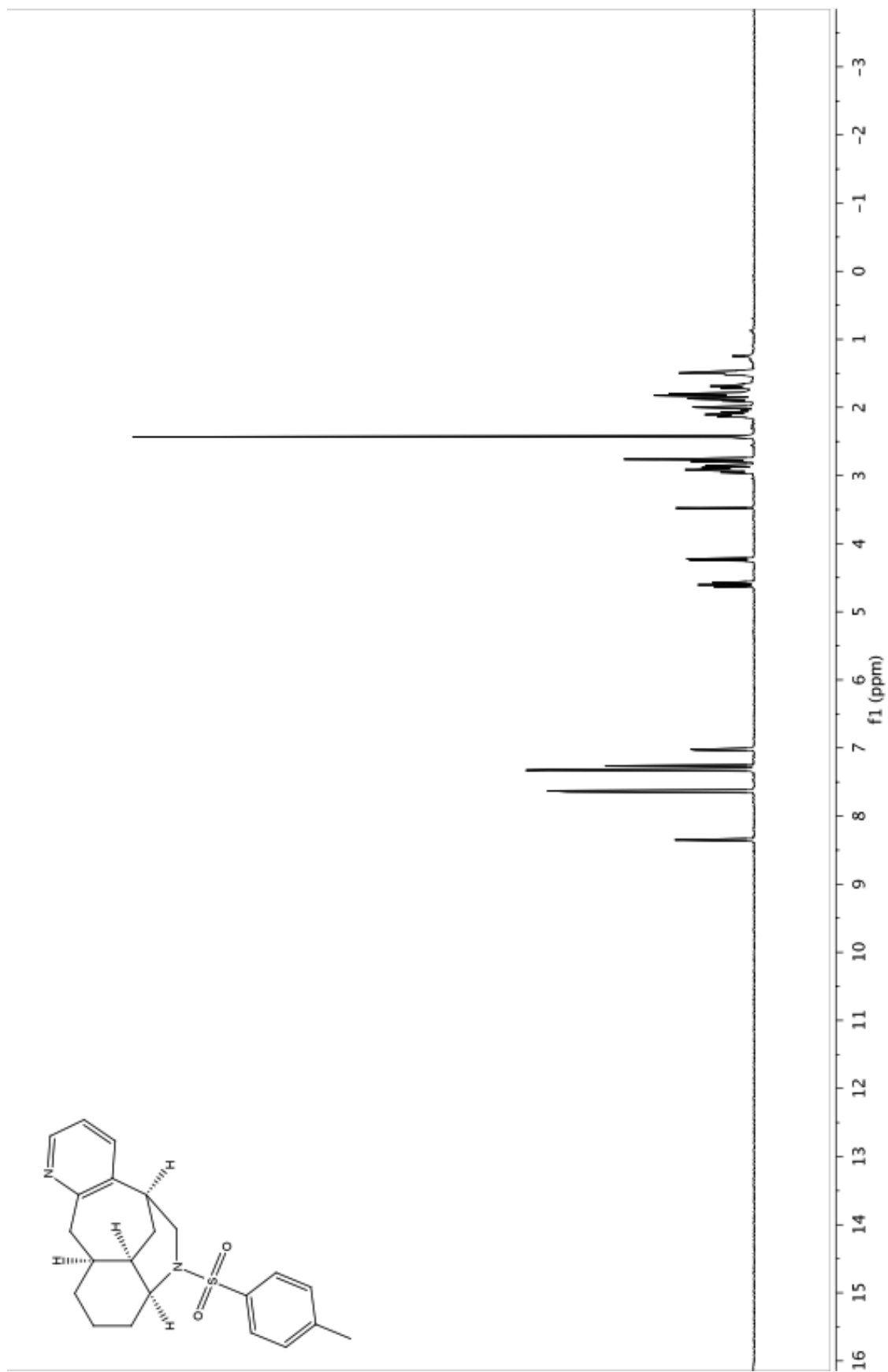
2.10 References

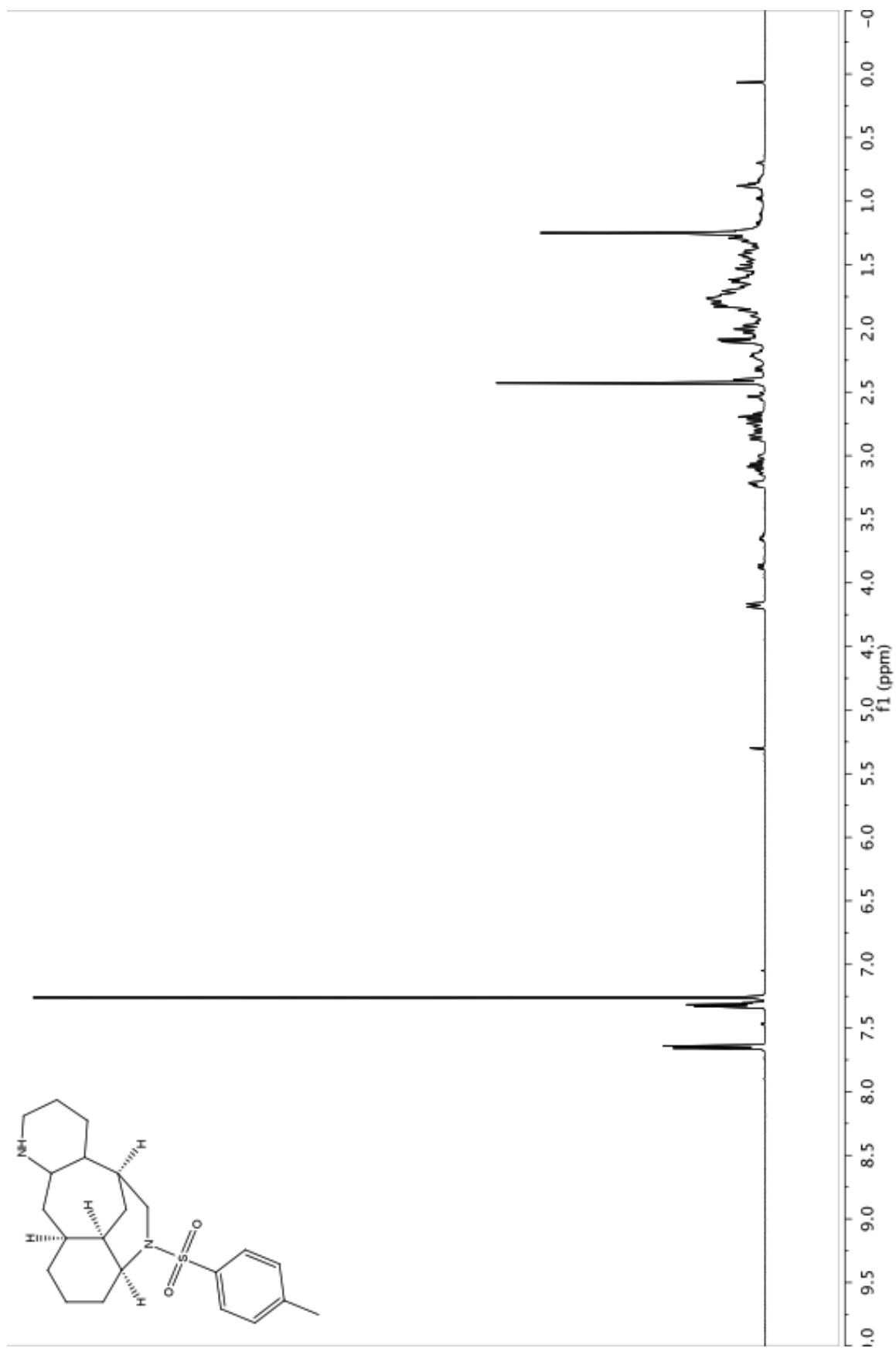
- 1 Szychowski, J.; Maclean, D. B. *Can. J. Chem.* **1979**, *57*, 1631.
- 2 Bisai, A.; West, S. P.; Sarpong, R. *J. Am. Chem. Soc.* **2008**, *130*, 7222.
- 3 West, S. P.; Bisai, A.; Lim, A. D.; Narayan, R. R.; Sarpong R. *J. Am. Chem. Soc.* **2009**, *131*, 11187.
- 4 Fenster, M. D. B.; Patrick, B. O.; Dake, G. R. *Org. Lett.* **2001**, *3*, 2109.
- 5 Liang, G.; Xu, Y.; Seiple, I. B.; Trauner, D. *J. Am. Chem. Soc.* **2006**, *128*, 11022.

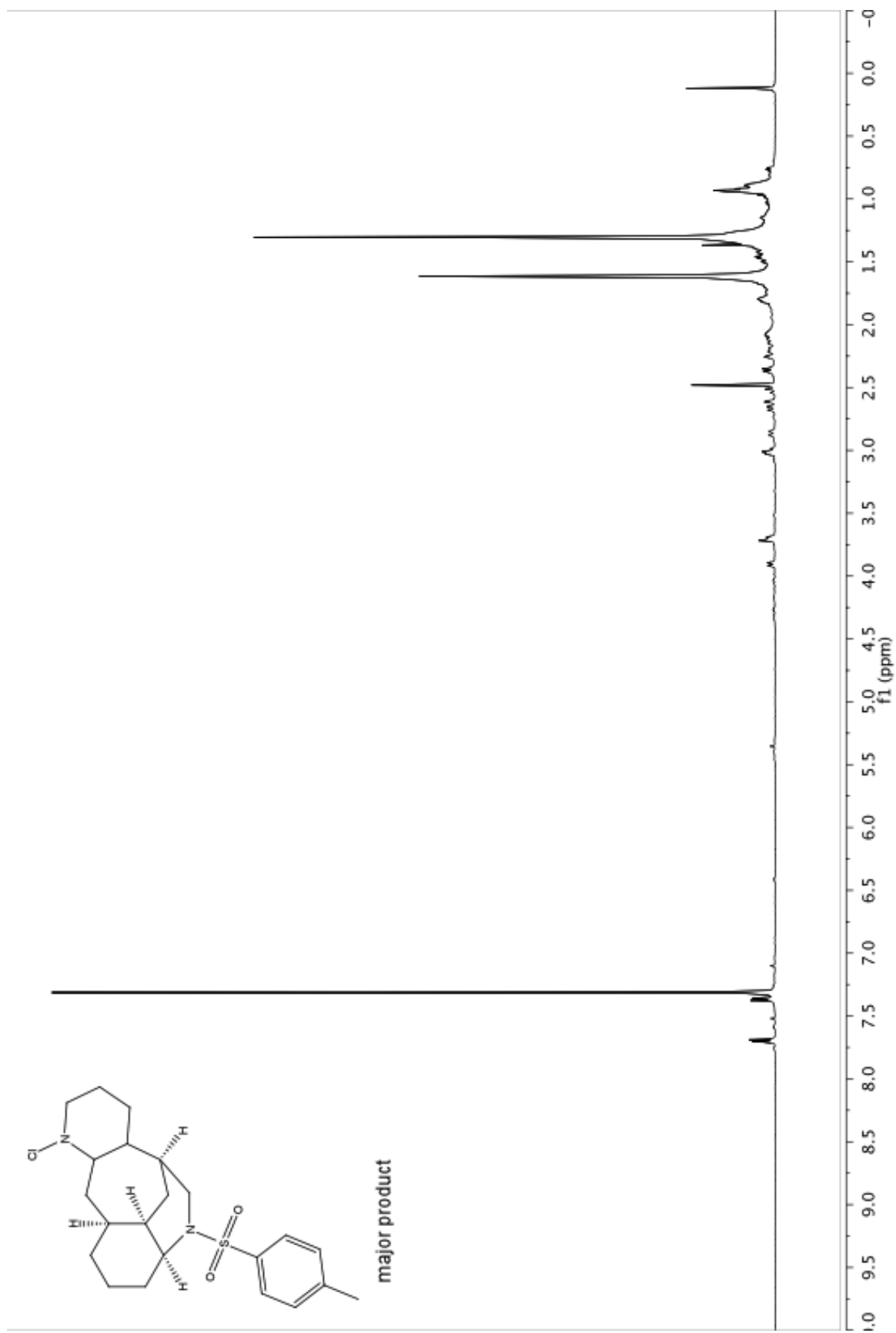
-
- ⁶ Hill, J.; Sutherland, J. K.; Crowley, P. J. *Chem. Soc. Perkin Trans. I* **1992**, 969.
- ⁷ Matsumoto, K.; Tokuyama, H.; Fukuyama, T. *Synlett* **2007**, 3137.
- ⁸ Chen, P.; Carroll, P. J.; Sieburth, S. McN. *Synthesis*, **2007**, 15, 2351.
- ⁹ Spicer, J. A. *et. al. J. Med. Chem.* **2007**, 50, 5090.
- ¹⁰ de la Hoz, A.; Prieto, M. P.; Rajzmann, M.; de Cózar, A.; Díaz-Ortiz, A.; Moreno, A.; Cossío, F. P. *Tetrahedron* **2008**, 64, 8169.
- ¹¹ Lanni, E. L.; Bosscher, M. A.; Ooms, B. D.; Shandro, C. A.; Ellsworth, B. A.; Anderson, C. E. *J. Org. Chem.*
- ¹² Yang, Z.-Y.; Xia, Y.; Xia, P.; Brossi, A.; Cosentino, L. M.; Lee, K.-H. *Bioorg. Med. Chem. Lett.* **2000**, 10, 1003.
- ¹³ McCarthy, A. R.; Hartmann, R. W.; Abell, A. D. *Bioorg. Med. Chem. Lett.* **2007**, 17, 3603.
- ¹⁴ Mabic, S.; Castagnoli Jr., N. *J. Org. Chem.* **1996**, 61, 309.
- ¹⁵ Kuethe, J. T.; Padwa, A. *Tetrahedron Lett.* **1997**, 38, 1505.
- ¹⁶ Mahoney, J. M.; Brestensky, D. M.; Stryker, J. M. *J. Am. Chem. Soc.* **1998**, 110, 291.
- ¹⁷ Li, X.; Kyne, R. E.; Ovaska, T. V. *Org. Lett.* **2006**, 8, 5153.
- ¹⁸ Sharma, P. K.; Kumar, S.; Kumar, P.; Nielsen, P. *Tetrahedron Lett.* **2007**, 48, 8704.
- ¹⁹ Inanaga, J.; Sakai, S.; Handa, Y.; Yamaguchi, M.; Yokoyama, Y. *Chem. Lett.* **1991**, 2117.
- ²⁰ Cabrera, A.; Alper, H. *Tetrahedron Lett.* **1992**, 33, 5007.
- ²¹ Brettle, R.; Shibib, S. M. *J. Chem. Soc. Perkin Trans. I* **1980**, 2912.
- ²² Donohoe, T. J.; McRiner, A. J.; Helliwell, M.; Sheldrake, P. *J. Chem. Soc. Perkin Trans. 1*, **2001**, 1435.
- ²³ Donohoe, T. J.; Mace, L.; Helliwell, M.; Ichihara, O. *Synlett* **2002**, 2, 331.
- ²⁴ Guthikonda, R. N.; Shah, S. K.; Pacholok, S. G.; Humes, J. L.; Mumford, R. A.; Grant, S. K.; Chabin, R. M.; Green, B. G.; Tsou, N.; Ball, R.; Fletcher, D. S.; Luell, S.; MacIntyre, D. E.; MacCoss, M. *Bioorg. Med. Chem. Lett.* **2005**, 15, 1997.
- ²⁵ MacCarthy, A. R.; Hartmann, R. W.; Abell, A. D. *Bioorg. Med. Chem. Lett.* **2007**, 17, 3603.
- ²⁶ Joshi, R. A.; Ravindranathan, T. *Ind. J. Chem. Sect. B* **1984**, 23, 260-262.
- ²⁷ Poon, K. W. C.; Dudley, G. B. *J. Org. Chem.* **2006**, 71, 3923.
- ²⁸ Grundl, M. A.; Trauner, D. *Org. Lett.* **2006**, 8, 23.
- ²⁹ Kuehne, M. E.; Bornmann, W. G.; Parsons, W. H.; Spitzer, T. D.; Blount, J. F.; Zubieta, J. *J. Org. Chem.* **1988**, 53, 3439.
- ³⁰ Zheng, S.; Chan, C.; Furuuchi, T.; Wright, B. J. D.; Zhou, B.; Guo, J.; Danishefsky, S. J. *Angew. Chem. Int. Ed.* **2006**, 45, 1754.
- ³¹ Sieck, O.; Ehwald, M. Liebscher, J. *Eur. J. Org. Chem.* **2005**, 663.
- ³² Burgess, L. E.; Gross, E. K. M.; Jurka, J. *Tetrahedron Lett.* **1996**, 37, 3255.
- ³³ Maryanoff, B. E.; Zhang, H.-C.; Cohen, J. H.; Turchi, I. J.; Maryanoff, C. A. *Chem. Rev.* **2004**, 104, 1431.
- ³⁴ Rodriguez, S.; Wipf, P. *Synthesis*, **2004**, 17, 2767.
- ³⁵ Kobayashi, J.; Morita, H. *Alkaloids (Academic Press)* **2005**, 61, 1.
- ³⁶ Ayer, W. A.; Berezows, J.; Law, D. A. *Can. J. Chem.* **1963**, 41, 649.

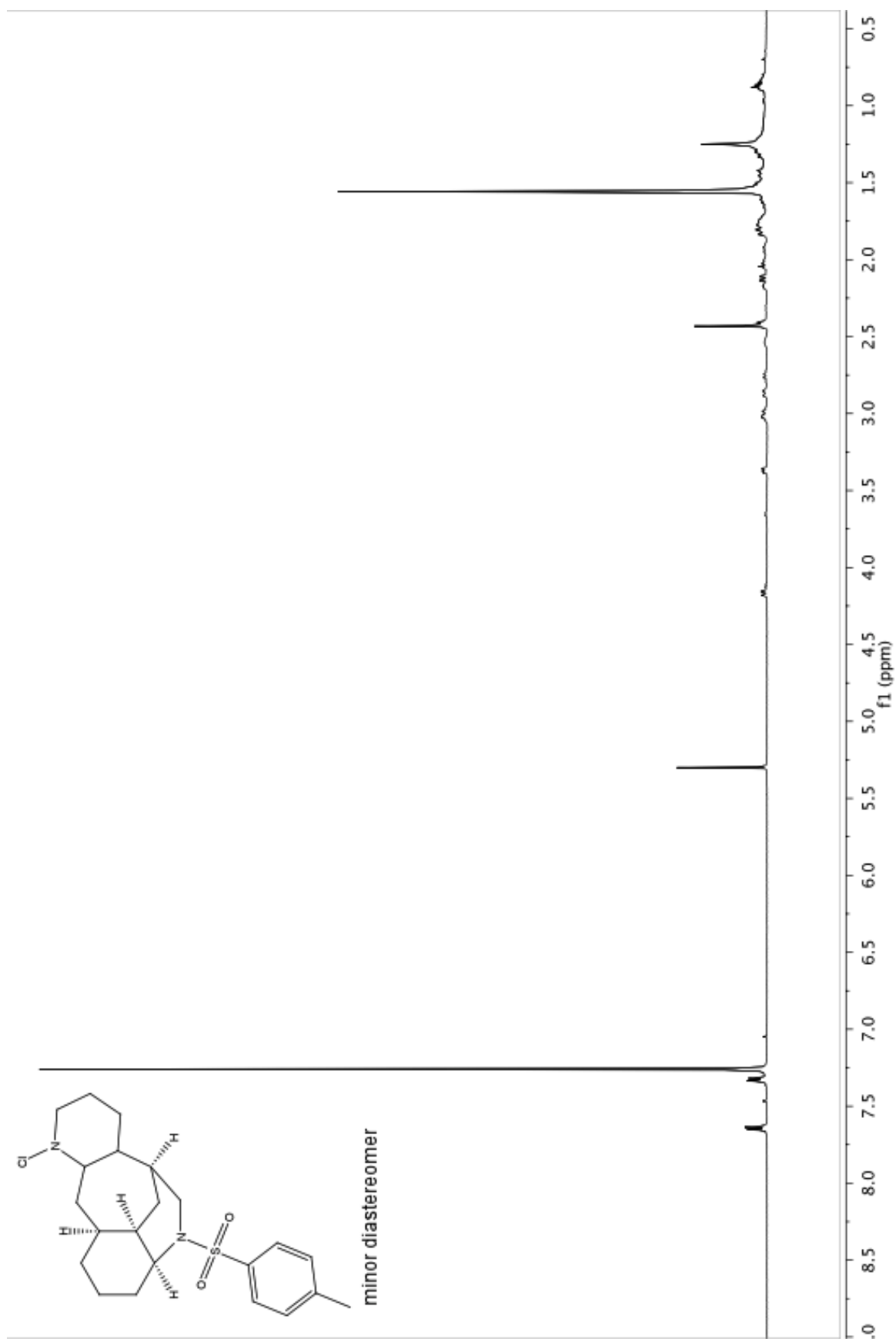
Appendix One: Spectra Relevant to Chapter Two

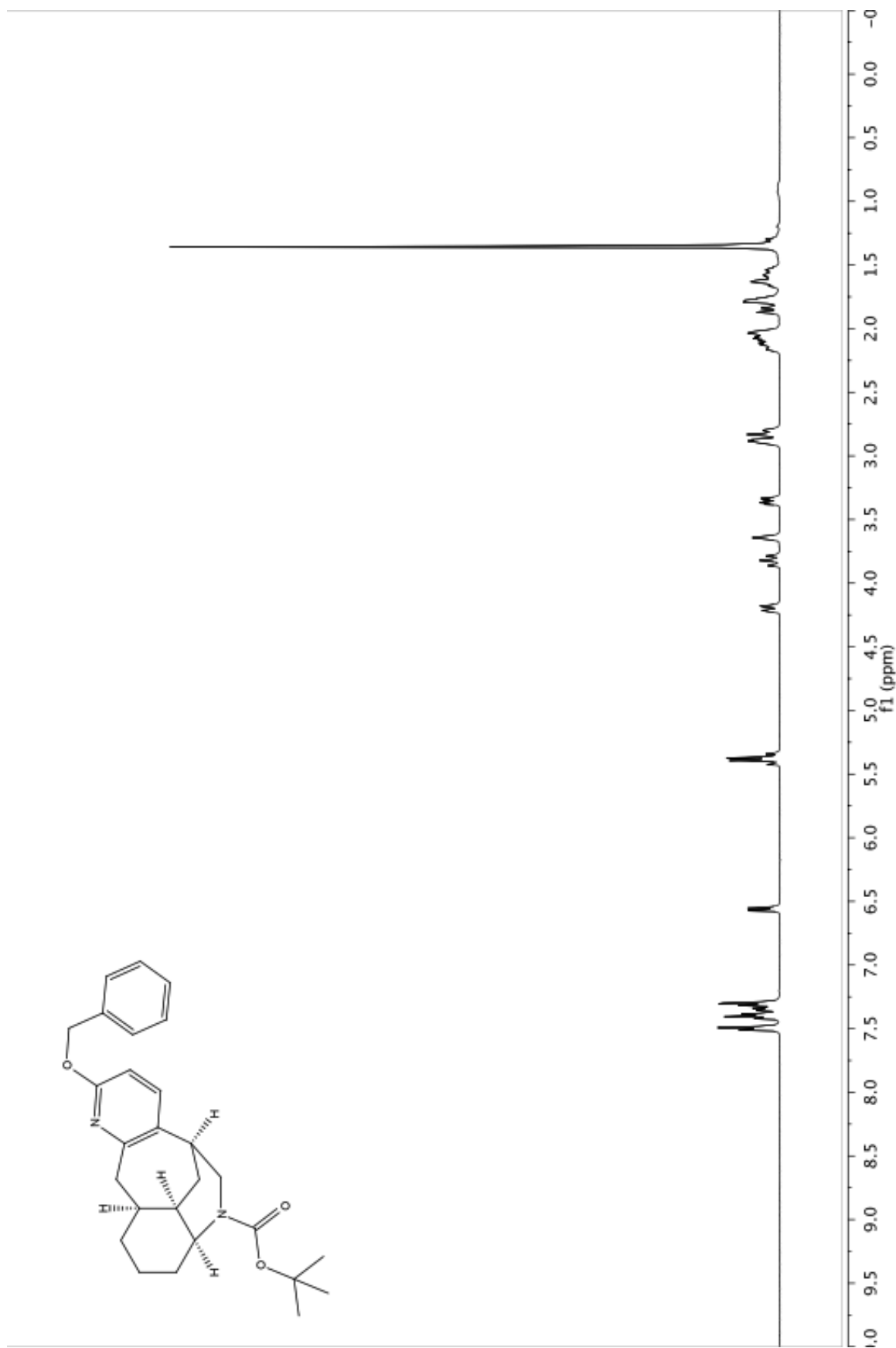


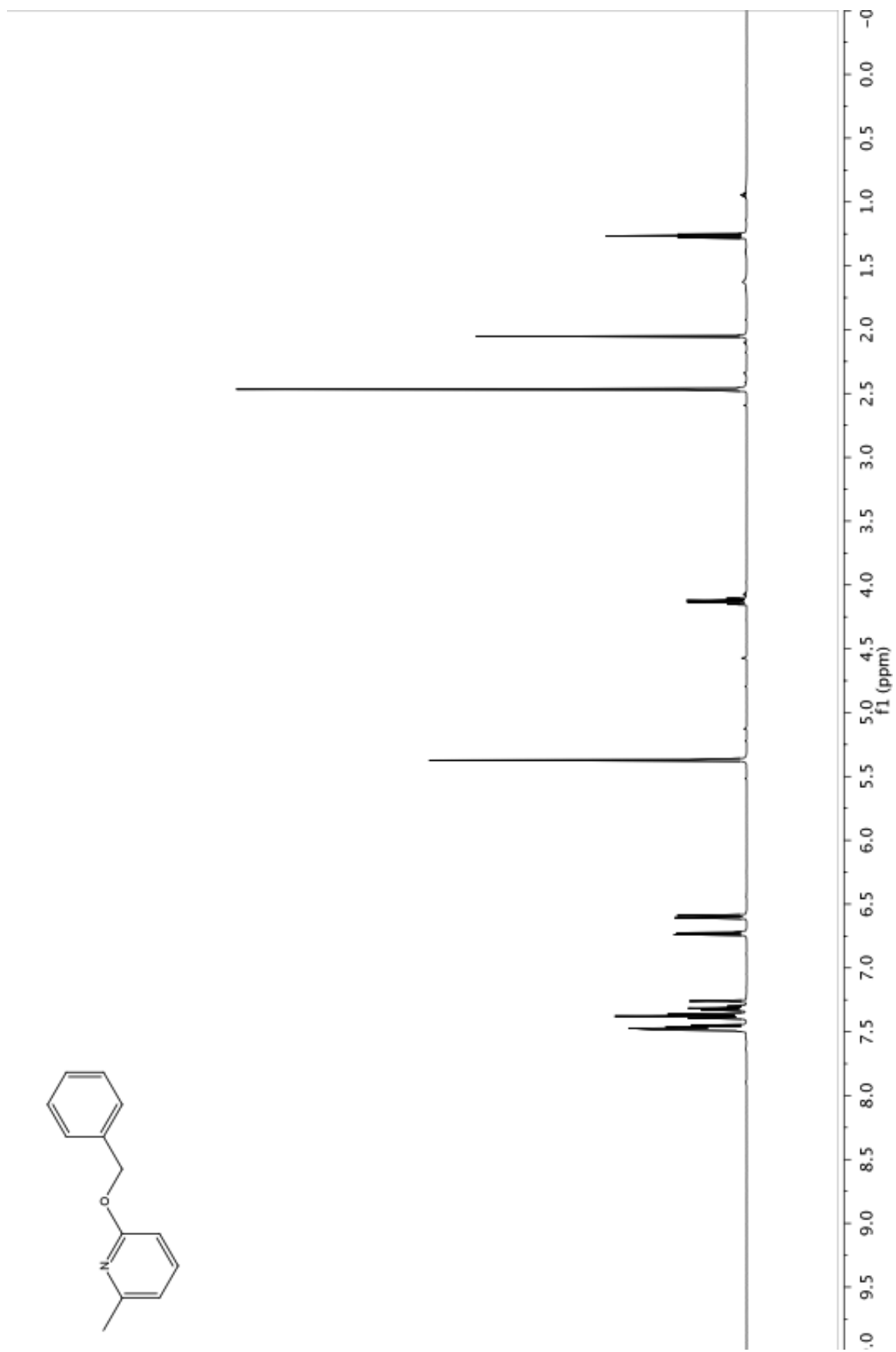
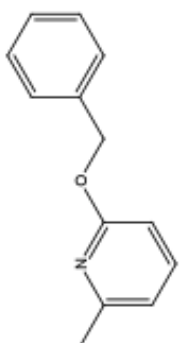


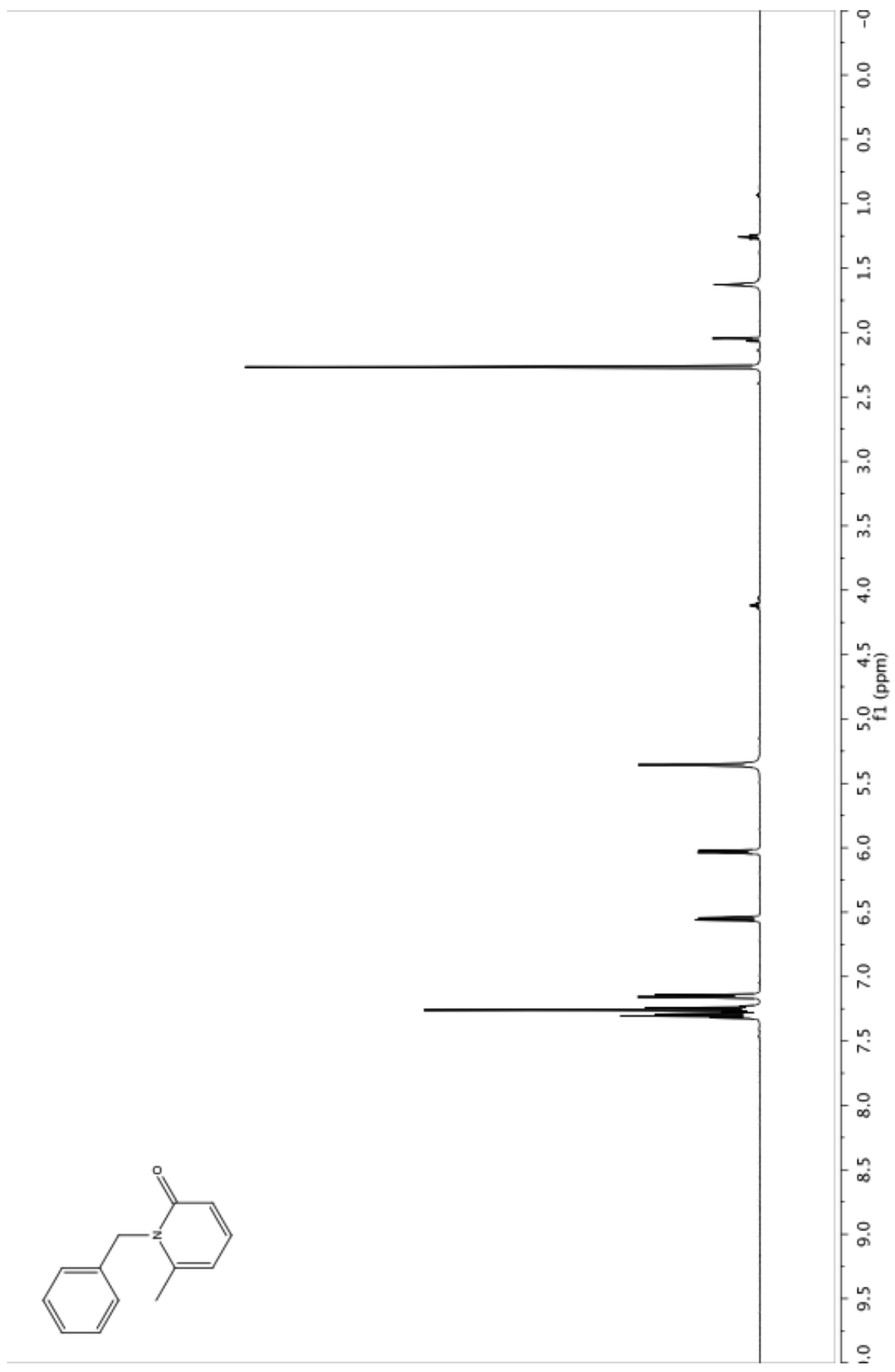


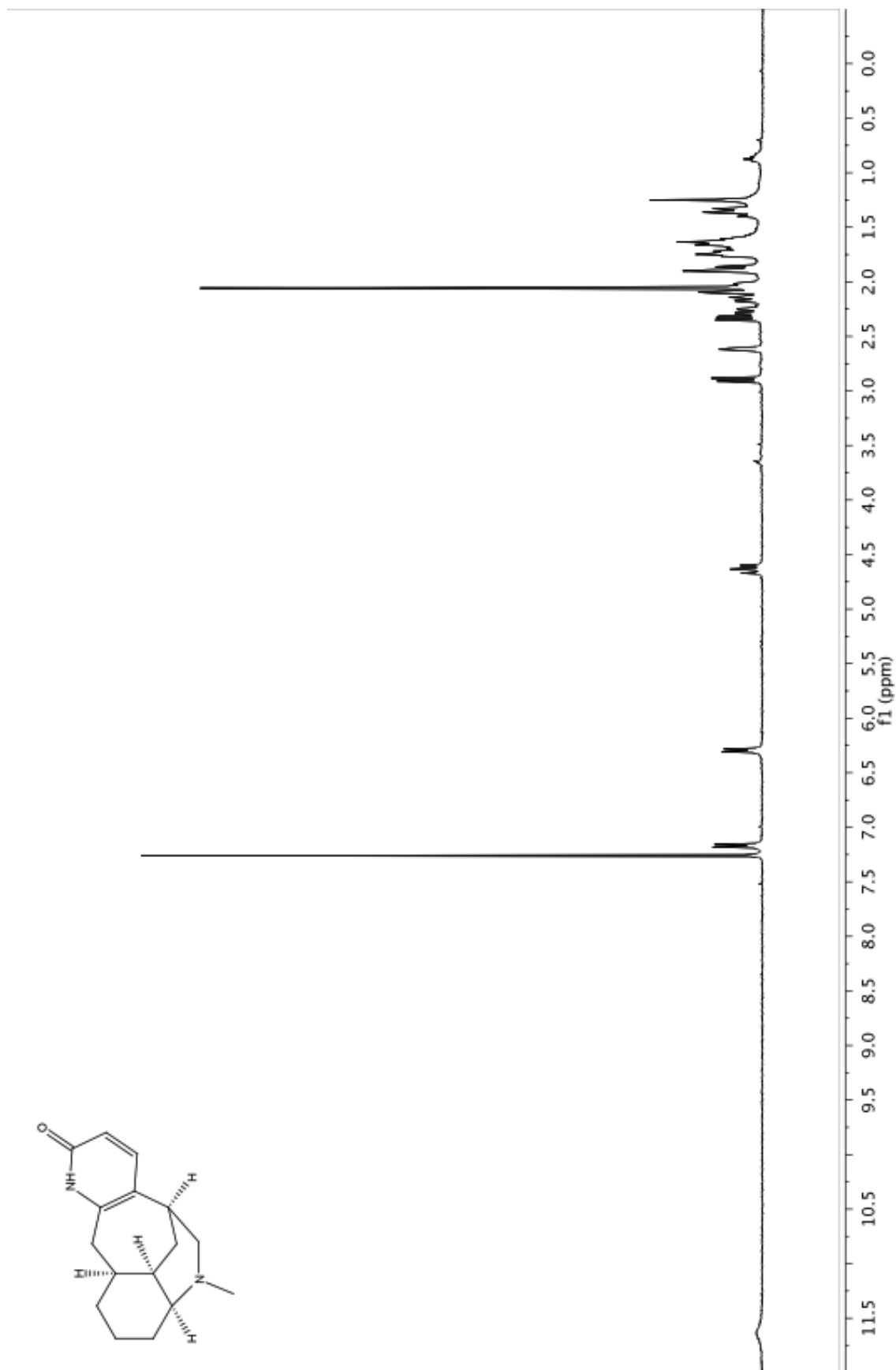


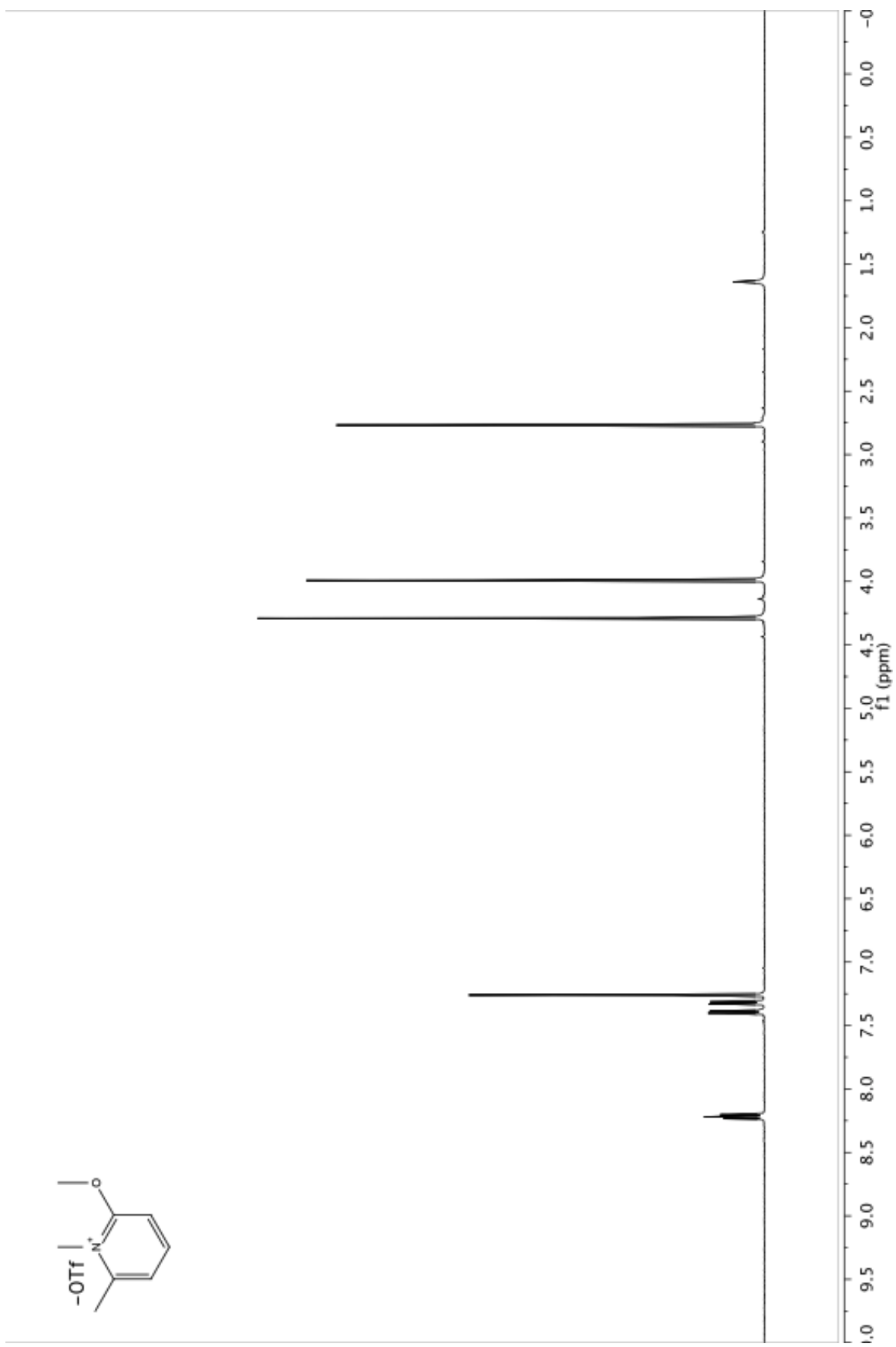
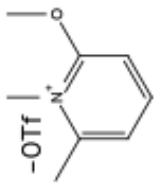


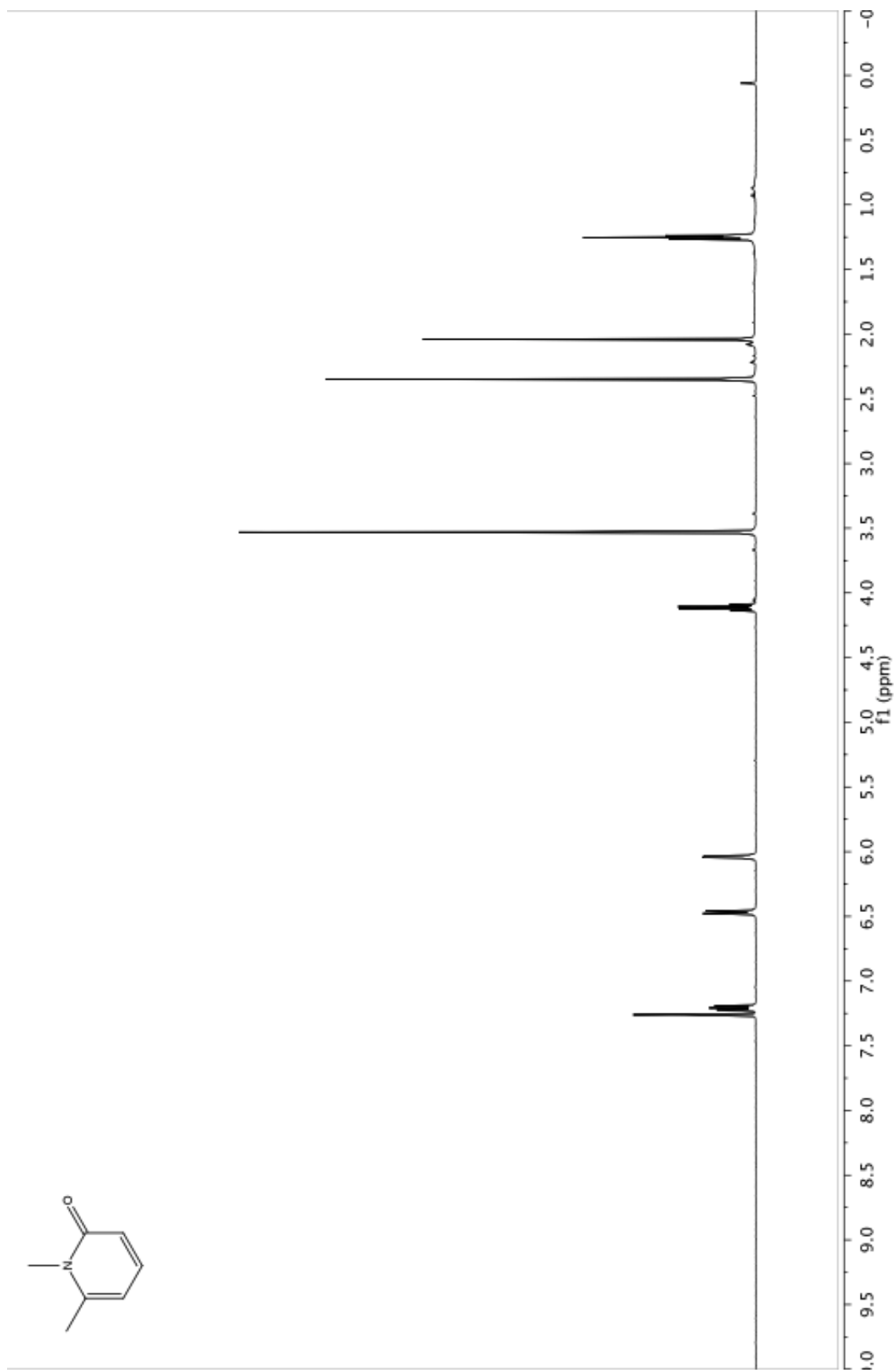
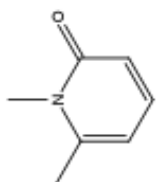


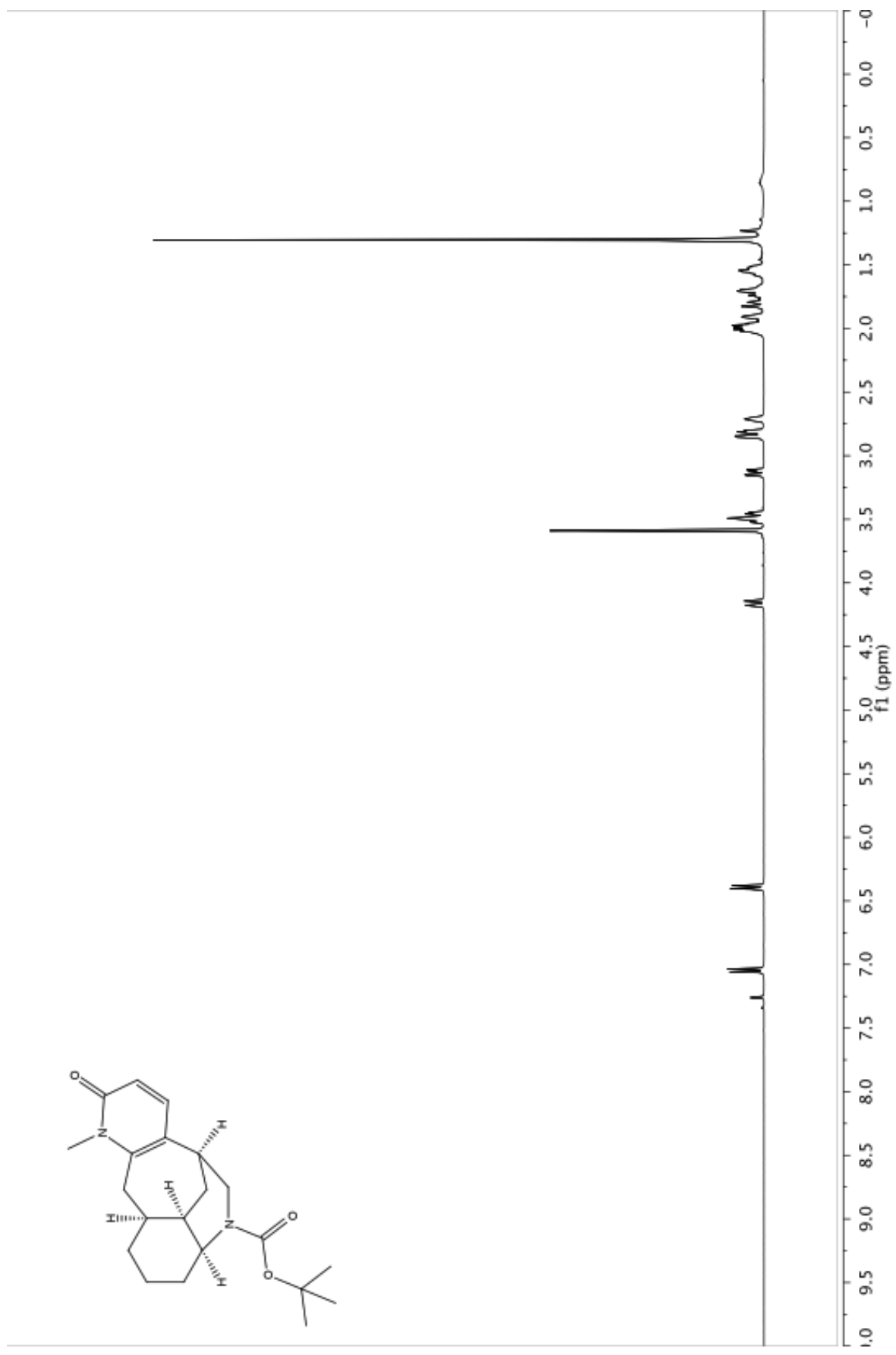


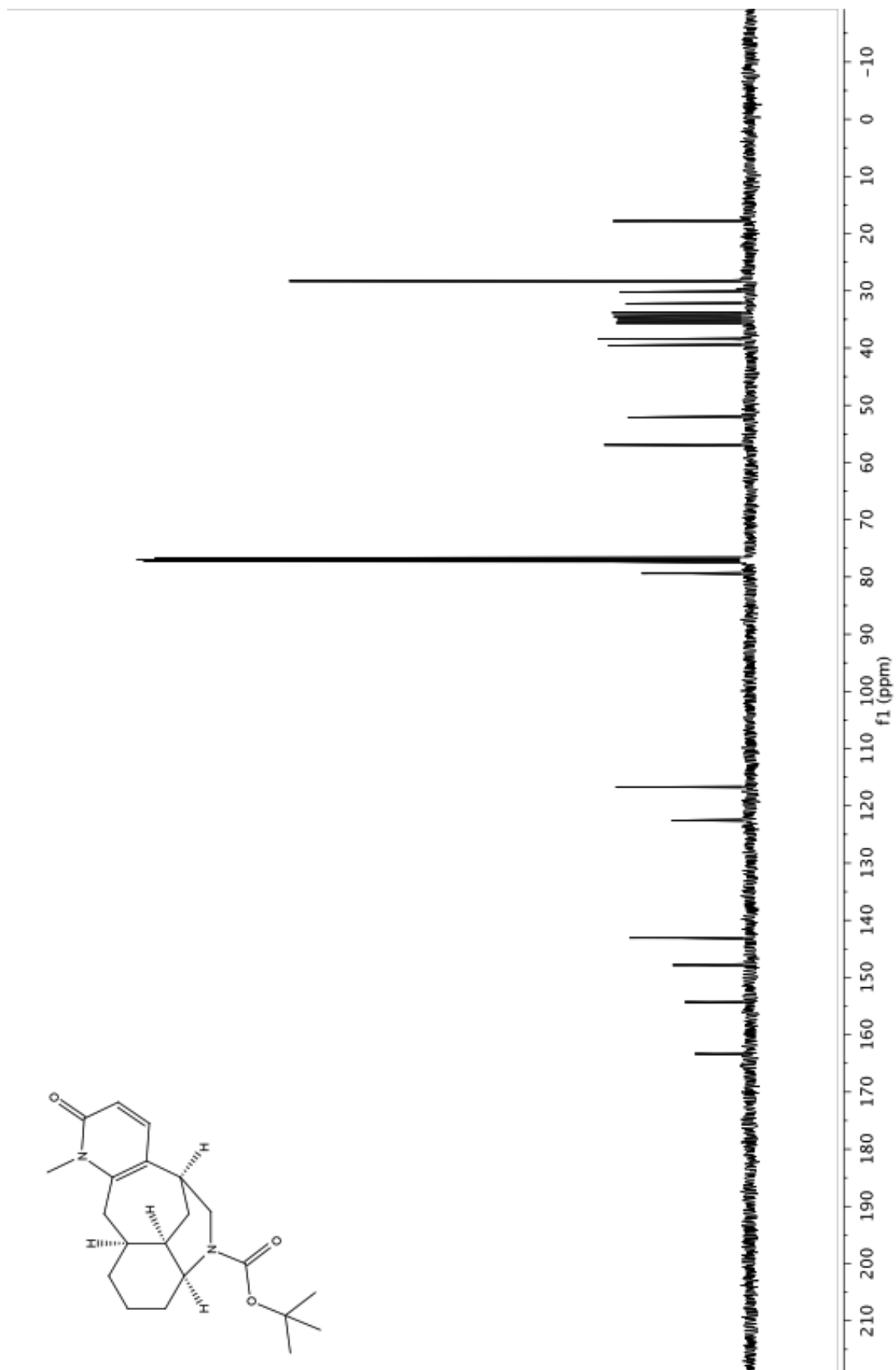


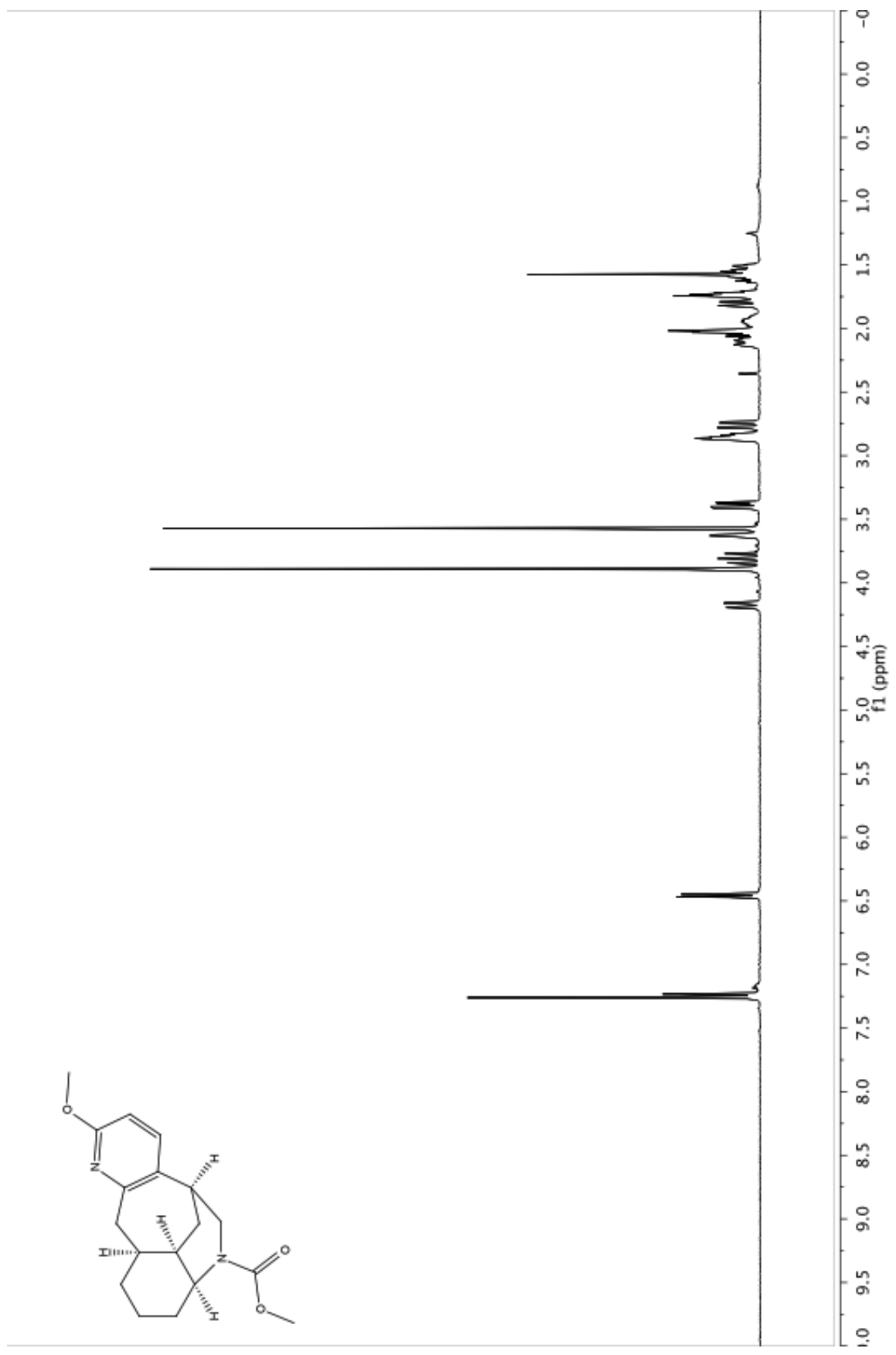


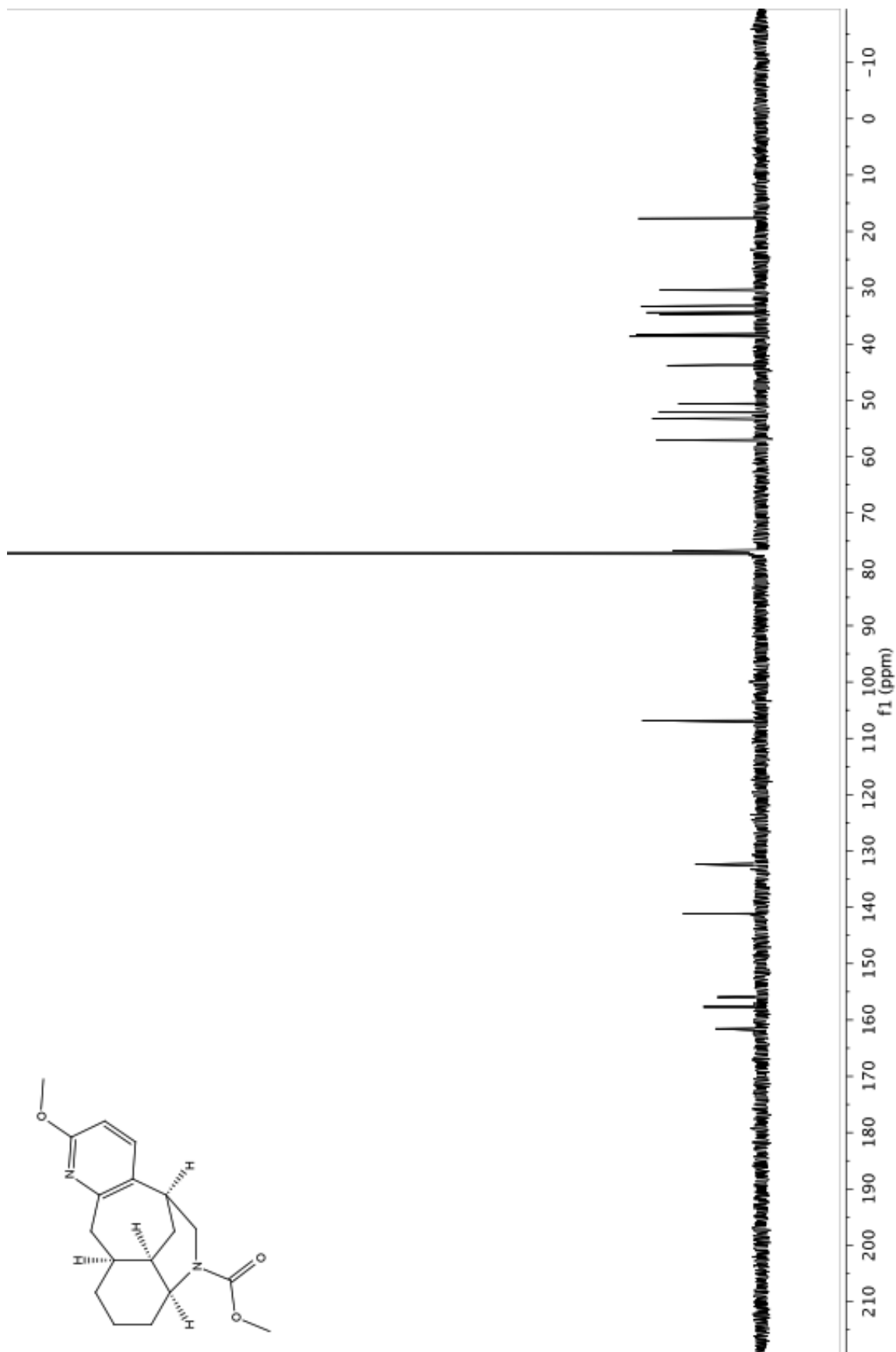


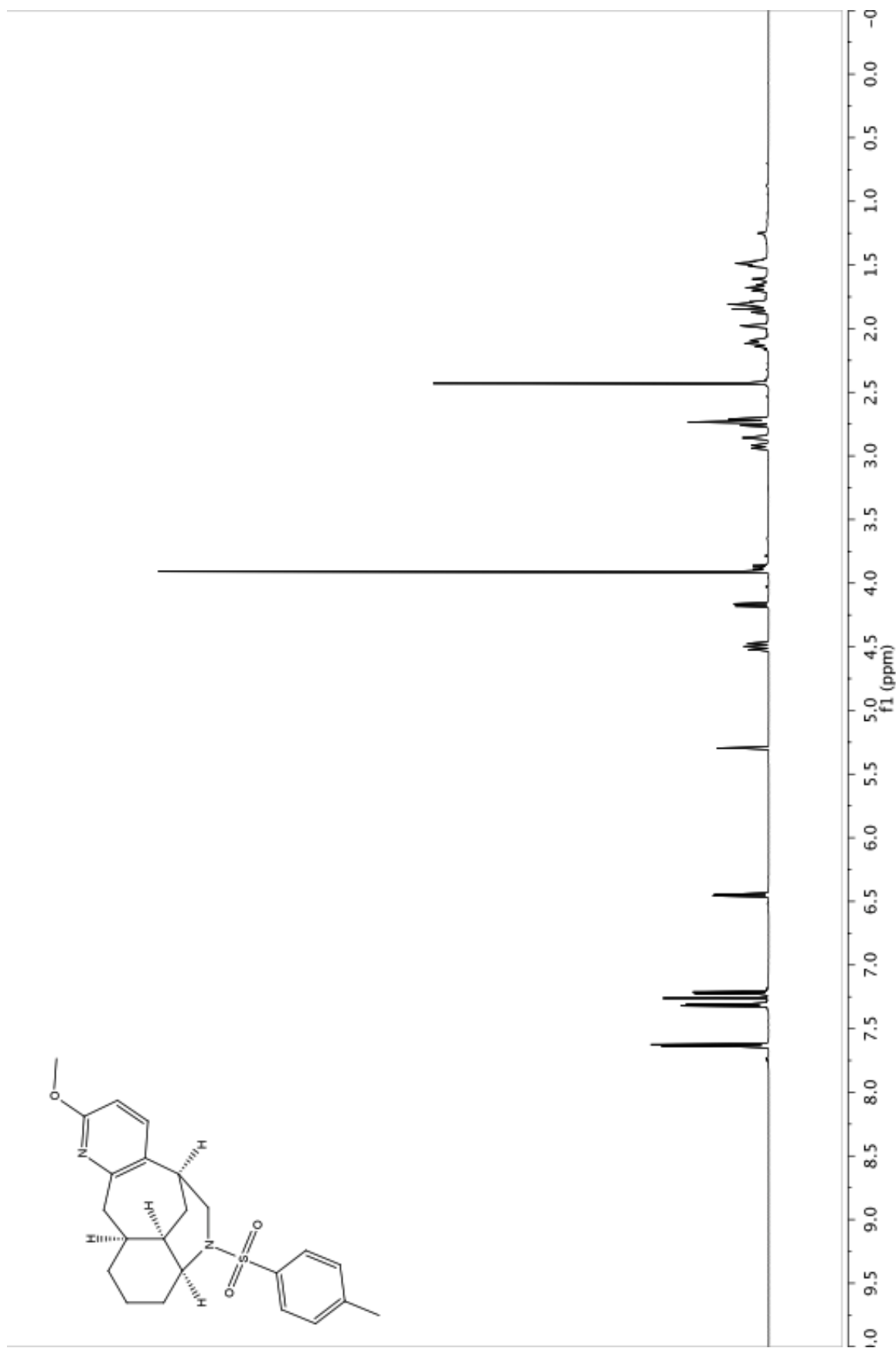


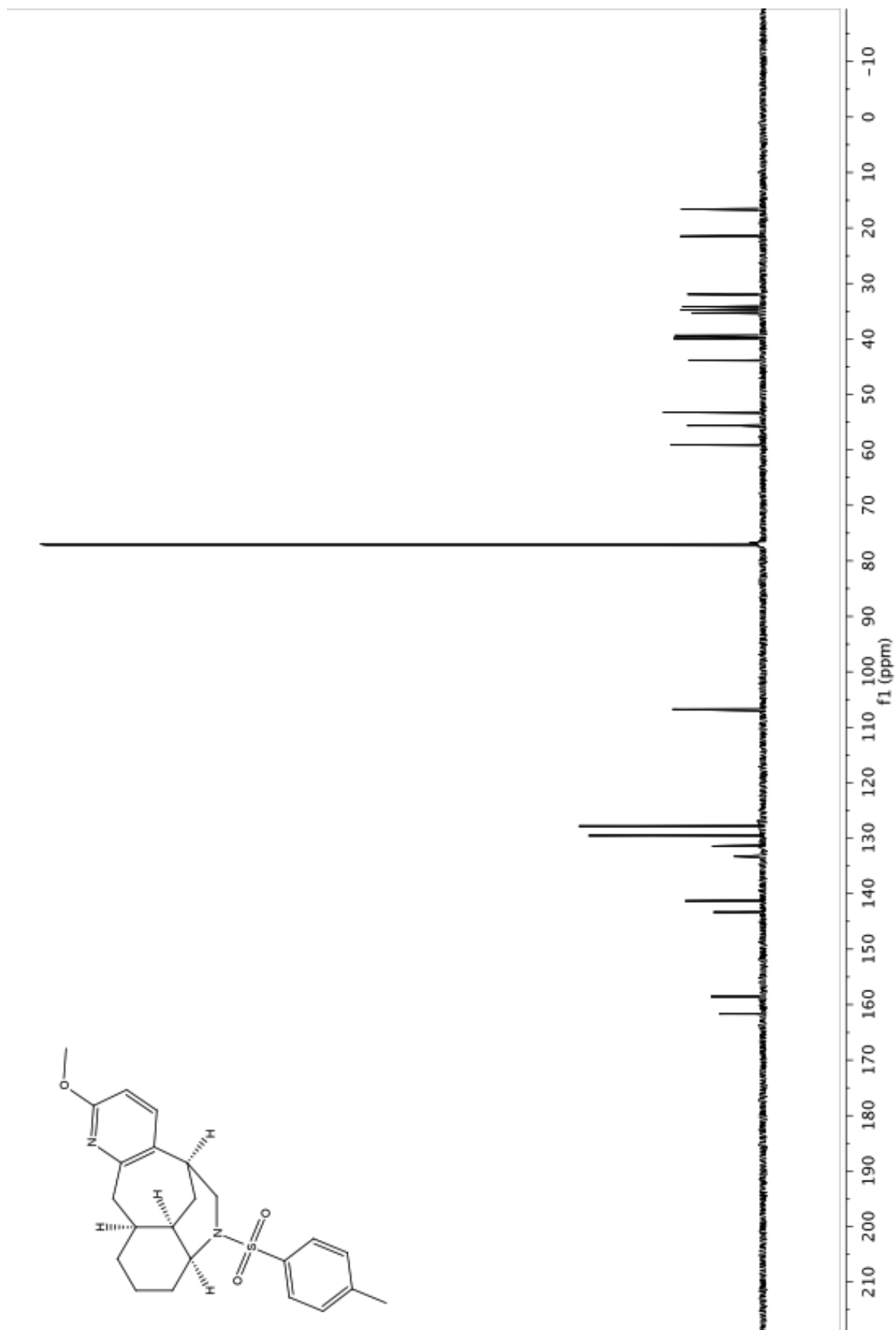


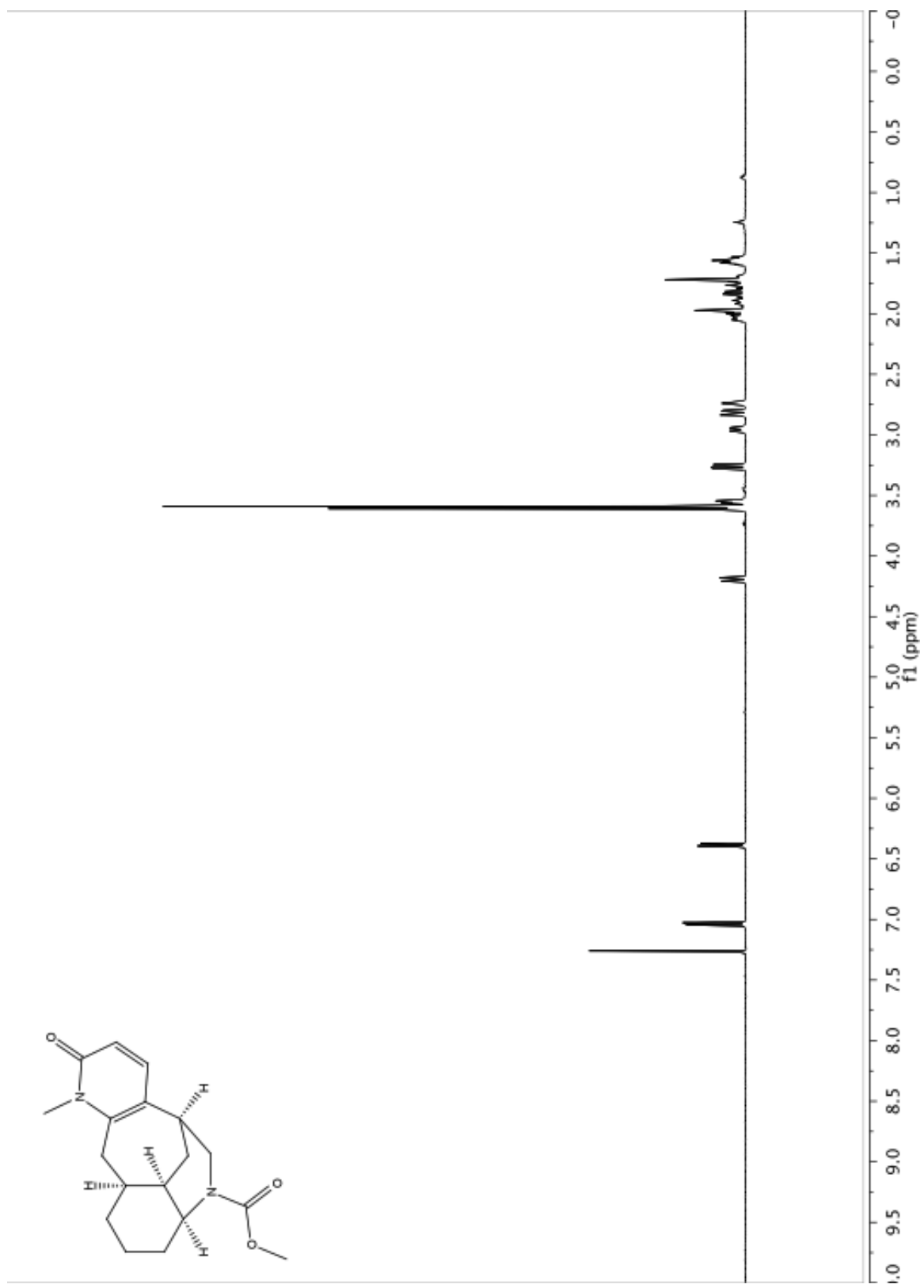


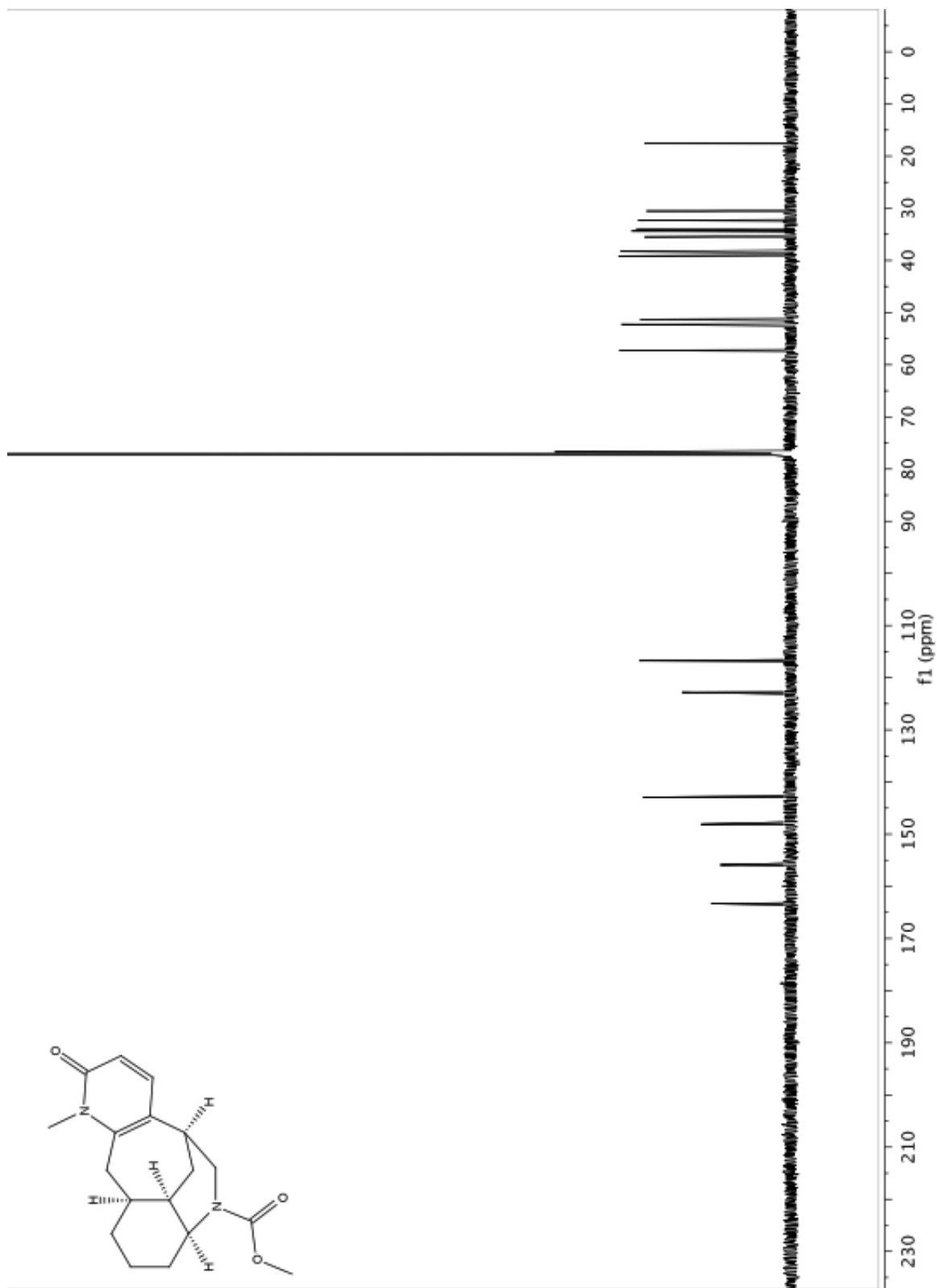


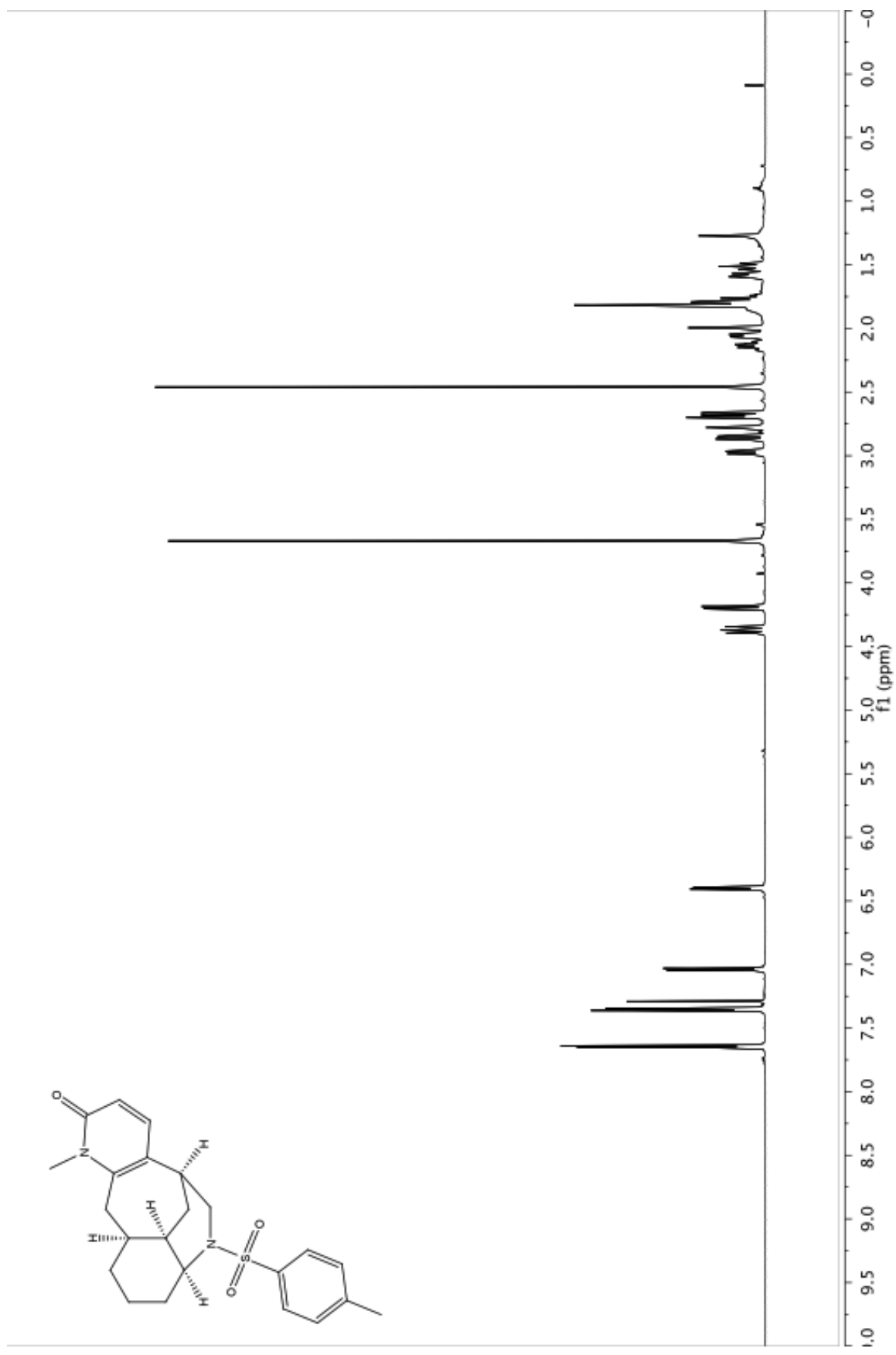


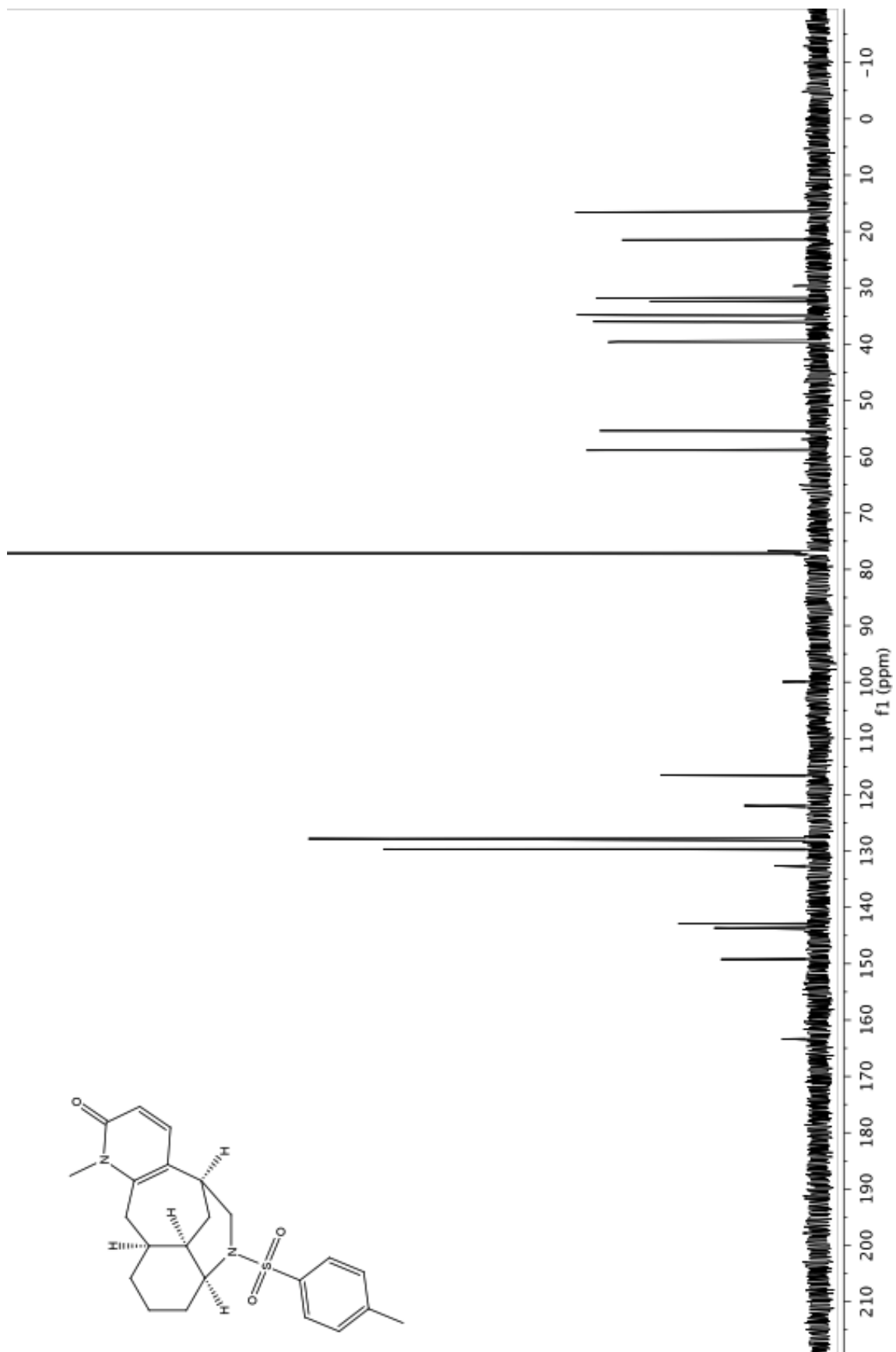


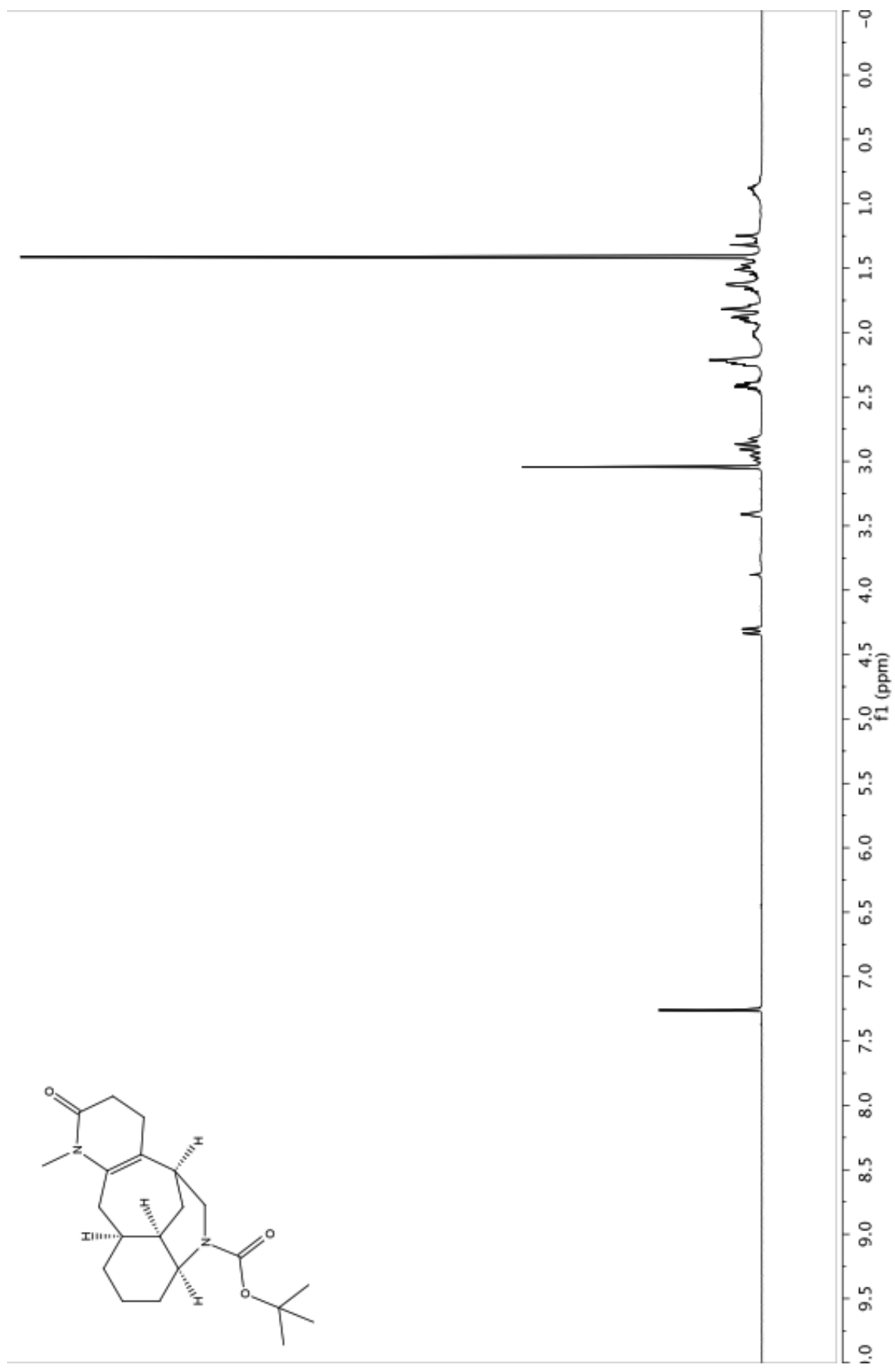


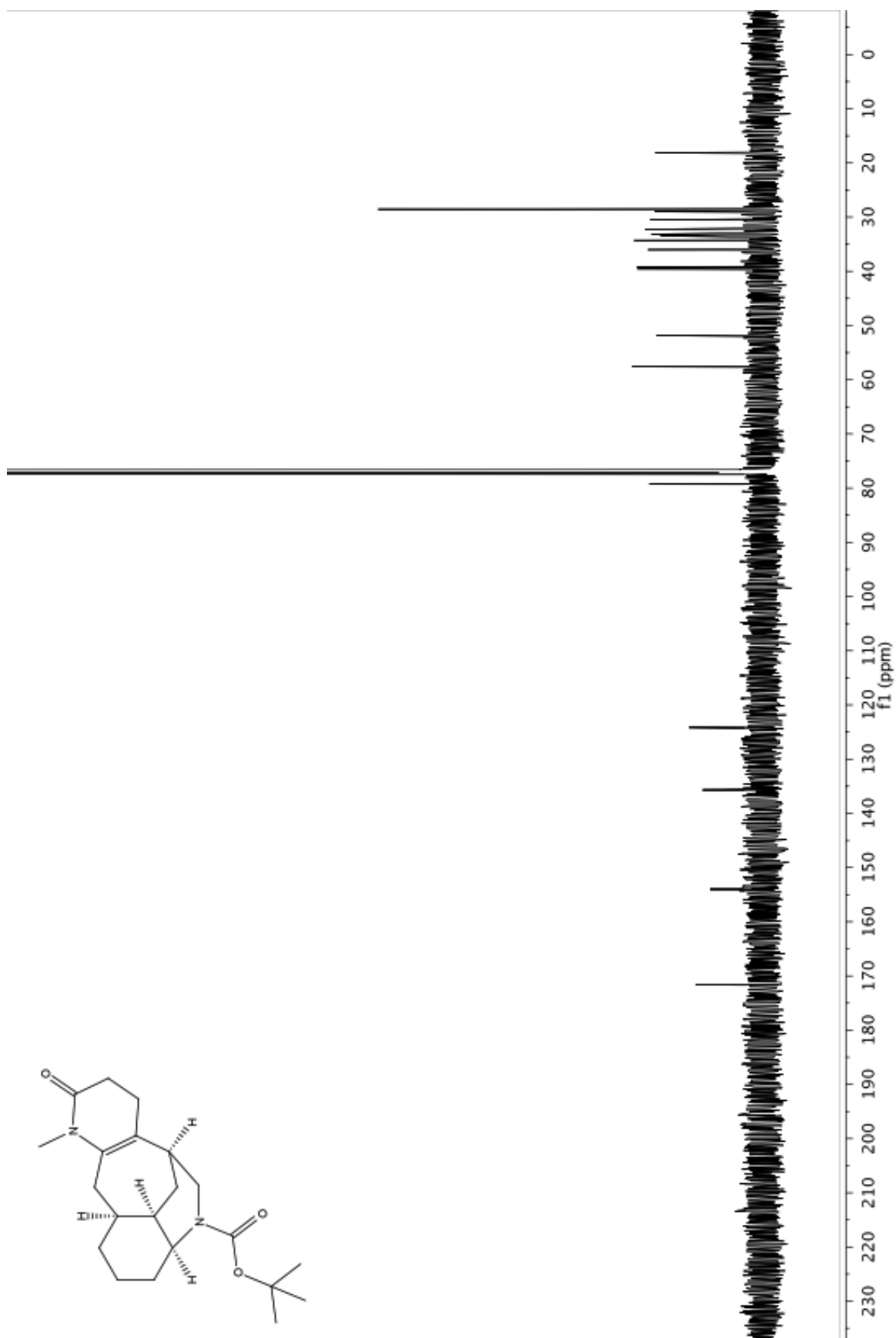


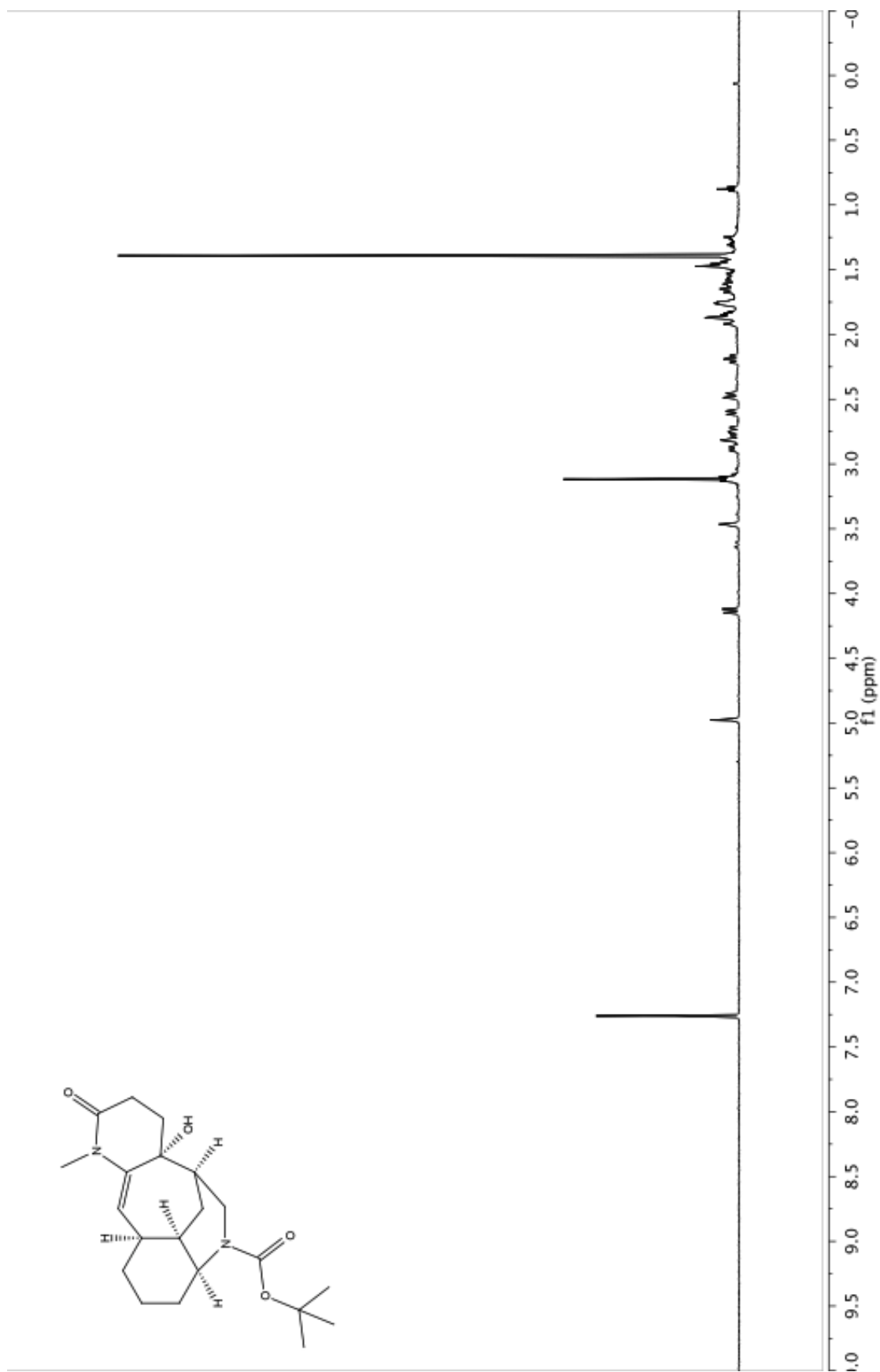


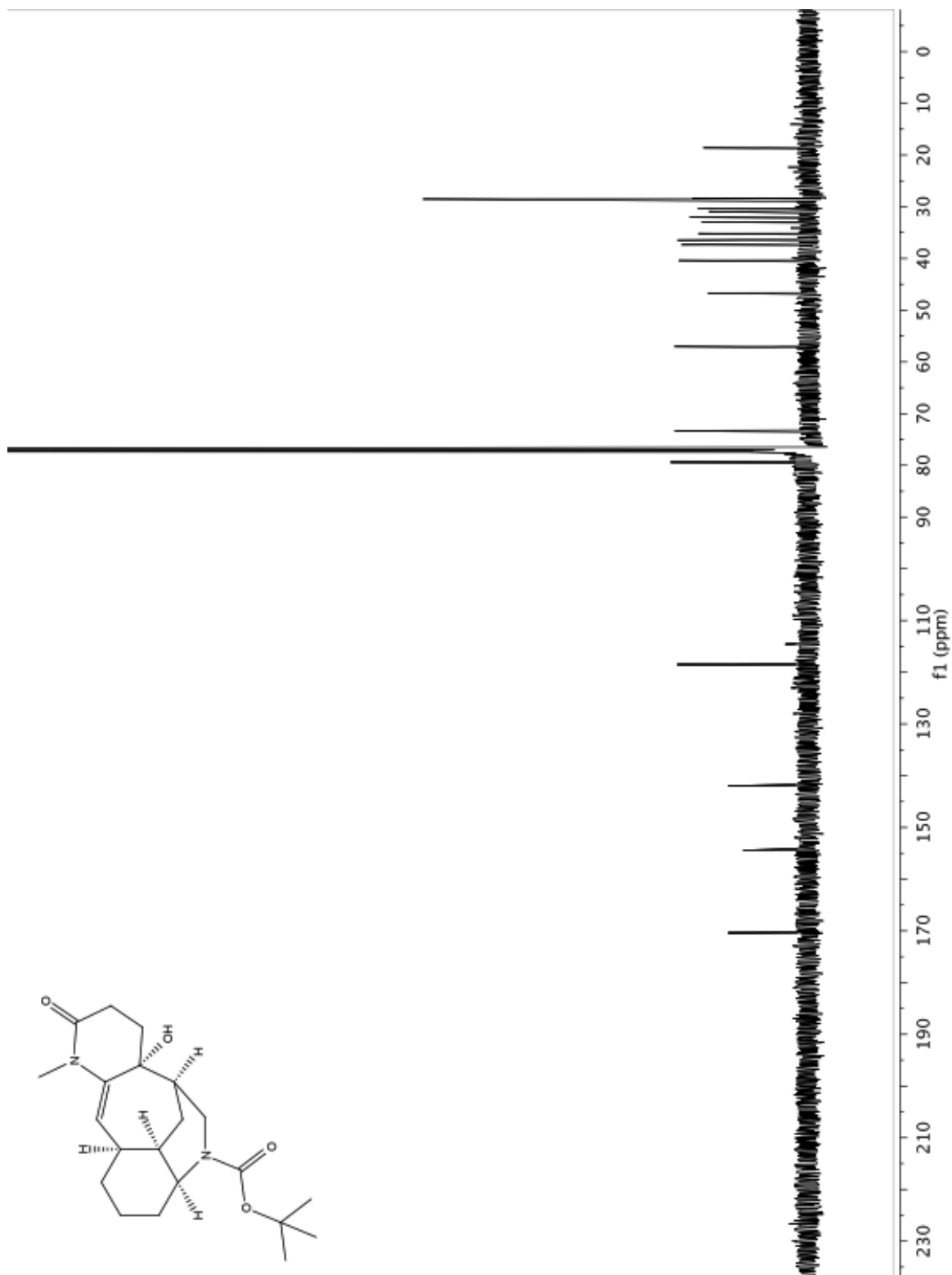




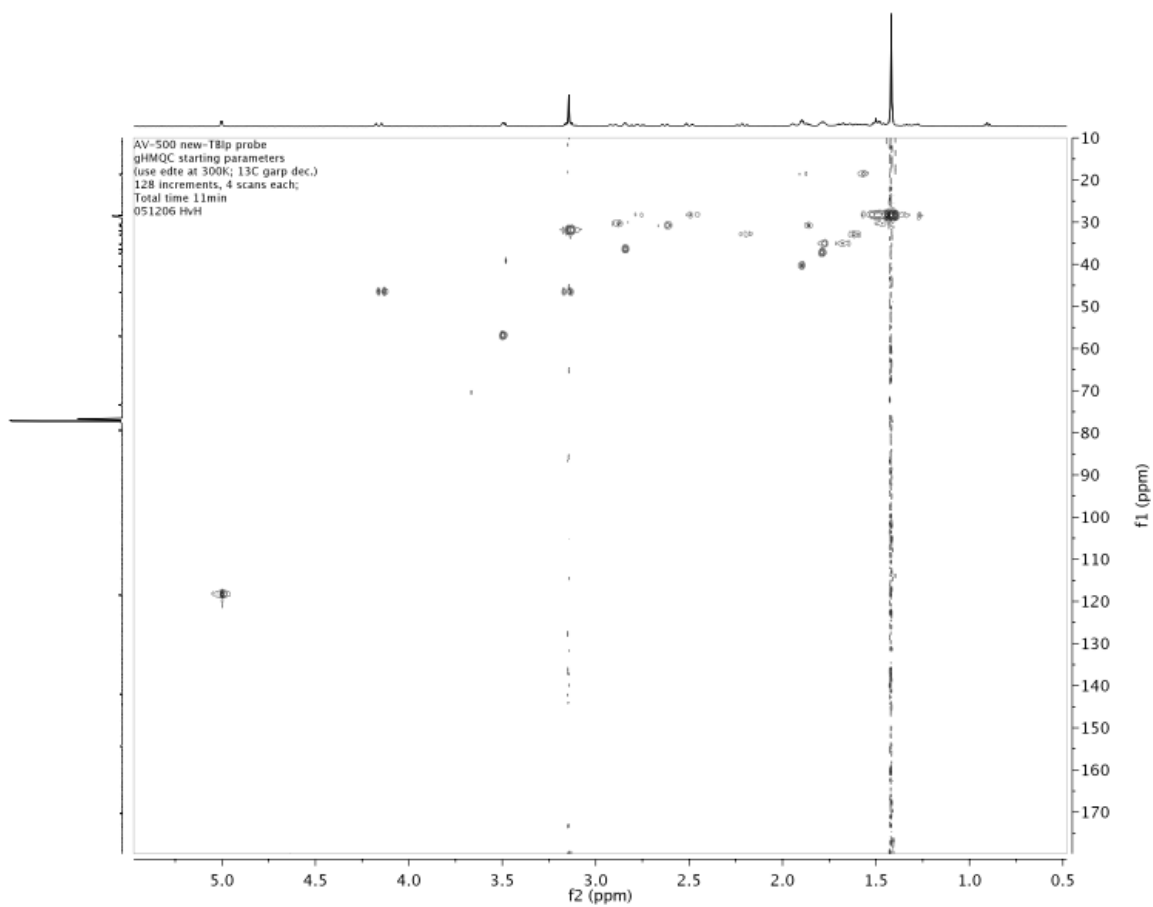




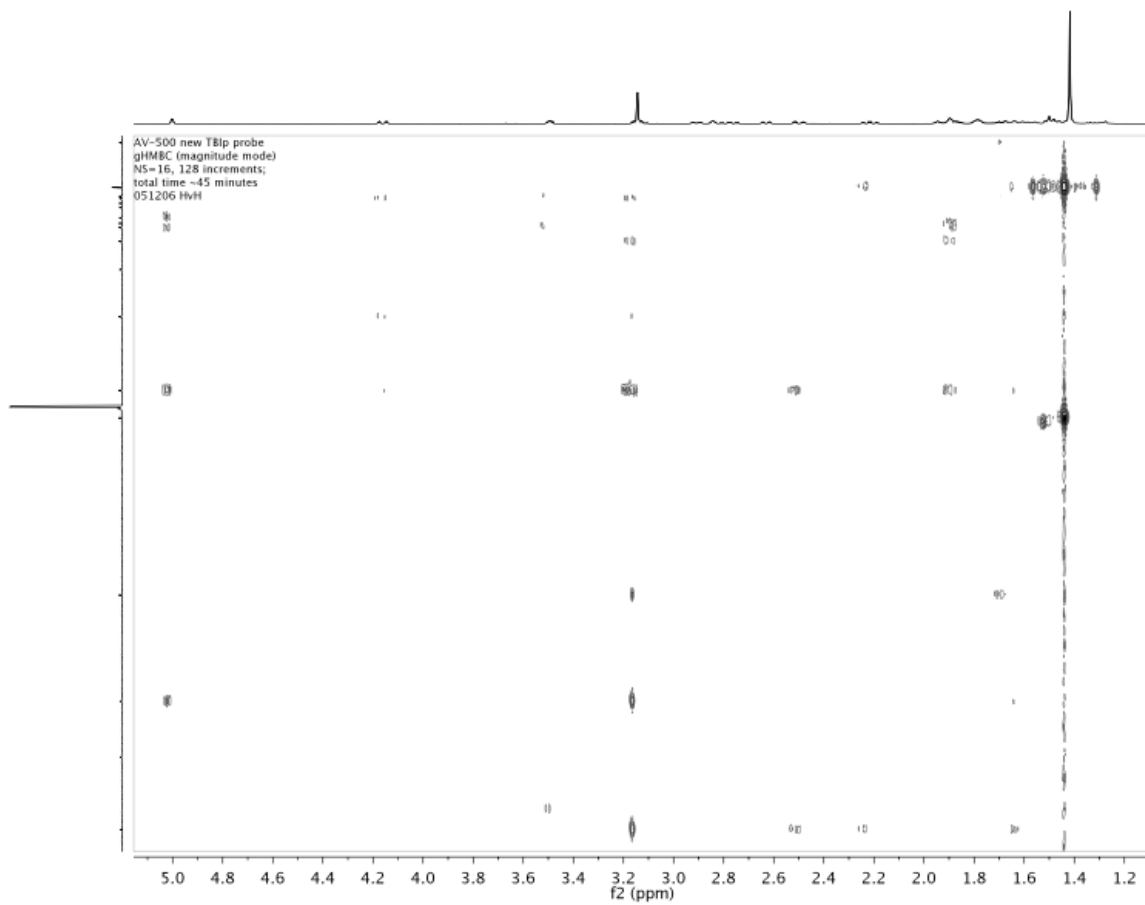




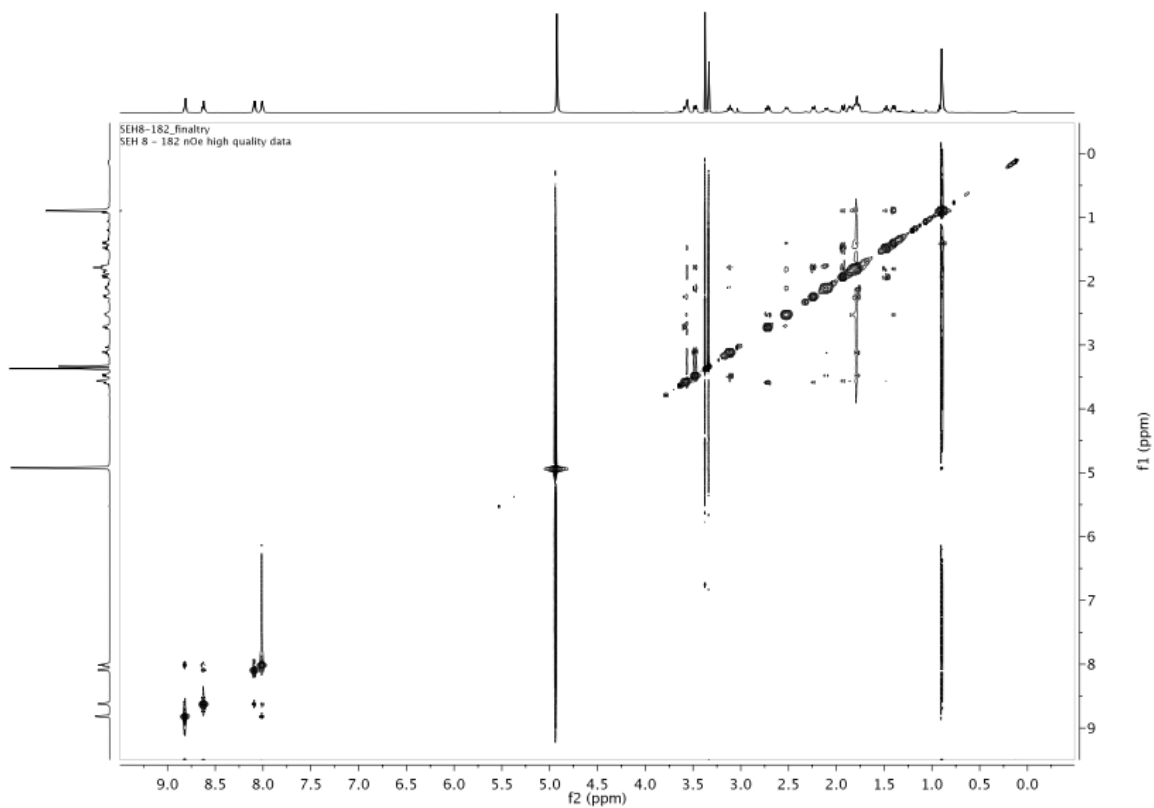
HMQC for enamide **2.108a**

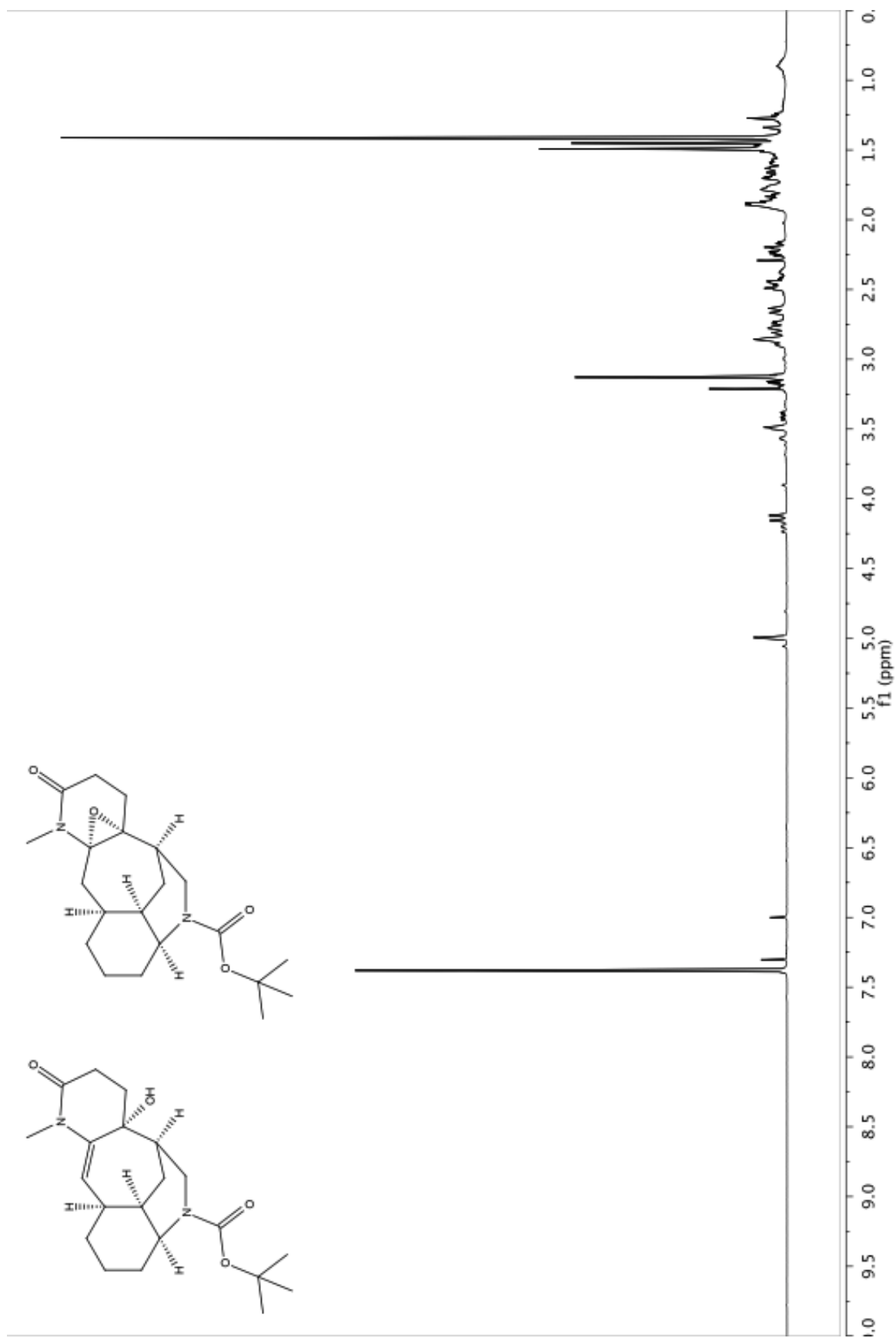


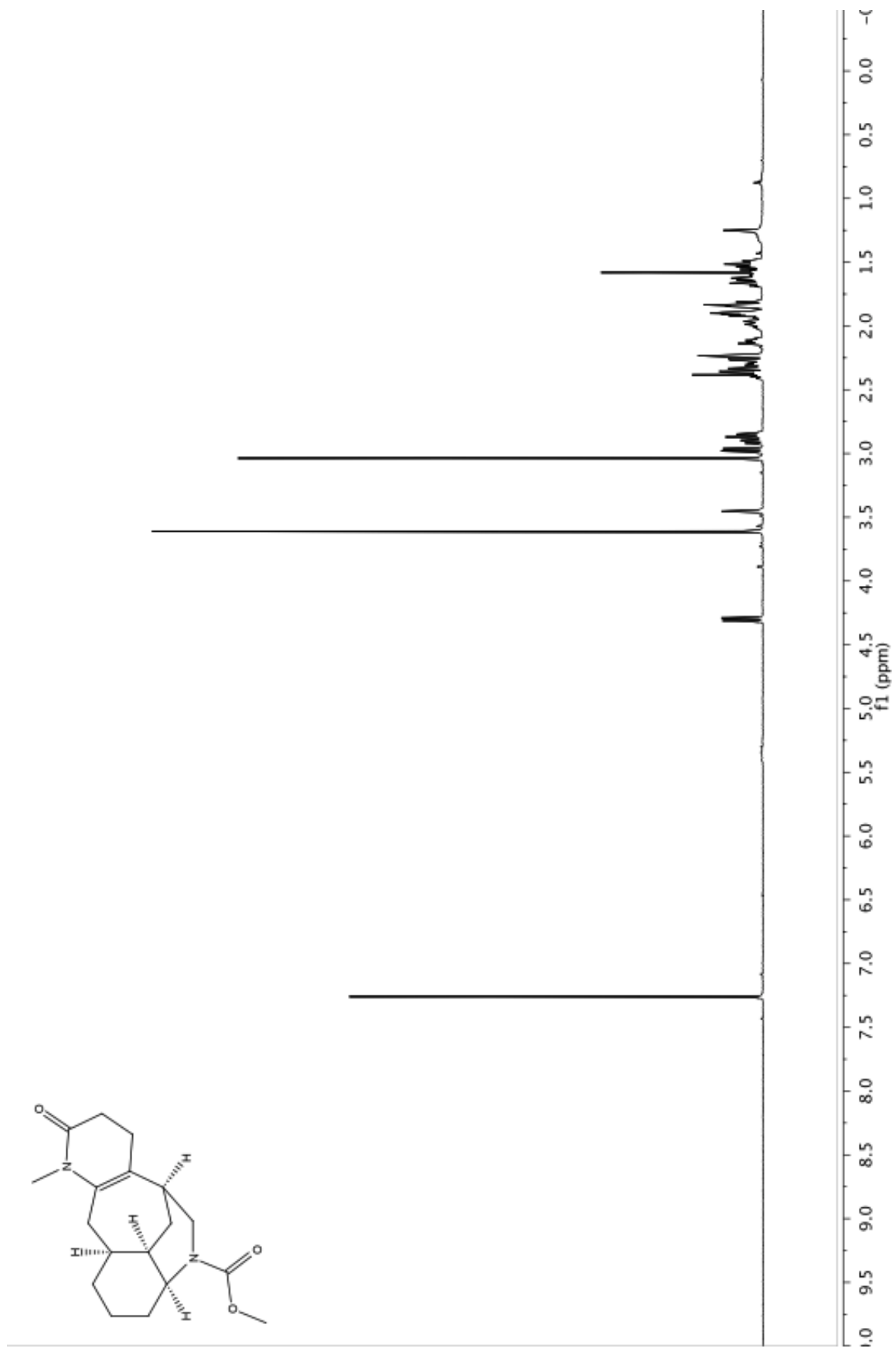
HMBC for enamide **2.108a**

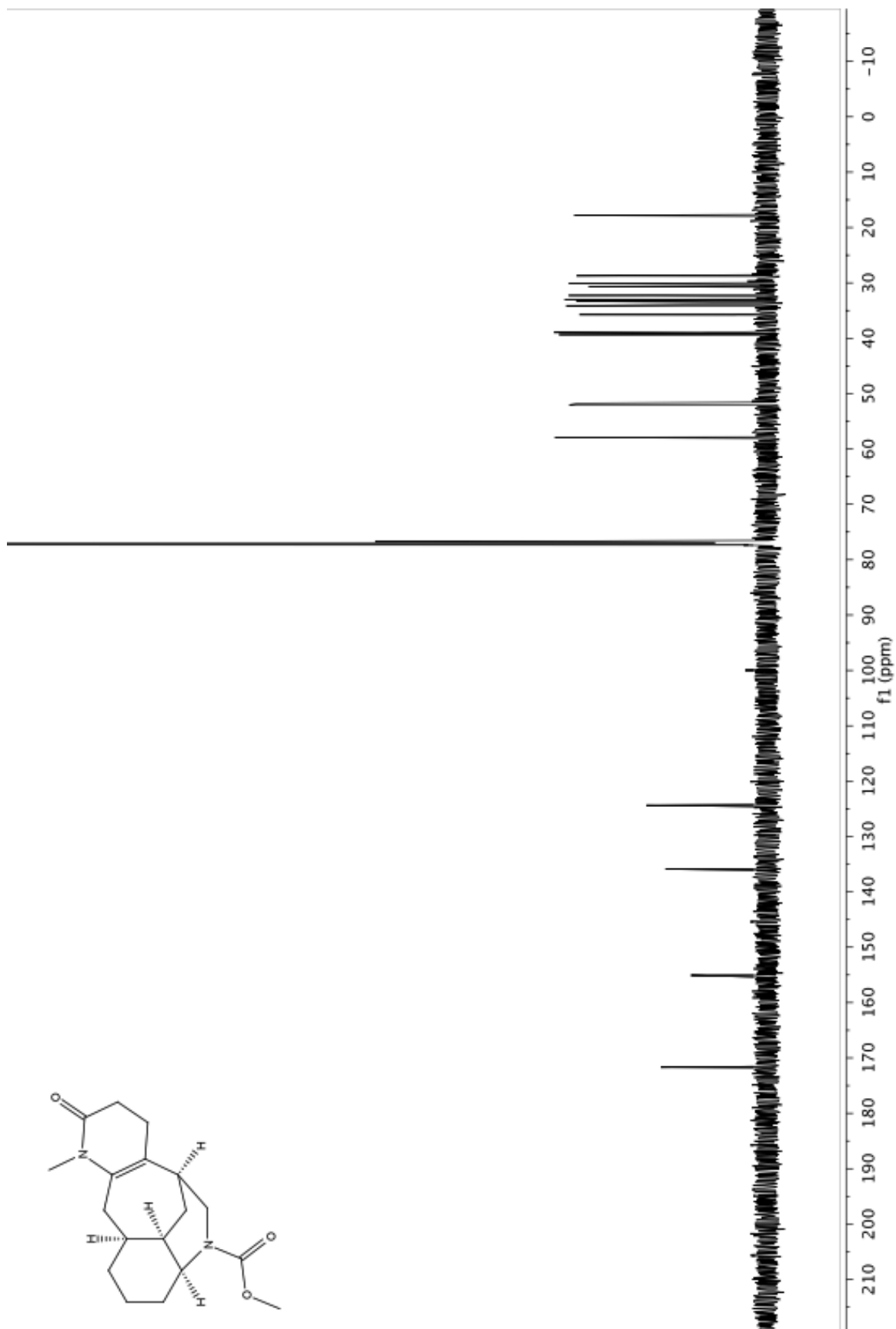


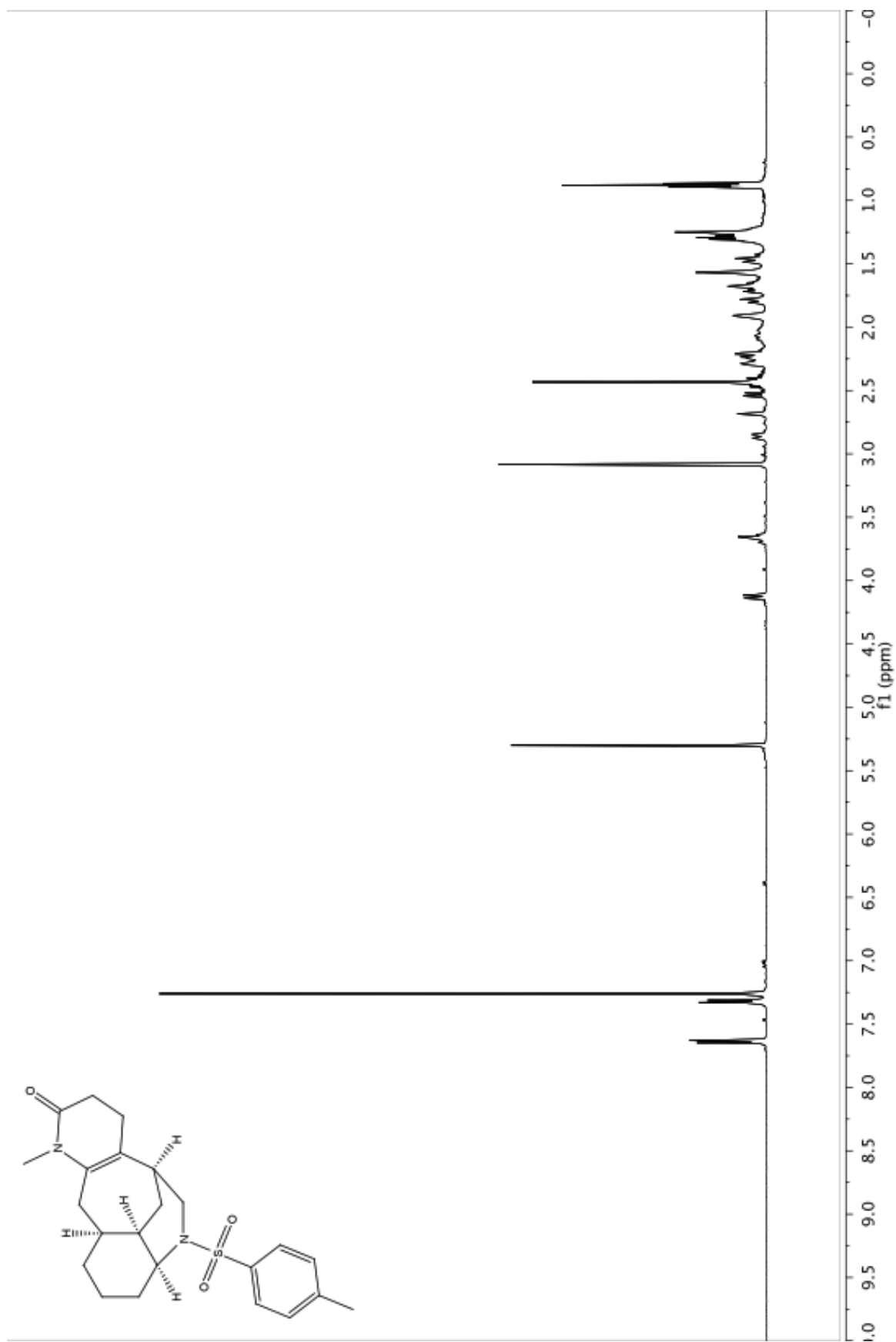
NOESY for enamide **2.108a**

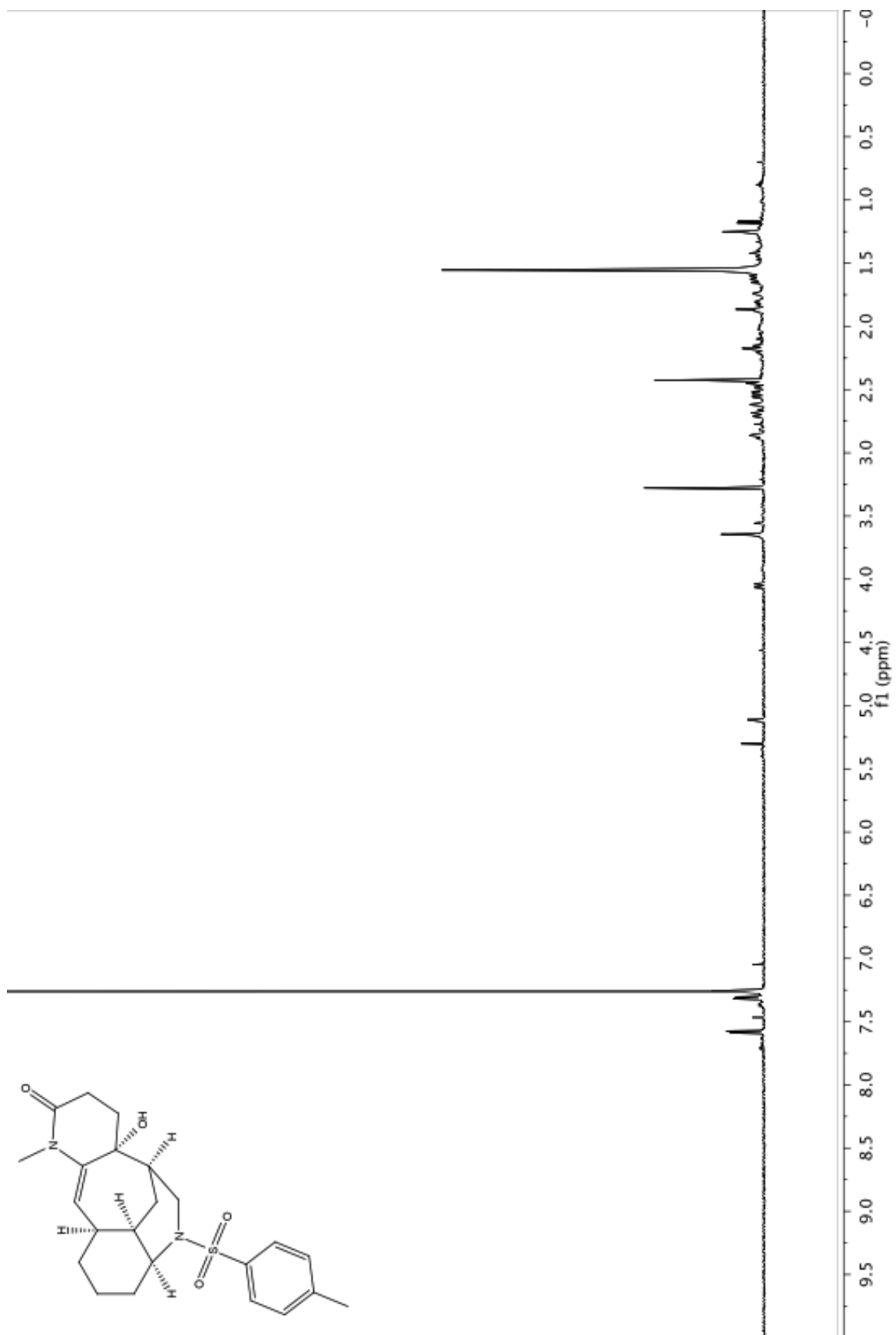


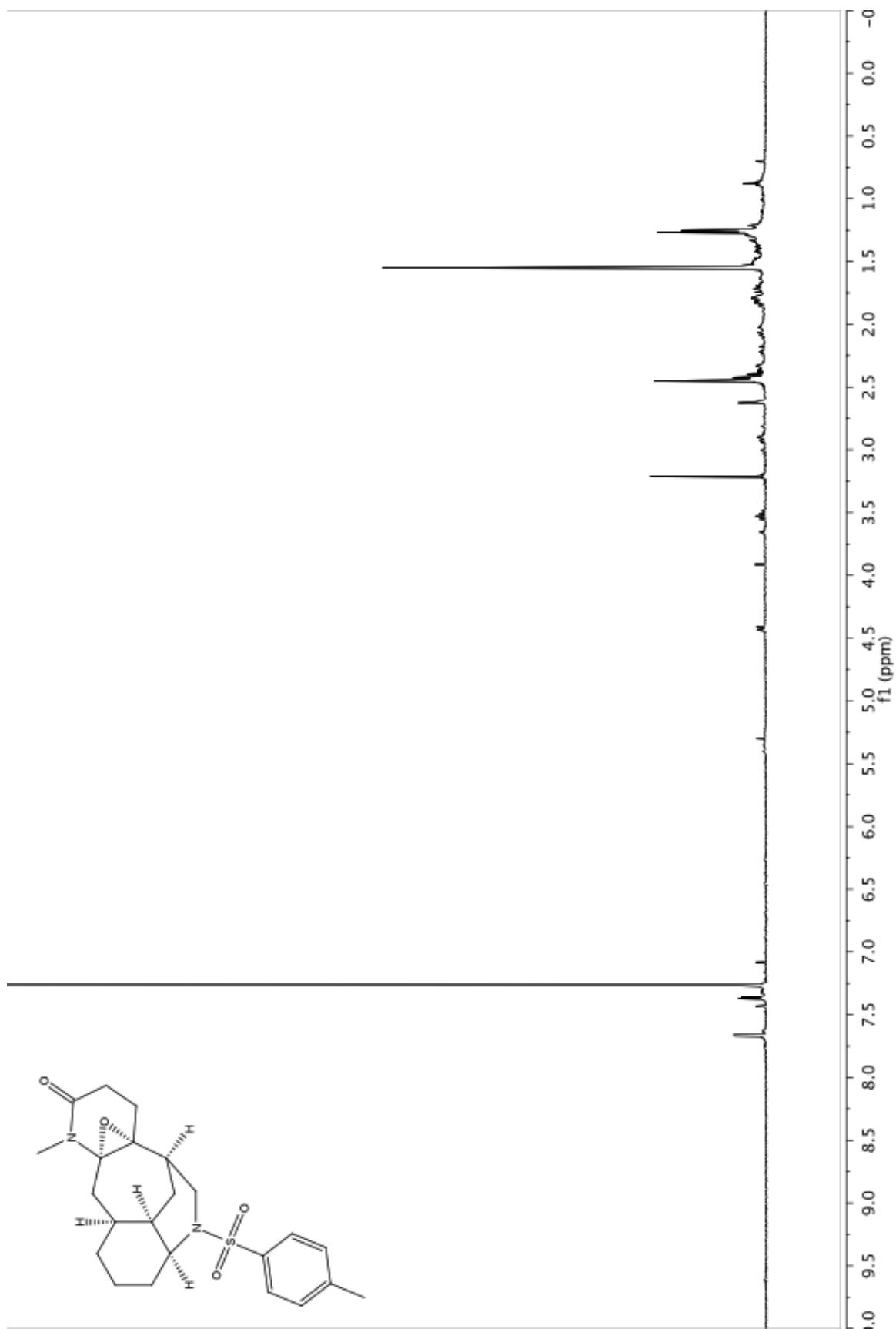


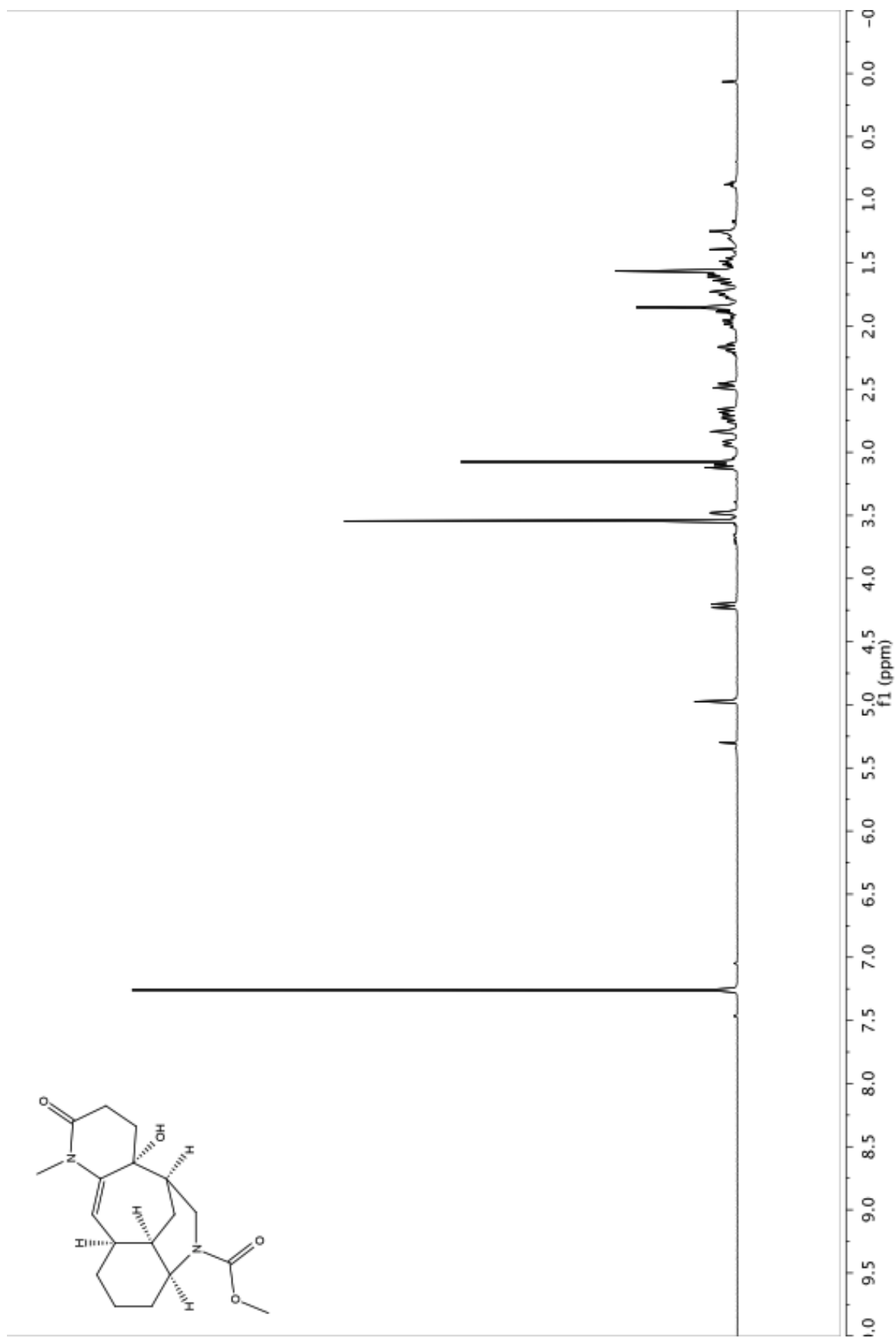


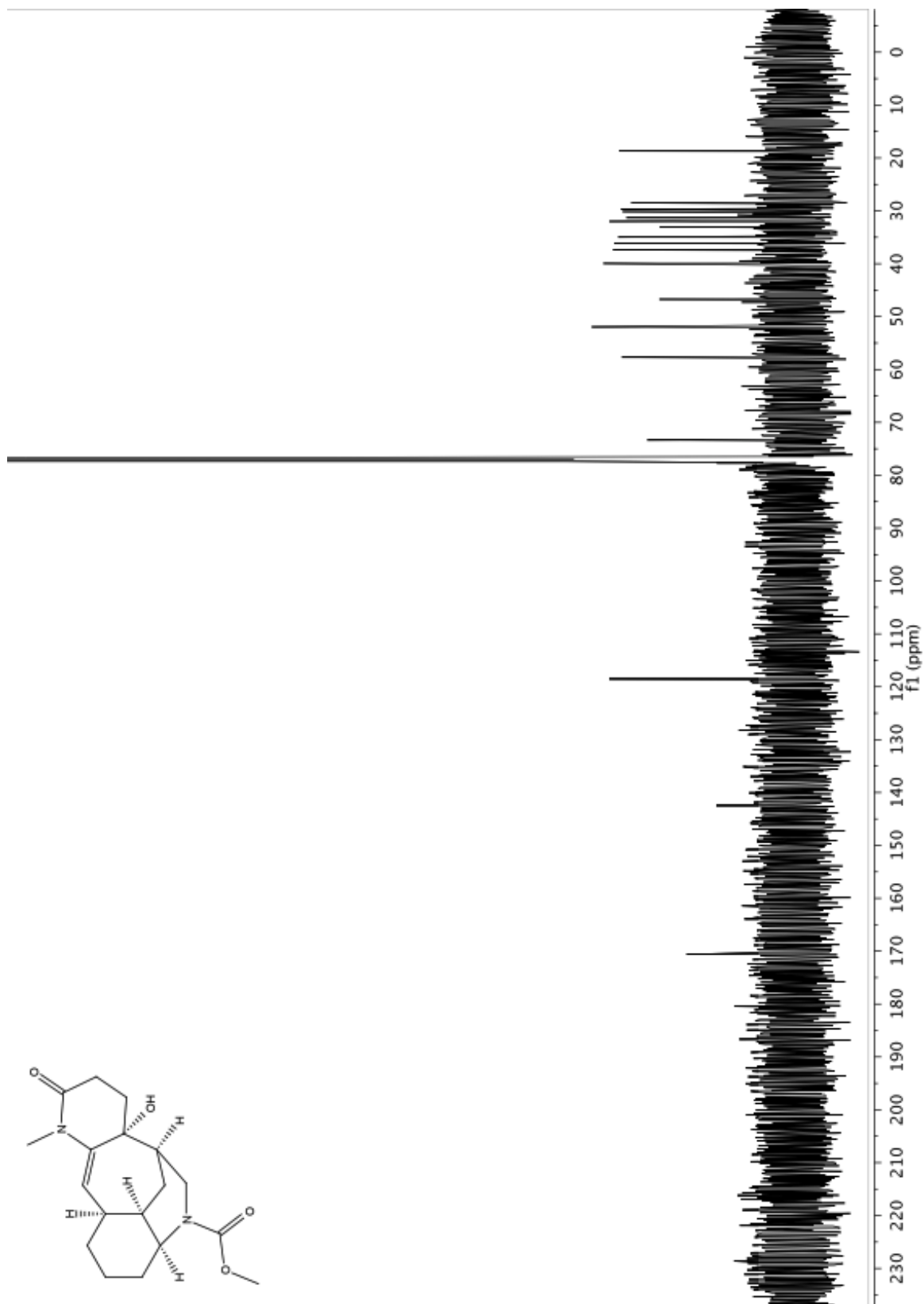


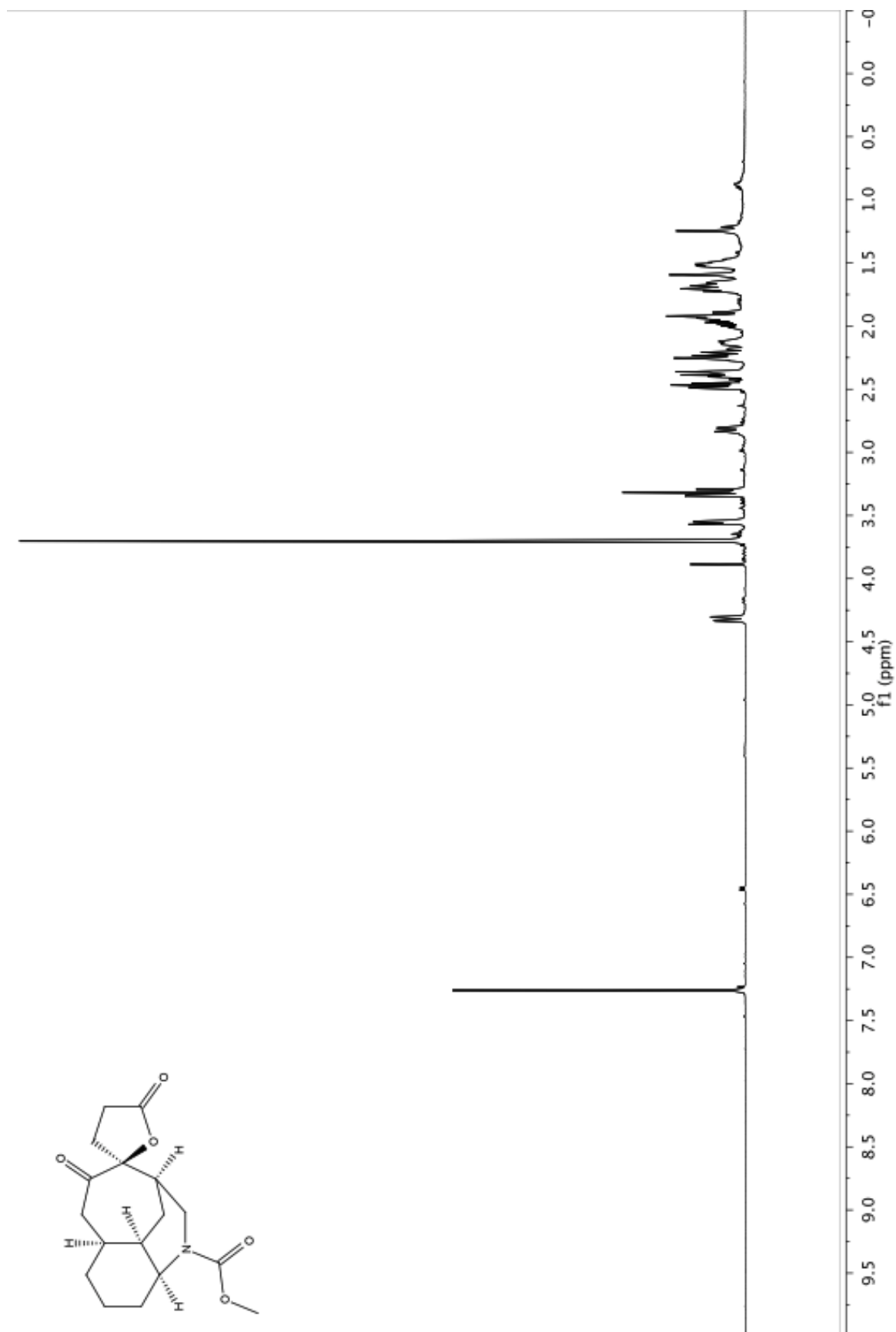


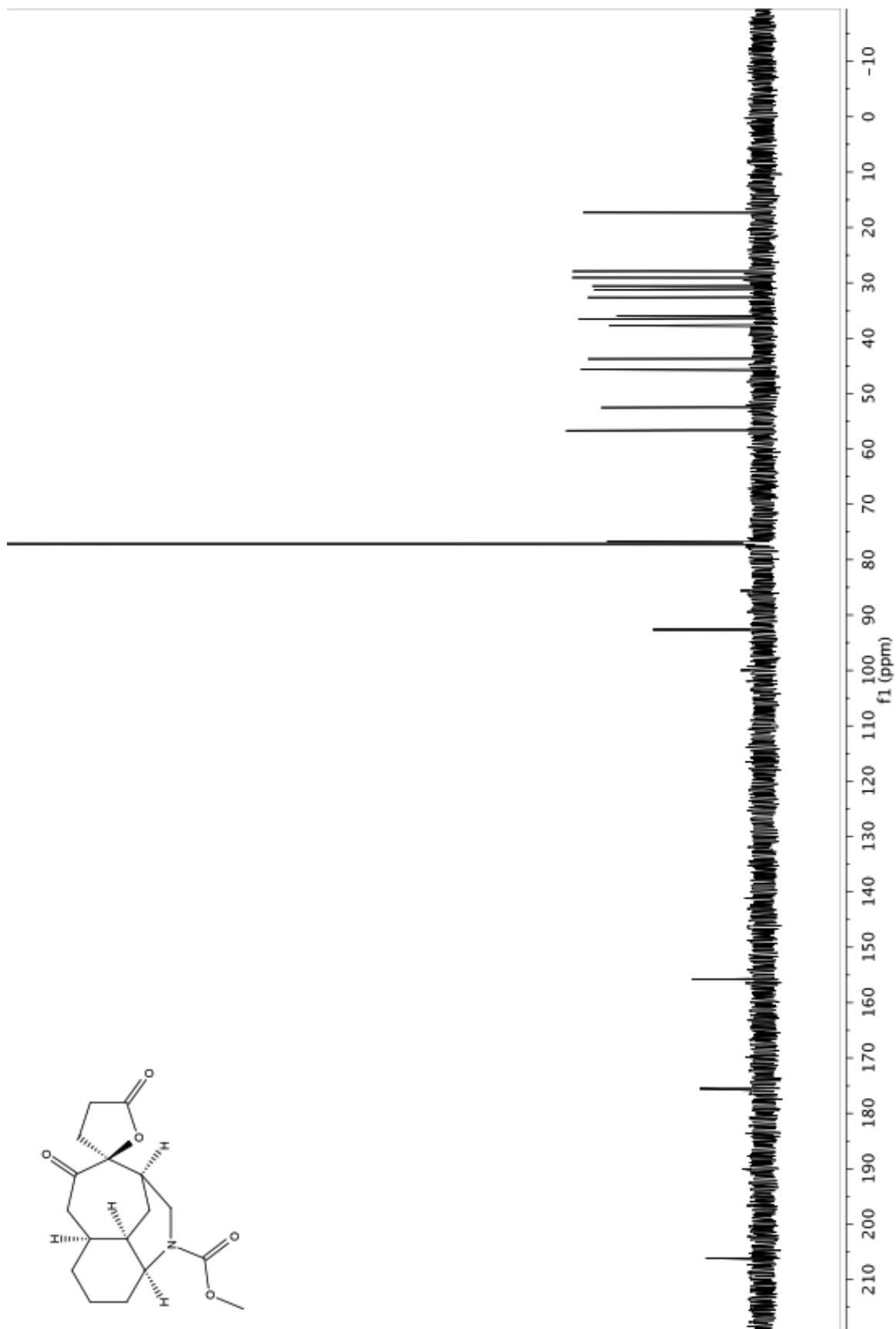


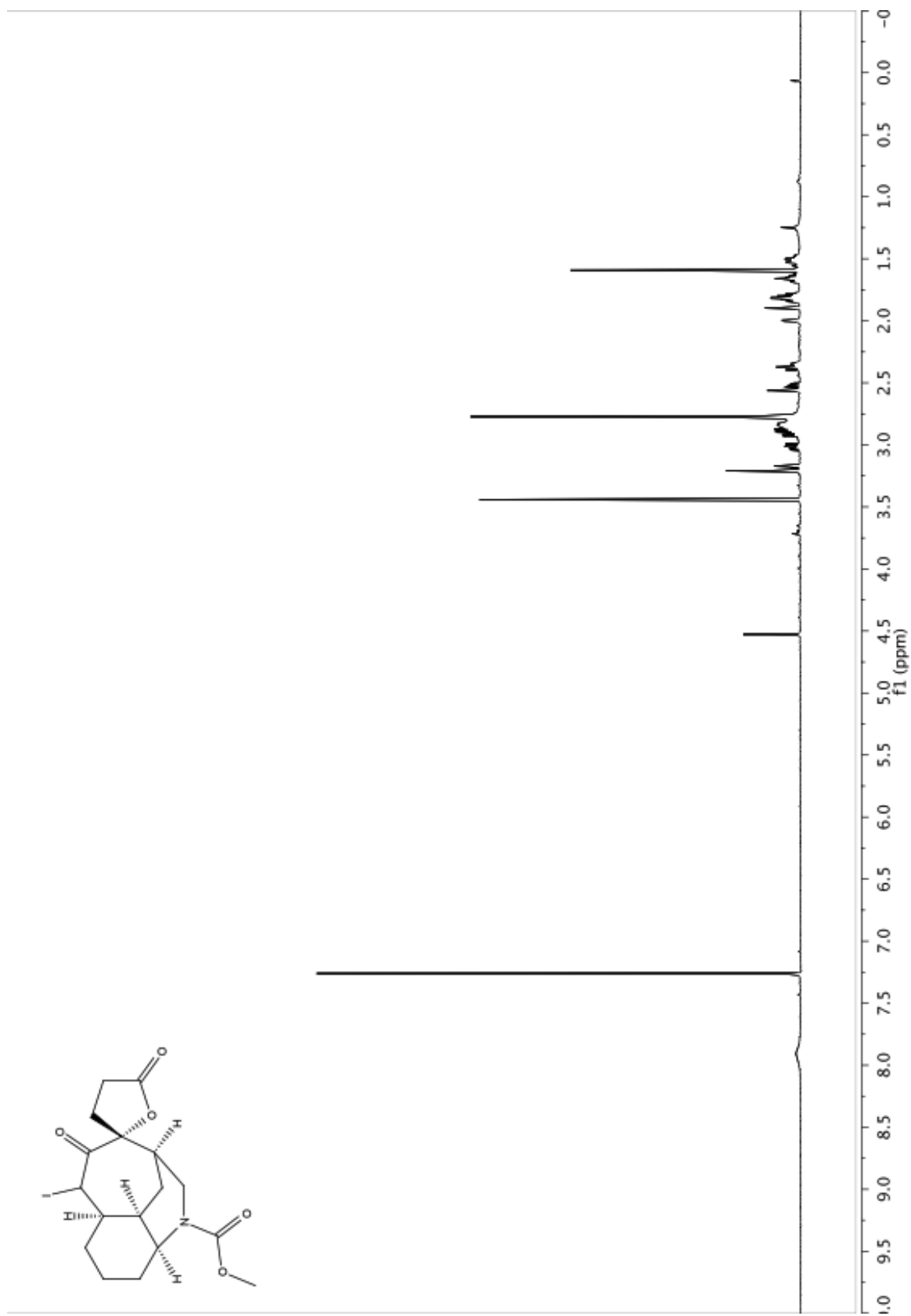


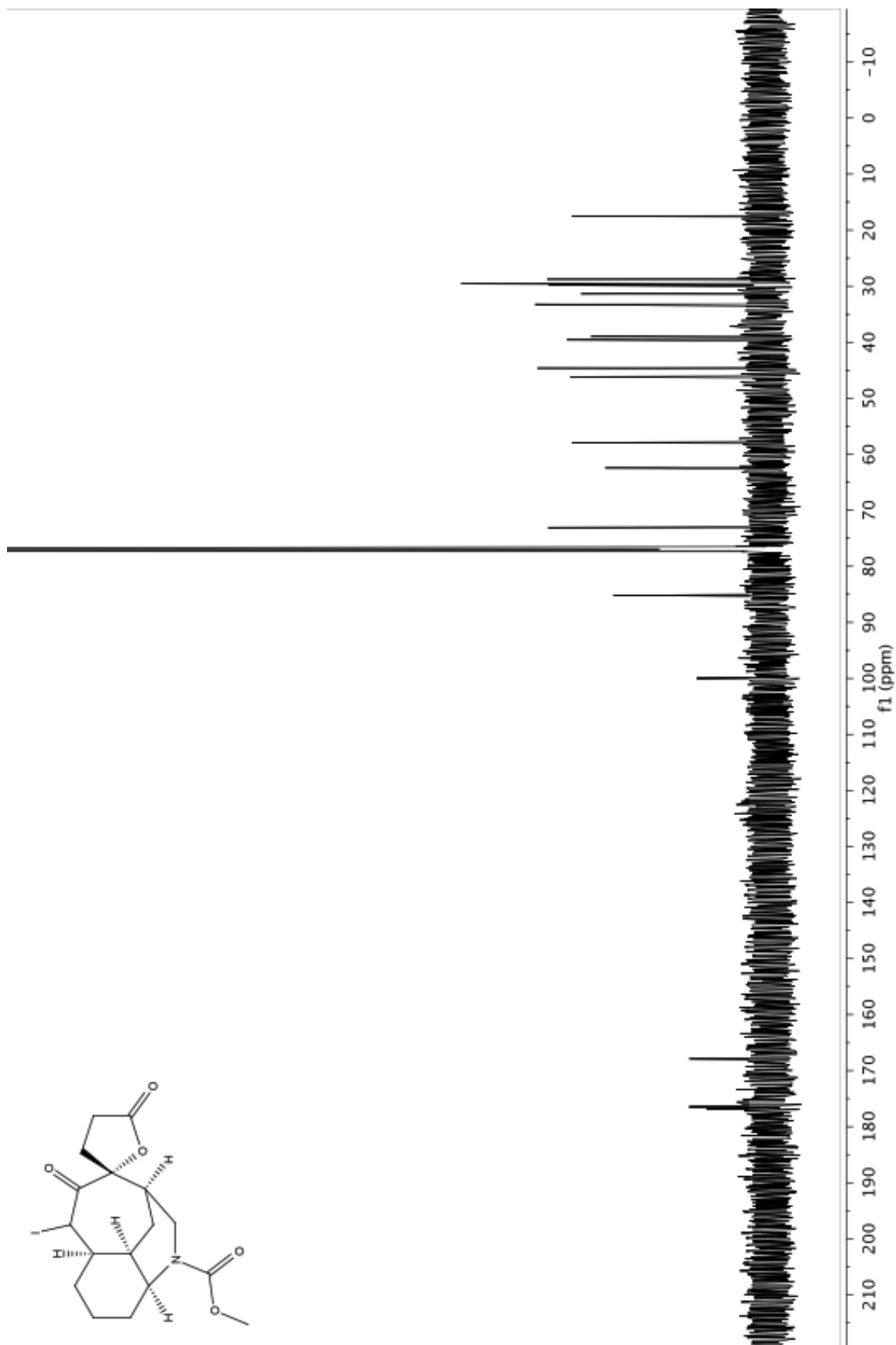












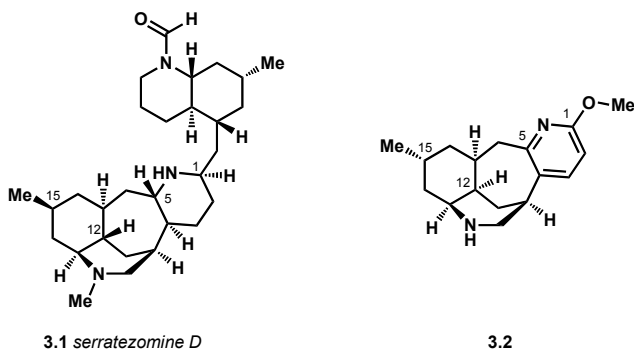
Chapter Three

Toward the Total Synthesis of Serratezomine D

3.1 Introduction

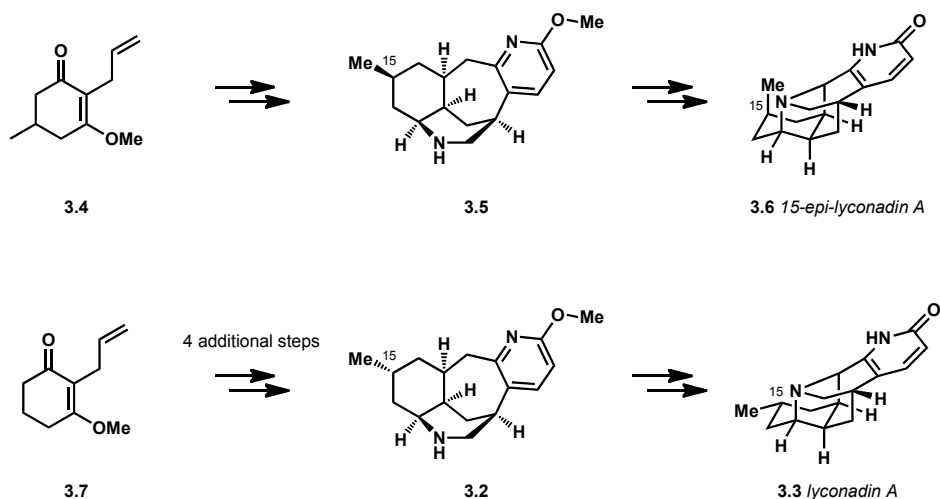
The isolation and structural elucidation of serratezomine D (**3.1**, Figure 3.1) was reported by Kobayashi and co-workers¹ while our studies toward the synthesis of spirolucidine and nankakurines A and B were underway. Serratezomine D immediately caught our attention as an ideal target for the unified approach to miscellaneous *Lycopodium* alkaloids. The tetracyclic core of serratezomine D is similar to tetracyclic amines such as **3.2** that have been synthesized in our laboratory.^{2,3} One of the most notable differences between **3.1** and **3.2** is the oxidation level of the pyridine ring in tetracycle **3.2**, which is a piperidine ring in **3.1**. The reduction of the methoxypyridine moiety of **3.2** was under investigation for the studies towards nankakurine B, and we foresaw the opportunity to apply our knowledge of this system's reactivity to a new target.

Figure 3.1 Serratezomine D and tetracycle **3.2**.



The other difference between common intermediate **3.2** and the tetracyclic core reported for serratezomine D is the stereochemistry at C-12 and C-15. To address this difference, we planned to take advantage of a lesson learned by Drs. West and Bisai in our laboratory during the synthesis of lyconadin A (**3.3**, see Scheme 3.1). One of the principal challenges in that synthesis proved to be achieving the correct stereochemistry at C-15. It was found that every attempt to bring in the methyl group at an early stage by beginning the synthesis with vinylogous ester **3.4** (Scheme 3.1) resulted in the synthesis of C-15 *epi*-tetracycle **3.5**, which in turn led to *epi*-lyconadin A (**3.6**).^{2,3} This was a drawback in the synthesis of lyconadin A that necessitated starting from vinylogous ester **3.7** and employing a four-step sequence to install the methyl group at a later stage; however, for the case of serratezomine D, we saw the opportunity to use this inherent stereochemical preference to our advantage.

Scheme 3.1 Stereochemistry of C-15.

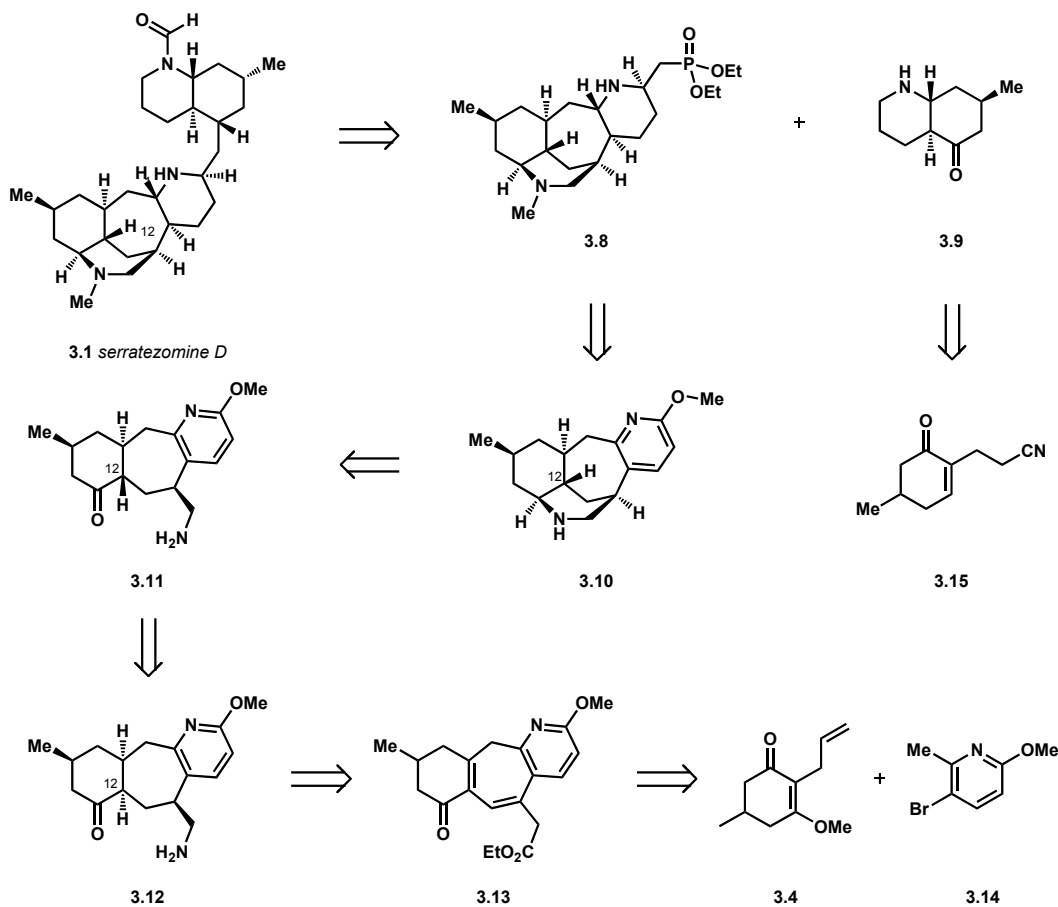


3.2 Retrosynthetic Analysis of Serratezomine D

Serratezomine D was envisioned to arise from the late-stage union of phosphonate **3.8** (Scheme 3.2) and ketone **3.9** through a Horner-Wadsworth-Emmons reaction. Phosphonate **3.8** would arise from the reduction and functionalization of the pyridine ring of **3.10**. Tetracycle **3.10** could be accessed from the intramolecular reductive amination of aminoketone **3.11**. Ketone **3.11** could be derived from the epimerization of ketone **3.12**, which was synthesized during initial studies toward lyconadin A.^{2,3} Ketone **3.12** arises from tricycle **3.13**, which ultimately comes from bromomethoxypicoline **3.14** and vinylogous ester **3.4**.

The key challenge that we wanted to explore in this synthesis was the transformation of ketone **3.11** to tetracycle **3.10**. Although the analogous reductive amination of aminoketone **3.12** to give tetracycle **3.2** has been demonstrated, this could prove much more challenging with substrate **3.11**. The epimerization of the C-12 stereocenter appears to add significant strain to caged structure **3.10**. We sought to determine whether the construction of the core of serratezomine D was possible through methods developed for tetracycle **3.12** and to gain insight into the strain inherent in **3.10** by doing so.

Scheme 3.2 Retrosynthesis of serratezomine D.



3.3 Model Study

Initial studies on the epimerization of the C-12 stereocenter and subsequent reductive amination were carried out on tricyclic ketone **3.16**, which does not bear the C-15 methyl group. This had been synthesized during the studies on nankakurine B and was already in hand. The transformation of *cis*-fused ketone **3.16** to *trans*-fused ketone **3.17** was expected to be thermodynamically favorable on the basis that this epimerization would allow both substituents on the cyclohexanone ring of **3.17** to reside in equatorial positions.

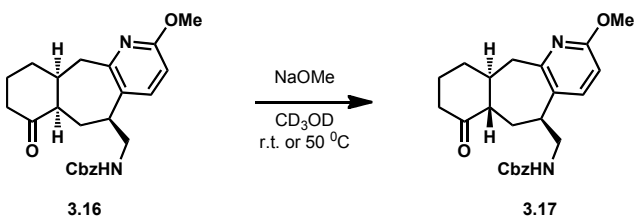
Initial attempts to effect the isomerization of **3.16** with potassium carbonate in methanol resulted in starting material (Table 3.1, entry 1). Employing *p*-toluenesulfonic acid afforded multiple products (entry 2). Utilizing pyrrolidine gave 50% conversion to product (entry 3). Using DBU as a base gave only starting material at room temperature, but began to show conversion at 45 °C (entries 4 and 5). It was found that increasing the number of equivalents of DBU led to higher conversion to product; however, the maximum conversion achieved with this reagent was 67% (entries 6 – 8). Employing sodium methoxide as the base gave the same result (entry 9).

Table 3.1 Model study of epimerization reaction.

Entry	Reagent	Solvent	Temp. (°C)	Result
1	K ₂ CO ₃	MeOH	r.t.	s.m.
2	p-TsOH	PhH	r.t.	mult. prods.
3	pyrrolidine	PhH	r.t.	50 % conversion
4	DBU	DCM	r.t.	s.m.
5	0.25 equiv. DBU	DCM	45	25 % conversion
6	1 equiv. DBU	DCM	45	55 % conversion
7	3 eqyuv. DBU	DCM	45	67 % conversion
8	6 equiv. DBU	DCM	45	67 % conversion
9	NaOMe	MeOH	r.t.	67 % conversion

The consistency with which a 66% conversion was obtained led us to speculate that perhaps this was the thermodynamic ratio of the product and starting material. To test this, the conversion of **3.16** to **3.17** in the presence of sodium methoxide was studied by NMR (Table 3.2). The reaction was run in deuterated methanol at both room temperature and 50 °C. It was found that at 50 °C, the reaction progressed to 66% conversion after approximately one day. The reaction run at room temperature required three days of stirring before 66% conversion was achieved. Both reactions reached the same 66% conversion that had been observed previously and did not progress further even after stirring for a week. We concluded that this 2:1 ratio between **3.17** and **3.16** does indeed represent the thermodynamic ratio.

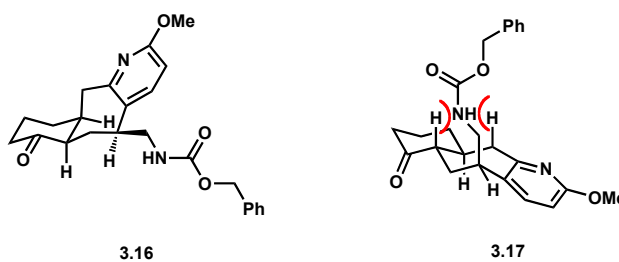
Table 3.2 Conversion of **3.16** to **3.17** over time.



Time	Conversion to 3.17 at r.t.	Conversion to 3.17 at 50 °C
1.5 h	12 %	45 %
3.5 h	22 %	54 %
5.5 h	26 %	58 %
26 h	52 %	65 %
2 d	59 %	66 %
3 d	63 %	66 %
10 d	65 %	66 %

We postulate that lack of a strong preference for the *trans*-fused 6,7-ring system of **3.17** over the *cis*-fused 6,7-system of **3.16** can be attributed to the CH₂NHCbz substituent on the seven-membered ring. In *cis*-fused ketone **3.16** (see Figure 3.2), this substituent is free to adopt a pseudo-equatorial orientation in which steric interaction with the remainder of the molecule is minimized. In *trans*-fused ketone **3.17**, the seven-membered ring is forced to undergo a conformational change that places this large substituent in a pseudo-axial orientation. It likely experiences a steric clash with the indicated pseudo-axial hydrogens.

Figure 3.2 Conformations of **3.16** and **3.17**.



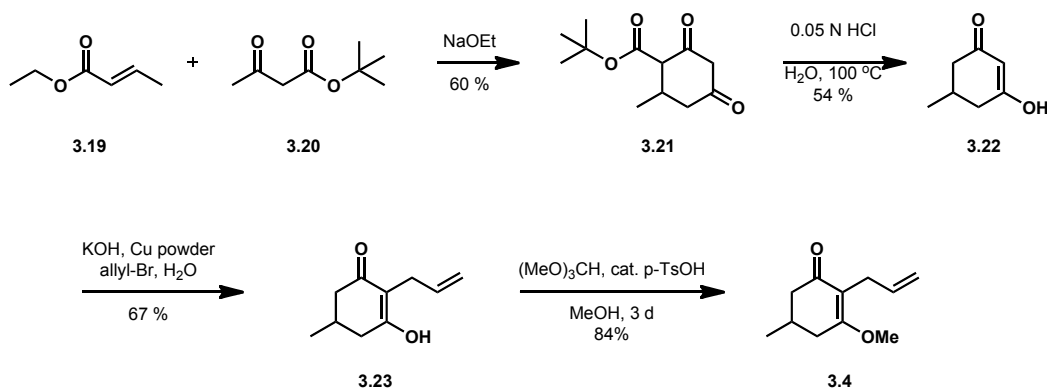
These difficulties in the epimerization of substrate **3.16** led us to abandon the model study at this stage and shift our focus to methylated ketone **3.18**.

3.4 Studies Toward the Tetracyclic Core of Serratezomine D

Synthesis of ketone **3.18** began with the construction of vinylogous ester **3.4** (Scheme 3.3). Ethyl crotonate (**3.19**) and *t*-butylacetoacetate (**3.20**) underwent

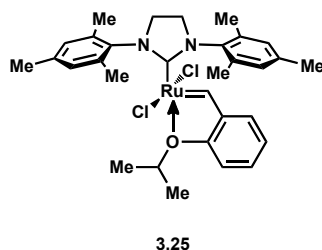
conjugate addition followed by a Claisen condensation to afford ester **3.21**. Heating **3.21** in the presence of dilute hydrochloric acid led to decarboxylation and isolation of vinylogous acid **3.22**.⁴ Allylation was accomplished by stirring in the presence of potassium hydroxide and allyl bromide to give allylated acid **3.23** in 67% yield. Acid **3.23** was transformed into vinylogous ester **3.4** by treatment with trimethyl orthoformate and catalytic *p*-toluenesulfonic acid.

Scheme 3.3 Synthesis of vinylogous ester **3.4**.

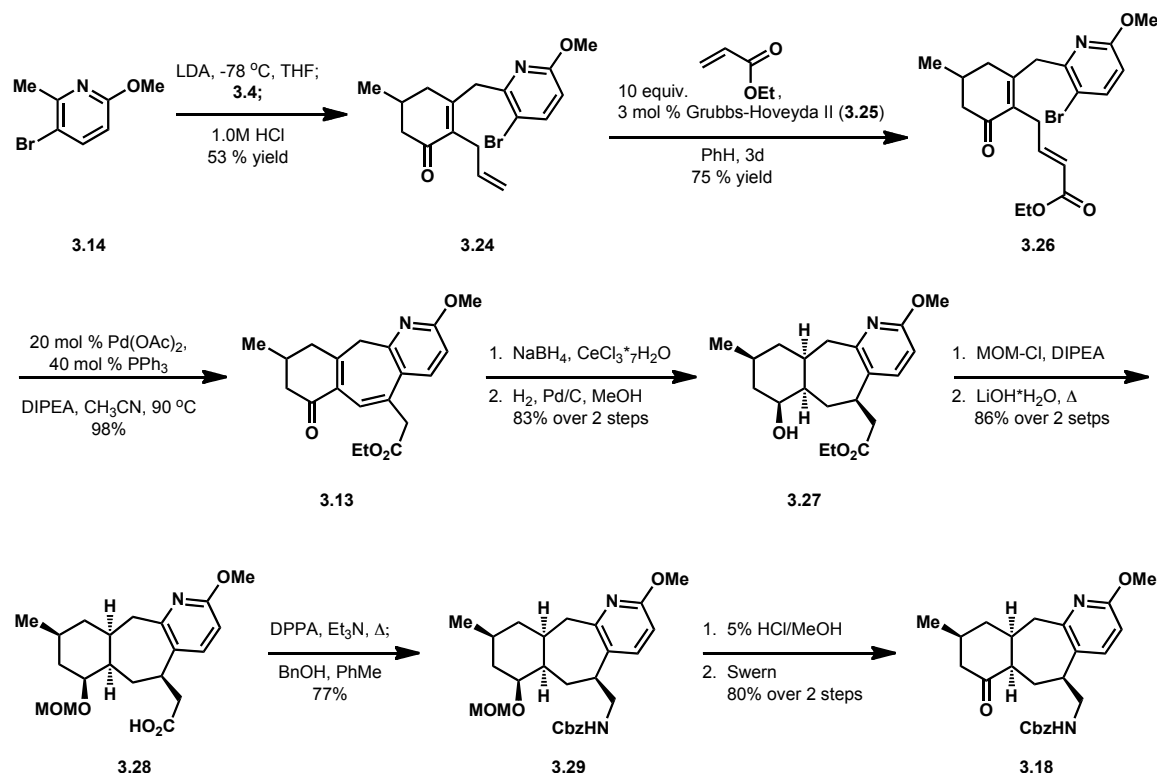


The synthesis of tricyclic ketone **3.18** was then carried out according to the route developed by West and Bisai (Scheme 3.4).^{2,3} The anion of methoxypicoline **3.14** was treated with vinylogous ester **3.4** at -78 °C. Subsequent hydrolysis with hydrochloric acid afforded enone **3.24** in 53% yield. Cross metathesis was carried out with the Grubbs-Hoveyda second generation catalyst **3.25** (see Figure 3.3) and ethyl acrylate to give enoic ester **3.26**. Ester **3.26** was converted to tricyclic **3.13** via a Heck reaction. Luche reduction of **3.13** was followed by hydrogenation to afford ester **3.27**. MOM protection of the hydroxyl group and subsequent hydrolysis of the ester functionality gave rise to acid **3.28**. A Curtius rearrangement was carried out in the presence of benzyl alcohol to afford amine **3.29**. Hydrolysis of the MOM ether and Swern oxidation afforded desired ketone **3.18**.

Figure 3.3 Grubbs-Hoveyda second generation catalyst.

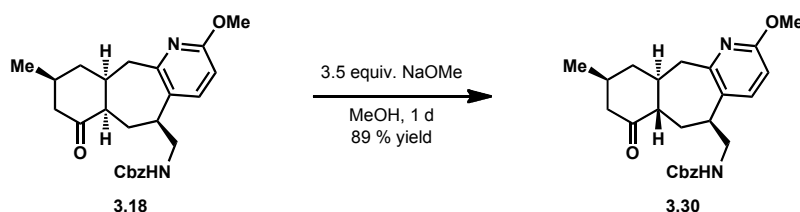


Scheme 3.4 Synthesis of tricyclic ketone **3.18**.



The epimerization of *cis*-fused ketone **3.18** to *trans*-fused ketone **3.30** was then investigated (Scheme 3.3). Gratifyingly, treatment of **3.18** with sodium methoxide in methanol resulted in complete conversion to the desired product **3.30** in high yield.

Scheme 3.5 Epimerization of ketone **3.18**.



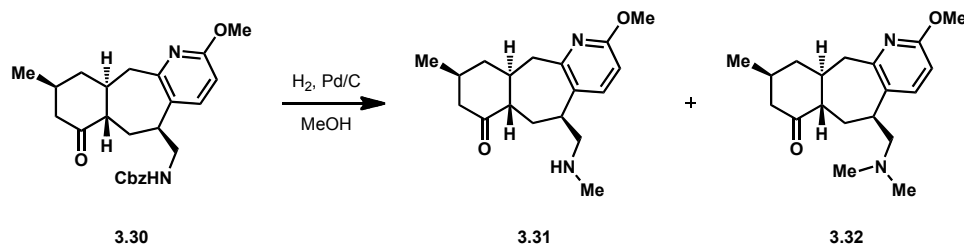
Ketone **3.30** bears all the requisite stereochemistry of the core of serratezomine D (**3.1**, see Figure 3.1). Having established a route to access this material, we were now in position to investigate the key reductive amination.

Hydrogenolysis of ketone **3.30** with palladium on carbon in methanol resulted in isolation of a mixture of amines **3.31** and **3.32** (Scheme 3.6). These were presumed to arise via the dehydrogenation of methanol to form formaldehyde, which could condense with the initial product of the hydrogenolysis reaction to form an iminium ion. The reductive reaction conditions could complete a reductive

amination to afford **3.31**. Amine **3.32** is merely the result of two reductive amination processes.

This initial result was discouraging. *Cis*-fused ketone **3.16** had only been observed to undergo adventitious methylation after the desired intramolecular reductive amination had already taken place; this suggested that the desired tetracycle-forming reductive amination was slower in the case of **3.30** than it was for **3.16**.

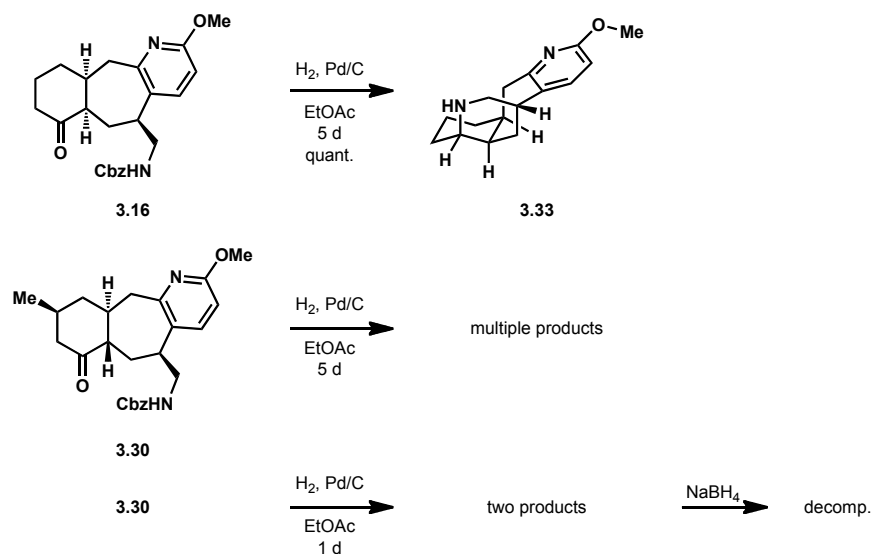
Scheme 3.6 Hydrogenolysis of ketone **3.30** in methanol.



Ketone **3.16** had been shown to undergo partial or complete intramolecular reductive amination to give **3.33** upon prolonged exposure to hydrogenolysis conditions (Scheme 3.7). Undesired methylation could be suppressed by using ethyl acetate as solvent. The success encountered in the case of ketone **3.16** inspired us to try a similar approach with **3.30**.

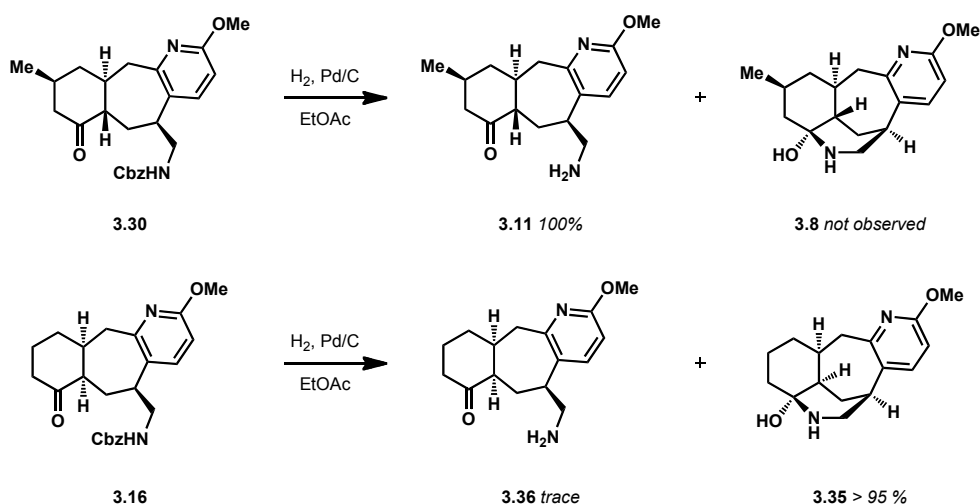
Treatment of **3.30** with 50 weight % palladium on carbon and hydrogen in ethyl acetate for 5 days resulted in the formation of multiple products that stemmed from overreduction of the substrate. Decreasing the reaction time to 1 d gave two products. Treatment of these two products with NaBH_4 failed to provide any of the desired tetracycle.

Scheme 3.7 Hydrogenolysis of ketones **3.16** and **3.30** in ethyl acetate.



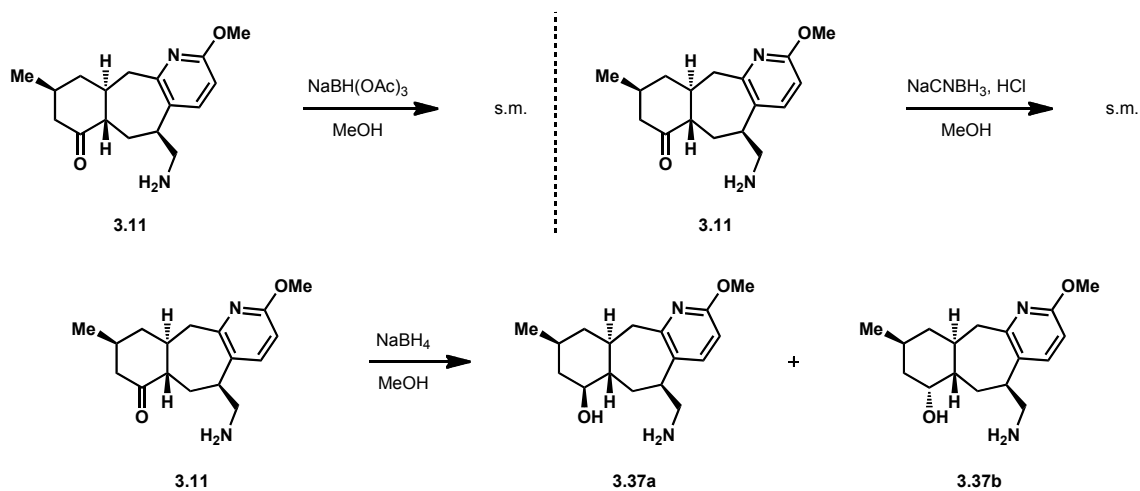
Decreasing the reaction time further to 12 h allowed for the isolation of aminoketone **3.11** (Scheme 3.8). Discouragingly, ¹H NMR indicated that this product existed entirely as the aminoketone tautomer (**3.11**), with no sign of the hemiaminal form (**3.34**). This was in stark contrast to substrate **3.16**, which was observed to exist almost exclusively in the hemiaminal form **3.35**.

Scheme 3.8 Hydrogenolysis of ketone **3.30** versus ketone **3.16** in EtOAc.



Several attempts were made to induce the intramolecular reductive amination of **3.11** to generate tetracycle **3.10** (Scheme 3.9). Treatment of **3.11** with sodium triacetoxyborohydride resulted in recovery of starting material. Sodium cyanoborohydride also failed to effect any of the desired reductive amination. Employing sodium borohydride resulted in reduction of **3.11** to afford alcohol **3.37** as a mixture of diastereomers at the carbon bearing the hydroxyl group.

Scheme 3.9 Attempted reductive amination of **3.11**.



These results seemed to indicate that several undesired reduction pathways of ketone **3.11** were more favored than the desired intramolecular reductive amination to afford **3.10**. This led us to conclude that forcing conditions would be necessary to build strained tetracyclic core **3.10**, and the reductive amination methodology developed to access tetracycle **3.2** would not be sufficient to effect this transformation.

3.5 Conclusion

Tricyclic ketone substrate **3.30** was built through the epimerization of ketone **3.18**. The suitability of extending a ring-closing intramolecular reductive amination first developed for the formation of tetracycle **3.2** to the generation of tetracycle **3.10** was evaluated. Tetracycle **3.10** was found to be too strained to be constructed in this manner. This high strain calls into question the validity of the proposed structure of serratezomine D (**3.1**).

3.6 Experimental Contributions

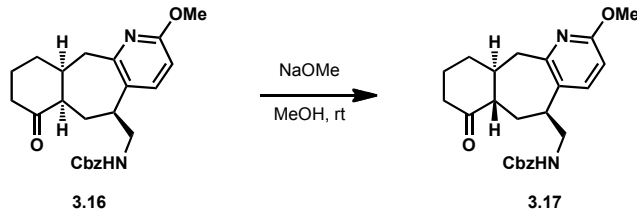
The synthesis of ketone **3.18** (Scheme 3.4) was pioneered by Alakesh Bisai and Scott West in our research group during their studies on the total synthesis of lyconadin A.

3.7 Experimental Methods

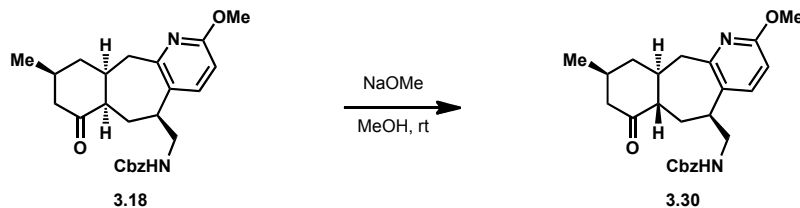
Materials and Methods

Unless otherwise stated, reactions were performed in oven-dried glassware fitted with rubber septa under a nitrogen atmosphere and were stirred with Teflon-coated magnetic stirring bars. Liquid reagents and solvents were transferred via syringe using standard Schlenk techniques. Tetrahydrofuran (THF) and diethyl ether (Et₂O) were distilled over sodium/benzophenone ketyl. Dichloromethane (CH₂Cl₂), toluene, and benzene were distilled over calcium hydride. Acetonitrile was distilled over potassium carbonate. *N,N*-Diisopropylethylamine (DIPEA) was distilled over calcium hydride prior to use. All other solvents and reagents were used as received unless otherwise noted. Reaction temperatures above 23 °C refer to oil bath temperature, which was controlled by an OptiCHEM temperature modulator. Thin layer chromatography was performed using SiliCycle silica gel 60 F-254 precoated plates (0.25 mm) and visualized by UV irradiation and anisaldehyde stain. SiliCycle Silia-P silica gel (particle size 40-63 μm) was used for flash chromatography. Melting points were recorded on a Laboratory Devices Mel-Temp 3.0 and are uncorrected. ¹H and ¹³C NMR spectra were recorded on Bruker AVB-400, DRX-500, AV-500 and AV-600 MHz spectrometers with ¹³C operating frequencies of 100, 125, 125 and 150 MHz, respectively. Chemical shifts (δ) are reported in ppm relative to the residual solvent signal (δ = 7.26 for ¹H NMR and δ = 77.0 for ¹³C NMR). Data for ¹H NMR spectra are reported as follows: chemical shift (multiplicity, coupling constants, number of hydrogens). Abbreviations are as follows: s (singlet), d (doublet), t (triplet), q (quartet), m (multiplet), br (broad). IR spectra were recorded on a Nicolet MAGNA-IR 850 spectrometer and are reported in frequency of absorption (cm⁻¹). Only selected IR absorbencies are reported. High resolution mass spectral data were obtained from the Mass Spectral Facility at the University of California, Berkeley.

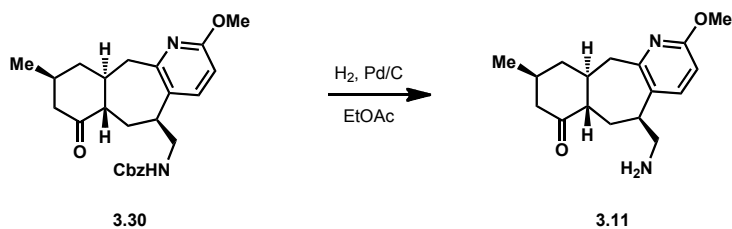
Experimental Procedures



Ketone 3.17: A round-bottom flask was charged with ketone **3.16** (2.7 mg, 0.00664 mmol), NaOMe (0.9 mg, 0.0167 mmol) and MeOH (1.0 mL). The reaction was stirred for 24 h, then poured into sat. NH_4Cl (2 mL). The mixture was extracted with DCM (3 x 10 mL). The combined organic extracts were dried over MgSO_4 , filtered and concentrated under vacuum to afford 2.4 mg (89% yield) of ketones **3.17** and **3.16** in a 2:1 ratio. R_f 0.38 (3:1 hexanes/EtOAc); $^1\text{H NMR}$ (600 MHz, CDCl_3) δ 7.39 – 7.27 (m, 6H), 6.48 (d, $J = 8.2$ Hz, 1H), 5.05 (s, 2H), 4.65 (br, s, 1H), 3.88 (s, 3H), 3.59 – 3.53 (m, 1H), 3.53 – 3.45 (m, 1H), 3.11 (dd, $J = 14.7, 9.0$ Hz, 1H), 3.05 – 2.96 (m, 2H), 2.50 (t, $J = 7.49$, 1H), 2.46 – 2.36 (m, 1H), 2.32 (dd, $J = 12.3, 6.0$ Hz, 2H), 2.09 (s, 1H), 2.00 (s, 1H), 1.76 – 1.63 (m, 4H) (for major rotamer).



Ketone 3.30: A round-bottom flask was charged with ketone **3.18** (36.6 mg, 0.0867 mmol), NaOMe (16.3 mg, 0.302 mmol) and MeOH (1.2 mL). The reaction was stirred for 24 h, then poured into sat. NH_4Cl (5 mL). The mixture was extracted with DCM (3 x 10 mL). The combined organic extracts were dried over MgSO_4 , filtered and concentrated under vacuum to afford 32.4 mg (89% yield) of ketone **3.30**. The crude material was used in the next step without purification. R_f 0.35 (2:1 hexanes/EtOAc); $^1\text{H NMR}$ (600 MHz, CDCl_3) δ 7.36 – 7.20 (m, 6H), 6.47 (d, $J = 8.2$ Hz, 1H), 5.07 – 4.99 (s, 2H), 4.77 (s, 1H), 3.88 (s, 3H), 3.58 – 3.50 (m, 1H), 3.46 (m, 1H), 3.08 (dd, $J = 14.7, 10.0$ Hz, 1H), 2.99 (m, 2H), 2.43 (t, $J = 11.4$ Hz, 1H), 2.39 – 2.26 (m, 2H), 2.06 – 1.93 (m, 2H), 1.89 – 1.80 (m, 1H), 1.65 (m, 2H), 1.41 (q, $J = 12.3$ Hz, 1H), 1.03 (d, $J = 6.4$ Hz, 3H) (for major rotamer); $^{13}\text{C NMR}$ (151 MHz, CDCl_3) δ 211.47, 162.15, 156.45, 156.23, 140.55, 136.44, 128.47, 128.41, 128.07, 127.95, 107.42, 66.65, 53.36, 53.31, 51.81, 49.52, 45.82, 42.86, 42.27, 41.93, 41.59, 36.11, 33.18, 28.71, 22.36, 22.28, 22.22 (for two rotamers); IR (film) ν_{max} 3347, 2952, 1699, 1597, 1538, 1479, 1426, 1312, 1268, 1141, 1035 cm^{-1} ; HRMS (ESI) m/z 423.2272 $[(\text{M}+\text{H})^+]$; calculated for $[\text{C}_{25}\text{H}_{31}\text{N}_2\text{O}_4]^+$: 423.2278]; MP 54 – 56 $^\circ\text{C}$.

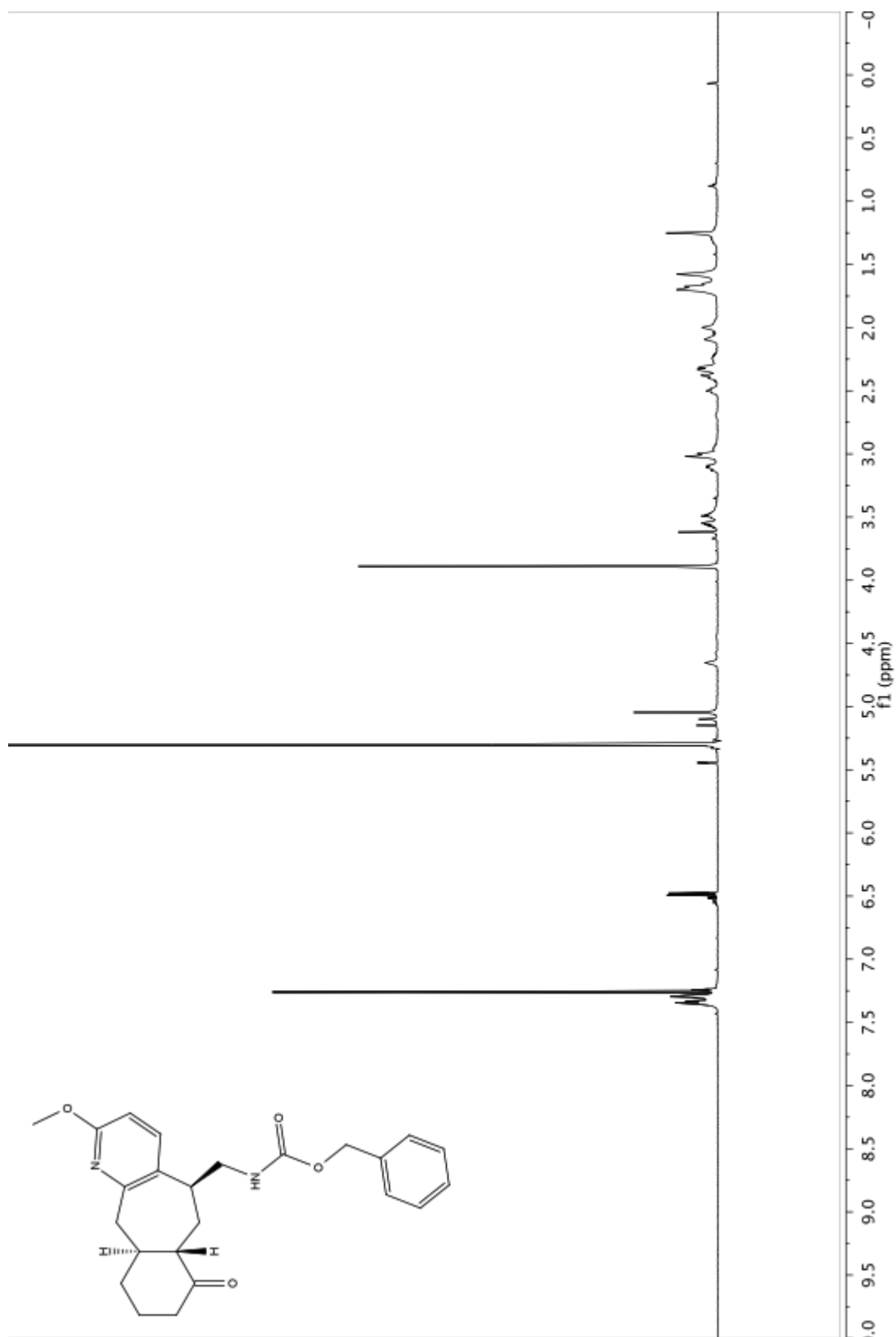


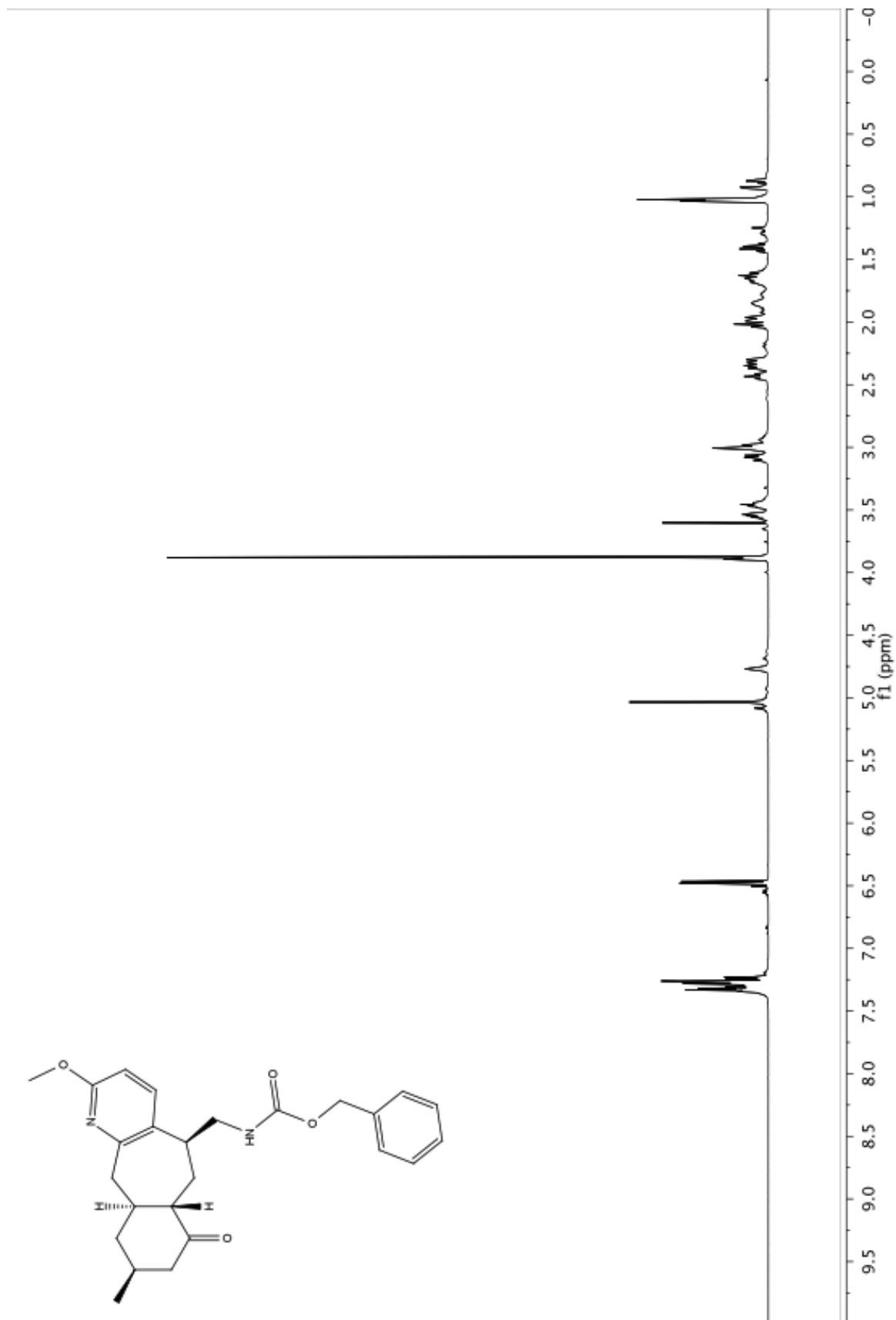
Ketone 3.11: Ketone **3.30** (1.4 mg, 0.00332 mmol) was dissolved in EtOAc (1 mL) and sparged with nitrogen for 5 minutes. 10% Pd on activated carbon (0.5 mg) was added and the reaction vessel was evacuated and backfilled with hydrogen 3 times. The reaction mixture was placed under a hydrogen atmosphere (1 atm. balloon) and stirred at rt for 1 d. The reaction mixture was filtered through a pad of celite and washed with MeOH (3 x 5 mL). The filtrate was concentrated under vacuum to provide 1.0 mg (quant. yield) of aminoketone **3.11**. $^1\text{H NMR}$ (500 MHz, CDCl_3) δ 7.28 (d, $J = 8.3$ Hz, 1H), 6.51 (d, $J = 8.2$ Hz, 1H), 4.56 (br, s, 1H), 3.90 (s, 3H), 3.62 (s, 2H), 3.54 (s, 1H), 3.44 (s, 1H), 3.13 – 2.96 (m, 3H), 2.47 – 2.28 (m, 3H), 2.01 (m, 2H), 1.89 (m, 1H), 1.63 (m, 1H), 1.09 – 1.00 (d, $J = 6.4$ Hz, 3H), 0.97 – 0.92 (2d, $J = 6.8, 3.2$ Hz, 1H).

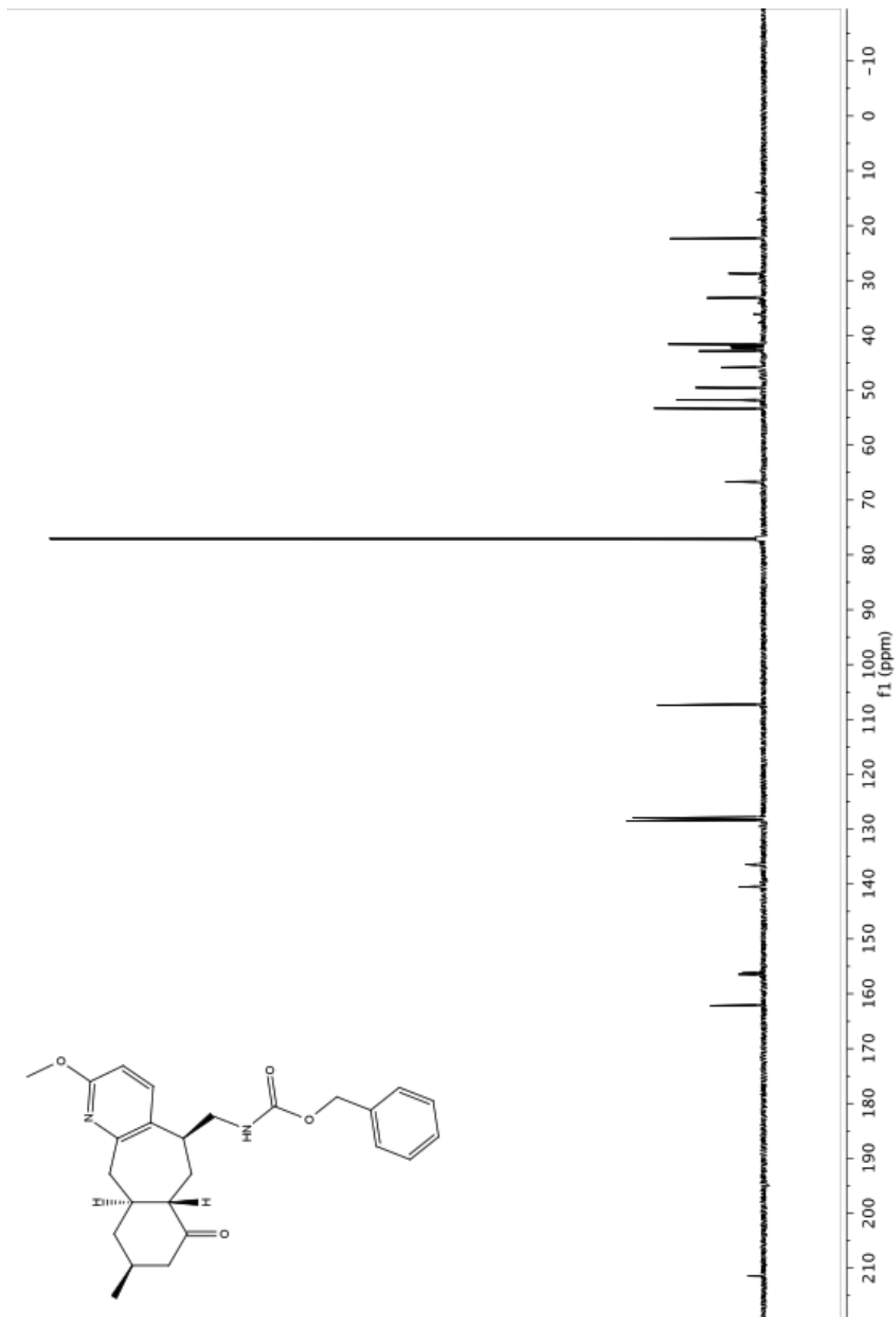
3.8 References

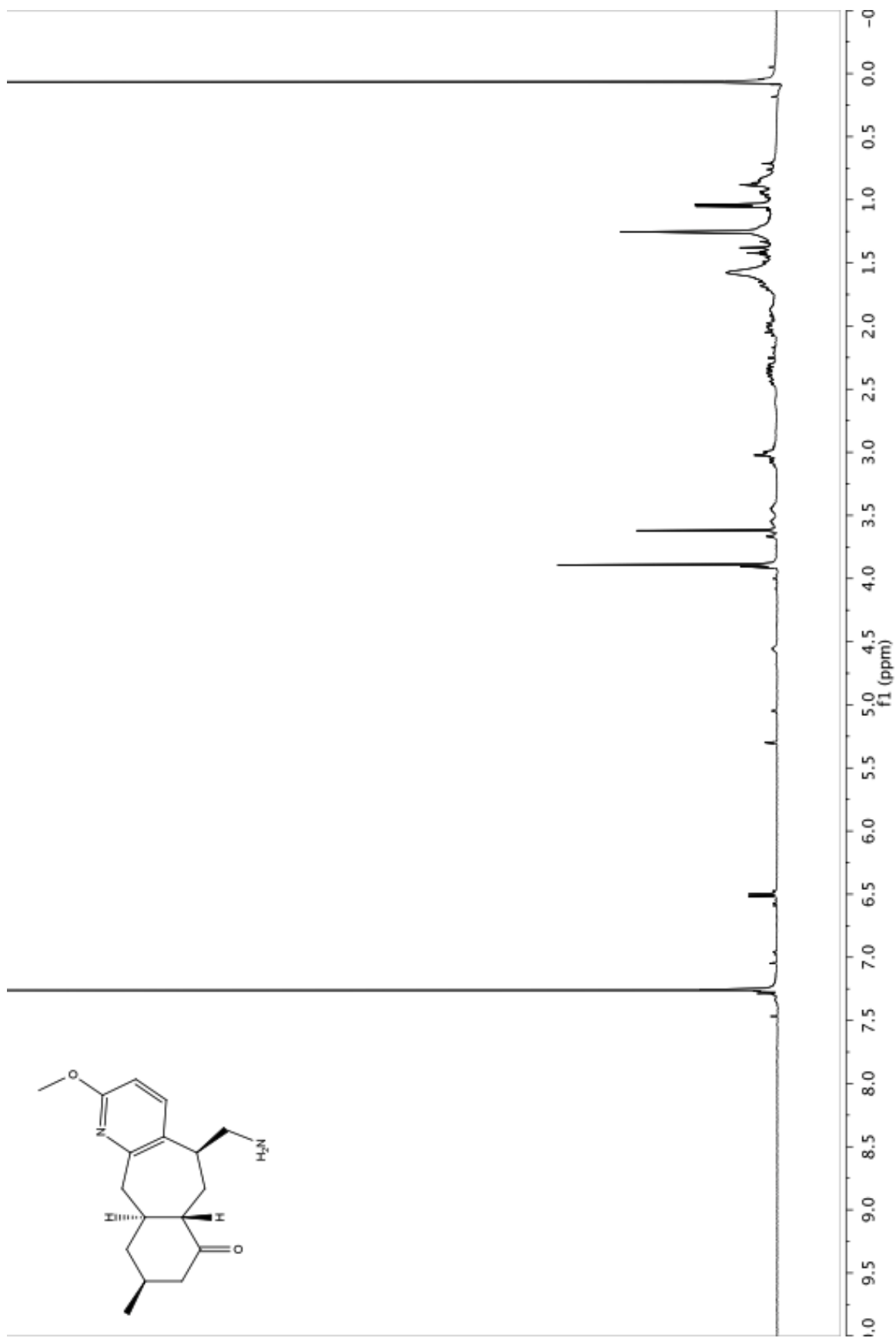
- ¹ Kubota, T.; Yahata, H.; Yamamoto, S.; Hayashi, S.; Shibata, T.; Kobayashi, J. *Bioorg. Med. Chem. Lett.* **2009**, *19*, 3577.
- ² Bisai, A.; West, S. P.; Sarpong, R. *J. Am. Chem. Soc.* **2008**, *130*, 7222.
- ³ West, S. P.; Bisai, A.; Lim, A. D.; Narayan, R. R.; Sarpong R. *J. Am. Chem. Soc.* **2009**, *131*, 11187.
- ⁴ Rajamannar, T.; Palani, N.; Balasubramanian, K. K. *Synth. Commun.* **1993**, *23*, 3095.

Appendix Two: Spectra Relevant to Chapter Three









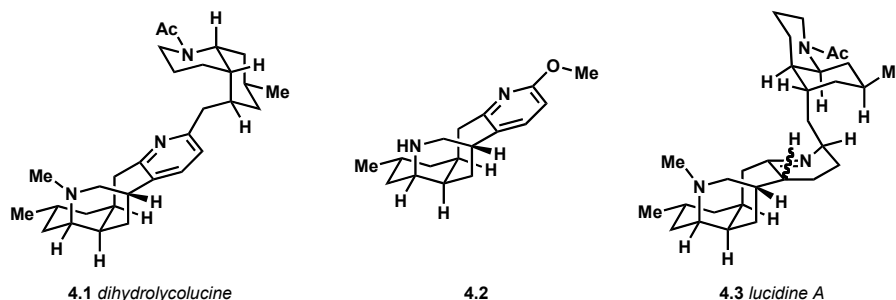
Chapter Four

Toward the Total Synthesis of Serratezomine E and Dihydrolycolucine

4.1 Introduction

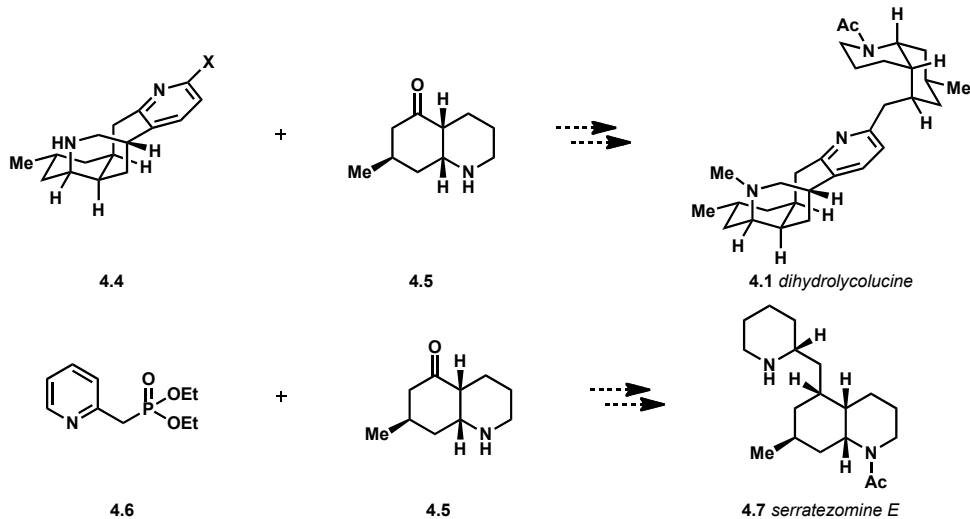
Another natural product that seemed an ideal target for the unified approach to *Lycopodium* alkaloids was dihydrolycolucine (**4.1**, Figure 4.1).¹ Dihydrolycolucine consists of a tetracyclic core along with an appended bicyclic portion. Of the various *Lycopodium* alkaloids that bear this structural motif, dihydrolycolucine possesses the most structurally similar core to tetracyclic intermediate **4.2**.^{2,3,4} Both compounds contain a pyridine moiety; this is in contrast to many of the other congeners in this class (*e.g.*, lucidine A,^{5,6} **4.3**) wherein this ring occurs at the imine oxidation level.

Figure 4.1 Dihydrolycolucine, tetracycle **4.2** and lucidine A.



The chief synthetic contribution that would arise from the synthesis of dihydrolycolucine would be the union of the tetracyclic pyridine core (**4.4**, Scheme 4.2) with the bicyclic ketone portion (**4.5**) to give the complete carbon skeleton of dihydrolycolucine and several other miscellaneous *Lycopodium* alkaloids.³ We recognized that the development of a general method to join pyridyl phosphonates such as **4.6** with bicyclic ketones such as **4.5** could also give us access to the tricyclic cores of a variety of phlegmarine-like natural products.⁴ In particular, serratezomine E (**4.7**) shares the configuration of all of its stereocenters with the analogous bicyclic portion of dihydrolycolucine.⁷ Serratezomine E, therefore, would be an ideal model to study the coupling chemistry. Methods initially developed for serratezomine E would then be applied to the synthesis of dihydrolycolucine.

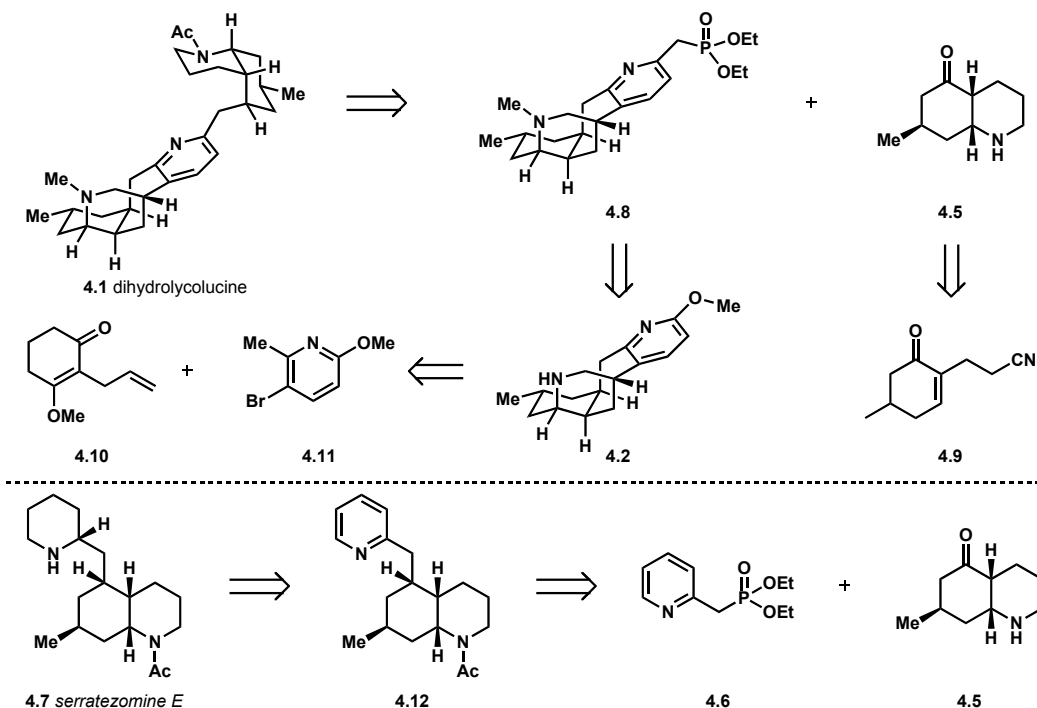
Scheme 4.2 dihydrolycolucine and serratezomine E as synthetic targets.



4.2 Retrosynthetic Analysis of Dihydrolycolucine and Serratezomine E

Dihydrolycolucine (4.1) was envisioned to arise from the Horner-Wadsworth-Emmons coupling of tetracyclic phosphonate 4.8 and bicyclic ketone 4.5⁸ (Scheme 4.3). Bicyclic ketone 4.5 could be generated from enone 4.9. Phosphonate 4.8 would arise from elaboration of tetracyclic amine 4.2, which can be built from vinyllogous ester 4.10 and bromomethoxypicoline 4.11.^{9,10}

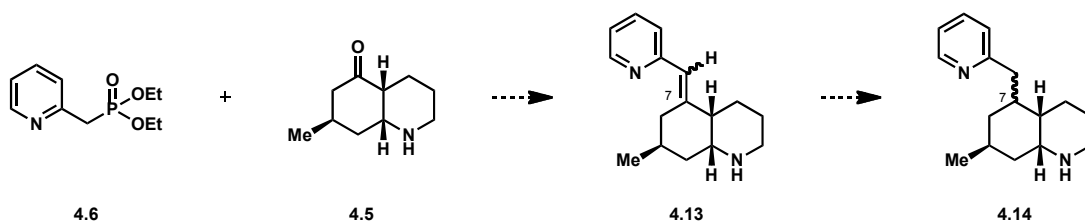
Scheme 4.3 Retrosynthesis of Dihydrolycolucine and Serratezomine E



Serratezomine E would arise from the reduction of tricyclic pyridone **4.12**. Pyridone **4.12** would stem from the union of ketone **4.5** and phosphonate **4.6** through a Horner-Wadsworth-Emmons reaction. Ketone **4.5** is the same intermediate targeted in the dihydrolycolucine synthesis.

We intended to employ serratezomine E as a platform for the exploration of methods of coupling bicycle **4.5** with a pyridine moiety (Scheme 4.4). This synthesis would allow us to determine the stereochemistry with which a Horner-Wadsworth-Emmons reaction to afford **4.13** and subsequent reduction of the olefin would take place. In particular, the stereochemistry this sequence would generate at C-7 of pyridine **4.14** was in question. Lessons learned on serratezomine E could give us valuable insight into the coupling that would give rise to dihydrolycolucine, for which characterization through spectroscopic methods is much more challenging because of its structural complexity.

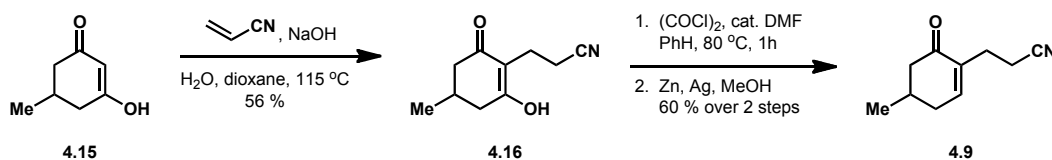
Scheme 4.4 Horner-Wadsworth-Emmons coupling of **4.5** and **4.6**.



4.3 Synthesis of Bicyclic Ketone

This synthetic effort commenced with the construction of enone **4.9** from vinylogous acid **4.15** (Scheme 4.5).¹¹ Dropwise addition of acrylonitrile into **4.15** at 115 °C resulted in conjugate addition to afford nitrile **4.16**. Nitrile **4.16** was converted to the corresponding vinylogous acid chloride by treatment with oxalyl chloride and catalytic DMF. Subsequent reduction using activated zinc metal and silver afforded enone **4.9**.

Scheme 4.5 Synthesis of nitrile **4.9**.

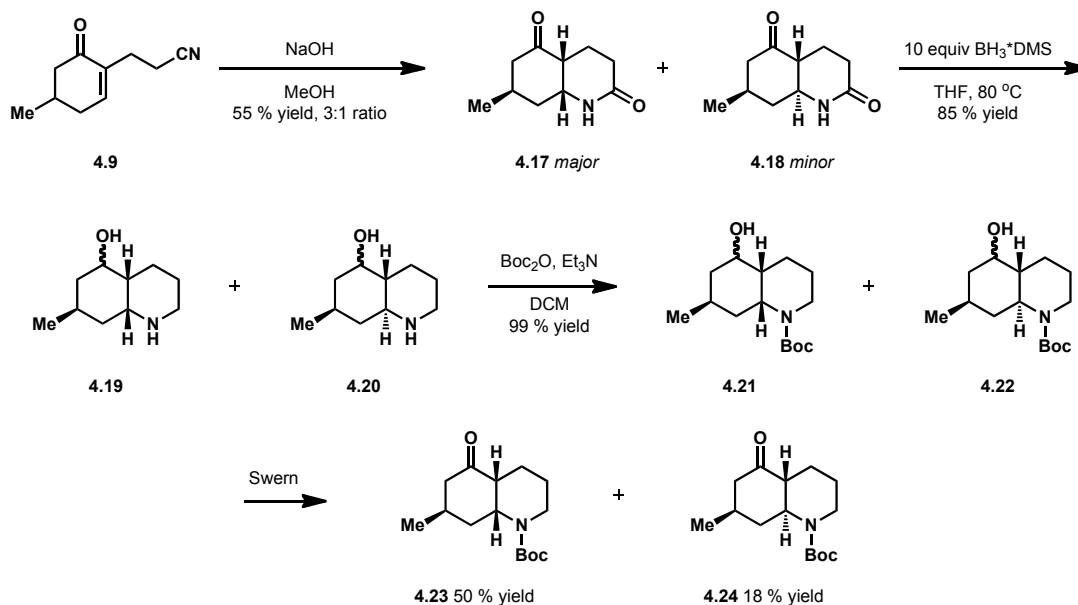


Enone **4.9** was heated in the presence of potassium hydroxide for 2 d to afford a mixture of bicyclic lactams **4.17** and **4.18** as a 3:1 ratio in a combined 55% yield (Scheme 4.6).¹¹ Separation of lactams **4.17** and **4.18** by column chromatography was not feasible at this stage. As such, the material was carried forward in the synthesis as a mixture of diastereomers.

A global reduction of lactams **4.17** and **4.18** was accomplished by heating in the presence of $\text{BH}_3\cdot\text{DMS}$. Each compound afforded a mixture of α - and β -hydroxy isomers (**4.19** and **4.20**), resulting in a product mixture consisting of four diastereomers. This was not cause for concern, however, as the hydroxyl group was to be oxidized to a carbonyl group shortly in the synthetic sequence.

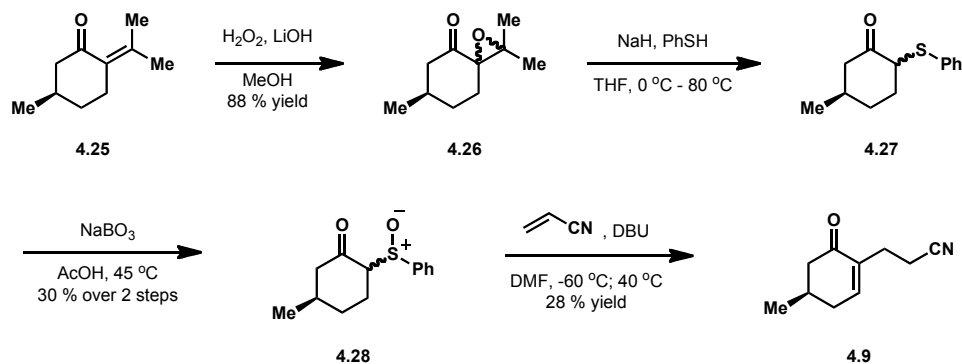
Boc protection of amines **4.19** and **4.20** afforded the four corresponding diastereomeric carbamates **4.21** and **4.22** in near quantitative yield. Swern oxidation of alcohols **4.21** and **4.22** afforded the desired ketone **4.23** in 50% yield and minor product **4.24** in 18% yield.

Scheme 4.6 Synthesis of racemic ketone **4.23**.



In order to achieve enantioselective total syntheses of dihydrolycolucine and serratezomine E, synthesis of ketone **4.23** in enantioenriched form was required. This entailed generating nitrile **4.9** in an asymmetric fashion. This was accomplished through the modification of a literature-precedented method.^{8,12,13} Synthesis of enantioenriched nitrile **4.9** began with (R)-(+)-pulegone (**4.25**, Scheme 4.7), a cheap and abundant commercially available material from the chiral pool that already contains the necessary stereocenter. Pulegone was epoxidized with hydrogen peroxide to afford **4.26** as a mixture of diastereomers. Treatment of **4.26** with sodium thiophenoxide in THF afforded thioether **4.27**. Thioether **4.27** was oxidized to the corresponding sulfoxide (**4.28**) with sodium perborate in acetic acid. Conjugate addition of **4.28** into acrylonitrile with DBU followed by *in situ* elimination of the sulfoxide functionality afforded enantioenriched nitrile **4.9**. Although several steps in this synthetic sequence are low-yielding, it provides access to nitrile **4.9** in multigram quantities.

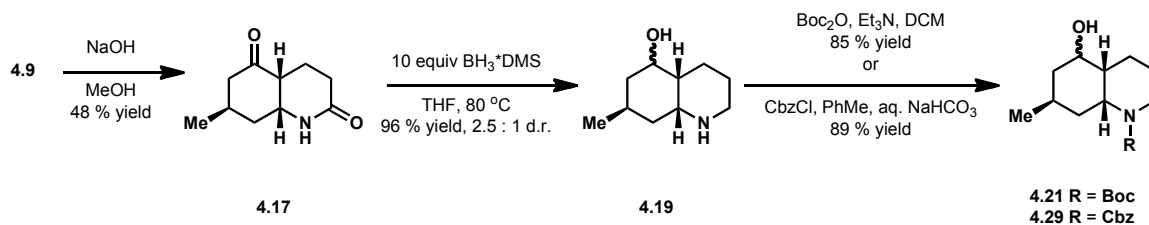
Scheme 4.7 Enantioselective synthesis of nitrile **4.9**.



Enone **4.9** was then treated with sodium hydroxide to afford lactam **4.17**. It was discovered that **4.17** could be recrystallized from ethyl acetate to afford the pure material in the form of large rectangular crystals in 48% yield.

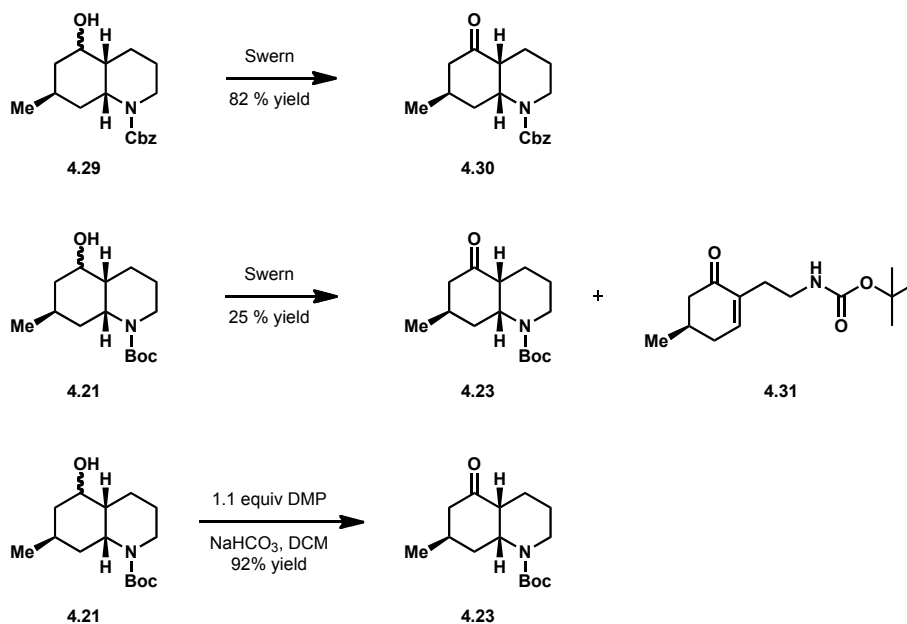
Lactam **4.17** was then carried through the remainder of the synthetic sequence initially developed for the racemic material. Reduction with $\text{BH}_3\cdot\text{DMS}$ gave alcohol **4.19** as a 2.5:1 mixture of hydroxyl group diastereomers. The identity of the major product was not determined. Boc protection could be achieved by treatment of **4.19** with Boc_2O and triethylamine to afford **4.21** in high yield; alternatively, alcohol **4.19** could be converted into the corresponding Cbz carbamate **4.29** in 89% yield.

Scheme 4.8 Synthesis of enantioenriched alcohols **4.21** and **4.29**.



Cbz-protected alcohol **4.29** could be converted to desired ketone **4.30** in 82% yield under Swern oxidation conditions (Scheme 4.9). However, it was found that when Boc-protected alcohol **4.21** was treated with Swern conditions on scales larger than 100 mg, the reaction was not clean and did not reach completion. Desired ketone **4.23** was isolated in an extremely modest 25% yield, and enone **4.31** was isolated as a reaction byproduct. This most likely stems from activation and subsequent elimination of the Boc carbamate under the reaction conditions. Happily, changing the oxidant to Dess-Martin periodinane resulted in isolation of ketone **4.23** in 92% yield.

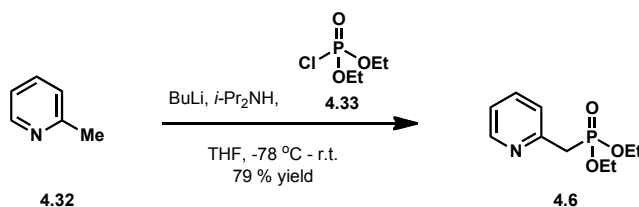
Scheme 4.9 Oxidation of alcohols **4.21** and **4.23** to the corresponding ketones.



4.4 Studies Toward Serratezomine E

With a route to enantioenriched ketones **4.23** and **4.30** secured, we turned our attention to the Horner-Wadsworth-Emmons coupling that would afford the tricyclic core of serratezomine E.¹⁴ Phosphonate **4.6** could be generated in one step from picoline **4.32** *via* deprotonation and quenching with chlorophosphonate **4.33** (Scheme 4.10).

Scheme 4.10 Synthesis of phosphonate **4.6**.



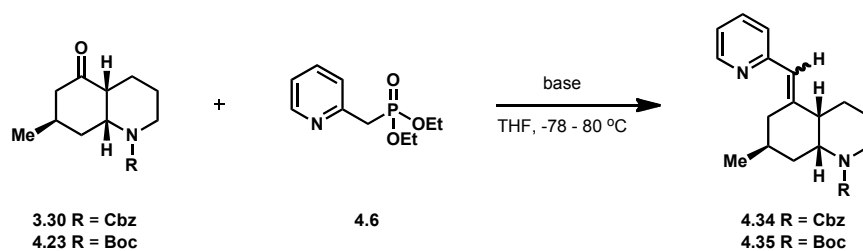
The Horner-Wadsworth-Emmons reaction of phosphonate **4.6** and ketone **4.30** was then investigated (Table 4.1). Amine bases were generated by deprotonation of the amine with butyllithium. Treatment of ketone **4.30** with LDA and 1.0 equiv of phosphonate **4.6** resulted in no conversion to product (entry 1). Increasing the amount of phosphonate **4.6** to 1.2 equiv resulted in 22% conversion to product (entry 2). Doubling the amount of LDA and phosphonate to 3.0 and 2.5 equiv, respectively, resulted in recovery of starting material (entry 3).

Further optimization was done employing 1.2 equivalents of phosphonate **4.6**. Switching from LDA to LiHMDS (2.0 equiv) gave 33% conversion when the reaction was heated for 6 h at 80 °C. Increasing the reaction time to 16 h resulted in

complete conversion to **4.34** as a 1:1 mixture of olefin isomers, which were isolated in 77% yield.

Using Boc-protected ketone **4.23** as a substrate revealed a clear dependence of yield on equivalents of LiHMDS. Increasing the amount of base from 1.3 to 1.5 equivalents increased the conversion from 39% to 56%. A further increase to 1.9 equivalents of base afforded complete conversion to product. Olefin **4.35** was isolated as a 1.5:1 mixture of alkene isomers in 57% yield. Employing 2.6 equivalents of base increased the isolated yield to 92%. The stereochemistry of the major product was not determined, as the olefin would be reduced in the subsequent step.

Table 4.1 Horner-Wadsworth-Emmons reaction conditions.

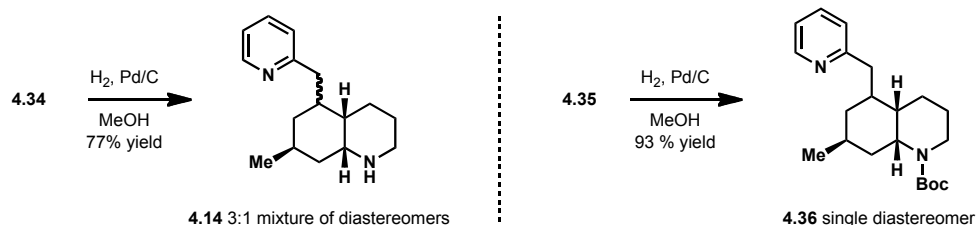


Entry	Substrate	Base	Equiv of Base	Equiv of 4.6	T (h)	Result	isolated yield	d.r.
1	4.30	LDA	1.7	1.0	48	s.m.	—	—
2	4.30	LDA	1.5	1.2	6	22 % conversion	—	1 : 1
3	4.30	LDA	3.0	2.5	6	s.m.	—	—
4	4.30	LiHMDS	2.0	1.2	6	33 % conversion	—	1 : 1
5	4.30	LiHMDS	2.2	1.1	16	complete conversion	77%	1 : 1
6	4.23	LiHMDS	1.3	1.1	16	39 % conversion	—	1.5 : 1
7	4.23	LiHMDS	1.5	1.3	16	56 % conversion	—	1.5 : 1
8	4.23	LiHMDS	1.9	1.1	16	complete conversion	57%	1.5 : 1
9	4.23	LiHMDS	2.6	1.2	16	complete conversion	92%	1.5 : 1

With optimum Horner-Wadsworth-Emmons conditions thus identified, the reduction of alkenes **4.34** and **4.35** was investigated. Hydrogenation of Cbz-protected tricycle **4.34** with palladium on carbon was expected to effect both a reduction of the alkene and hydrogenolysis of the Cbz group. In the event, these reaction conditions afforded complete conversion of alkene **4.34** to amine **4.14**. Amine **4.14** was isolated as a 3:1 mixture of diastereomers.

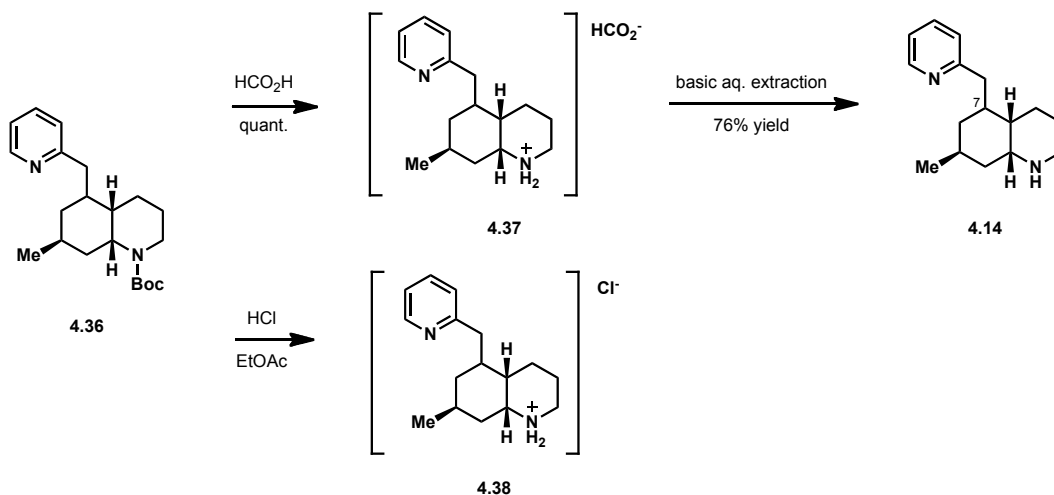
Hydrogenation of Boc-protected tricycle **4.35** was expected to reduce the alkene but leave the protecting group intact. To our delight, hydrogenation of Boc-protected substrate **4.35** afforded a single isomer of **4.36** in 93% yield.

Scheme 4.11 Reduction of olefins **4.34** and **4.35**.



The Boc protecting group could be removed from **4.36** by stirring in neat formic acid to afford salt **4.37** (Scheme 4.12) after removal of volatiles. Alternatively, a basic aqueous extraction of **4.37** gave secondary amine **4.14**. The Boc group could also be removed from **4.36** by treatment with anhydrous 3.0 M hydrochloric acid in ethyl acetate. Removal of volatiles afforded HCl salt **4.38**. This was a suitable substrate for the determination of the stereochemistry at C-7 using NOESY studies.

Scheme 4.12 Removal of Boc protecting group of **4.36**.



The stereochemistry at C-7 was expected to control the conformation of the molecule because the C-7 pyridylmethylene substituent is the largest of the substituents on the C-7 – C-15 cyclohexane ring. If hydrogenation occurred from the top face to form tricycle **4.14a**, the molecule should sit in the conformation illustrated in Figure 4.2. This conformation results in three substituents residing in equatorial positions while one substituent is axial. If hydrogenation occurred from the bottom face to form tricycle **4.14b**, this would be expected to sit in the indicated conformation. This conformation results in two axial and two equatorial substituents. The pyridylmethylene substituent is sterically larger than the methyl group, and thus this is expected to prefer an equatorial orientation.

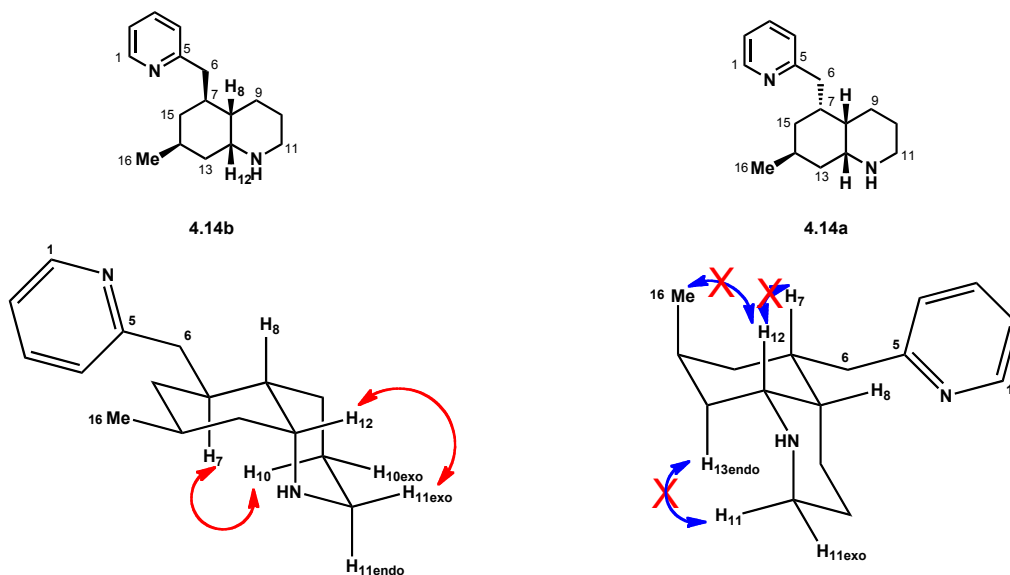
NOESY data were consistent with structure **4.14a**. A NOESY cross-peak between H-7 and H-10_{endo} is a strong indicator that H-7 resides in an endo position

wherein the cupping of the molecule brings it into close proximity with the C-8 – C-12 piperidine ring. In structure **4.14b**, the exo orientation of H-7 places it on the opposite face of the C-7 – C-15 cyclohexane ring from C-10, making a NOESY cross-peak between these two protons unlikely.

A NOESY correlation between H-12 and H-11_{endo} indicates that the C-8 – C-12 piperidine ring adopts a chair conformation and these two protons are in axial positions, which is consistent with structure **4.14a**. In structure **4.14b**, H-12 is in an equatorial position on the piperidine ring, making a NOESY cross-peak with either proton at C-11 unlikely.

Further support for structure **4.14a** over structure **4.14b** comes from the lack of NOESY cross-peaks between H-7 and H-12, as well as between H-12 and the protons of C-16. This means that it is highly unlikely that these three atoms reside in axial orientations on the C-7 – C-15 chair-conformation of the cyclohexane ring, as would be expected for **4.14b**. The absence of any detectable NOESY cross-peak between H-13_{endo} and H-11_{endo} lends further support to this hypothesis, as it suggests that C-13 and C-11 are not in close proximity.

Figure 4.2 Conformations and selected NOESY correlations of **4.14a** and **4.14b**.



The stereochemistry at C-7 in **4.14a** is epimeric to that of the natural product serratezomine E (**4.7**, see Figure 4.1). It is also epimeric to the analogous portion of dihydrolycolucine.

Having developed a method of coupling pyridyl phosphonate **4.6** with bicyclic ketone **4.23**, the next step was to apply this reaction to the more structurally complex natural product dihydrolycolucine.

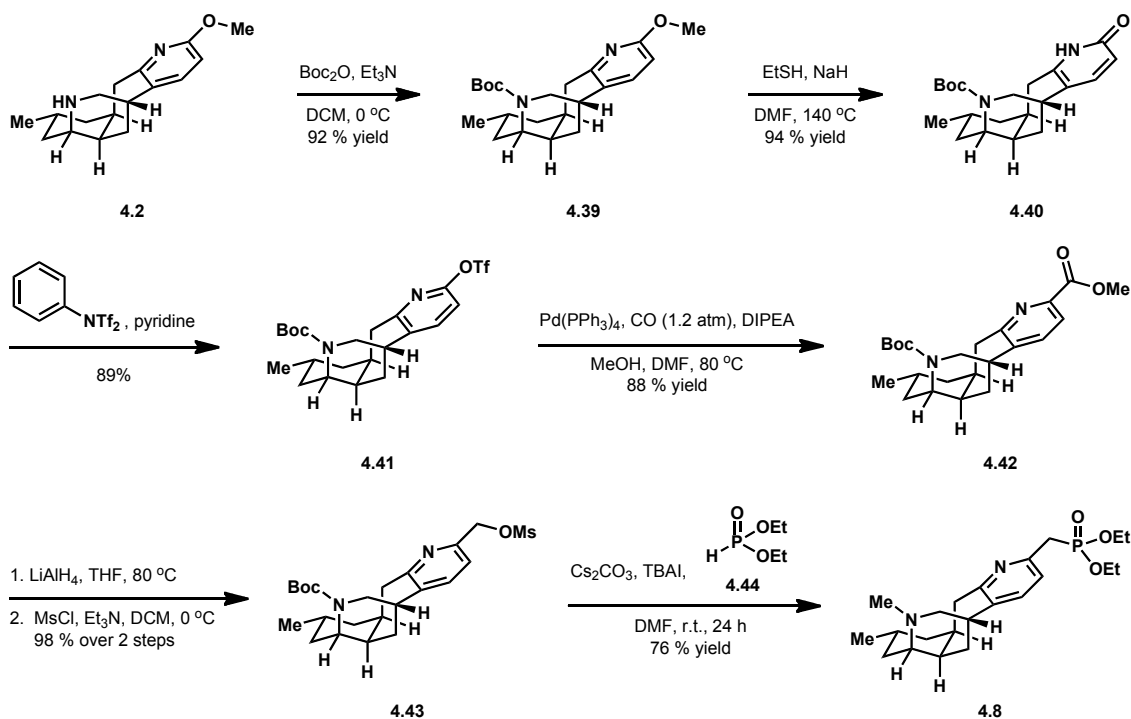
4.5 Studies Toward Dihydrolycolucine

The synthesis of the tetracyclic phosphonate portion of dihydrolycolucine (**4.8**, see Scheme 4.13) was carried out by Alakesh Bisai in the Sarpong group. This synthesis commenced with enantioenriched tetracycle **4.2**, which had been synthesized *en route* to lyconadin A.^{9,10} Tetracycle **4.2** was converted into the corresponding Boc carbamate **4.39** in high yield. Pyridone **4.40** was generated from **4.39** by treatment with NaSEt at 140 °C. Subsequent treatment with Comins reagent afforded pyridine triflate **4.41**.

An extensive screen of cross coupling reactions was carried out on pyridine triflate **4.41**. Surprisingly, functionalization of C-1 of **4.41** was found to be very difficult. However, it was found that treatment of triflate **4.41** with Pd(PPh₃)₄ in methanol under 1.2 atms of carbon monoxide provided ester **4.42** in 88% yield.

Ester **4.42** was reduced to the corresponding alcohol by heating in the presence of LiAlH₄. Subsequent treatment with mesyl chloride furnished mesylate **4.43**. The mesylate was displaced by stirring in the presence of phosphonate **4.44** and Cs₂CO₃ to afford desired phosphonate **4.8**.

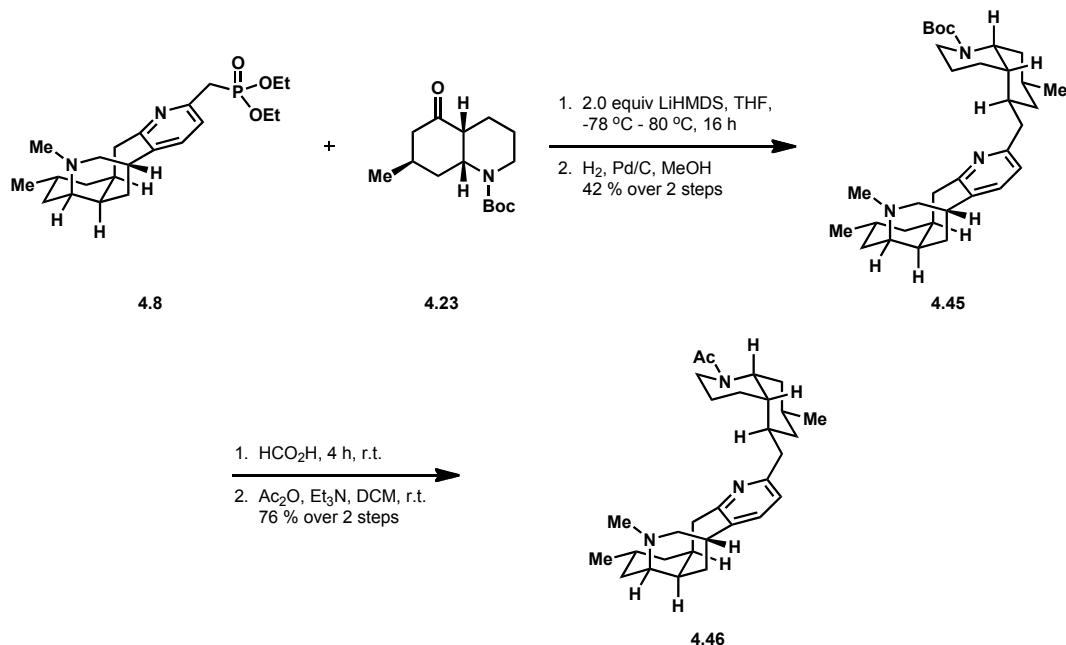
Scheme 4.13 Synthesis of phosphonate **4.8**.



Phosphonate **4.8** and bicyclic ketone **4.23** were then subjected to Horner-Wadsworth-Emmons coupling. Subsequent hydrogenation, according to the method employed in the studies toward serratezomine E, afforded pyridine **4.45** as a single diastereomer. The stereochemistry at C-1' was presumed to be set in an analogous fashion to the corresponding stereocenter of the serratezomine E core (**4.14a**, see Figure 4.2). The Boc group of **4.45** could be converted into an acetate by treatment

with formic acid followed by acetic anhydride to afford 1'-*epi*-dihydrolycolucine (**4.46**).

Scheme 4.14 Completion of 1'-*epi*-dihydrolycolucine.



4.6 Conclusion

The enantioselective total synthesis of 1'-*epi*-dihydrolycolucine was completed in 26 steps. Tetracyclic amine **4.2** was demonstrated to be a suitable common intermediate for the synthesis of multiple natural products as part of a unified approach to the miscellaneous *Lycopodium* alkaloids. The key union of the tetracyclic core (**4.8**) and the bicyclic ketone (**4.23**) was accomplished through a Horner-Wadsworth-Emmons coupling and subsequent hydrogenation that provided a single diastereomer of product **4.45**. The tricyclic core of serratezomine E was assembled through an analogous protocol, and the facial selectivity of the hydrogenation of alkene **4.35** was determined through NOESY studies. A route was developed to access enantioenriched ketone **4.23**, which could be applied to the synthesis of other miscellaneous *Lycopodium* alkaloids.

4.7 Experimental Contributions

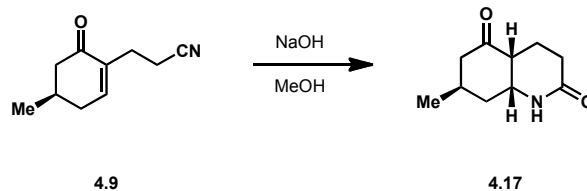
Significant contributions to this work were made by Alakesh Bisai and Scott West. The synthesis of enantioenriched tetracycle **4.2** was pioneered by them for the synthesis of lyconadin A (see Section 1.6.3).^{9,10} The elaboration of tetracycle **4.2** into 1'-*epi*-dihydrolycolucine was carried out by Dr. Bisai (Schemes 4.13 and 4.14).

4.8 Experimental Methods

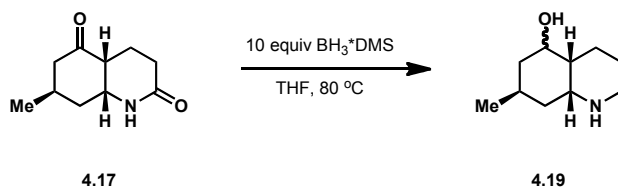
Materials and Methods

Unless otherwise stated, reactions were performed in oven-dried glassware fitted with rubber septa under a nitrogen atmosphere and were stirred with Teflon-coated magnetic stirring bars. Liquid reagents and solvents were transferred via syringe using standard Schlenk techniques. Tetrahydrofuran (THF) and diethyl ether (Et₂O) were distilled over sodium/benzophenone ketyl. Dichloromethane (CH₂Cl₂), toluene, and benzene were distilled over calcium hydride. Acetonitrile was distilled over potassium carbonate. *N,N*-Diisopropylethylamine (DIPEA) was distilled over calcium hydride prior to use. All other solvents and reagents were used as received unless otherwise noted. Reaction temperatures above 23 °C refer to oil bath temperature, which was controlled by an OptiCHEM temperature modulator. Thin layer chromatography was performed using SiliCycle silica gel 60 F-254 precoated plates (0.25 mm) and visualized by UV irradiation and anisaldehyde stain. SiliCycle Silia-P silica gel (particle size 40-63 μm) was used for flash chromatography. Melting points were recorded on a Laboratory Devices Mel-Temp 3.0 and are uncorrected. ¹H and ¹³C NMR spectra were recorded on Bruker AVB-400, DRX-500, AV-500 and AV-600 MHz spectrometers with ¹³C operating frequencies of 100, 125, 125 and 150 MHz, respectively. Chemical shifts (δ) are reported in ppm relative to the residual solvent signal (δ = 7.26 for ¹H NMR and δ = 77.0 for ¹³C NMR). Data for ¹H NMR spectra are reported as follows: chemical shift (multiplicity, coupling constants, number of hydrogens). Abbreviations are as follows: s (singlet), d (doublet), t (triplet), q (quartet), m (multiplet), br (broad). IR spectra were recorded on a Nicolet MAGNA-IR 850 spectrometer and are reported in frequency of absorption (cm⁻¹). Only selected IR absorbencies are reported. High resolution mass spectral data were obtained from the Mass Spectral Facility at the University of California, Berkeley. Enantiomeric excesses (*ee*'s) were determined on a Shimadzu VP Series Chiral HPLC. A Perkin-Elmer 241 polarimeter with a sodium lamp was used to determine specific rotations and concentrations are reported in g/dL.

Experimental Procedures

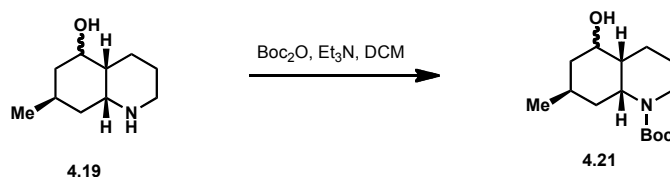


Lactam 4.17: To a round-bottom flask charged with sodium hydroxide (156 mg, 3.90 mmol) and methanol (25.0 mL) was added enantioenriched enone **4.9** (219.2 mg, 1.33 mmol). The solution was heated at reflux for 48 h. The reaction was allowed to cool to rt and quenched with AcOH (250 μ L). Volatiles were removed under vacuum and the solids were dissolved in CHCl_3 (50 mL). The organic layer was extracted with H_2O (2 x 15 mL), dried over MgSO_4 , filtered and concentrated under vacuum. Recrystallization of the mixture from ethyl acetate (25 mL) provided 117 mg (48% yield) of lactam **4.17** as clear rectangular crystals. R_f 0.20 (19:1 DCM/MeOH); $[\alpha]_D^{20} = -56.4^\circ$ (c 0.59, CHCl_3); $^1\text{H NMR}$ (600 MHz, CDCl_3) δ 6.46 (s, 1H), 4.11 (dd, $J = 7.6, 3.3$ Hz, 1H), 2.52 (m, 2H), 2.47 – 2.40 (m, 2H), 2.26 (dd, $J = 18.2, 6.5$ Hz, 1H), 2.20 – 2.05 (m, 1H), 2.05 – 1.97 (m, 1H), 1.90 (ddd, $J = 14.4, 5.7, 3.1$ Hz, 1H), 1.68 (ddd, $J = 19.2, 11.4, 5.3$ Hz, 1H), 1.65 – 1.57 (m, 1H), 1.04 (d, $J = 6.5$ Hz, 3H); $^{13}\text{C NMR}$ (151 MHz, CDCl_3) δ 208.54, 173.09, 53.94, 49.54, 44.82, 38.81, 27.91, 27.39, 21.66, 20.07; **IR** (film) ν_{max} 3224, 2955, 2929, 2886, 1710, 1674, 1642, 1471, 1446, 1320, 1246, 1183 cm^{-1} ; **HRMS** (ESI) m/z 182.1175 [(M+H) $^+$]; calculated for $[\text{C}_{10}\text{H}_{16}\text{NO}_2]^+$: 182.1176].

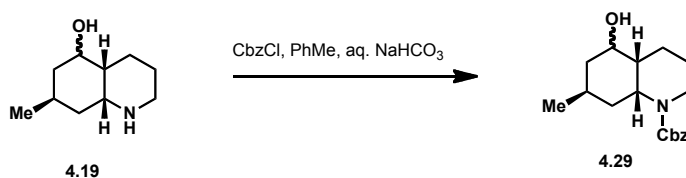


Alcohol 4.19: A round-bottom flask equipped with a reflux condenser was charged with lactam **4.17** (225.4 mg, 1.23 mmol) and THF (6.2 mL). $\text{BH}_3\cdot\text{DMS}$ (1.2 mL, 12.7 mmol) was added dropwise over 10 minutes and the solution was refluxed for 8 h. The reaction was cooled to 0 $^\circ\text{C}$ and quenched with MeOH (3 mL) and 2.0 M HCl (3 mL). The mixture was heated at 90 $^\circ\text{C}$ for 30 min, then allowed to cool to rt. Volatile organics were removed under vacuum and the mixture was partitioned between 3.0 M NaOH (5 mL) and DCM (15 mL). The aqueous layer was extracted with DCM (3 x 20 mL). The combined organic extracts were dried over MgSO_4 , filtered and concentrated under vacuum to afford 197.2 mg (95% yield) of alcohol **4.19** as a 2.5:1 mixture of diastereomers. The colorless oil was used in the next step without purification. Major diastereomer: $^1\text{H NMR}$ (600 MHz, CDCl_3) δ 3.98 (d, $J = 1.7$ Hz, 1H), 3.14 (dd, $J = 11.0, 5.2$ Hz, 1H), 2.93 (s, 1H), 2.71 (m, 1H), 2.29 – 2.11 (m, 2H), 1.94 – 1.84 (m, 2H), 1.76 – 1.59 (m, 2H), 1.51 – 1.45 (m, 1H), 1.45 – 1.37 (m, 1H), 1.27 (ddd, $J = 13.9, 12.7, 3.8$ Hz, 1H), 1.12 – 1.03 (m, 1H), 0.91 (t, $J = 5.7$ Hz, 3H).

Minor diastereomer: $^1\text{H NMR}$ (diagnostic peaks) (600 MHz, CDCl_3) δ 4.10 (td, $J = 10.6, 4.3$ Hz, 1H), 3.72 – 3.63 (m, 1H), 3.02 (d, $J = 2.7$ Hz, 1H), 2.05 – 1.98 (m, 1H), 1.24 – 1.16 (m, 1H).

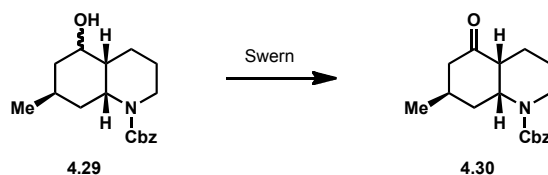


***N*-Boc-protected alcohol 4.21:** To a solution of alcohol **4.19** (197.2 mg, 1.16 mmol), triethylamine (490 mL, 3.53 mmol) and DCM (5 mL) was added a solution of Boc_2O (513.3 mg, 2.35 mmol) in DCM (1 mL). The solution was stirred for 14 h, then poured into water (10 mL) and extracted with DCM (3 x 20 mL). The combined organic extracts were dried over MgSO_4 , filtered and concentrated under vacuum. The crude material was purified by flash chromatography (9:1 hexanes/EtOAc to 3:1 hexanes/EtOAc) to afford 267.4 mg (85% yield) of alcohol **4.21** as a 2.5:1 mixture of diastereomers. A sample of each diastereomer was purified for analysis. Major diastereomer: R_f 0.32 (2:1 hexanes/EtOAc); $[\alpha]^{20}_D = -38.4^\circ$ (c 0.77, CHCl_3); $^1\text{H NMR}$ (600 MHz, CDCl_3) δ 4.30 (br, d, $J = 79.5$ Hz, 1H), 4.08 – 3.99 (m, 1H), 3.93 (br, s, 1H), 2.79 (br, s, 1H), 2.15 (dt, $J = 7.3, 5.2$ Hz, 1H), 2.09 – 1.99 (m, 1H), 1.88 (td, $J = 13.0, 5.3$ Hz, 1H), 1.69 (m, 2H), 1.62 – 1.47 (m, 2H), 1.44 (s, 9H), 1.42 – 1.32 (m, 2H), 1.19 (br, s, 1H), 1.07 (br, d, $J = 6.0$ Hz, 3H); $^{13}\text{C NMR}$ (151 MHz, CDCl_3) δ 154.89, 79.23, 67.40, 42.31, 34.43, 28.44, 26.56, 24.92, 18.74, 16.52; **IR** (film) ν_{max} 3423, 2929, 1668, 1417, 1366, 1163 cm^{-1} ; **HRMS** (ESI) m/z 292.1889 $[(M+\text{Na})^+]$; calculated for $[\text{C}_{15}\text{H}_{27}\text{NO}_3\text{Na}]^+$: 292.1883]. Minor diastereomer: R_f 0.45 (2:1 hexanes/EtOAc); $[\alpha]^{20}_D = +1.3$ (c .45, CHCl_3); $^1\text{H NMR}$ (600 MHz, CDCl_3) δ 4.61 (dt, $J = 12.8, 4.6$ Hz, 1H), 3.98 – 3.90 (m, 1H), 3.88 (d, $J = 2.6$ Hz, 1H), 2.78 (m, 1H), 2.14 – 2.02 (m, 1H), 2.01 – 1.91 (m, 1H), 1.88 – 1.79 (m, 1H), 1.76 – 1.65 (m, 3H), 1.53 – 1.39 (m, 4H), 1.457 (s, 9H) 1.31 – 1.22 (m, 1H), 1.495 (d, $J = 7.5$ Hz, 3H); $^{13}\text{C NMR}$ (151 MHz, CDCl_3) δ 155.21, 79.14, 73.41, 44.66, 42.61, 38.84, 33.28, 28.64, 28.47, 27.32, 25.38, 23.15, 21.26; **IR** (film) ν_{max} 3448, 2928, 1669, 1455, 1417, 1365, 1269, 1148, 1009 cm^{-1} .

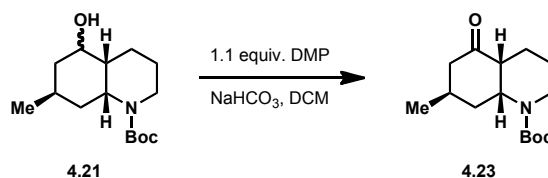


***N*-Cbz-protected bicyclic alcohol 4.29:** To a mixture of alcohol **4.19** (191 mg, 1.16 mmol), toluene (8 mL) and sat. NaHCO_3 (8 mL) was added benzyl chloroformate (250 μL). The mixture was stirred at rt for 2.5 h, then extracted with EtOAc (3 x 8 mL). The combined organic extracts were dried over MgSO_4 , filtered and concentrated under vacuum. The crude material was purified by flash chromatography (2:1 hexanes/EtOAc) to afford 311 mg (89% yield) of *N*-Cbz-protected alcohol **4.29** as a

colorless liquid. **R_f** 0.48 (1:1 hexanes/EtOAc); $[\alpha]^{20}_{\text{D}} = -58.2^{\circ}$ (*c* 0.50, CHCl₃); **¹H NMR** (600 MHz, CDCl₃) δ 7.34 (m, 5H), 5.11 (m, 2H), 4.18-4.21 (m, 1H), 4.10-4.12 (m, 1H), 4.05-4.09 (m, 1H), 3.97-3.99 (m, 1H), 3.73-3.79 (m, 1H), 2.81-2.90 (m, 1H), 1.93-2.02 (m, 2H), 1.68-1.73 (m, 2H), 1.60-1.62 (m, 1H), 1.31-1.42 (m, 2H), 1.04-1.09 (m, 1H), 0.94 (d, *J* = 6.6 Hz, 3H) (for major rotamer); **¹³C NMR** (125 MHz) δ 155.4, 155.3, 137.0, 136.9, 128.4, 128.3, 127.9, 127.8, 127.6, 127.4, 71.1, 71.0, 67.0, 66.9, 52.0, 51.7, 41.2, 41.0, 39.73, 39.71, 37.6, 37.5, 31.8, 31.1, 28.8, 28.6, 28.5, 25.1, 24.8, 22.2, 21.8, 17.3 (for two rotamers).

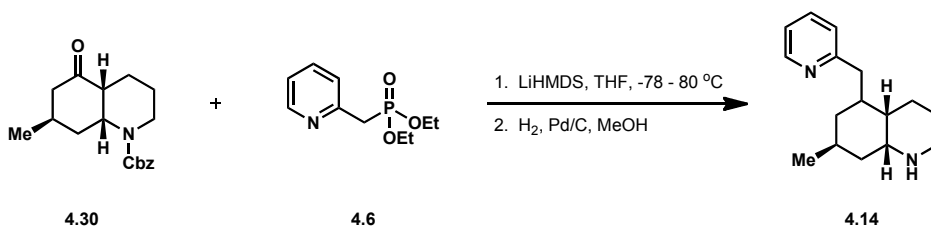


Ketone 4.30: A round-bottom flask charged with DMSO (480 μ L, 6.72 mmol) and DCM was cooled to -78°C . Oxalyl chloride (112 μ L, 1.26 mmol) in DCM (1.0 mL) was added dropwise over 2 min. After stirring for 20 min. at -78°C , *N*-Cbz protected alcohol **4.29** (256 mg, 0.840 mmol) in DCM (4 mL) was added dropwise to the reaction mixture over 4 min. The solution was stirred at -78°C for 2.5 h. Triethylamine (936 μ L, 6.72 mmol) was added to the reaction dropwise over 8 min. and it was allowed to warm to rt. The reaction was stirred at rt for 2.5 h, then poured into water (10 mL) and extracted with DCM (2 x 10 mL). The combined organic extracts were dried over MgSO₄, filtered and concentrated under vacuum. The crude material was purified by flash chromatography (2:1 hexanes/EtOAc) to afford 208 mg (82% yield) as a colorless oil. **R_f** 0.40 (2:1 hexanes/EtOAc); $[\alpha]^{20}_{\text{D}} = -67.7^{\circ}$ (*c* 0.52, CHCl₃); **¹H NMR** (500 MHz, CDCl₃) δ 7.33 (m, 5H), 5.10 (dd, *J* = 39.5, 12.0 Hz, 2H), 4.68 (m, 1H), 4.10 (d, *J* = 12.0 Hz, 1H), 2.90 (t, *J* = 13.0 Hz, 1H), 2.61 (dd, *J* = 14.7, 6.1 Hz, 1H), 2.52 (m, 1H), 2.35 (br, s, 1H), 2.25 (m, 1H), 2.06 (d, *J* = 14.5 Hz, 1H), 1.71 (m, 3H), 1.53 (m, 1H), 1.45 (br, 1H), 0.99 (d, *J* = 6.5 Hz, 3H); **¹³C NMR** (125 MHz) δ 213.2, 155.5, 137.1, 128.9, 128.5, 128.2, 67.6, 51.9, 48.7, 44.4, 39.3, 29.3, 27.6, 24.7, 24.1, 19.6; **IR** (film) ν_{max} 2923, 2360, 2352, 1698, 1508, 1422, 1375, 1255, 1080 cm^{-1} ; **HRMS** (ESI) *m/z* 302.1760 [(*M*+*H*)⁺; calculated for [C₁₈H₂₄NO₃]⁺: 302.1711].

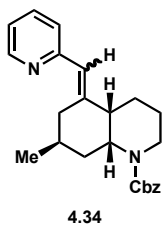


Ketone 4.23: To a mixture of alcohol **4.21** (241 mg, 0.895 mmol), NaHCO₃ (460.7 mg, 5.48 mmol) and DCM (4.5 mL) was added DMP (454 mg, 1.07 mmol). The mixture was stirred at rt for 1 h. Sat. NaHCO₃ (2 mL) and sat. NaHSO₃ (2 mL) were added and the mixture was stirred for 2 h. The mixture was extracted with DCM (3 x 10 mL). The combined organic extracts were dried over MgSO₄, filtered and

concentrated under vacuum. The crude material was purified by flash chromatography (9:1 hexanes/EtOAc to 6:1 hexanes/EtOAc) to afford 220 mg (92% yield) of ketone **4.23** as a colorless oil. R_f 0.52 (2:1 hexanes/EtOAc); $[\alpha]_D^{20} = -42.7^\circ$ (c 0.33, CHCl_3); $^1\text{H NMR}$ (500 MHz, CDCl_3) δ 4.55-4.60 (m, 1H); 3.99-4.03 (m, 1H), 2.80 (dt, $J = 13.0, 2.0$ Hz, 1H), 2.59 (dd, $J = 14.5, 6.0$ Hz, 1H), 2.48-2.52 (m, 1H), 2.34 (m, 1H), 2.21 (dt, $J = 13.0, 5.0$ Hz, 1H), 2.05 (m, 1H), 1.66-1.73 (m, 3H), 1.47-1.50 (m, 1H), 1.44 (m, 1H), 1.43 (s, 9H), 0.99 (d, $J = 7.5$ Hz, 3H); $^{13}\text{C NMR}$ (125 MHz) δ 212.9, 155.0, 80.2, 52.1, 48.3, 44.4, 38.9, 29.1, 28.8, 27.6, 24.8, 24.3, 19.5; **IR** (film) ν_{max} 3405, 2093, 1642, 1523, 1410, 1375, 1285, 1080, 999 cm^{-1} ; **HRMS** (ESI) m/z 268.1913 $[(\text{M}+\text{H})^+]$; calculated for $[\text{C}_{15}\text{H}_{26}\text{NO}_3]^+$: 268.1868].

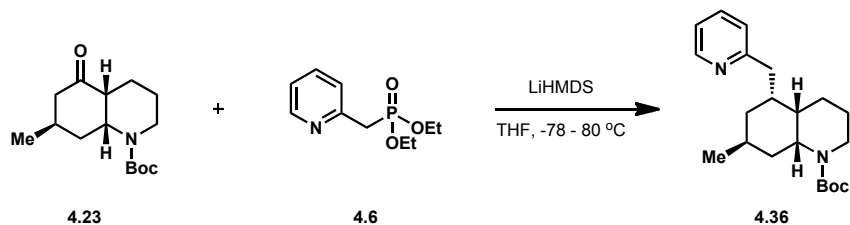


Tricycle 4.14: A Schlenk flask was charged with hexamethyl disilazane (30 μL , 0.141 mmol) and THF (1.5 mL) and cooled to -78°C . Butyllithium (60 μL , 2.5 M in THF, 0.150 mmol) was added dropwise and the reaction was stirred for 25 minutes. A solution of phosphonate **4.6** (16.3 mg, 0.0711 mmol) in THF (1 mL) was added dropwise to the reaction. After stirring for 20 minutes, a solution of ketone **4.30** (19.9 mg, 0.0660 mmol) in THF (1 mL) was added dropwise to the reaction. The flask was sealed and allowed to warm to rt. After stirring at rt for 15 minutes, the reaction was heated at 80°C for 14 h. The reaction was allowed to cool to rt, then quenched by addition of sat. NaHCO_3 (0.5 mL). The reaction mixture was filtered through a pad of celite and the solid residue was washed with EtOAc (3 x 5 mL) and DCM (3 x 5 mL). The combined organic extracts were dried over MgSO_4 , filtered and concentrated under vacuum to afford 19.2 mg (77% yield) of alkene **4.34** as a 1:1 mixture of *cis* and *trans* isomers. The crude material was used in the next step without purification.

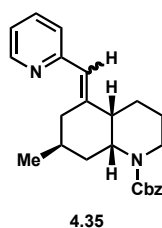


Alkene **4.34** (19.2 mg, 0.0582 mmol) was dissolved in MeOH (1 mL) and sparged with nitrogen for 5 minutes. 10% Pd on activated carbon (9.0 mg) was added and the reaction vessel was evacuated and backfilled with hydrogen 3 times. The reaction mixture was placed under a hydrogen atmosphere (1 atm. balloon) and stirred at rt for 2 h. The reaction mixture was filtered through a pad of celite and

washed with MeOH (3 x 5 mL). The filtrate was concentrated under vacuum to provide 13.2 mg (93% yield) of tricyclic pyridine **4.14** as a 3:1 mixture of diastereomers. Major diastereomer: $^1\text{H NMR}$ (600 MHz, CDCl_3) δ 8.52 (d, $J = 4.8$ Hz, 1H), 7.56 (d, $J = 7.8$ Hz, 1H), 7.13 (d, $J = 7.8$ Hz, 1H), 7.09 (m, 1H), 3.10-3.13 (m, 1H), 2.89 (m, 1H), 2.67-2.71 (m, 1H), 2.29-2.38 (m, 2H), 2.12 (m, 1H), 1.56-1.72 (m, 4H), 1.41-1.50 (m, 2H), 1.29-1.36 (m, 2H), 1.24 (s, br, 1H), 1.09-1.19 (m, 2H), 0.96 (d, $J = 7.2$ Hz, 1H), 0.87 (q, $J = 12.0$ Hz, 1H), 0.75 (d, $J = 6.0$ Hz, 1H); $^{13}\text{C NMR}$ (125 MHz) δ 161.8, 149.1, 135.9, 123.6, 120.7, 56.7, 48.0, 42.7, 42.0, 40.9, 40.8, 33.5, 27.0, 26.6, 22.6, 21.3.



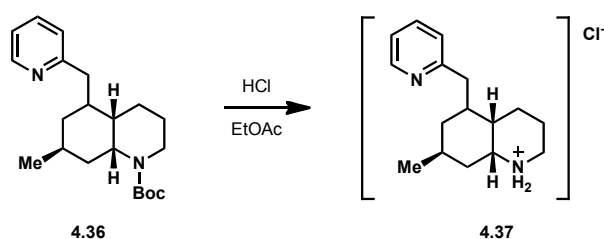
Tricycle 4.36: A Schlenk flask was charged with hexamethyl disilazane (280 μL , 1.32 mmol) and THF (6 mL) and cooled to -78 $^{\circ}\text{C}$. Butyllithium (500 μL , 2.5 M in THF, 1.25 mmol) was added dropwise and the reaction was stirred for 25 minutes. A solution of phosphonate **4.6** (190.0 mg, 0.829 mmol) in THF (4 mL) was added dropwise to the reaction. After stirring for 20 minutes, a solution of ketone **4.23** (174.1 mg, 0.652 mmol) in THF (4 mL) was added dropwise to the reaction. The flask was sealed and allowed to warm to rt. After stirring at rt for 15 minutes, the reaction was heated at 80 $^{\circ}\text{C}$ for 13 h. The reaction was allowed to cool to rt, then quenched by addition of sat. NaHCO_3 (2 mL). The reaction mixture was filtered through a pad of celite and the solid residue was washed with EtOAc (3 x 10 mL) and DCM (3 x 10 mL). The combined organic extracts were dried over MgSO_4 , filtered and concentrated under vacuum. The crude material was purified by flash chromatography (9:1 hexanes/EtOAc to 6:1 hexanes/EtOAc) to afford 223.3 mg (92% yield) of alkene **4.35** as a 1.5:1 mixture of *cis* and *trans* isomers.



Alkene 4.35 major product: R_f 0.45 (2:1 hexanes/EtOAc); $[\alpha]_D^{20} = -20.2^{\circ}$ (c 0.12, CHCl_3); $^1\text{H NMR}$ (600 MHz, CDCl_3) major rotamer: δ 8.57 (d, $J = 4.1$ Hz, 1H), 7.60 (m, 1H), 7.13 (d, $J = 7.8$ Hz, 1H), 7.07 (m, 1H), 6.29 (d, $J = 3.4$ Hz, 1H), 4.20 (dt, $J = 12.8, 4.8$ Hz, 1H), 4.03 – 3.95 (m, 1H), 3.55 (dt, $J = 12.3, 4.4$ Hz, 1H), 2.76 (td, $J = 13.3, 3.0$ Hz, 1H), 2.62 (dd, $J = 13.3, 4.1$ Hz, 1H), 2.20 (d, $J = 5.3$ Hz, 1H), 2.10 (m, 1H), 1.93 (m, 1H), 1.85 – 1.78 (m, 1H), 1.77 – 1.63 (m, 3H), 1.59 – 1.44 (m, 1H), 1.41 (s, 9H), 1.33

(m, 1H), 1.00 (d, $J = 7.2$ Hz, 3H); minor rotamer: (diagnostic peaks) δ 8.54 (d, $J = 4.3$ Hz, 1H), 4.38 (dt, $J = 12.7, 4.8$ Hz, 1H), 3.89 (d, $J = 13.4$ Hz, 1H), 3.51 – 3.42 (m, 1H), 2.84 (td, $J = 13.2, 2.4$ Hz, 1H), 1.05 (d, $J = 7.2$ Hz, 3H); $^{13}\text{C NMR}$ (151 MHz, CDCl_3) for two rotamers: δ 156.53, 155.14, 154.61, 149.34, 149.22, 146.37, 146.12, 135.91, 135.81, 126.08, 126.02, 123.42, 120.80, 120.74, 79.15, 48.49, 47.41, 39.17, 38.81, 38.33, 38.20, 29.42, 28.84, 28.52, 28.46, 28.38, 28.30, 25.29, 24.92, 24.32, 24.20, 17.94, 17.68; **IR** (film) ν_{max} 2929, 1683, 1585, 1471, 1412, 1391, 1271, 1160, 1139, 1093 cm^{-1} ; **HRMS** (ESI) m/z 343.2384 [(M+H) $^+$; calculated for $[\text{C}_{21}\text{H}_{31}\text{N}_2\text{O}_2]^+$: 343.2380]. Minor diastereomer: $^1\text{H NMR}$ (600 MHz, CDCl_3) major rotamer, diagnostic peaks: δ 6.53 (br, s, 1H), 4.58 (br, s, 1H), 3.19 (br, s, 1H), 2.50 (dt, $J = 12.8, 4.6$ Hz, 1H), 2.20 (br, s, 2H), 0.90 (br, s, 3H).

Alkene **4.35** (163.2 mg, 0.477 mmol) was dissolved in MeOH (8.4 mL) and sparged with nitrogen for 5 minutes. 10% Pd on activated carbon (83.5 mg) was added and the reaction vessel was evacuated and backfilled with hydrogen 3 times. The reaction mixture was placed under a hydrogen atmosphere (1 atm. balloon) and stirred at rt for 2 h. The reaction mixture was filtered through a pad of celite and washed with MeOH (3 x 15 mL). The filtrate was concentrated under vacuum to provide 153 mg (93% yield) of tricyclic pyridine **4.36**. R_f 0.36 (2:1 hexanes/EtOAc); $[\alpha]^{20}_{\text{D}} = +6.2^\circ$ (c 0.15, CHCl_3); $^1\text{H NMR}$ (500 MHz, CDCl_3) δ 8.53 (d, $J = 4.2$ Hz, 1H), 7.57 (dt, $J = 7.8, 1.8$ Hz, 1H), 7.11 (d, $J = 7.8$ Hz, 1H), 7.09-7.10 (m, 1H), 4.35-4.37 (m, 1H), 3.89-3.91 (m, 1H), 2.92-2.95 (dd, $J = 13.2, 6.6$ Hz, 1H), 2.70-2.77 (m, 2H), 1.88-1.98 (m, 2H), 1.83 (m, 1H), 1.64-1.72 (m, 1H), 1.55-1.59 (m, 2H), 1.48-1.54 (m, 1H), 1.48 (s, 9H), 1.40-1.46 (m, 1H), 1.32-1.38 (m, 1H), 1.24 (s, br, 1H), 1.06-1.12 (m, 1H), 1.04 (d, $J = 7.2$ Hz, 3H); $^{13}\text{C NMR}$ (125 MHz) δ 161.4, 155.2, 149.4, 136.1, 123.7, 121.0, 79.1, 46.6, 45.0, 41.1, 39.0, 38.8, 32.5, 28.9, 28.5, 27.4, 26.4, 25.2, 22.4. **IR** (film) ν_{max} 3424, 2093, 1641, 1486, 1192 cm^{-1} ; **HRMS** (ESI) m/z [(M+H) $^+$; calculated for $[\text{C}_{21}\text{H}_{31}\text{N}_2\text{O}_2]^+$: 343.2380].



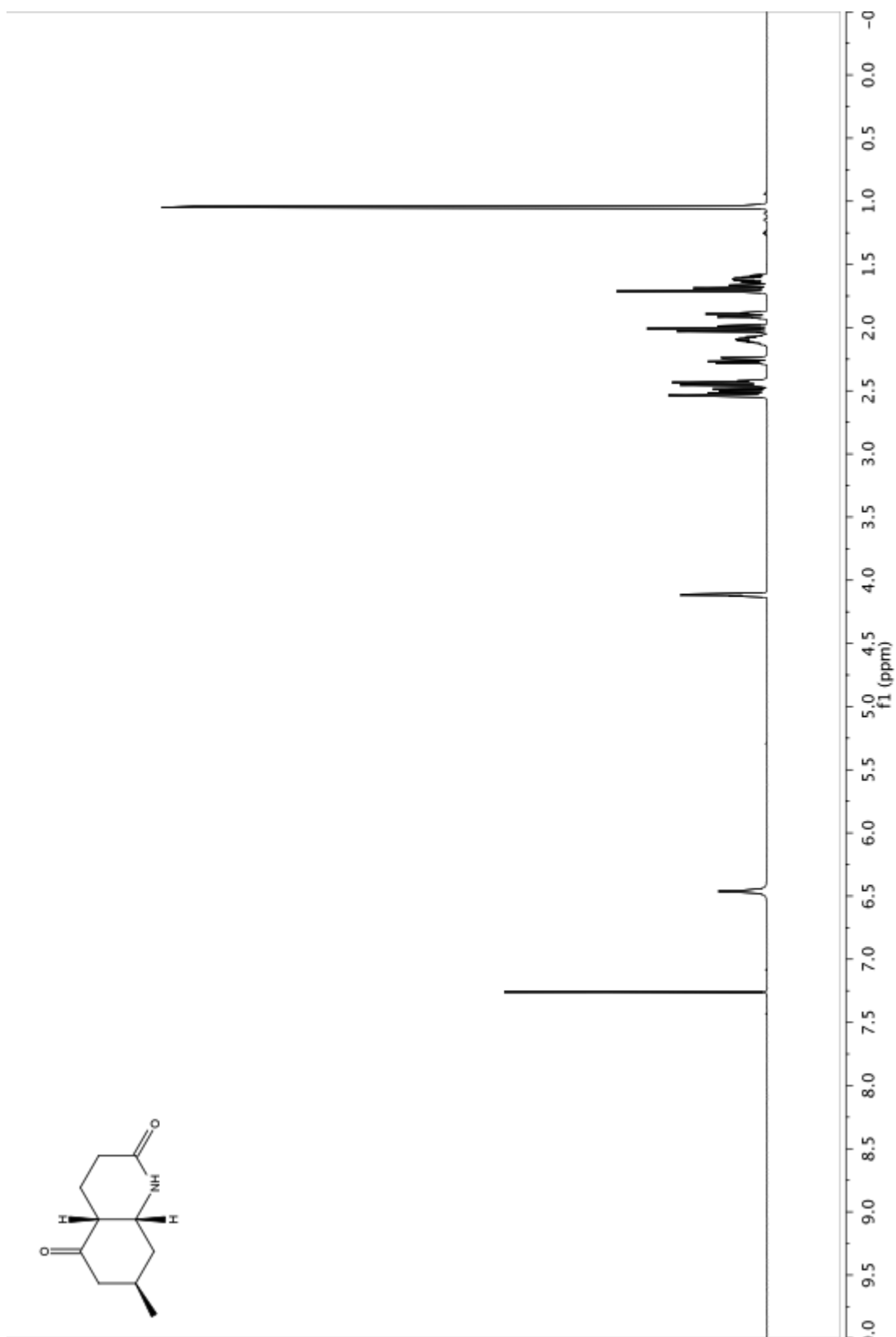
HCl salt 4.37: A vial was charged with EtOAc (600 mL) and acetyl chloride (210 mL, 2.95 mmol). EtOH (180 mL, 3.08 mmol) was added and the solution was stirred for 30 min. Pyridine **4.36** (13.2 mg, 0.0383 mmol) was added and the reaction was stirred at rt for 2 h. Volatiles were removed under vacuum to afford 10.8 mg (quant. yield) of HCl salt **4.37** as a white crystalline solid. $[\alpha]^{20}_{\text{D}} = -23.6^\circ$ (c 0.93, MeOH); $^1\text{H NMR}$ (500 MHz, CD_3OD) δ 8.82 (d, $J = 5.4$ Hz, 1H), 8.62 (t, $J = 7.4$ Hz, 1H), 8.09 (d, $J = 7.7$ Hz, 1H), 8.01 (t, $J = 6.4$ Hz, 1H), 3.66 – 3.51 (m, 2H), 3.48 (d, $J = 10.1$ Hz, 1H), 3.12 (t, $J = 12.2$ Hz, 1H), 2.80 – 2.64 (m, 1H), 2.52 (d, $J = 10.0$ Hz, 1H), 2.22 (m, 1H), 2.17 – 2.00 (m, 1H), 1.93 (d, $J = 13.9$ Hz, 1H), 1.90 – 1.69 (m, 3H), 1.48 (t, $J = 14.0$ Hz, 1H),

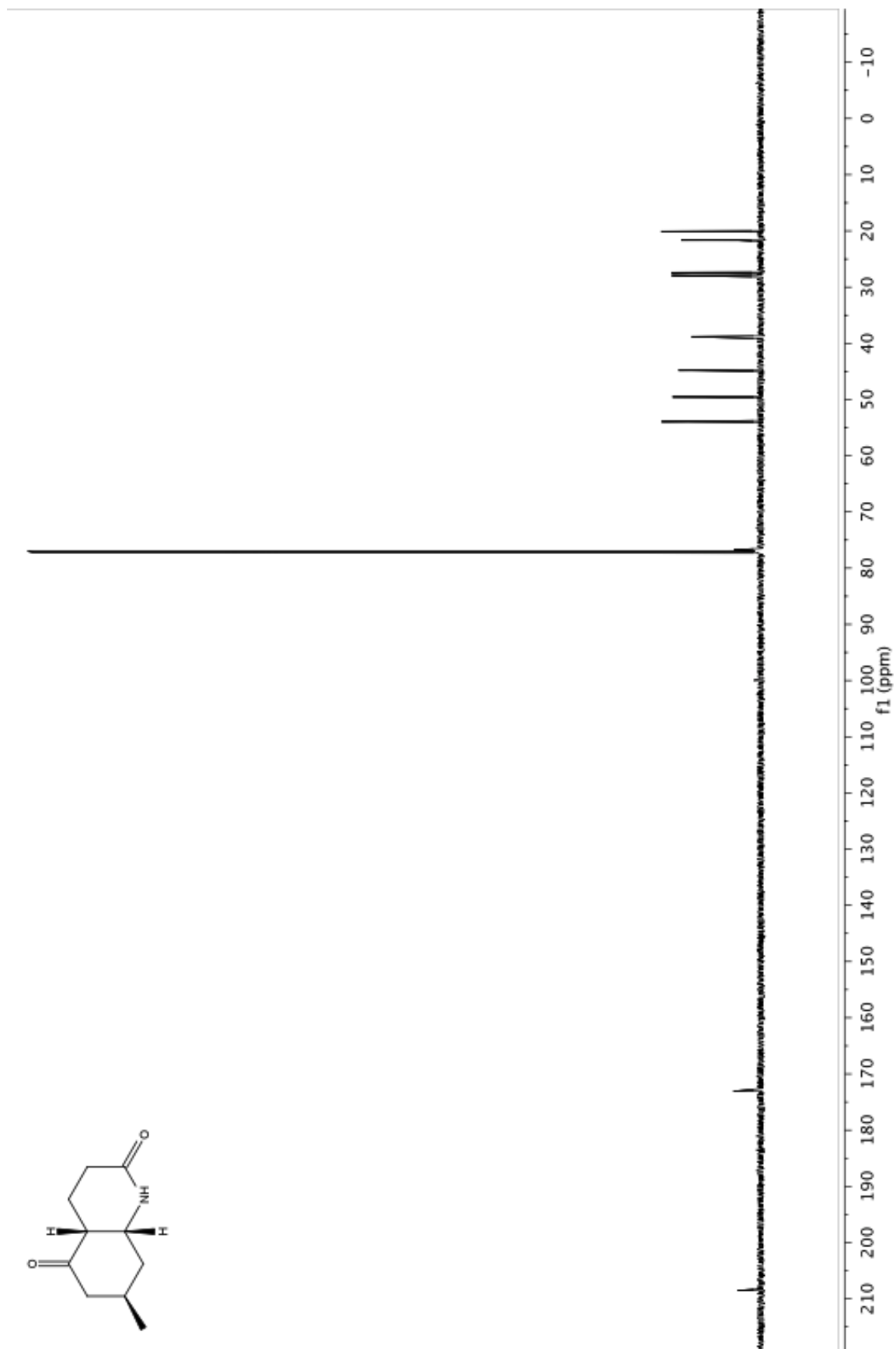
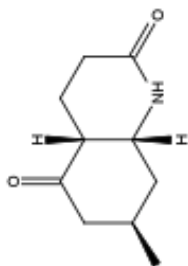
1.43 – 1.32 (m, 1H), 0.97 – 0.80 (m, 4H); ¹³C NMR (151 MHz, CD₃OD) δ 155.84, 146.69, 141.17, 128.38, 125.07, 56.42, 45.26, 38.75, 38.38, 37.00, 36.76, 32.94, 25.44, 23.65, 20.77, 17.06; HRMS (ESI) m/z 245.2014 [(M+H)⁺]; calculated for [C₁₆H₂₅N₂O₂₅]⁺: 245.2012]; MP decomp. At 193 – 194 °C. COSY, HMQC and NOESY data for **2.108a** is included with ¹H and ¹³C.

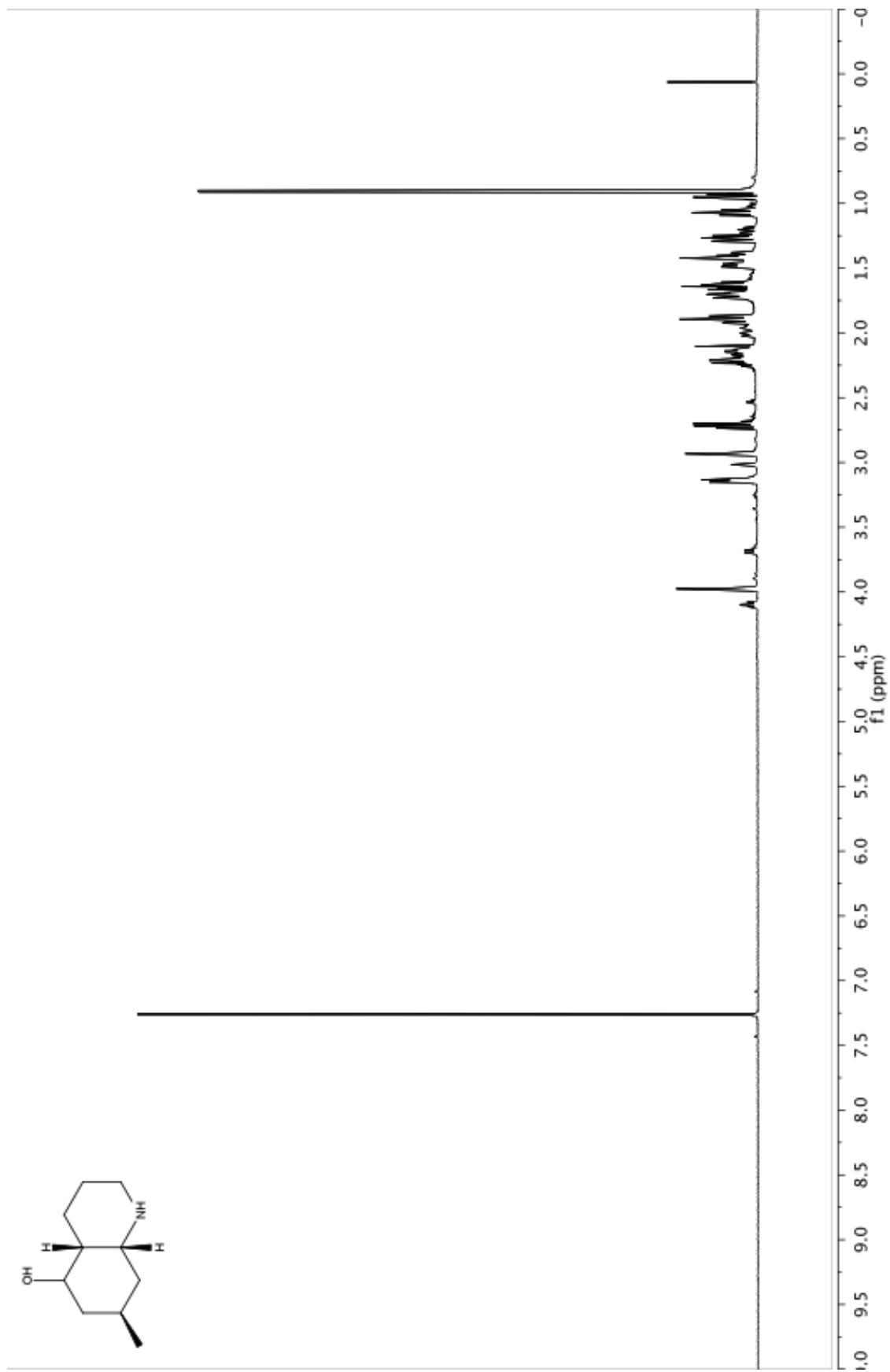
4.9 References

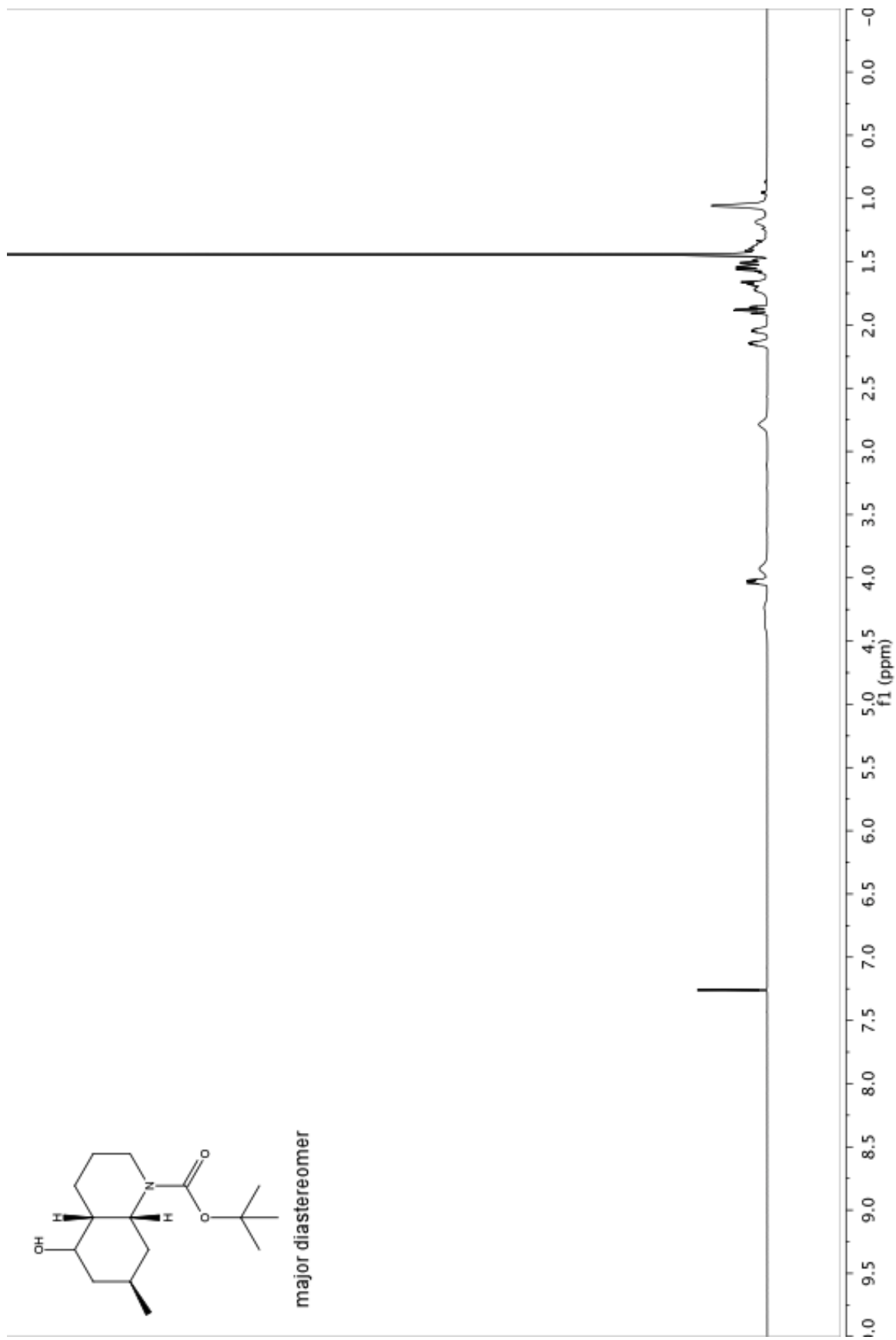
- ¹ Ayer, W. A.; Browne, L. M.; Nakahara, Y.; Tori, M.; Delbaere, L. T. J. *Can. J. Chem.* **1979**, *57*, 1105.
- ² Ma, X.; Gang, R. *Nat. Prod. Rep.* **2004**, *21*, 752.
- ³ Kobayashi, J.; Morita, H. *Alkaloids (Academic Press)* **2005**, *61*, 1.
- ⁴ Hirasawa, Y.; Kobayashi, J.; Morita, H. *Heterocycles* **2009**, *77*, 679.
- ⁵ Ayer, W. A.; Berezows, J.; Law, D. A. *Can. J. Chem.* **1963**, *41*, 649.
- ⁶ Tori, M.; Shimoji, T.; Shimura, E.; Takaoka, S.; Nakashima, K.; Sono, M.; Ayer, W. *Phytochemistry* **2000**, *53*, 503.
- ⁷ Kubota, T.; Yahata, H.; Yamamoto, S.; Hayashi, S.; Shibata, T.; Kobayashi, J. *Bioorg. Med. Chem. Lett.* **2009**, *19*, 3577.
- ⁸ Kozak, J. A.; Dake, G. R. *Angew. Chem. Int. Ed.* **2008**, *47*, 4221.
- ⁹ Bisai, A.; West, S. P.; Sarpong, R. *J. Am. Chem. Soc.* **2008**, *130*, 7222.
- ¹⁰ West, S. P.; Bisai, A.; Lim, A. D.; Narayan, R. R.; Sarpong R. *J. Am. Chem. Soc.* **2009**, *131*, 11187.
- ¹¹ Szychowski, J.; MacLean, D. B. *Can. J. Chem.* **1979**, *57*, 1631.
- ¹² Reusch, W.; Johnson, C. K. *J. Org. Chem.* **1963**, *28*, 2557.
- ¹³ Mutti, S.; Daubie C.; Decalogne, F.; Fournier, R.; Rossi, P. *Tetrahedron Lett.* **1996**, *37*, 3125.
- ¹⁴ Chackalamannil, S.; Xia, Y.; Greenlee, W. J.; Clasby, M.; Doller, D.; Tsai, H.; Asberom, T.; Czarniecki, M.; Ahn, H.-S.; Boykow, G.; Foster, C.; Agans-Fantuzzi, J.; Bryant, M.; Lau, J.; Chintala, M. *J. Med. Chem.* **2005**, *48*, 5884.

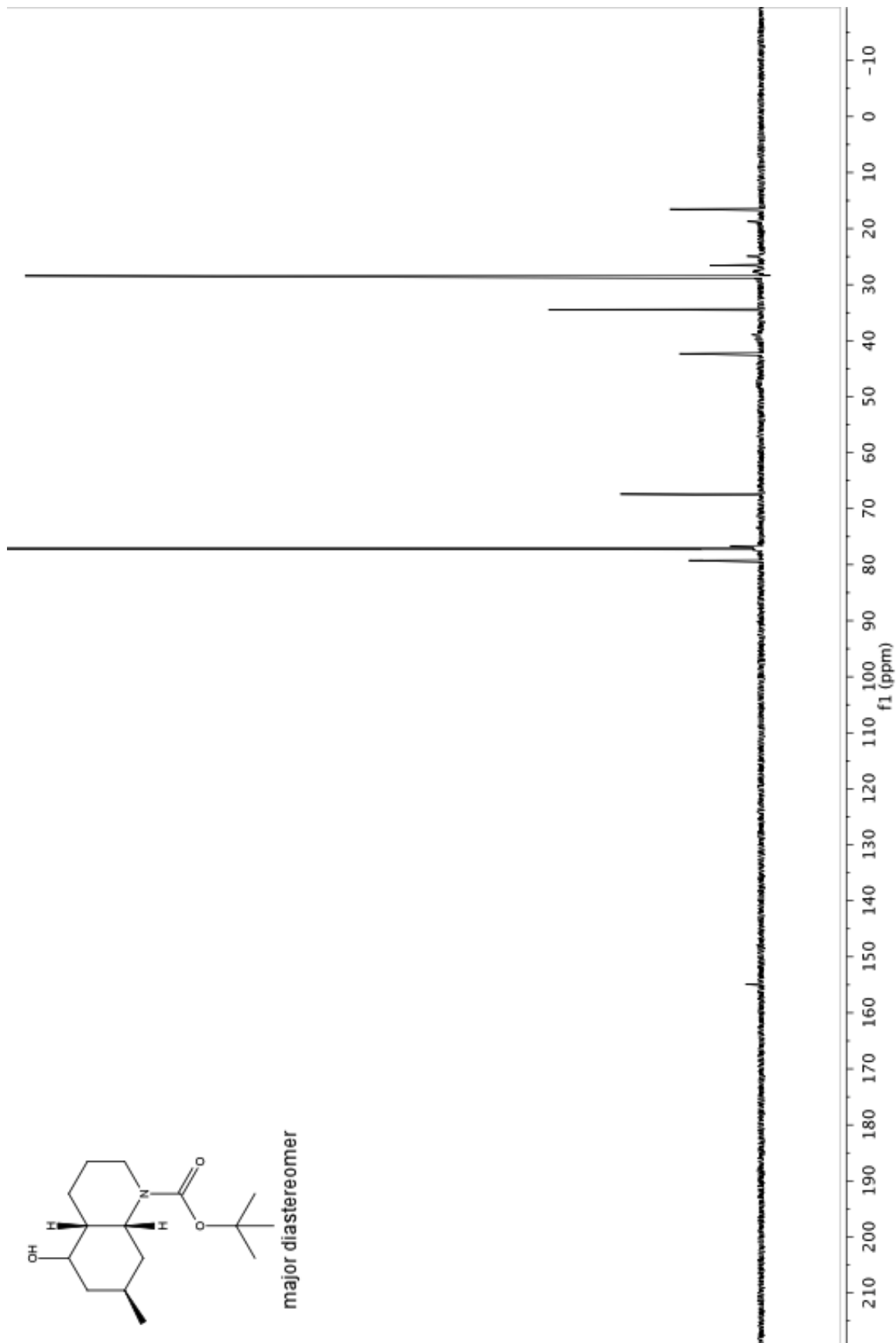
Appendix Three: Spectra Relevant to Chapter Four

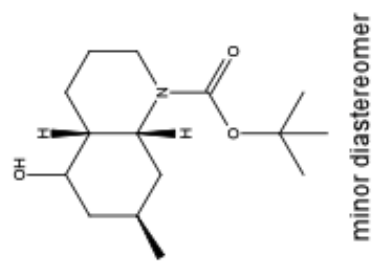
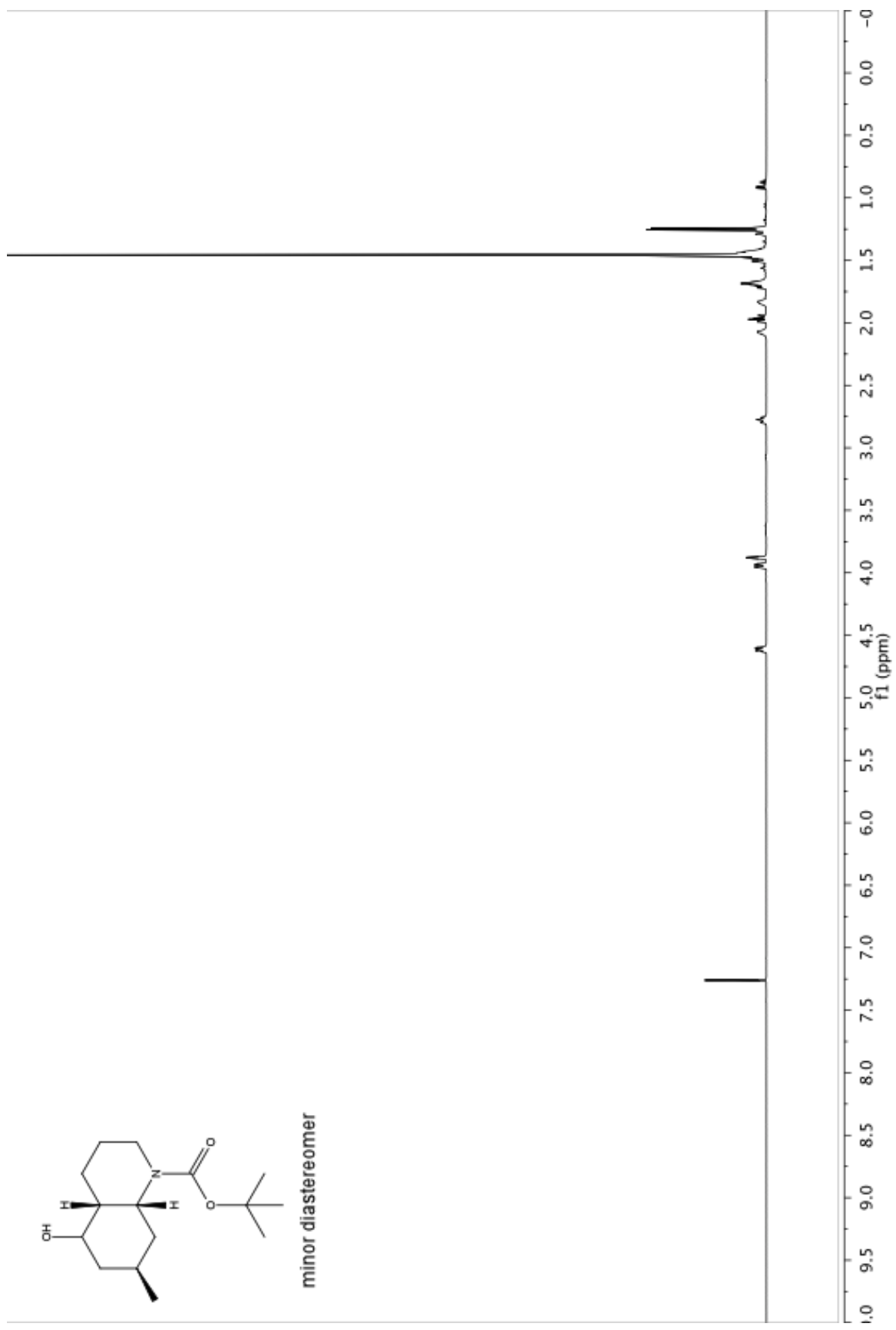


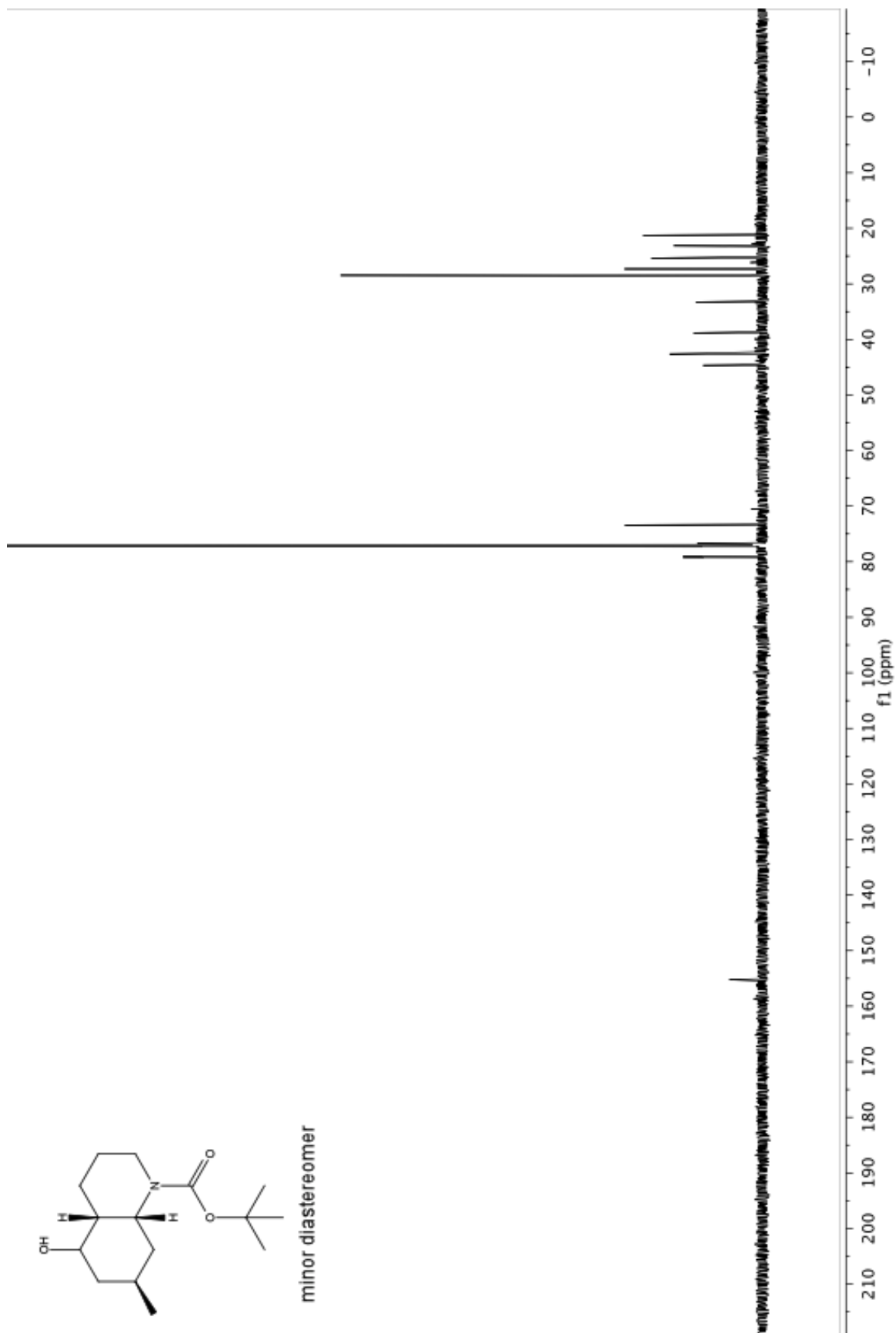


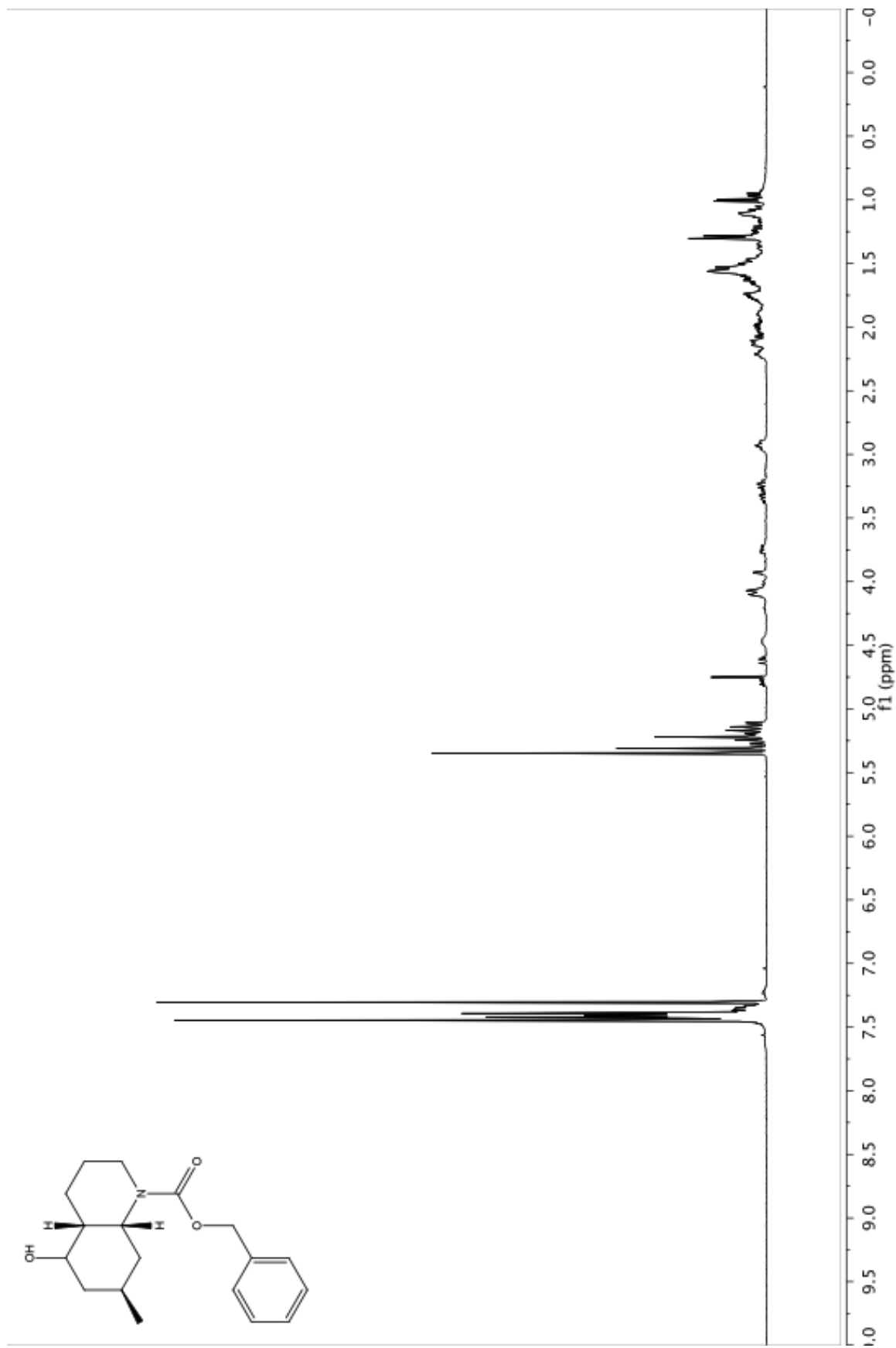


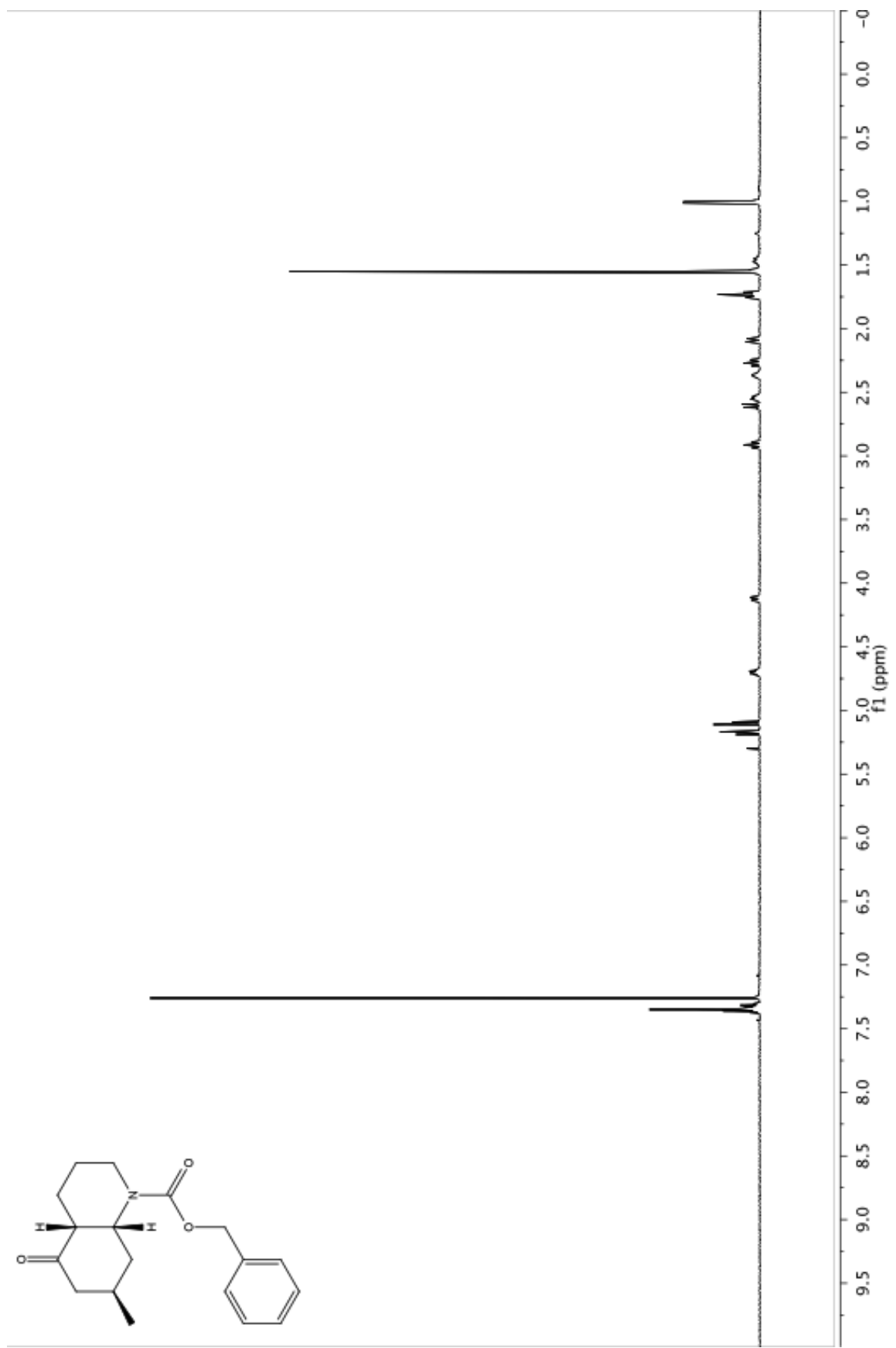


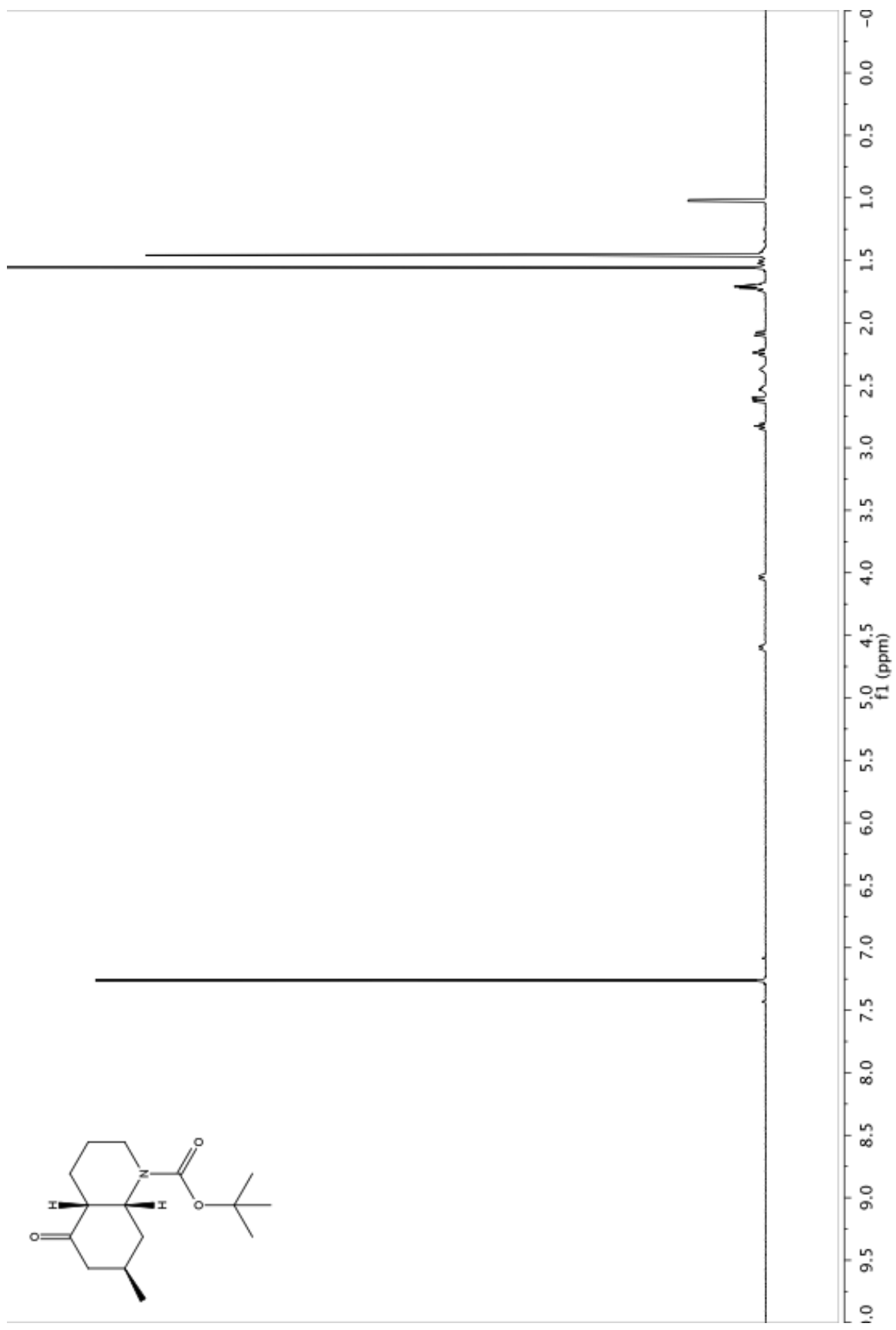


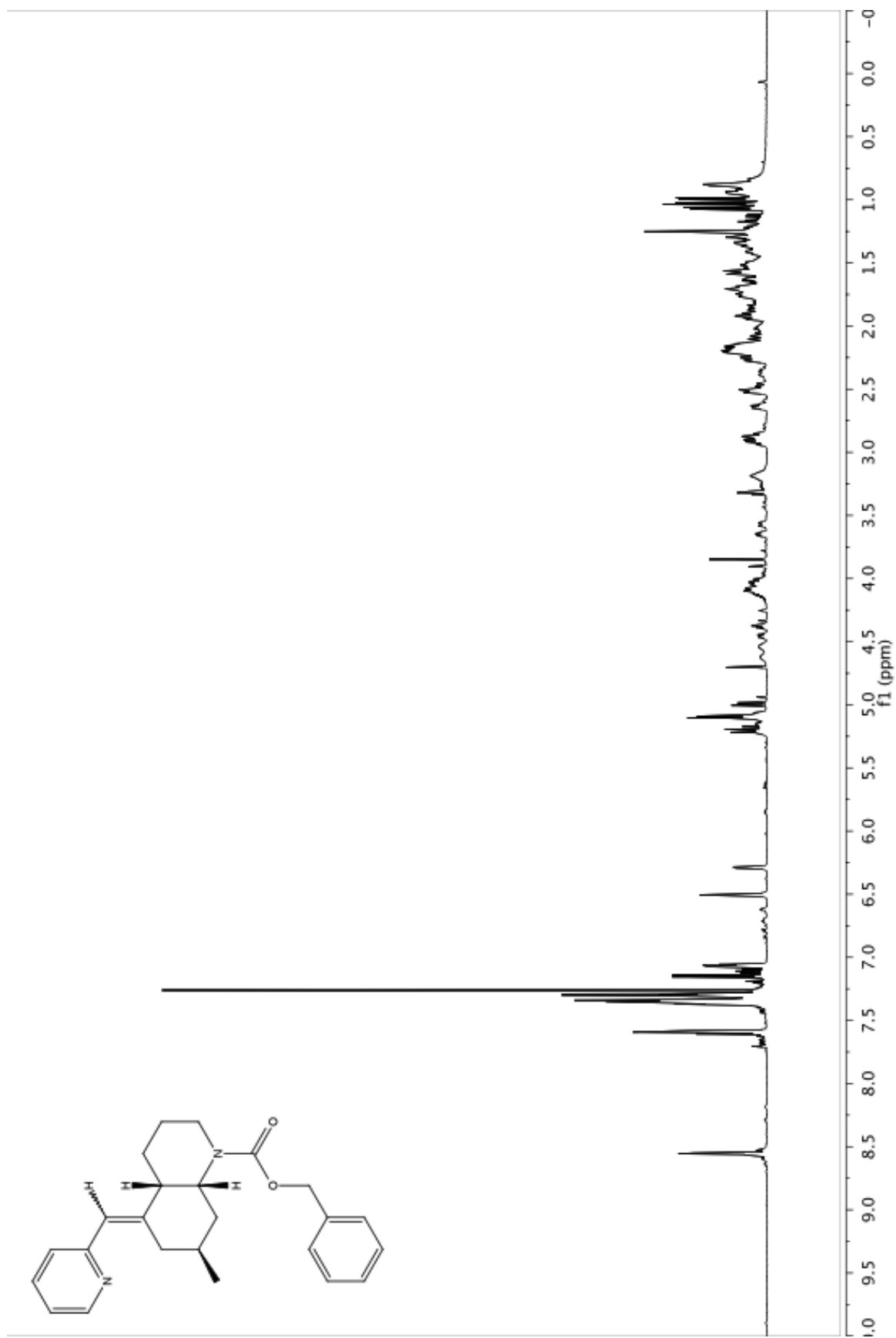


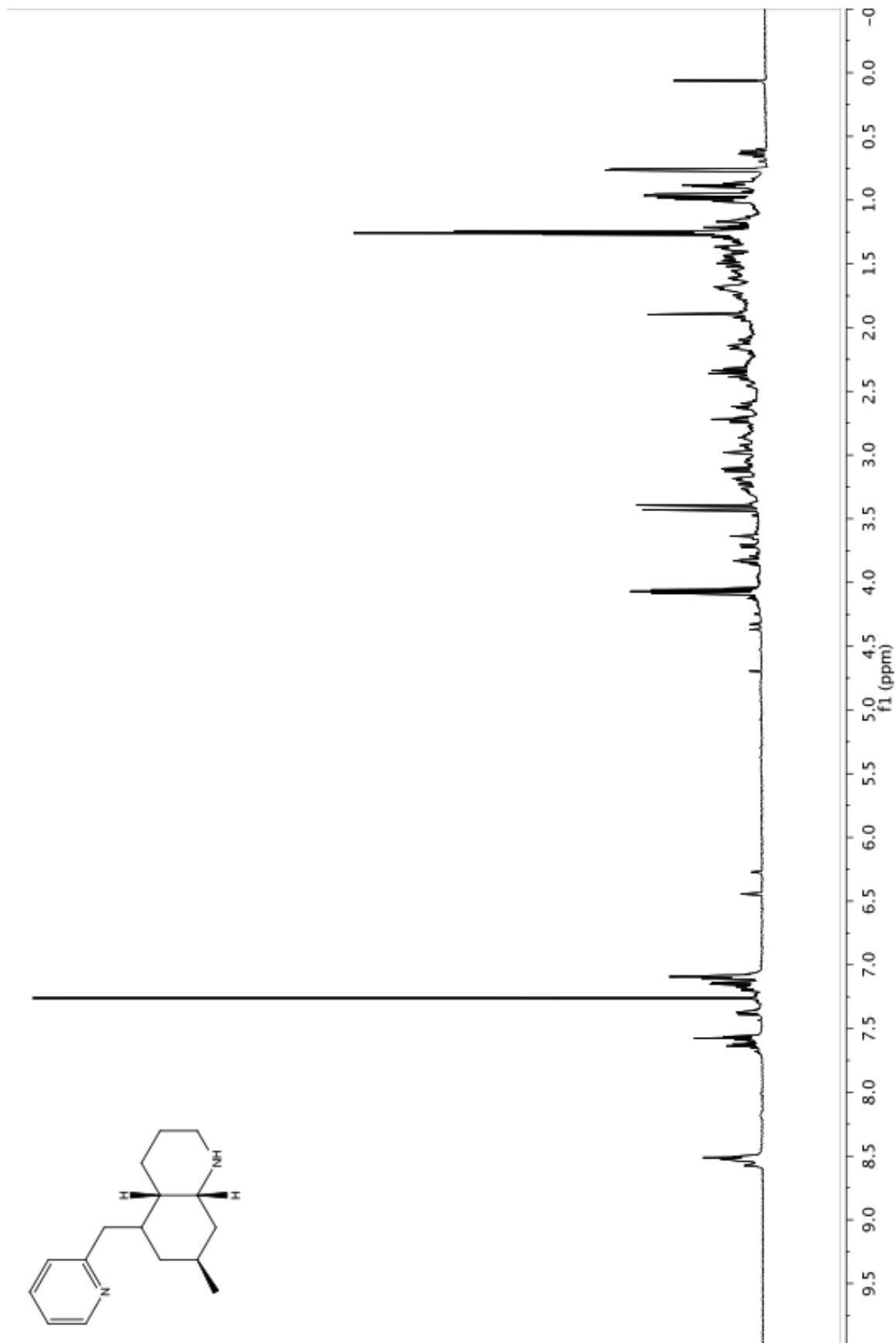


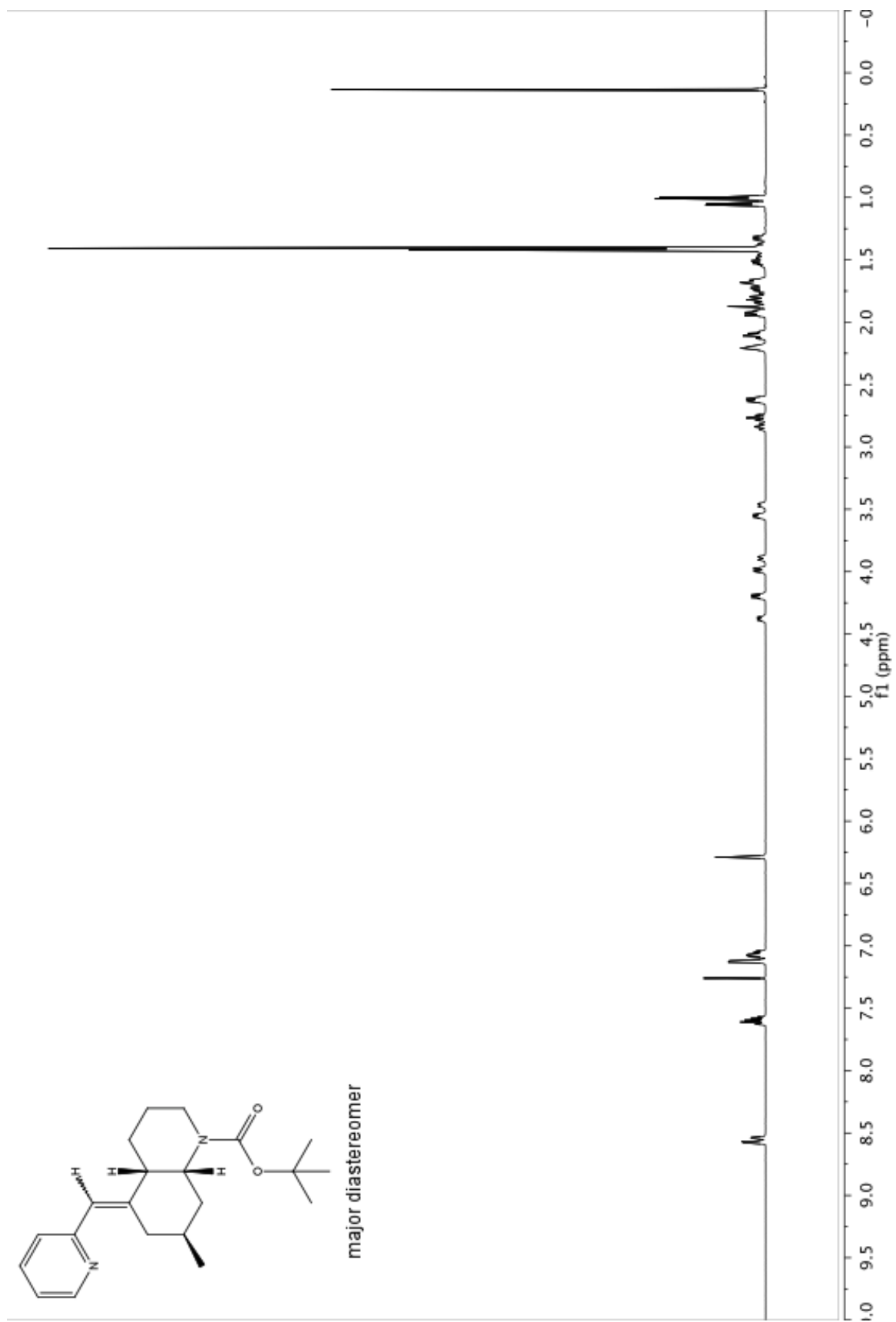


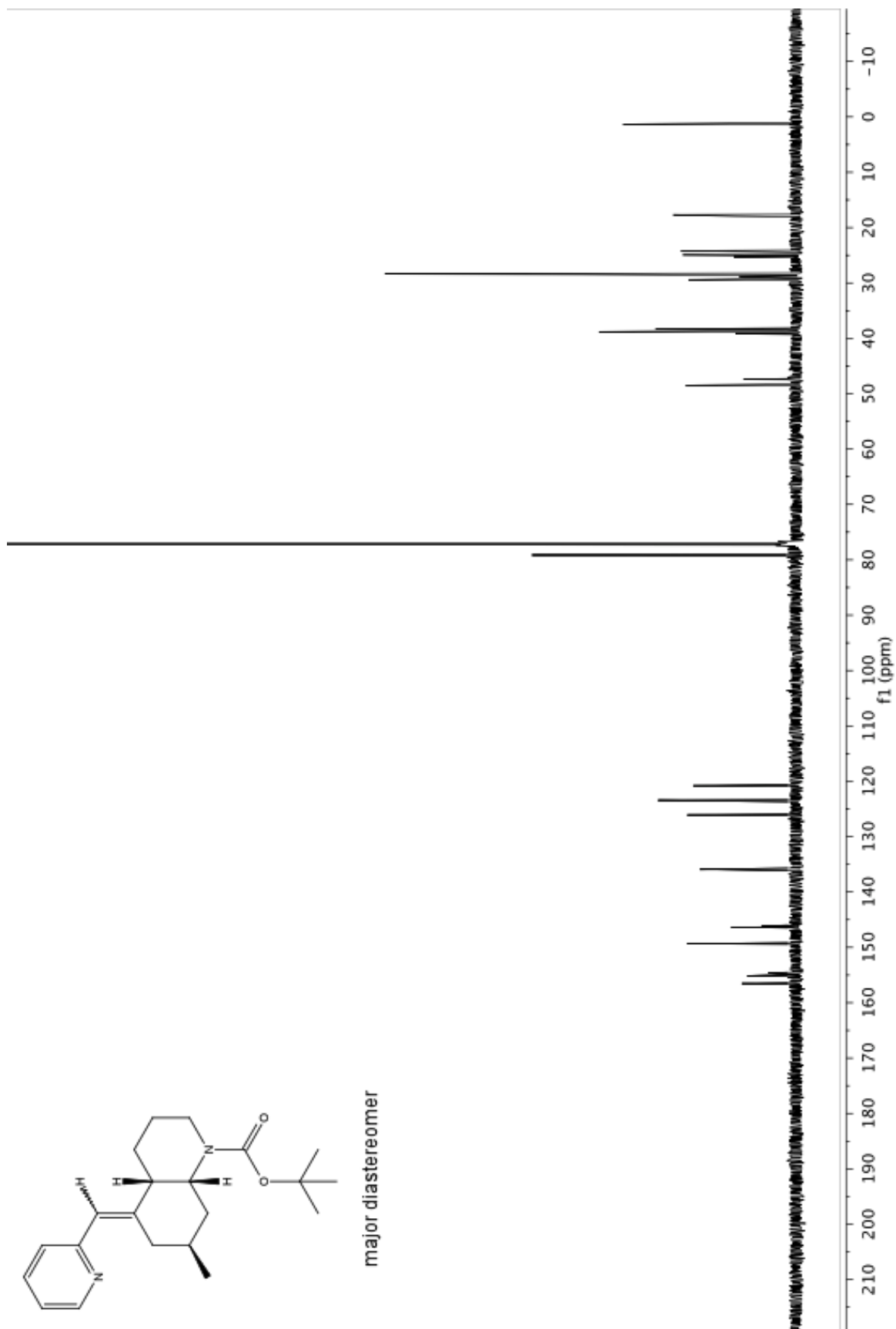


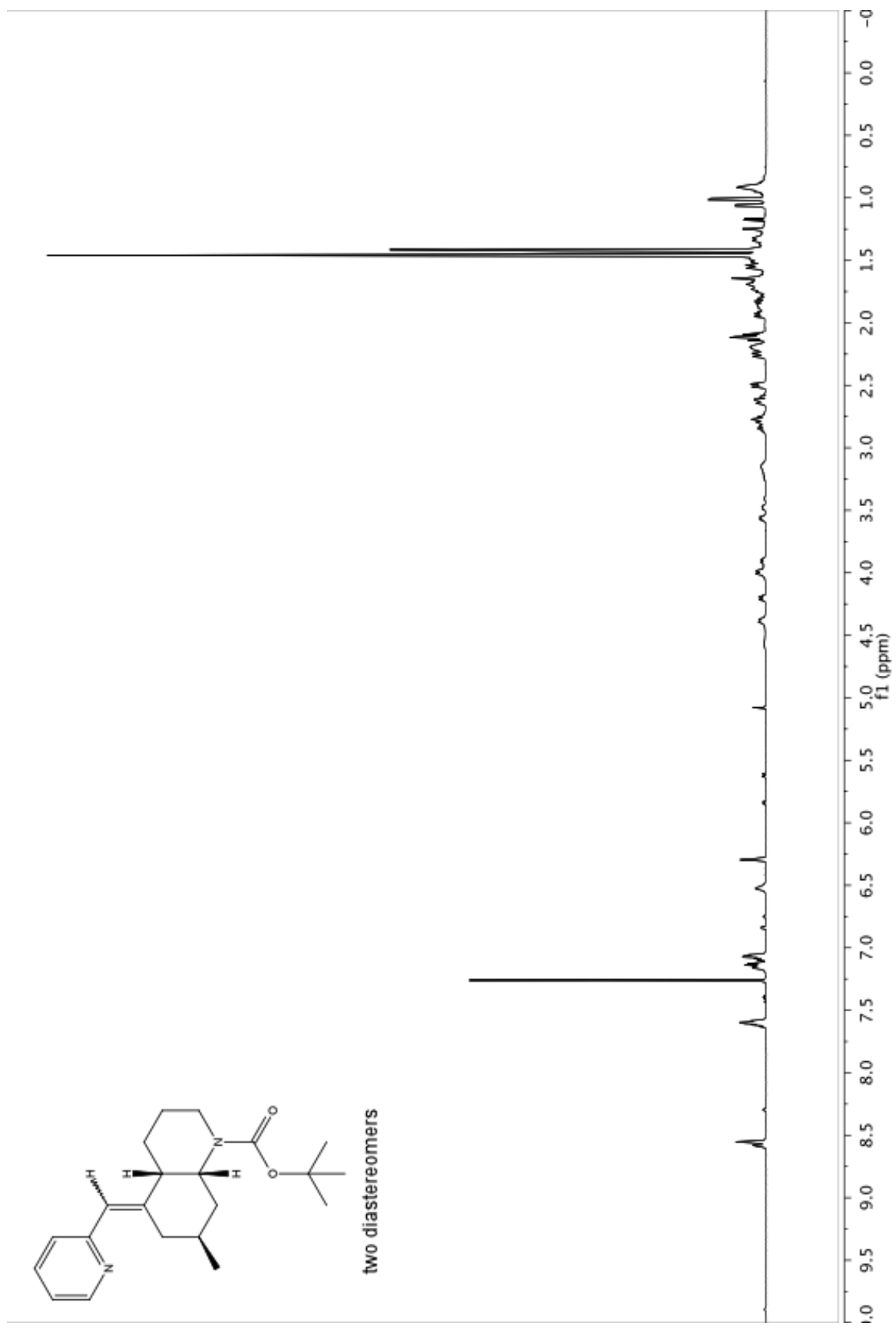


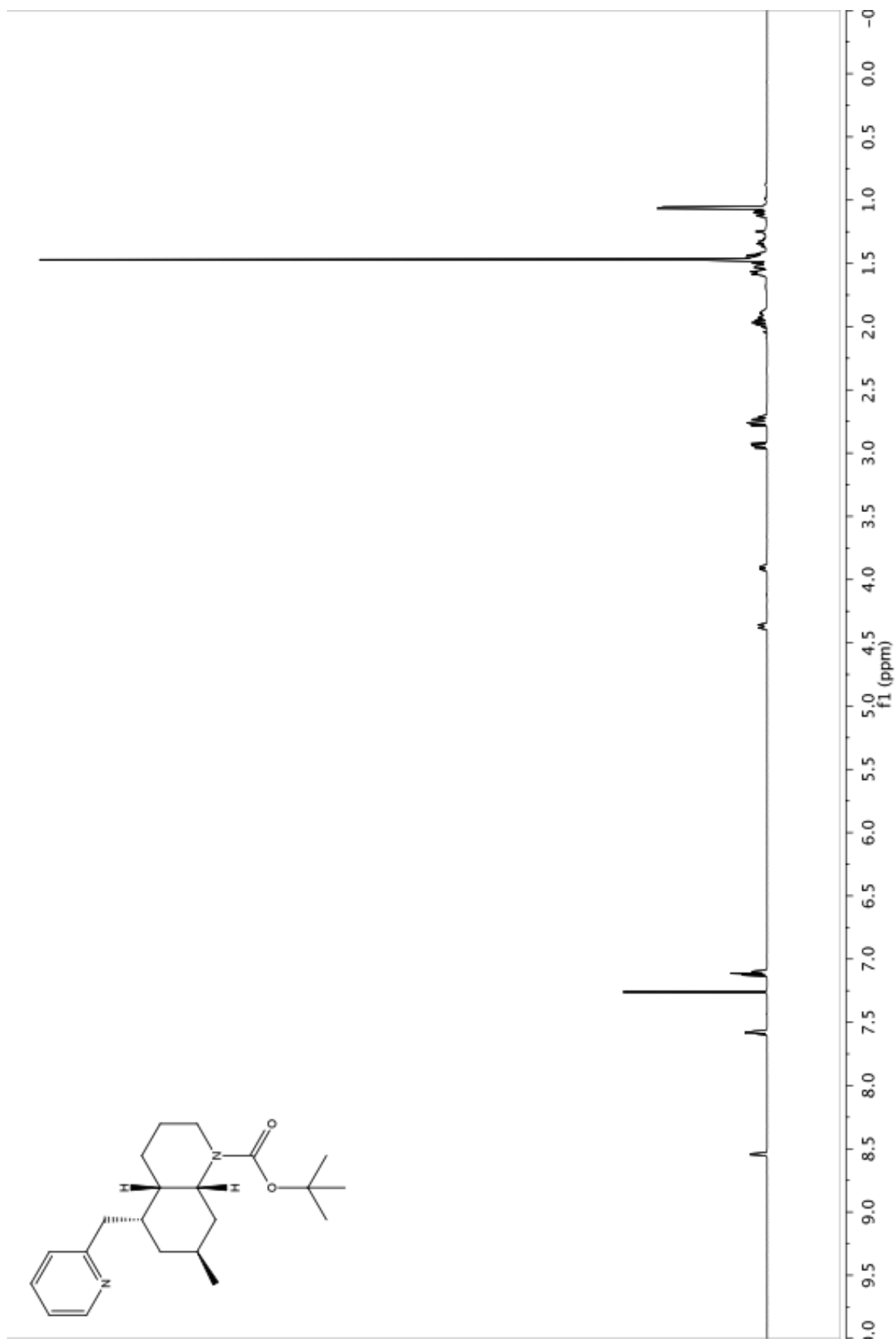


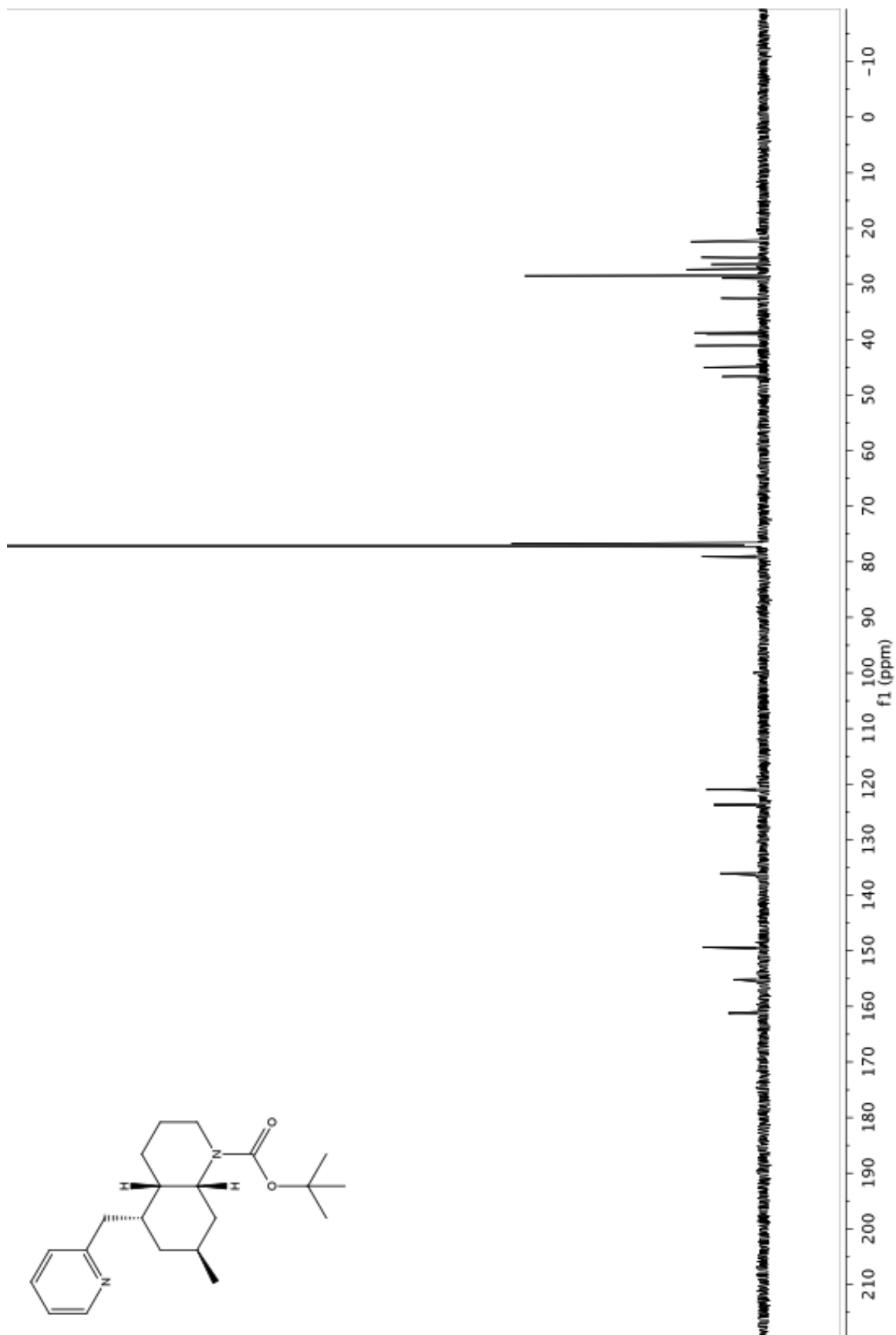


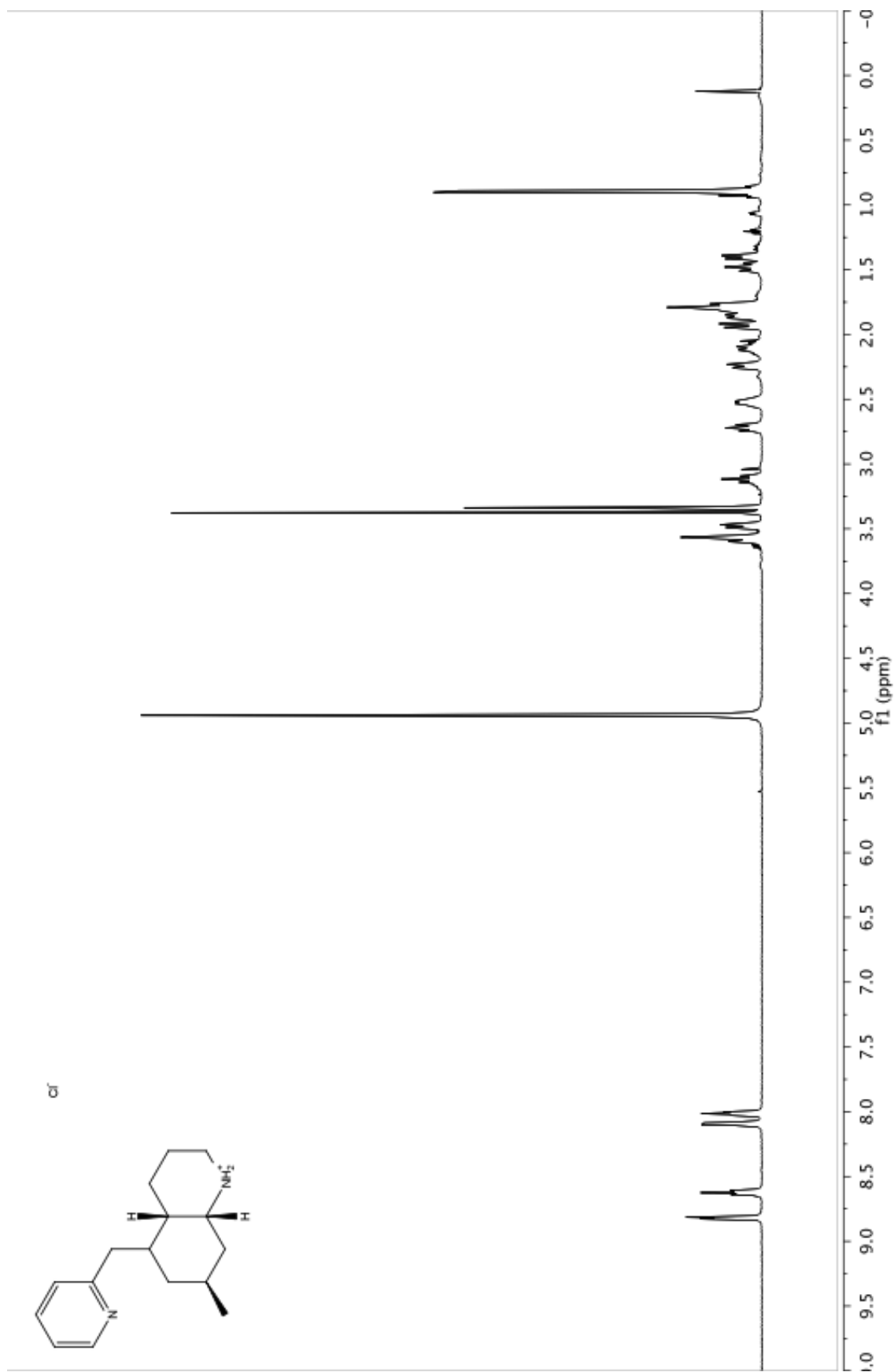


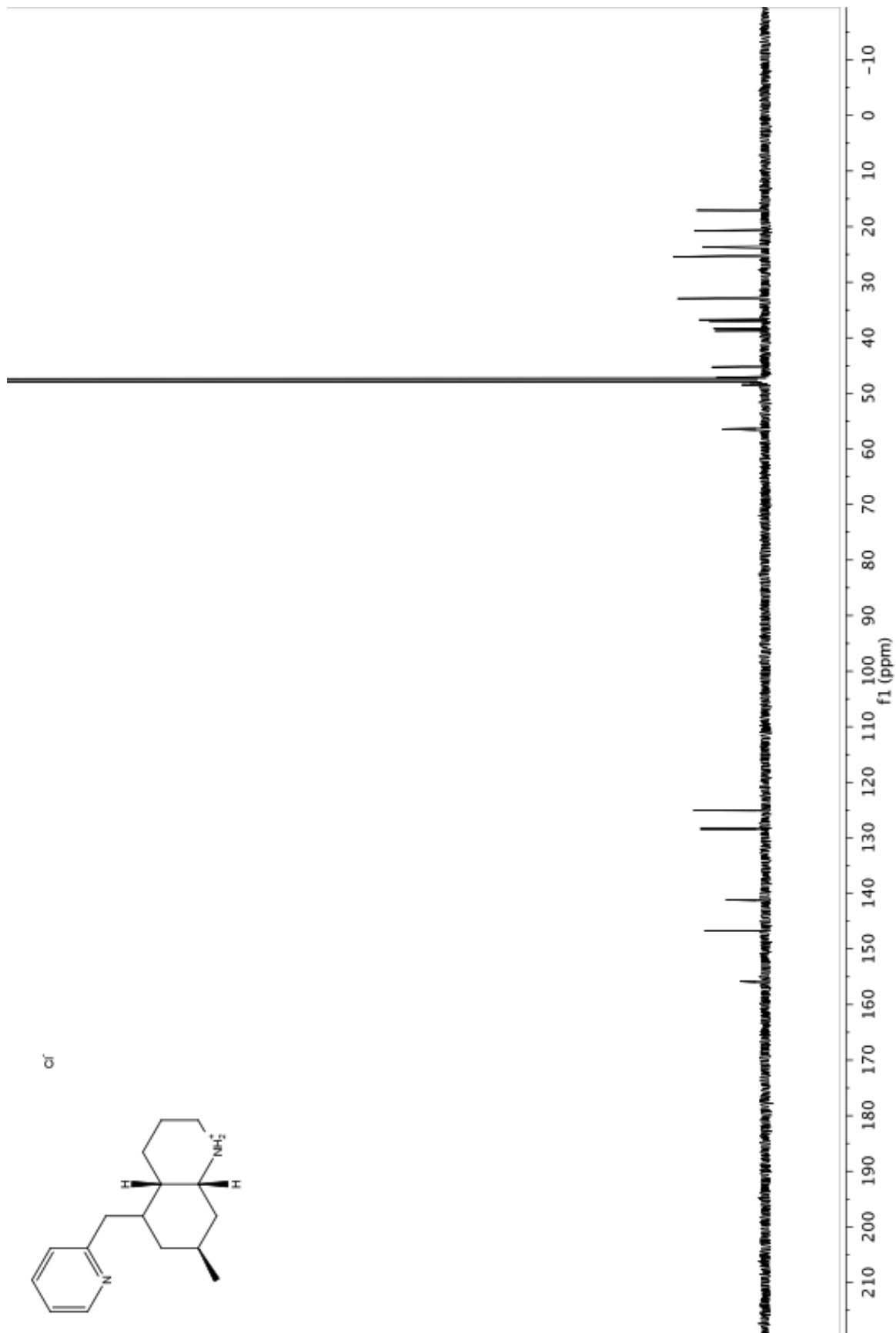




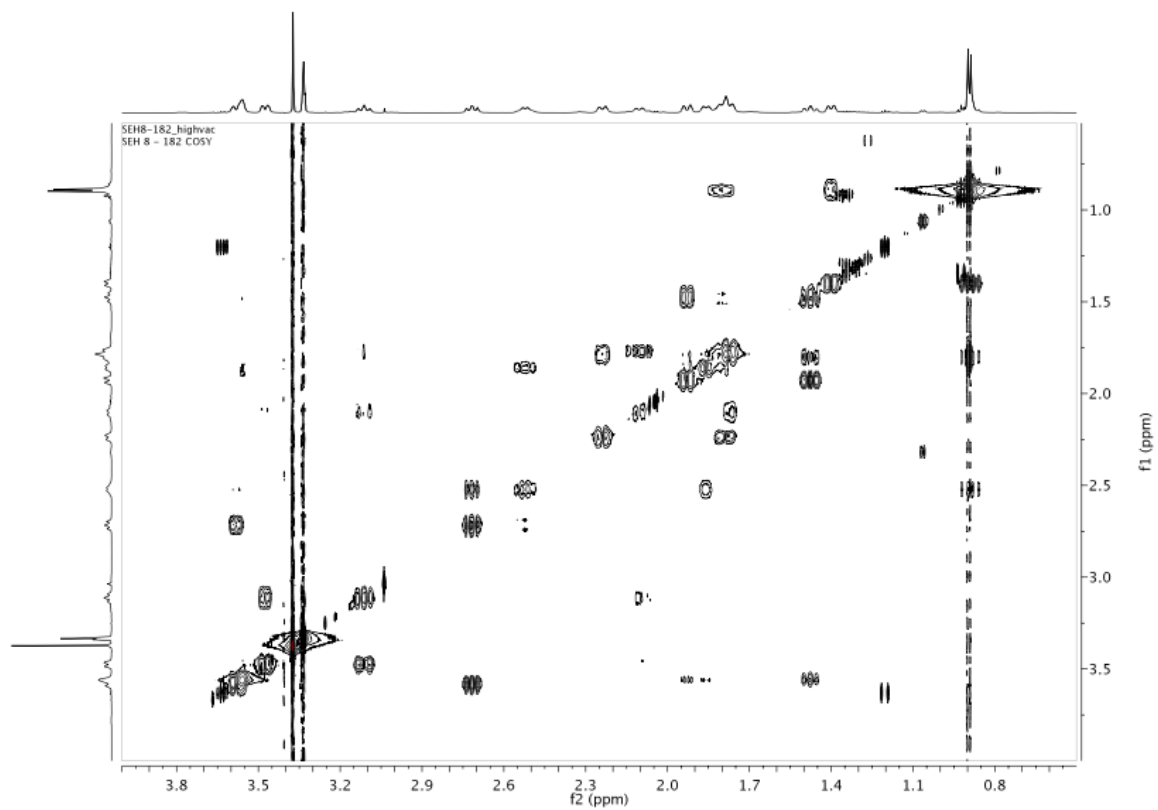




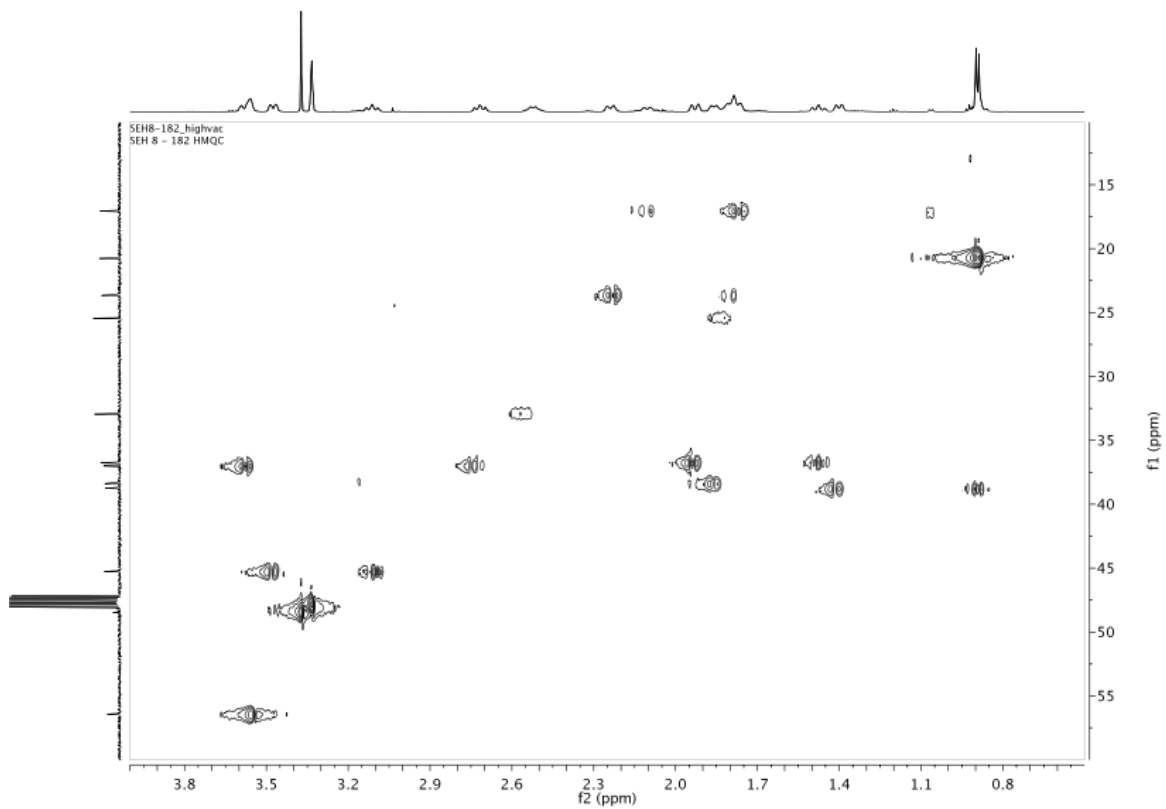




COSY for HCl salt **4.37**



HMQC for HCl salt **4.37**



NOESY for HCl salt **4.37**

